INSTITUTE OF SEISMOLOGY
UNIVERSITY OF HELSINKI
REPORT S-67

LITHOSPHERE 2018

TENTH SYMPOSIUM ON STRUCTURE, COMPOSITION AND EVOLUTION OF THE LITHOSPHERE

PROGRAMME AND EXTENDED ABSTRACTS

Edited by

Ilmo Kukkonen, Suvi Heinonen, Hanna Silvennoinen, Fredrik Karell, Elena Kozlovskaya, Arto Luttinen, Kaisa Nikkilä, Vesa Nykänen, Markku Poutanen, Pietari Skyttä, Eija Tanskanen, Timo Tiira and Kati Oinonen

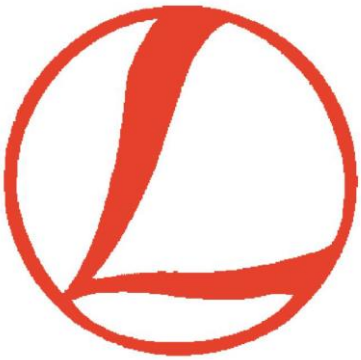

University of Oulu,
November 14-16, 2018

Oulu 2018

Series Editor-in-Chief: Timo Tiira

Guest Editors: Ilmo Kukkonen, Suvi Heinonen, Hanna Silvennoinen, Fredrik Karell, Elena Kozlovskaya, Arto Luttinen, Kaisa Nikkilä, Vesa Nykänen, Markku Poutanen, Pietari Skyttä, Eija Tanskanen, Timo Tiira and Kati Oinonen

Publisher: Institute of Seismology
P.O. Box 68
FI-00014 University of Helsinki
Finland
Phone: +358-294-1911 (switchboard)
http://www.helsinki.fi/geo/seismo/

ISSN 0357-3060
ISBN 978-952-10-9594-8 (print)
Juvenes Print Oulu
Oulu 2018
ISBN 978-952-10-9595-5 (pdf)

LITHOSPHERE 2018

TENTH SYMPOSIUM ON STRUCTURE, COMPOSITION AND EVOLUTION OF THE LITHOSPHERE

PROGRAMME AND EXTENDED ABSTRACTS

University of Oulu, Finland
November 14-16, 2018

CONTRIBUTING ORGANIZATIONS

Finnish National Committee of the International Lithosphere Programme (ILP)
Aalto University
Geological Survey of Finland (GTK)
National Land Survey of Finland, Finnish Geospatial Research Institute (FGI)
University of Helsinki
University of Turku
University of Oulu
Åbo Akademi University

ORGANIZING COMMITTEE AND EDITORS

Ilmo Kukkonen	University of Helsinki (ilmo.kukkonen@helsinki.fi)
Suvi Heinonen	Geological Survey of Finland (suvi.heinonen@gtk.fi)
Hanna Silvennoinen	University of Oulu (hanna.silvennoinen@oulu.fi)
Fredrik Karell	Geological Survey of Finland (fredrik.karell@gtk.fi)
Elena Kozlovskaya	University of Oulu (elena.kozlovskaya@oulu.fi)
Arto Luttinen	University of Helsinki (arto.luttinen@helsinki.fi)
Kaisa Nikkilä	Åbo Akademi University (kaisa.nikkila@abo.fi)
Vesa Nykänen	Geological Survey of Finland (vesa.nykanen@gtk.fi)
Markku Poutanen	Finnish Geospatial Research Institute FGI (markku.poutanen@nls.fi)
Pietari Skyttä	University of Turku (pimisk@utu.fi)
Eija Tanskanen	Finnish Meteorological Institute (eija.tanskanen@fmi.fi)
Timo Tiira	University of Helsinki (timo.tiira@helsinki.fi)
Kati Oinonen	University of Helsinki (kati.oinonen@helsinki.fi)

References of Lithosphere Symposia Publications

Pesonen, L.J., Korja, A. and Hjelt, S.-E., 2000 (Eds.). Lithosphere 2000 - A Symposium on the Structure, Composition and Evolution of the Lithosphere in Finland. Programme and Extended Abstracts, Espoo, Finland, October 4-5, 2000. Institute of Seismology, University of Helsinki, Report S-41, 192 pages.

Lahtinen, R., Korja, A., Arhe, K., Eklund, O., Hjelt, S.-E. and Pesonen, L.J., 2002 (Eds.). Lithosphere 2002 – Second Symposium on the Structure, Composition and Evolution of the Lithosphere in Finland. Programme and Extended Abstracts, Espoo, Finland, November 12-13, 2002. Institute of Seismology, University of Helsinki, Report S-42, 146 pages.

Ehlers, C., Korja A., Kruuna, A., Lahtinen, R. and Pesonen, L.J., 2004 (Eds.). Lithosphere 2004 – Third Symposium on the Structure, Composition and Evolution of the Lithosphere in Finland. Programme and Extended Abstracts, November 10-11, 2004, Turku, Finland. Institute of Seismology, University of Helsinki, Report S-45, 131 pages.

Kukkonen, I.T., Eklund, O., Korja, A., Korja, T., Pesonen, L.J. and Poutanen, M., 2006 (Eds.). Lithosphere 2006 – Fourth Symposium on the Structure, Composition and Evolution of the Lithosphere in Finland. Programme and Extended Abstracts, Espoo, Finland, November 9-10, 2006. Institute of Seismology, University of Helsinki, Report S-46, 233 pages.

Korja, T., Arhe, K., Kaikkonen, P., Korja, A., Lahtinen, R. and Lunkka, J.P., 2008 (Eds.). Lithosphere 2008 – Fifth Symposium on the Structure, Composition and Evolution of the Lithosphere in Finland. Programme and Extended Abstracts, Oulu, Finland, November 5-6, 2008. Institute of Seismology, University of Helsinki, Report S-53, 132 pages.

Heikkinen, P., Arhe, K., Korja, T., Lahtinen, R., Pesonen, L.J. and Rämö, T., 2010 (Eds.). Lithosphere 2010 – Sixth Symposium on the Structure, Composition and Evolution of the Lithosphere in Finland. Programme and Extended Abstracts, Helsinki, Finland, October 27-28, 2010. Institute of Seismology, University of Helsinki, Report S-55, 154 pages.

Kukkonen, I.T., Kosonen, E., Oinonen, K., Eklund, O., Korja, A., Korja, T., Lahtinen, R., Lunkka, J.P. and Poutanen, M., 2012 (Eds.). Lithosphere 2012 – Seventh Symposium on the Structure, Composition and Evolution of the Lithosphere in Finland. Programme and Extended Abstracts, Espoo, Finland, November 6-8, 2012. Institute of Seismology, University of Helsinki, University of Helsinki, S-56, 116 pages.

Eklund, O., Kukkonen, I.T., Skyttä, P., Sonck-Koota, P., Väisänen, M. and Whipp, D., 2014 (Eds.). Lithosphere 2014 – Eighth Symposium on the Structure, Composition and Evolution of the Lithosphere in Finland. Programme and Extended Abstracts, Turku, Finland, November 4-6, 2014. Institute of Seismology, University of Helsinki, S-62, 126 pages.

Kukkonen, I.T., Heinonen, S., Oinonen, K., Arhe, K., Eklund, O., Karell, F., Kozlovskaya, E., Luttinen, A., Lahtinen, R., Lunkka, J., Nykänen, V., Poutanen, M., Tanskanen, E. and Tiira T. (Eds.), 2016. Lithosphere 2016 – Ninth Symposium on the Structure, Composition and Evolution of the Lithosphere in Finland. Programme and Extended Abstracts, Espoo, Finland, November 9-11, 2016. Institute of Seismology, University of Helsinki, Report S-65, 156 pages.

Kukkonen, I.T., Heinonen, S., Silvennoinen, H., Karell, Kozlovskaya, E., Luttinen, A., Nikkilä, K., Nykänen, V., Poutanen, M., Skyttä, P., Tanskanen, E., Tiira, T. and Oinonen, K. (Eds.), 2018. Lithosphere 2018 – Tenth Symposium on the Structure, Composition and Evolution of the Lithosphere. Programme and Extended Abstracts, Oulu, Finland, November 14-16, 2018. Institute of Seismology, University of Helsinki, Report S-67, 134 pages.

Keywords (GeoRef Thesaurus, AGI): lithosphere, crust, upper mantle, Fennoscandia, Finland, Precambrian, Baltic Shield, symposia

TABLE OF CONTENTS

PREFACE

The Finnish National committee of the International Lithosphere Programme (ILP) organises every second year the LITHOSPHERE symposium, which provides a forum for lithosphere researchers to present results and reviews as well as to inspire interdisciplinary discussions. The tenth symposium - LITHOSPHERE 2018 – comprises 39 presentations. The extended abstracts (in this volume) provide a good overview on current research on structure and processes of solid Earth.

The three-day symposium is hosted by the University of Oulu and it will take place on the Linnanmaa campus in Oulu in November 14-16, 2018. The participants will present their results in oral and poster sessions. Posters prepared by graduate and postgraduate students will be evaluated and the best one will be awarded. The invited talk is given by Prof. Ulrich Riller (Universität Hamburg, Institut für Geologie).

This special volume ***"LITHOSPHERE 2018"*** contains the programme and extended abstracts of the symposium in alphabetical order.

Helsinki, October 31, 2018

Ilmo Kukkonen, Suvi Heinonen, Hanna Silvennoinen, Fredrik Karell, Elena Kozlovskaya, Arto Luttinen, Kaisa Nikkilä, Vesa Nykänen, Markku Poutanen, Pietari Skyttä, Eija Tanskanen, Timo Tiira and Kati Oinonen

Lithosphere 2018 Organizing Committee

LITHOSPHERE 2018 Symposium
Programme

Wednesday, Nov 14

09:00 - 10:00 Registration at the University of Oulu, Saalasti Auditorium

10:00 - 10:05 Opening: I. Kukkonen

10:05- 12:05 Session 1: Lithosphere structure and evolution from upper crust to asthenosphere
Chair: Ilmo Kukkonen

10:05 - 10:50 **Ulrich Riller [Invited]**
Multi-scale deformation during large impact cratering

10:50 - 11:15 **M. Ivandic, R. Carbonell, R. Roberts and D. Marti**
Towards a pan-European Deep Seismic Sounding (DSS) European database: Promoting the impact, preservation, and accessibility of the existing wealth of controlled source seismic data

11:15 - 11:40 **O.M. Muravina, V.N. Glaznev and M.V. Mints**
3D-density model of the Earth crust for central part of the East-European platform

11:40 – 12.05 **T. Kreitsmann, L.J. Pesonen, S. Hietala, J. Lerssi, J. Nenonen and J. Plado**
Summanen, a new meteorite impact structure in Central Finland

12:05 - 13:00 Lunch

13:00-14:15 Session 2: Lithosphere structure and evolution from upper crust to asthenosphere (cont.)
Chair: E. Kozlovskaya

13:00-13:25 **U. Autio, M. Smirnov, M. Cherevatova, T. Korja and T. Bauer**
Analysis of magnetotelluric array data from the central Finnish Lapland – tectonic implications

13:25 - 13:50 **J. Nevalainen, E. Kozlovskaya and H. Jänkävaara**
EPOS Anthropogenic Hazard: Pyhäsalmi Episode

13:50 - 14:15 **G. Gislason, S. Heinonen, J. Konnunaho, K. Moisio, J. Nevalainen and H. Salmirinne**
KOSE - Koillismaa Seismix Exploration survey: Details and first results

14:15 - 14:45 Coffee/Tea

14:45-16:50 Session 3: Lithosphere evolution, structures and mineral resources
Chair: E. Tanskanen

14:45-15:10 **P. Skyttä**
Fragmentation of the Archaean crust and its influence on the evolution of the overlying Proterozoic sequences (Northern Finland)

15:10-15:35 **S. Reimers, J. Engström and U. Riller**
The Kynsikangas shear zone, Southwest Finland: Importance for understanding deformation kinematics and rheology of lower crustal shear zones

15:35- 16:00 **S. Heinonen, M. Malinowski, G. Gislason, F. Hlousek, S. Buske and E. Koivisto**
COGITO-MIN seismic reflection profiling for mineral exploration in Polvijärvi, Finland

16:00-16:25 **E. Koivisto, M. Malinowski, S. Heinonen, C. Cosma, K. Vaittinen, M. Wojdyła, M. Riedel, M. Chamarczuk and the COGITO-MIN Working Group**
Seismic mineral exploration at different scales in the Outokumpu Ore District, Eastern Finland

16:25- 16:50 **J. Engström, F. Karell and J. Kuva**
The relationship between Structural Geology, Anistropy of Magnetic Susceptibility (AMS) and X-ray Computed Tomography (μ-CT) in high-grade metamorphic rocks in SW Finland

16:50- 17:30 Session 4: Poster introductions
Chair: K. Nikkilä
5 min talks with five slides max in the auditorium

17:30 – 19:30 Poster viewing and networking with refreshments

Posters

P01. J. Palosaari, S. Lund, J. Kauppila, O. Eklund, R-M. Latonen, T. Lindfors, J-H. Smått, E. Björnvik, S. Sirkiä, J. Peltonen, S. Raunio, R. Blomqvist, J. Marmo and S. Lukkari
Identification of Potential Flake Graphite Ores in the Fennoscandian Shield and Utilization of Graphene (FennoFlakes)

P02. J. Kara, J. Manninen, T. Leskelä, P. Skyttä, M. Väisänen, M. Tiainen and H. Leväniemi
Characterisation of the structural evolution and structural control of the gold mineralisations in the Kullaa area, SW Finland

P03. T. Kauti, P. Skyttä and A. Salo
Delineating the network of dolerite dykes within the Archaean Siilinjärvi carbonatite complex

P04. I. Pitkälä, J. Kara, T. Leskelä, P. Skyttä, M. Väisänen, H. Leväniemi, J. Hokka, M. Tiainen, Y. Lahaye
Shear zones and structural analysis of the Loimaa area, SW Finland

P05. J. Woodard
Oxygen isotopes in zircon from Palaeoproterozoic post-collisional carbonatites and lamprophyres in the Fennoscandian Shield

P06. T. Veikkolainen and I.T. Kukkonen
Heat flow and heat production in relation to geoneutrino signal near Pyhäsalmi mine

P07. S. Väkevä, E. Koivisto, G. Hillers, M. Chamarczuk and M. Malinowski:
3C Seismic Interferometry at the Polymetallic Kylylahti Deposit, Outokumpu District, Finland

P08. S. Hietala, J. Plado and L. J. Pesonen
Economical aspect of meteorite impact craters in Fennoscandia and Baltic countries

P09. P. Koskenniemi, J. Kortström, K. Piipponen, M. Uski and T. Vuorinen
Seismic monitoring of a hydraulic fracture stimulation

P10. T. Vehkamäki, M. Väisänen, Y. Lahaye, M. Kurhila and B. Johanson
U-Pb zircon, monazite and xenotime geochronology of cordierite-anthophyllite and felsic volcanic rocks in Orijärvi, southern Finland

Thursday, Nov 15

09:30-12:05 Session 5: Archaean and Proterozoic lithosphere structure and evolution
Chair: S. Heinonen

09:30-09:55 **A. Saukko, K. Nikkilä, O. Eklund and M. Väisänen**
Felsic MASH zone in southernmost Finland

09:55-10:20 **H. Leväniemi, S. Mertanen, M. Melamies, T. Karinen, S. Heinonen and T. Niiranen**
Intensity and Characteristics of Natural Remanent Magnetisation for Magnetic Data Interpretation in Sodankylä, Northern Finland

10:20- 10:50 Coffee/Tea

10:50- 11:15 **S. Väkevä, T. Tiira, T. Janik, T. Veikkolainen, T. Skrzynik, A. Heinonen, K. Komminaho and A. Korja**
Refraction seismic studies along the Kokkola–Kymi transect, Central Fennoscandia

11:15-11:40 **N. Afonin, E. Kozlovskaya, J. Karjalainen, T. Pirttisalo, S. Heinonen, S. Buske**
Retrieving of surface and body waves from ambient seismic noise, recorded during XSodEX experiment

11:40- 12:05 **J. Karjalainen, E. Kozlovskaya, T. Pirttisalo, S. Heinonen, S. Buske**
Ambient noise measurements and HVSR analysis in the XSoDEx project

12:05-13:00 Lunch

14:00 -14:00 **Session 6: Visit to the Oulu Mining School Research Centre**

13:30-16:30 **Session 7: Crustal structures and mineral resources**
Chair: D. Whipp

14:00- 14:25 **T. Leskelä, J. Kara, I. Pitkälä, P. Skyttä, M. Väisänen, M. Tiainen, H. Leväniemi, J. Hokka, Y. Lahaye**
Geochronology, geochemistry and structural setting of the Uunimäki gold mineralisation, SW Finland

14:25- 14:45 **M. Holma and P. Kuusiniemi**
Underground muography: The raise of geoparticle physics as a soil, orebody and rock realm imaging method

14:45- 15:05 Coffee/Tea

15:05- 15:30 **J. O. Eisermann and U. Riller**
Reconciling the kinematic importance of the GPS velocity field in the Southern Andes with scaled analogue experiments

15:30-15:55 **P. L. Göllner, J. O. Eisermann and U. Riller**
Strain partitioning along the South American convergent margin between 42°S and 47°S: Insights from lineament analysis

15:55 –16:15 **E.I. Tanskanen**
Magnetic disturbances driven by currents in the solid Earth and ionosphere

16:15-16:40 **H. Jänkävaara**
Preliminary studies of long-period array methods with Northern Finland Seismological Network

Friday, Nov 16

9:30-10:20 Session 8: Neotectonics, geothermal energy

Chair: P. Skyttä

9:30-9:55 **J. Mattila, A. Ojala, T. Ruskeeniemi, J.-P. Palmu, M. Markovaara-Koivisto, N. Nordbäck, R. Sutinen**
On the displacement-length ratios of postglacial faults

9:55-10:20 **M. Markovaara-Koivisto, T. Ruskeeniemi, P. Hänninen and R. Sutinen**
Groundwater monitoring in postglacial faults -effect of atmospheric pressure and tide

10:20- 10:40 Coffee/Tea

10:40-11:05 **R. Sutinen and A. Ojala**
Subglacial deformations adjacent to Ristonmännikkö PGF

11:05–11:30 **I.T. Kukkonen**
Geothermal energy from deep bedrock in Finland – Geophysical and geological constraints

11:30- 12:00 Time for discussion and team meetings

12:00 - 13:00 Lunch

13:00-13:50 Session 9: Short communications
Chair: F. Karell

13:00 – 13:10 **E. Kozlovskaya, J. Narkilahti, J. Nevalainen, H. Silvennoinen, H. Jänkävaara**
FIN-EPOS Research Infrastructure at the University of Oulu

13:10 – 13:20 **J. Järvinen, S. Piippo, S. Silvennoinen, S. Kultti, E. Koivisto**
New digital learning materials for teaching in geosciences

13:20 – 13:30 **Kari Strand**
New scientific ocean drilling (IODP) opportunities for polar region geosciences

13:30 – 13.40 **Ilmo Kukkonen & DAFNE WG**:
ICDP project proposal Drilling Active Faults in Northern Europe (DAFNE)

13:40– 13:50 **E. Kozlovskaya**
INFACT: Innovative, Non-Invasive and Fully Acceptable Exploration Technologies

13:50- 14:00 Final discussion and poster award

14:00 Closing of symposium

EXTENDED ABSTRACTS

For color versions of figures, see the web version of the publication,
http://www.seismo.helsinki.fi/ilp/lito2018/

Retrieving of surface and body waves from ambient seismic noise, recorded during XSodEX experiment

N. Afonin[1], E. Kozlovskaya [1,2], J. Karjalainen[1], T. Pirttisalo [1], S. Heinonen [2], S. Buske [3]

[1]Oulu Mining School, Faculty of Technology, University of Oulu, Finland
[2] Geological Survey of Finland
[3] TU Bergakademie Freiberg , Germany (TUBAF)

E-mail: nikita.afonin@oulu.fi

In this article, we describe the first results of passive seismic data analysis, collected during XSodEX seismic experiment. Application of advanced technique of retrieving Empirical Greens Functions allowed to extract both surface and body waves from ambient seismic noise.

Keywords: ambient seismic noise, passive seismic interferometry, surface and body waves retrieving

1. Introduction

At present, passive seismic methods of applied geophysics are rapidly developing. These methods are very good tool for solution of many applied tasks, where information about elastic properties of the rocks in near-surface layers is needed (microseismic zonation, groundwater and microearthquakes sources study etc.). In some situations, such as measuring near active industrial object or other areas with high level of seismic noise, application of passive seismic techniques is the only option (Place and Malemhir, 2015, Cheng et al., 2015; Shirzad and Shomali, 2014; Vidal et al., 2014, Panea et al., 2014, etc.). In this study, we described the first results of analysis of ambient noise recorded during XSodEx seismic experiment. Retrieving surface and body waves from the noise is based on splitting of all records to time windows with surface or body waves only and calculation of crosscorrelation function separately for these parts. The main idea of data processing has been taken from works by Vidal et al. (2014) and Panea et al. (2014).

2. Description of the passive seismic experiment

For extraction of surface and body waves from ambient seismic noise, we used continuous passive seismic data recorded since 21.08.2017 to 23.08.2017 with the sampling frequency of 500 Hz along the profile of total length of about 950 m with intersensor spaces about 10-15 m. The equipment consisted of 38 DSU-SA 3C MEMS and 60 1C SG-5 seismic sensors with the autonomous RAUD eX data acquisition units produced by Sercel Ltd. The profile was located near roads and river, which may be sources of continuous seismic noise.

For evaluation of surface and body wave parts of empirical Greens functions, we particularly used the procedure, described on Panea et al. (2014). The algorithm of the data processing includes spectral whitening of seismic noise records, splitting of all records to time windows of 1 minutes length, calculation of crosscorrelation functions. After this visual inspection of calculated crosscorrelation functions had been apllied. The main criteria of separation were apparent velocity, which must be higher for body waves.

After visual inspection, time windows have been merged into two new records contained only body waves or both surface and body waves. After this, we calculated crosscorrelation functions separately for these records and stacked correspondent functions for different locations of a virtual source (figure 1).

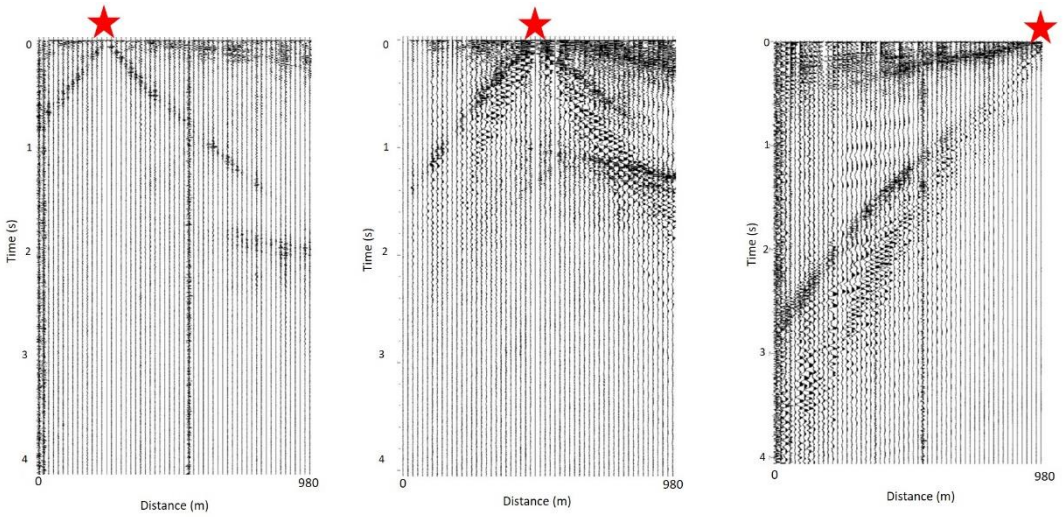

Figure 1. Empirical Greens functions with both surface and body waves parts, calculated for different positions of virtual sources (marked by the red stars).

As one can see on figure 1, application of this procedure, allowed to get signals as generated by active sources, located on positions of virtual sources (red starts on figure 3). On these correlograms, there are refracted and reflected body waves and surface waves.

3. Conclusions

In present study, we showed the first results of application advanced technique of passive data processing. This procedure includes visual inspection of crosscorrelation functions, calculated for short time records of seismic noise. It makes it possible to extract both surface and body waves parts of empirical Greens functions. From our results we can conclude that sources of seismic noise have inhomogeneous distribution and were located near one side of profile, in general. But principles of seismic interferometry and virtual source method make it possible to change position of virtual source and, therefore get signal as in active seismic experiments.

4. Acknowledgements

The study is a part of XSodEx experiment carried out as a joint effort of the Geological Survey of Finland, TU Bergakademie Freiberg , Germany and University of Oulu (OMS and SGO) . The study was supported by Grant No. 311666 of the Academy of Finland.

References:

Place, J. A. P., A. Malehmir, K. Högdahl, C. Juhlin, and K. Persson Nilsson, 2015, Seismic characterization of the Grängesberg iron deposit and its mining-induced structures, central Sweden: Interpretation, 3, SY41–SY56, doi: 10.1190/INT-2014-0212.1.

Cheng, F., Xia, J., Xu, Y., Xu, Z., and Pan, Y., 2015, A new passive seismic method based on seismic interferometry and multichannel analysis of surface waves: Journal of Applied Geophysics, 117, 126-135.

Shirzad, T., Shomali, Z. H., 2015, Extracting seismic body and Rayleigh waves from the ambient seismic noise using the rms-stacking method: Seismological Research Letters, 86(1), 173-180.

Vidal, C. A., Draganov, D., Van der Neut, J., Drijkoningen, G., and Wapenaar, K., 2014, Retrieval of reflections from ambient noise using illumination diagnosis. Geophysical Journal International, 198(3), 1572-1584.

Panea, I., Draganov, D., Almagro Vidal, C., and Mocanu, V., 2014, Retrieval of reflections from ambient noise recorded in the Mizil area, Romania: Geophysics, 79(3), Q31-Q42.

Analysis of magnetotelluric array data from the central Finnish Lapland – tectonic implications

U. Autio[1], M. Smirnov[2], M. Cherevatova[3], T. Korja[2] and T. Bauer[2]

[1]Oulu Mining School, University of Oulu, Finland
[2]Dep. of Civil, Environmental and Natural Resources Engineering, Luleå University of Technology, Sweden
[3]Applied Geophysics Group, University of Münster, Germany
E-mail: uula.autio@oulu.fi

Tectonic implications of recent magnetotelluric investigations in the central Finnish Lapland are presented. The site array covers the Central Lapland Granitoid Complex and parts of the Central Lapland Greenstone Belt, the Peräpohja Belt and the Kuusamo Belt. Thus, the study area is located in the (heavily reworked) Archaean part of the Fennoscandian shield. Reflecting the complex tectonic history, the data set bears highly anomalous imprints and requires three-dimensional conductivity models for explanation. However, at the same time, a dominant ~E-W trend is evident in strike indicators. Preferred inversion model shows major crustal conductors in the vicinity of the belts. The model is generally complex, but the E-W trend observed in the data is reflected also in the model. Most likely cause for the conductors are deeply buried graphite/sulphide bearing metasediments. The results favour a tectonic model where extension and compression in the area has took place dominantly in the present ~N-S direction.

Keywords: Fennoscandia, magnetotelluric, conductivity, crust, tectonic

1. Background

The central Finnish Lapland (Fig 1.) is located in the Archaean part of the Fennoscandian shield. The area has been heavily reworked in the Palaeoproterozoic tectonic processes. As a result, we are now looking at the Central Lapland Granitoid Complex (CLGC) flanked by the Central Lapland Greenstone Belt (CLGB), the Peräpohja Belt (BP) and the Kuusamo Belt (KB). The Archaean crust outcrops in the south (Pudasjärvi Complex, PC) and in the east, and at least partly underlies the Palaeoproterozoic units.

In the context of the MaSca-project (Cherevatova et al., 2015), data from total of 79 magnetotelluric (MT) sites were acquired in 2014 (Fig. 1a, black symbols). The period range (0.001-10000 s) and the site spacing (~15 km) allows to image the geoelectric structure in the crustal and lithospheric scales. One of the main goals of the research is to provide constraints for the structure and the tectonic evolution of the lithosphere in the northern Fennoscandia.

2. Results

Dimensionality indicators (the phase tensor skew) reveal pronounced 3-D effects in all except the eastern part of the study area. Despite the 3-D effects, a common N80ºE trend is also evident in the strike indicators (the phase tensor orientation). Conductivity models were obtained by inverting the data set using the 3-D code ModEM. Note that data also from previous investigations have been included in the analysis (Fig. 1a). The preferred model reveals dominantly E-W striking crustal conductors in the vicinity of the northern and the southern belts (CLGB, PB and KB). The most notable conductor is found in the north, near the border of the CLGC and the CLGB at mid-crustal depth. It has complex geometry and very high conductance (> 10000 S). Also in the south major crustal conductors exist in the PB and near the border of the KB and the CLGC. However, the exact nature of the conductors in the PB remains unclear due to unstable inversion results. Most part of the CLGC shows as a prominent resistor, separating the northern and the southern conductors.

The conductors represent most likely graphite/sulphide bearing metasediments, which are abundant in the near-surface. They were originally deposited in the rift basins during the extensional stage and subsequently deeply buried in the crustal collisions. Generally, the results

support the recent tectonic evolution model by Nironen (2017), which indicates that a major N-S component both in the extensional and the compressional stages was present in the study area.

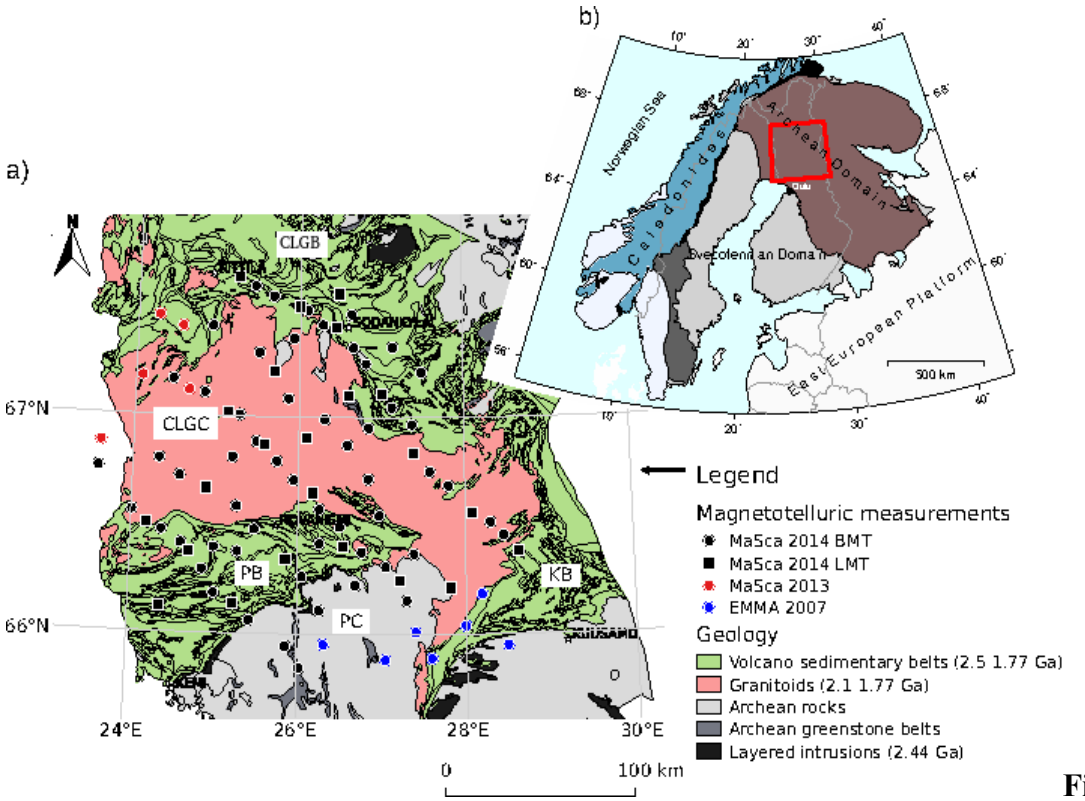

Figure 1. Location map. a) Magnetotelluric sites on a geological map (Korsman et al. 1997). CLA=Central Lapland Area, CLGC=Central Lapland Granitoid Complex, KB=Kuusamo Belt, PB=Peräpohja Belt, PC=Pudasjärvi Complex b) Large scale geological domains. The red rectangle encircles the extents of the study area.

References:

Cherevatova, M., Smirnov, M. Y., Jones, A., Pedersen, L., & MaSca Working Group, 2015. Magnetotelluric array data analysis from north-west Fennoscandia, Tectonophysics, 653, 1–19.

Korsman, K., Koistinen, T., Kohonen, J., Wennerström, M., Ekdahl, E., Honkamo, M., Idman, H., & Pekkala, Y., 1997. Geological map of Finland 1:1000 000 , Geological Survey of Finland.

Nironen, M., 2017. Structural interpretation of the Peräpohja and Kuusamo belts and Central Lapland, and a tectonic model for northern Finland, Geological Survey of Finland, Report of Investigation , 234, 53.

Reconciling the kinematic importance of the GPS velocity field in the Southern Andes with scaled analogue experiments

Jan Oliver Eisermann[1] and Ulrich Riller[1]

[1]Universität Hamburg, Institute of Geology, Hamburg, Germany
E-mail: Jan.Oliver.eisermann@uni-hamburg.de

Keywords: lithosphere, crust

1. Introduction

With a length of about 1000 km, the Liquiñe-Ofqui Fault Zone (LOFZ) in the Southern Andean Volcanic Zone (SAVZ) ranks among the largest intra-arc fault zones on Earth. The fault zone is generally believed to have formed in a transpressive setting attributed to oblique subduction of the Nazca Plate below the South American Plate. The LOFZ is commonly regarded as a vertically dipping, narrow dextral fault zone composed of two NNE-trending lineaments connected through a number of step-over faults.

2. Objective

West of the LOFZ, GPS sites indicate uniform NE-directed velocities on the order of several centimetres per year, indicating that the plate interface is currently locked (Fig. 1). East of the LOFZ, GPS velocities diminish abruptly to a few millimetres per year with a west-directed motion. At 36°S, GPS vectors change from NE-directed to SE-directed velocities (Fig. 1). The observed GPS velocity field has been associated with the effect of post-seismic mantle relaxation after the 1960 Valdivia earthquake (Moreno et al. 2011).

The GPS velocity field in the SAVZ indicates a strong spatial correlation with the LOFZ, in particular at its northern terminus. Thus, the velocity field seems to be kinematically related to deformation associated with the LOFZ. Specifically, west of the LOFZ velocities are co-linear with the obliquity in plate convergence and indicate an absence of deformation partitioning in this area. By contrast, the abrupt West-East GPS velocity gradient at the LOFZ points not only to a large component of dextral displacement, but also to a considerable shortening on the LOFZ.

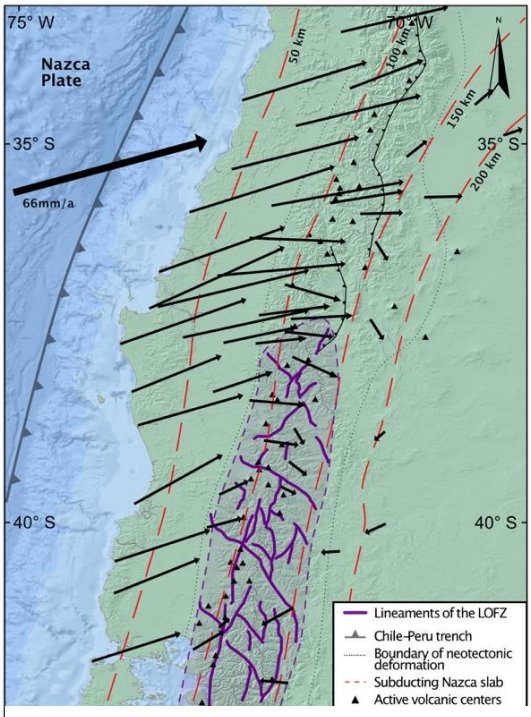

Figure 1. GPS velocity field in the SAVZ. Note large deviations of GPS vectors at the northern LOFZ as defined by lineaments.

3. Method

In order to test, to what extent the GPS velocity pattern is kinematically related to the LOFZ, we conducted a series of analogue experiments using our *MultiBox*, which was specifically designed to simulate transpression. The box consists of two halves, each of which contains a piston, whereby one halve is mobile and moves relative to the fixed one parallel to the box midline,

thereby inducing a velocity discontinuity. A large spectrum in deformation regimes can be generated by varying the displacement rates of the pistons and the mobile box halve. The large size of the *MultiBox* (1 m x 1 m x 30 cm) guarantees high accuracy in length scaling. The computer-controlled system is a prerequisite for high reproducibility of experimental results.

Our experiments are scaled to the average thicknesses of undeformed lower and upper crust. Experiments consist of a 3 cm thick layer of a silicone-corundum mixture simulating the ductile lower crust, and a 0.5 cm thick layer of quartz sand with Mohr-Coulomb rheology for the brittle upper crust. Each horizontal piston is fitted with a short vertical base plate in the shape of an L. These base plates carry a portion of the overlaying silicone and sand layers, simulating crustal blocks, and avoid localization of deformation at the pistons. A 20 cm wide area between the L-shaped pistons, in which material is detached from the base plate of the box, localizes the model mountain range. The experimental set-up allows for evenly distributed deformation, leading to spontaneous upper crustal deformation in and between the converging crustal blocks. The set-up includes a strength gradient in the quartz sand layer, which portrays the influence of different slab dips on the strength of the crust.

4. Quantitative assessment

Two cameras record the surface evolution during the experiments. Utilizing a state-of-the-art 3D digital image correlation system, individual increments of surface displacement and topography can be quantified with high accuracy. Moreover, a number of derivatives, such as strain intensity and rotation, of the measured vector field provides new insights into the structural and morphological evolution of crust undergoing transpression.

5. Results

We observed a change in the orientation and the magnitude of model velocity vectors, the patterns of which are remarkably similar to those of the GPS velocity field along the LOFZ and north of it. Deformation in our models is predominantly accomplished by oblique reverse faults. Within the fault zone, geometrically and kinematically linked faults allow us to define individual rhomb-shaped blocks. Most importantly, faulting appears to be distributed over a wide zone suggesting that the LOFZ is an orogen-scale fault zone. Our models do not indicate deformation partitioning (Fig. 2). Thus, post-seismic mantle relaxation does not seem to be the cause of the observed GPS velocity field. Our experiments are in agreement with a strong (upper) crust in the north and may, thus, account for the observed GPS velocity field associated the LOFZ. Purely vertical strike-slip faults, as a result of deformation partitioning, in a transpressive setting are not observed in our experiments. Collectively, our experimental structural and kinematic observations agree well with current GPS vectors in the SAVZ. Finally, our experiments indicate that the LOFZ may not propagate toward the north.

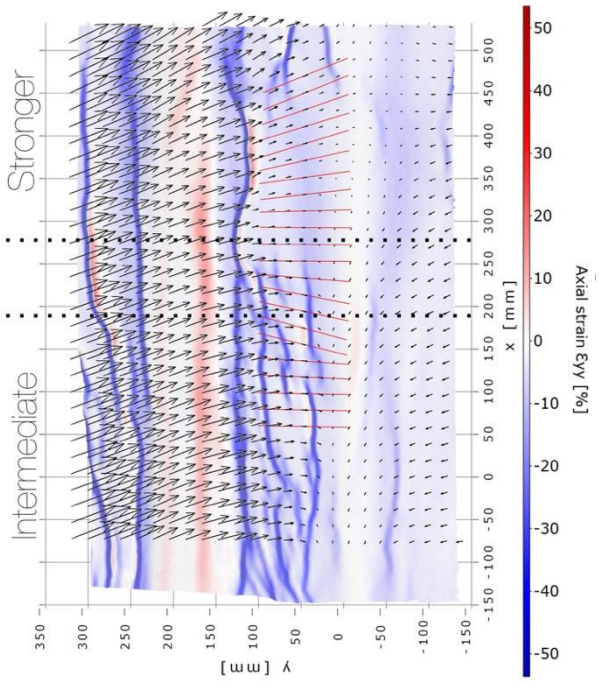

References:

M. Moreno, D. Melnick, M. Rosenau, J. Bolte, J. Klotz, H. Echtler, J. Baez, K. Bataille, J. Chen, M. Bevis, H. Hase, O. Oncken, Heterogeneous plate locking in the South–Central Chile subduction zone: Building up the next great earthquake, Earth and Planetary Science Letters, Volume 305, Issues 3–4, 2011, Pages 413-424, ISSN 0012-821X,

J. D. Pesicek, E. R. Engdahl, C. H. Thurber, H. R. DeShon, D. Lange; Mantle subducting slab structure in the region of the 2010 M8.8 Maule earthquake (30–40°S), Chile, Geophysical Journal International, Volume 191, Issue 1, 1 October 2012, Pages 317–324

Rosenau, M., D. Melnick, and H. Echtler (2006), Kinematic constraints on intra-arc shear and strain partitioning in the southern Andes between 38°S and 42°S latitude, Tectonics, 25, TC4013, doi: 10.1029/2005TC001943.

The relationship between Structural Geology, Anistropy of Magnetic Susceptibility (AMS) and X-ray Computed Tomography (μ-CT) in high-grade metamorphic rocks in SW Finland

J. Engström[1], F. Karell[1] and J. Kuva[1]

[1]Geological Survey of Finland, P.O. Box 96, 02151 Espoo Finland.
E-mail: jon.engstrom@gtk.fi

Anisotropy of magnetic susceptibility (AMS) has proven to be an excellent tool for examinations on mineral fabrics, magma flow and deformation of rocks. The magnetic anisotropy of rocks depends on the anisotropy of individual grains and their spatial arrangement. Structural geological mapping, micro-structural and X-ray computed tomography (μ-CT) scanning together with AMS has been utilized at two research sites (Olkiluoto and Kynsikangas) in SW Finland. The study indicates that the magnetic lineation and foliation can represent various structures within the metamorphic fabrics. The AMS data measured in the high-grade metamorphic rocks at the study sites show both α-lineation and β-lineation within the metamorphic minerals which gives new information about the deformation history of the areas.

Keywords: Anistropy of Magnetic Susceptibility (AMS), X-ray Computed Tomography (μ-CT), high-grade rocks, α-lineation and β-lineation

1. Introduction

Profound insights in understanding the structural evolution are important in several socio-economic aspects, especially civil engineering and the mining industry. Structural geology is important for understanding the tectonic ductile deformation in metamorphic rocks at surface but also deeper in the crust. Ductile deformation (lineation and foliation) is traditionally defined through structural geological studies performed at scales ranging from outcrop to microscopic. Through these studies it is possible to define the spatial preferred orientation (SPO) of minerals, such as foliation planes, fold axis and mineral lineation.

In nature, however, majority of deformed rocks do not develop clear mineral lineation, and some deformed metamorphic rocks do not even develop well-defined foliation planes. Combined use of modern techniques and traditional methods allows us to do a more detailed analysis of these structural metamorphic features. AMS has been a very useful tool in the fabric analysis of such deformed rocks and there have been several studies that have equated the three principal axes of the AMS ellipsoid (K1>K2>K3) with the three principal axes of the strain ellipsoid (X > Y > Z) (Tarling and Hrouda, 1994; Borradaile and Henry, 1997; Ferré et al., 2014). X-ray computed tomography (μ-CT) is an excellent tool for evaluating the minerals and structures in 3D at different scales. Combined use of AMS and μ-CT is a good, non-destructive tool for understanding complex microstructures and SPOs of minerals (Sayab et al. 2017) to understand their deformation history and geological evolution.

2. Study and methods

Structural geological mapping, thin section analysis and AMS together with μ-CT has been utilized at two research sites (Olkiluoto and Kynsikangas) in SW Finland. The Olkiluoto site has been studied as a site for the Finnish high-level Nuclear Waste, while the Kynsikangas shear zone is major ductile crustal shear zone that is of regional importance for the tectonic history of Southern Finland. Both sites are located within high-grade (amphibolite to granulite facies) metagranitoids and migmatic rocks. Even though the metamorphic environment is the same, the structural geology varies significantly. The Olkiluoto site is dominated by metatexitic to diatexitic rocks, which are intensively folded during several phases of ductile deformation. Kynsikangas is dominated by metatonalitic to migmatitic rocks. The major ductile shear zone has pervasively affected the rocks, which are dominated by steep foliations and stretching

lineations with left lateral shear in the horizontal plane. Samples from both sites were measured with AMS and imaged with μ-CT.

3. Results and Discussion

The study indicates that the magnetic lineation and foliation can represent various structures within the metamorphic fabrics. The AMS data obtained from the high-grade migmatites in Olkiluoto, shows predominantly β-lineation within the metamorphic minerals. The intensively folded migmatitic rock in Olkiluoto lacks stretching lineation while folding at all scales is evident throughout the site. Since the fold axis (β-lineation) orientations coincide with the main magnetic mineral direction, it is apparent that the metamorphic minerals within the samples are aligned parallel to the fold axis orientation. However, the AMS data from Kynsikangas exhibits a magnetic lineation, which is parallel to the stretching lineation (α-lineation) measured in the field. The central part of the Kynsikangas ductile shear zone is displaying a prolate shape for the minerals measured by AMS, thus indicating the biggest rate of stretching at this part of the zone. These structural features are important for determining the internal structure and kinematic evolution of the shear zone. The 3D-images from the μ-CT scans confirmed the SPO of the minerals and gave even more details about the meso-scale structural features. This data enhances the geological interpretation and gives new insight to the structural and tectonic evolution during the latter part of Svecofennian Orogen.

4. Conclusion

Our study concludes that in addition to foliation, also α-lineation and β-lineation measured in field can be defined with AMS studies. The AMS equipment is a cost-efficient and fast measurement technique to acquire additional structural data and μ-CT is an excellent complementary, non-destructive method to study the same samples. However, since several structural geological features can be defined by AMS, it is necessary to highlight the importance of thorough structural geological investigation prior to carrying out independent AMS studies, especially for complex structural domains.

References:

Borradaile, G.J., Henry, B., 1997. Tectonic applications of the magnetic susceptibility and its anisotropy. Earth Sci. Rev. 42, 49–93.

Ferré, E.C., Gébelin, A., Till, J.L., Sassier, C., Burmeister, K.C., 2014. Deformation and magnetic fabrics in ductile shear zones: a review. Tectonophysics 629, 179–188.

Tarling, D.H., Hrouda, F. 1993. The Magnetic Anistropy of Rocks. Chapman and Hall London. 217 p.

Sayab, M., Miettinen, A., Aerden, D., Karell, F. 2017. Orthogonal switching of AMS axes during type-2 fold interference: Insights from integrated X-ray computed tomography, AMS and 3D petrography. Journal of Structural Geology 103, 1-16

KOSE - Koillismaa Seismix Exploration survey: Details and first results

G. Gislason[1], S. Heinonen[1], J. Konnunaho[1], K. Moisio[2], J. Nevalainen[2] and H. Salmirinne[1]

[1]Geological Survey of Finland, P.O. Box 96, FI-02151 Espoo, Finland
[2]Oulu Mining School, University of Oulu, Oulu, Finland

E-mail: gardar.gislason@gtk.fi

We acquired 2D seismic reflection data in Koillismaa, Finland in April, 2018. The survey took 7 working days and spanned 8.5 km seismic line across an unknown buried gravity/magnetic anomaly, between the western intrusions and the eastern Näränkävaara intrusion, within the Koillismaa Layered Intrusion Complex. The aim of the survey was to estimate the depth and dip of the geological feature causing the anomaly. The seismic data was acquired using wireless receivers with 20 m spacing and a dynamite source with 40 m spacing. The Koillismaa seismic data show heavily varying traveltimes of adjacent traces, due to near-surface conditions such as thickness of snow, frost and characteristics of the overburden. In the pre-stack processed data there are clear reflectors visible, which encourages future processing efforts.

Keywords: seismic reflection profiling, upper crust, mineral potential, Koillismaa

1. Introduction

Presently, a significant part of the mineral resources of the European Union is located in Finland, within the Fennoscandian shield. Throughout its history, GTK has evaluated ore potential related to orthomagmatic Ni-Cu-PGE-Co and V-Ti-Fe-Cr deposits across the country. As a part of this activity, GTK's current, nationwide, Ni-Cu-Co mineral potential project (2016-2018) is focused on poorly explored areas and produces new geodata from prospective areas using modern exploration methods as deep penetrating geophysical surveys (e.g., seismic methods).

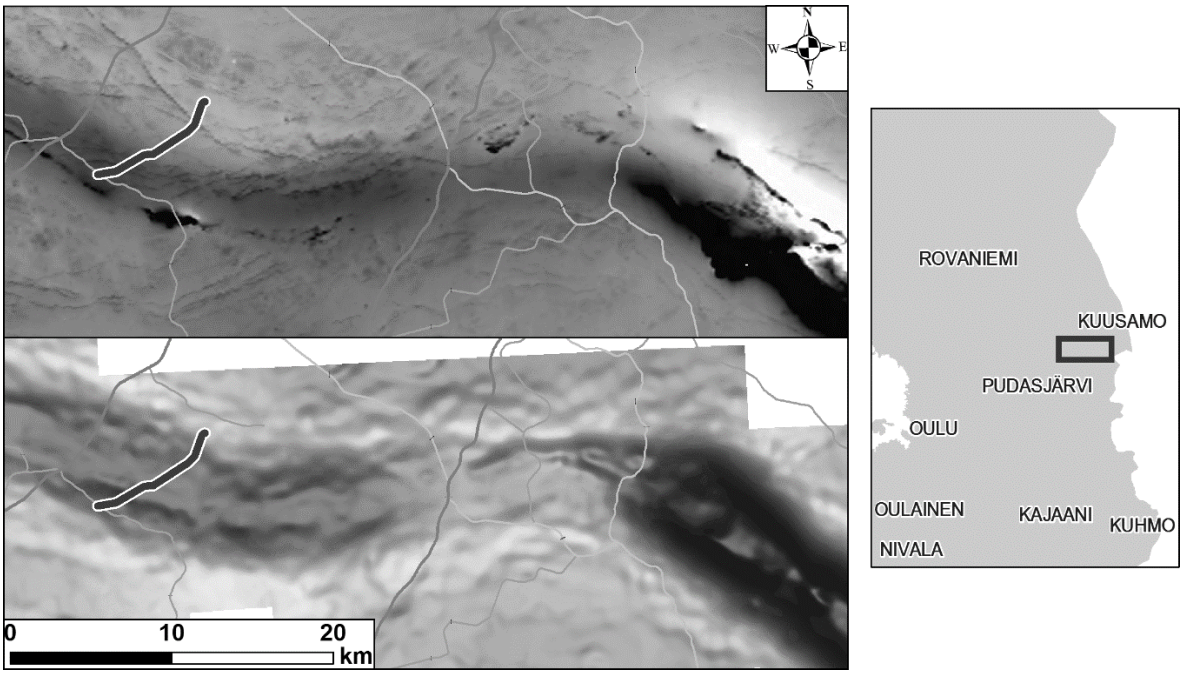

Figure 3. Magnetic (top) and Bouguer anomaly (bottom) maps of the survey site where white and black are low and high values, respectively. The Bouguer map has values from -33 to 23 mgal. The lighter lines are roads and the seismic survey line is shown in dark grey with a white stroke.

Many 2.45 to 2.5 Ga mafic-ultramafic layered intrusions in Finland host significant PGE-Ni-Cu and V-Ti-Fe-V deposits such as Suhanko, Koillismaa, Koitelainen and Akanvaara (Iljina et al. 2015). Based on the ore potential of these intrusions, GTK has carried out a seismic survey in the Koillismaa area, located in north-eastern Finland, around 100 km south of the Arctic Circle. It belongs to a discontinuous layered intrusion belt, about 300 km in length, which begins in Tornio and continues eastwards via Penikat and Koillismaa to Näränkävaara and from there into Russia.

A seismic survey was carried out across ca. 50 km long and ca. 5 km wide gravity and magnetic anomaly between the western intrusions and the eastern Näränkävaara intrusion within the Koillismaa Layered Intrusion Complex (Figure 1). Based on speculation around the anomaly, it is thought to be an Archean greenstone belt or a feeder channel for Koillismaa layered intrusions. Reflection seismics is expected to shed light in to the nature of the anomaly source.

Previous interpretations of the Bouguer gravity anomalies suggest a dyke intrusion of about 2.5 – 4 km width and a depth to the top part around 1 – 2 km. Koillismaa Seismic Exploration (KOSE) survey was aimed to estimate the depth and dip of this hypothesised dyke intrusion.

2. Survey and data acquisition

The KOSE 2D seismic reflection data were acquired during 7 working days in April, 2018. The survey was a collaboration between GTK, which provided manpower and a seismic source (dynamite), and Oulu Mining School, which provided receivers (Figure 2a) and manpower. The receivers used in the KOSE survey were wireless Sercel Unites. With a combination of 55 1C receivers and 35 3C receivers, making a total of 90 receivers, a roll-on split spread configuration was used. We sorted 1C and 3C stations together in a group of 18 (5 total groups) to achieve an even distribution of the geophones. With 10 meter receiver spacing, one spread was 1800 m and each roll was 360 m. Dynamite was used as a source and we acquired a total of 197 shot gathers with a source spacing of 40 m along an 8.5 km long line. Each source point was drilled to approximately 2 m depth. Because of thick snow coverage in the area, each receiver location was dug on the side of the road, with help of an excavator (Figure 2b).

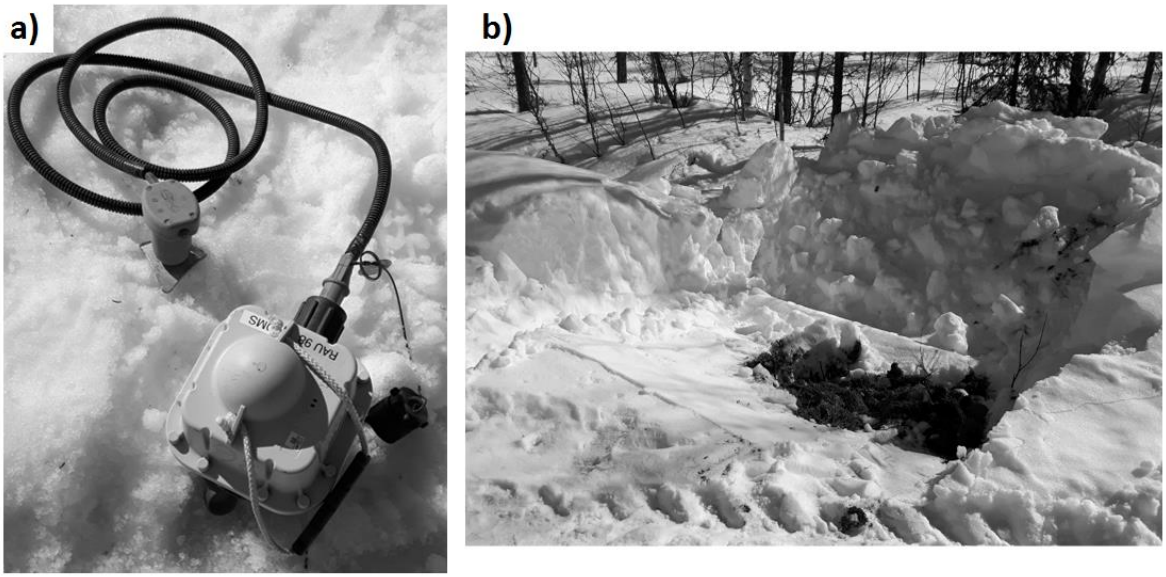

Figure 4. *a)* Wireless geophone and its data logger used in the survey. The 1C, 3C distribution was 1-3-1-1-3-1-1-3-1-1-3-1-3-1-1-3-1-3. *b)* Heavy snow was in the area and an excavator was used to dig for geophone locations.

The Sercel Unite receivers require a connection to GPS satellite in order to calibrate the internal clock and acquire the GPS coordinates of the data logger position. Besides triggering the

explosions, we used Seismic Source Boom Box to record exact GPS time of each explosion. Wireless receivers were recording continuously during the survey and we collected data loggers to the basecamp every evening for data harvesting. The correct data window was extracted from the receivers by using the GPS time measured with the Boom Box.

3. Data processing

The raw data (Figure 3a), show substantial delays in first breaks. With 20 m receiver spacing, the sudden delay or advance of adjacent traces, gives indication of highly varied velocity structures in the subsurface, namely in the overburden. Water saturated or frozen ground can also be a contributing factor to the nonlinear travel times. Time delays caused by the near surface variations mean that the later arrivals, such as reflections from the geological features of interest, will not stack coherently even if velocity field would be accurately determined. Thus, careful static corrections play crucial role in the processing of the Koillismaa seismic reflection data.

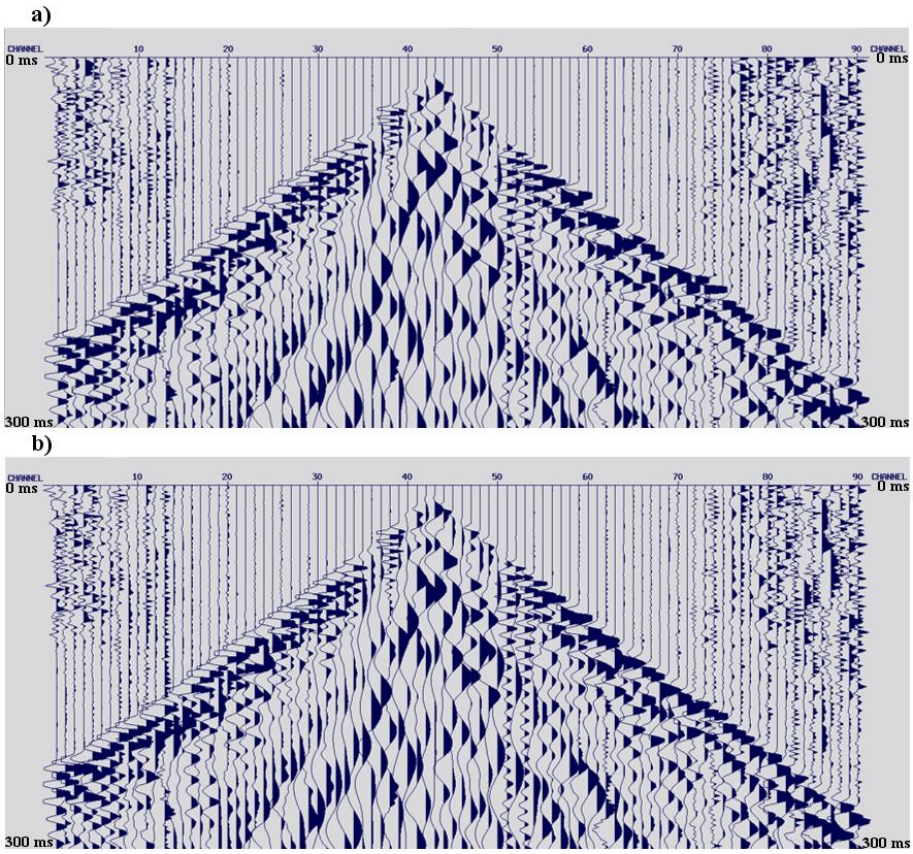

Figure 5: Raw wiggle plot of Shot #25 with a) AGC applied and b) AGC and statics applied. The plot goes from 0 to 300 ms TWT.

The first step of the data processing is picking first breaks, after which a starting model of the subsurface velocity variation is created. The subsurface model is iteratively modified according to the comparison between picked first arrivals and calculated arrivals based on the model and source-receiver locations. This refraction statics analysis is used to deliver the time shifts that are required to correct the data into one reference datum. In Figure 3, we show a raw shot gather before and after static corrections.

In Figure 4, the first 1000 ms TWT of shot #25 (same as in Figure 3) is shown. The raw data are completely overwhelmed by low frequency noise, airwaves and multiples. Using a bandpass filter of 40-45-275-300 Hz, airwave mute, spiking deconvolution, 3000 m/s median

filter, FK mute and a coherency filter, the signal-to-noise ratio of the data is substantially increased. In Figure 4b, around 400-550 m/s TWT, we can detect a couple of reflectors.

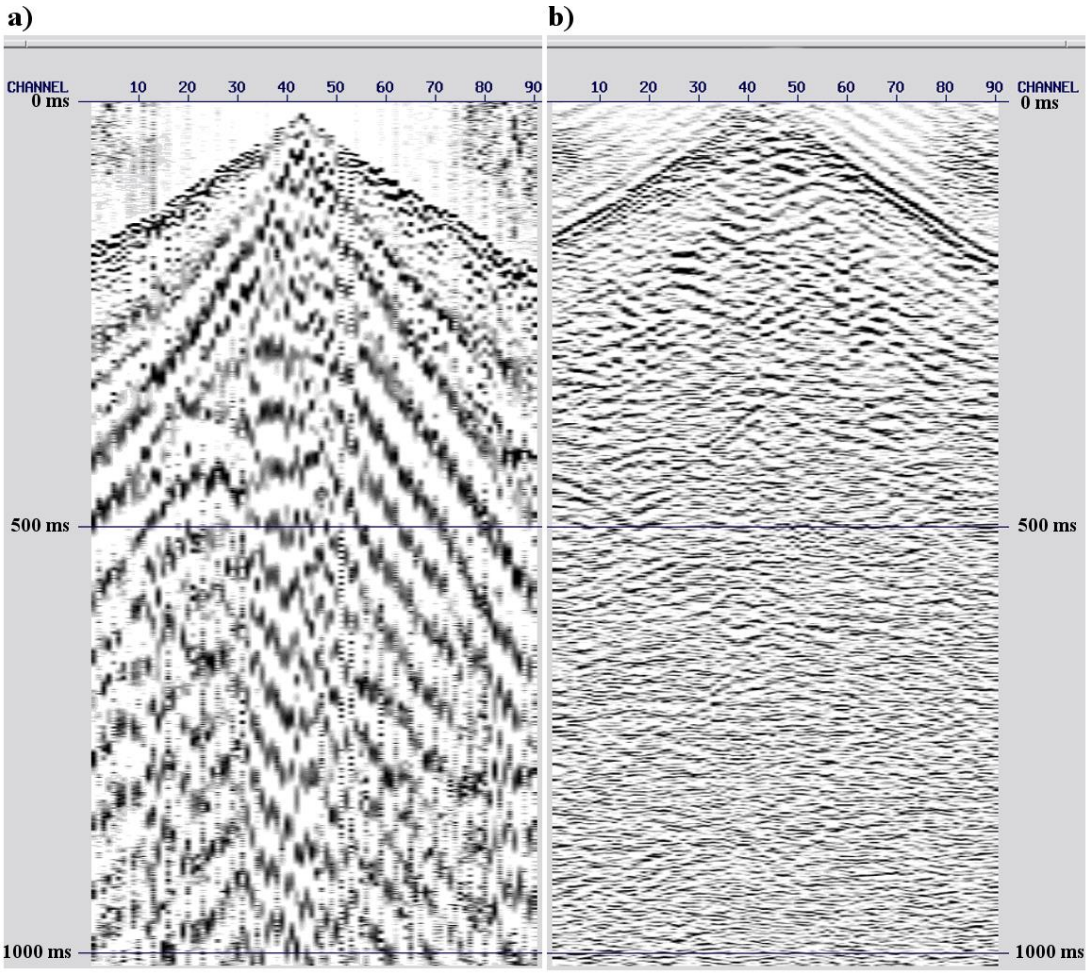

Figure 6: The first 1000 ms TWT of Shot #25; a) the raw data with AGC applied and b) pre-stack processed data.

4. Conclusion and future work

Geological Survey of Finland and Oulu University acquired seismic reflection data in Kuusamo during spring 2018. The data were acquired by using dynamite as sources at every 40 m and wireless receivers with 20 m spacing. The first insights into the 2D reflection data acquired from the KOSE project show, that, although the data are quite noisy, that reflectors are seen in the raw shot gathers which is encouraging for the future interpretation of the seismic profile.

References:

Iljina, M., Maier, W.D. and Karinen, T., 2015. PGE-(Cu-Ni) Deposits of the Tornio-Näränkävaara Belt of Intrusions (Portimo, Penikat, and Koillismaa) *in* Maier, D., Lahtinen, R., O'Brien, H.:Mineral Deposits of Finland, Elsevier, p. 133-164

Strain partitioning along the South American convergent margin between 42°S and 47°S: Insights from lineament analysis

P. L. Göllner, J. O. Eisermann and U. Riller

Institut für Geologie, Universität Hamburg, Bundesstraße 55, 20146 Hamburg
E-mail: paul.leon.goellner@uni-hamburg.de

We present a novel model for strain partitioning in the Southern Andes. Based on reassessment of structural and thermochronological data and identification of new lineaments, we highlight the complexity of intra-arc deformation in this area. The Southern Andes have previously been interpreted as a prime example for strain partitioning in the upper plate of a subduction system that is characterized by oblique plate convergence. In this system, the Liquiñe-Ofqui Fault Zone (LOFZ) is interpreted as the master fault accommodating chiefly margin-parallel slip. Our study highlights the importance of vertical displacements on the LOFZ and other major faults and the distribution of transpressive deformation across the entire width of the Southern Andes. Collectively, these results question the importance previously assigned to the LOFZ in terms of strain partitioning.

Keywords: strain partitioning, crustal deformation, Southern Andes

1. Introduction

The partitioning of strain at convergent margins into a margin-normal and margin-parallel components is a well-documented phenomenon at obliquely convergent plate boundaries. In such tectonic settings, margin-parallel slip is thought to be accommodated by large intra-arc shear zones, such as the Liquiñe-Ofqui Fault Zone (LOFZ) in the Southern Andes.

The LOFZ cuts the Patagonian Batholith and the modern Andean volcanic arc along-strike for more than 1000 km. Northward displacement of the Chiloé Block, a detached forearc sliver, points to an overall dextral displacement on the LOFZ, corresponding to the angle of convergence. In the context of the tectonic framework, which is based on limited ground truth, the LOFZ is commonly regarded as a vertically dipping, narrow fault zone composed of two NNE-trending lineaments connected through a number of step-over faults. In this study, we highlight the complexity of strain partitioning in the Southern Andes and discuss the role of the LOFZ in the tectonic setting by means of detailed lineament analysis in combination with a compilation of published kinematic and thermochronological data.

2. Methods

ASTER GDEM 2 high-resolution digital elevation models (DEMs) with 30m horizontal and 1m vertical resolution form the base for our lineament analysis. DEMs were processed into shaded relief models, drainage models and aspect maps from which the lineaments were extracted. Apatite fission track data, compiled by Thompson et al. (2010) were used to calculate exhumation rates following the method by Thompson (2002). Exhumation rates were subsequently interpolated using an inverse distance weighting method. Where the coverage of fission track data was sufficiently high, lineaments were taken as barriers in the interpolation to enhance gradients in the interpolation.

3. Results

Between 42° S and 47° S, DEM-analysis reveals a network of interconnected lineaments trending predominantly N-S, NE-SW, and NW-SE. A number of these lineaments display mutual offsets. Apatite fission track data show enhanced exhumation in the central cordillera where drastic changes in exhumation rate spatially coincide with the intersection of lineaments. Here, individual fault-bound blocks display specific exhumation rates.

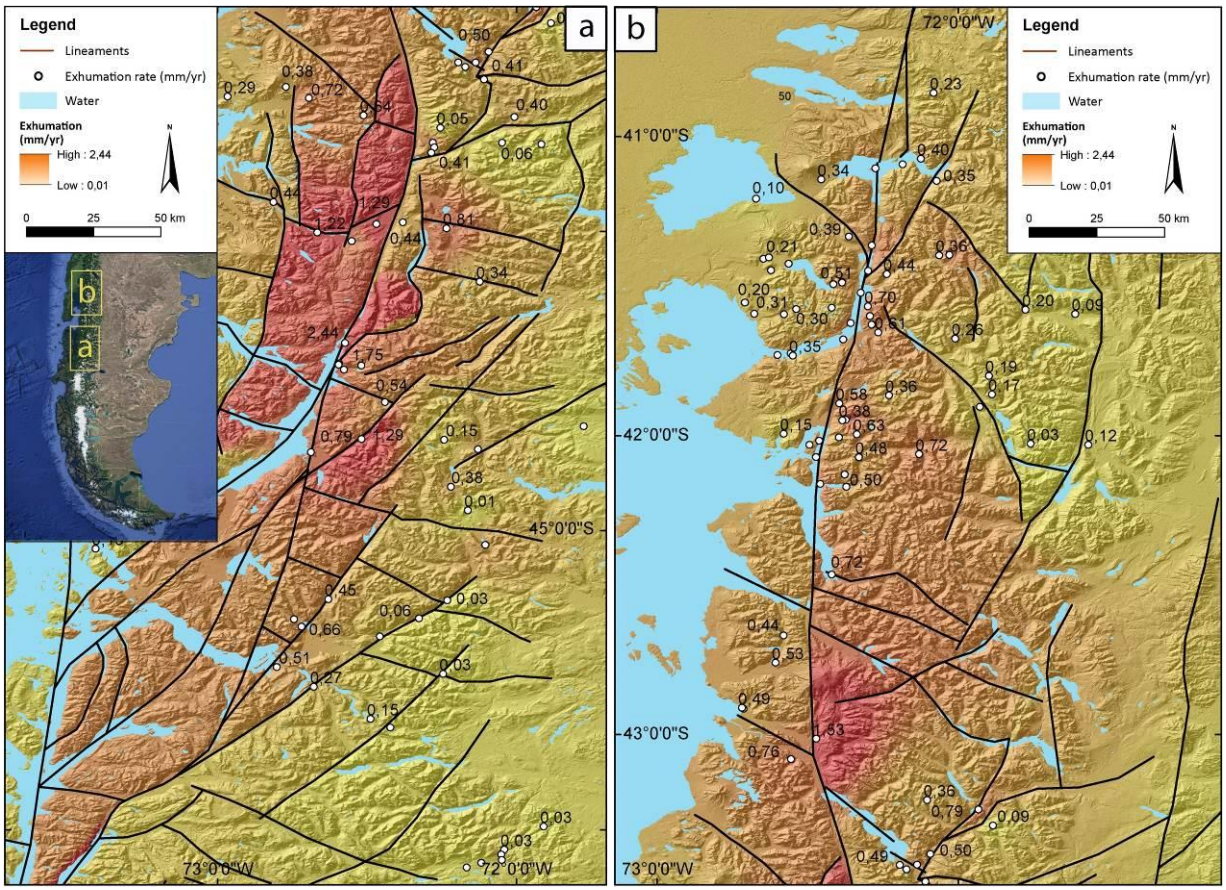

Figure 1. Interpolated exhumation rates and lineaments in the Southern Andean cordillera between (a) 43°S and 46°S and (b) between 43.5° and 40.5°S.

4. Discussion and Conclusion

In contrast to the pre-existing, rather crude structural and kinematic view on strain partitioning in the Southern Andes and the role of the LOFZ, our reassessment of thermochronological and structural data requires reconsideration of the intra-arc deformation. Most importantly, deformation appears to be distributed across the entire width of the Southern Andes and the fore-arc sliver is displaced on a network of structural discontinuities, rather than merely on the LOFZ. Moreover, variations in exhumation rates of individual fault-bound blocks call for significant vertical displacements during deformation. Collectively, the results question the simplicity of kinematic models of elastic strain partitioning.

5. References

Thompson, S.N., 2002. Late Cenozoic geomorphic and tectonic evolution of the Patagonian Andes between latitudes 42°S and 46°S: An appraisal based on fission-track results from the transpressional intra-arc Liquiñe-Ofqui fault zone, Geological Society of America Bulletin, 114, 1159-1173.

Thompson, S.N., Brandon, M.T., Tomkin, J.H., Reiners, P.W., Vásquez, C., Wilson, J., 2010. Glaciation as a destructive and constructive control on mountain building, Nature, 467, 313-317.

COGITO-MIN seismic reflection profiling for mineral exploration in Polvijärvi, Finland

S.Heinonen[1], M. Malinowski[2], G. Gislason[1], F. Hlousek[3], S. Buske[3] and E. Koivisto[4]

[1]Geological Survey of Finland, PO Box 96, 02151 Espoo, Finland
[2]Insitute of Geophysics, Polish Academy of Science, 64 Ksiecia Janusza St., 01-452 Warsaw, Poland
[3]Institute of Geophysics and Geoinformatics, TU Bergakademie Freiberg, Gustav-Zeuner-Str. 12, 09596 Freiberg, Germany
[4]Department of Geosciences and Geography, PO BPx 68, 00014 University of Helsinki, Finland
E-mail: suvi.heinonen@gtk.fi

The COGITO-MIN project acquired high-resolution seismic reflection profiles in the Kylylahti polymetallic mine area in the Outokumpu region, Finland. Acquisition was performed along two segmentally straight lines using both vibroseis and dynamite sources, and wireless receivers with 10 m spacing. The processing of these data poses typical challenges for hardrock environment such as need for static corrections due to varying overburden thickness and difficulty in suppressing source related noise. Final seismic images reveal steep reflectors that correlate with the black schist intercalations in the mica schist. The most obvious reflectors in the profiles are at 5-8 km depth attributed to mafic dykes on top of Archean basement rocks. Reflectivity around the known mineralization is prominent but discontinuous due to complex internal structure caused by folding and faulting.

Keywords: lithosphere, Fennoscandia, Kylylahti, massive sulphide, seismic exploration

1. Introduction

The COGITO-MIN (COst-effective Geophysical Imaging Techniques for supporting Ongoing MINeral exploration in Europe) project has been developing cost-effective seismic mineral exploration methods. The COGITO-MIN project is coordinated by the University of Helsinki and participated by both research institutions and industry partners from Finland and Poland (Geological Survey of Finland, Institute of Geophysics, Polish Academy of Sciences, Boliden, Vibrometric and Geopartner). One part of the project was to acquire two seismic reflection profiles in the Kylylahti polymetallic (Cu, Au, Zn, Co and Ni) sulphide mine area located within famous Outokumpu mining district in Finland in 2016. The acquisition of these data was encouraged by the positive results achieved in the HIRE project (High Resolution reflection seismics for ore exploration 2007-2010). Based on the HIRE data, Kukkonen et al. (2012) concluded that the ore-hosting rock association can be imaged with seismic methods as strongly reflective packages in the Outokumpu region.

2. Field data acquisition

The COGITO-MIN 2D seismic reflection data were acquired during two weeks in August-September 2016 using equipment owned by company Geopartner. Both seismic profiles were approximately 6 km long and had a fixed spread of Wireless Seismic RT2 10 Hz high sensitivity geophones spaced at 10 m interval. The receiver lines were deployed along segmentally straight lines in terrain varying from fields to forest, coppice and swamps. Despite the partly challenging terrain conditions, the telemetric data transmission between the receivers and recording van was working well and it was possible to harvest the data for QC purposes during the acquisition.

Two INOVA UniVib 9.5-ton trucks were used as seismic sources. Vibroseis sources were used along the roads with a 16-s long linear upsweep from 4 to 220 Hz. Vibroseis trucks could not access some parts of the seismic profiles and thus it was necessary to use dynamite explosions to fill the gaps that non-existing roads would have caused to the source coverage. The charge size used was 120 g or 240, depending of the terrain condition. Explosions were fired in about 2 m deep shot holes. Some gaps caused by the infrastructure (safety distance 50 m), rivers and lakes

were unavoidable to otherwise uniform 20 m source spacing. Both seismic sources performed well and clear first break energy is visible over the whole offset range.

3. Geology of the Kylylahti sulphide deposit

The Kylylahti sulfide deposit is located within the North Karelia Schist Belt east of the suture zone between the Archean Karelian craton and the Paleoproterozoic Svecofennian island arc complex (Gaal et al., 1975). The dominant rock type of the area is mica schist that has black schist intercalations (Figure 1). The massive sulfide deposits of the region are associated with variably sized fragments and lenses of serpentinized mantle peridotites that have been tectonically emplaced upon and within younger metasediments (Koistinen, 1981). The ore-hosting serpentinized mantle peridotites and other Outokumpu assemblage rocks are typically enclosed within black schists. According to a petrophysical study by Luhta (2018), black schists containing high levels of sulfide have high acoustic impedances compared to surrounding mica schists making them a plausible target for seismic imaging.

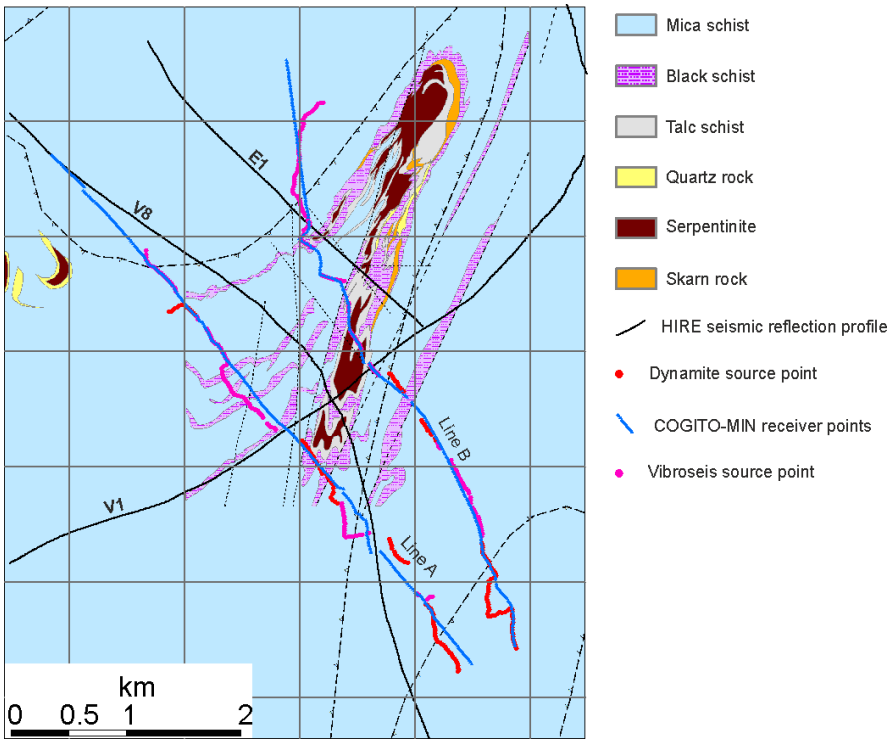

Figure 1. The COGITO-MIN seismic reflection profiling was done along two parallel profiles approximately perpendicular to the known Kylylahti massive sulfide deposit and intersecting the seismic reflection profiles acquired in the area during the HIRE project. © Bedrock of Finland –DigiKP

4. Data processing

The time processing of the COGITO-MIN data followed the procedure presented in Heinonen et al. (2018). We tested three different imaging strategies in order to acquire as good image of the subsurface reflectivity as possible. These approaches are (1) DMO followed by post-stack migration (Figure 2a), (2) pre-stack time migration with the same velocities as used for the DMO (Figure 2b) and (3) pre-stack depth migration with the Fresnel Volume migration (FVM) technique (Buske et al., 2009; Hlousek et al., 2015) using constant velocity. Unlike (1) and (2), the FVM was calculated in a 3D volume taking true source and receiver locations into account. The dimensions of the migration volume are larger than the actual profile length in order to preserve the reflection energy originating from the dipping features outside of the receiver line.

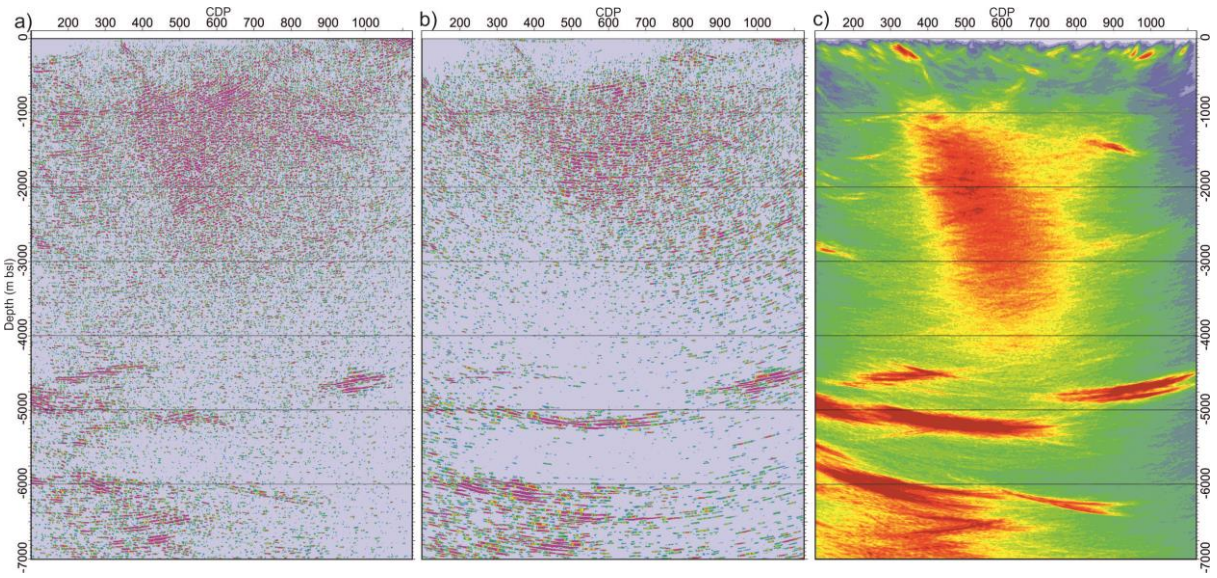

Figure 2. Comparison of results from different data imaging approaches: (a) DMO + post-stack time migration (b) pre-stack time migration and (c) coherency based Fresnel volume pre-stack depth migration along the COGITO-MIN reflection profile A.

5. Results

One of the most apparent feature in the COGITO-MIN seismic reflection data are the prominent reflectors at 5 to 8 km depth that can be mapped all over the Outokumpu area with the network of previously acquired HIRE seismic reflection profiles. According to Heinonen et al. (2016), these reflectors likely result from amphibolite dykes in the Archean basement. Seismic images in the vicinity of the known Kylylahti massive sulphide deposit are characterized by prominent but discontinuous reflectivity. This reflectivity has been attributed to the steep folding and frequent lithological changes of the Outokumpu assemblage rocks in the Kylylahti area. Additionally, large thrust faults interpreted from aerogeophysical maps and geological surface observations are making the general reflectivity pattern to appear fairly complex.

In the COGITO-MIN data, steep reflectors in the shallow (<500 m) part of the seismic sections are imaged especially clear in FVM migration result (Figure 2c). These features are not imaged in the previously acquired HIRE seismic reflection profiles. Steep reflectors are correlating with black schist interlayers within otherwise mica schist dominating geological environment. Kukkonen et al. (2012) interpreted similar clearly defined, rather thin but more moderately dipping reflectors to originate from the old fault zones that have been lubricated by the black schists.

7. Conclusions

The seismic reflection profiles acquired within the COGITO-MIN project provide new insight to the deep geology of the Kylylahti polymetallic mine area in the Outokumpu region, Finland. Usage of wireless geophones and both vibroseis and explosive sources enabled acquisition of high quality data set in challenging terrain. The overall features of the seismic reflection images are similar in post- and pre-stack time migrated seismic data, while pre-stack depth migration algorithm is most clearly imaging the steeply dipping reflectors.

Acknowledgements

The COGITO-MIN project has been funded through the ERA-MIN network. At the national level, the funding comes from Tekes in Finland and the NCBR in Poland. Leica Geosystems Oy is thanked for providing their SmartNet for the project use.
*COGITO-MIN Working Group: M. Chamarczuk, C. Cosma, N. Enescu, G. Gislason, S. Heinonen, S. Juurela, E. Koivisto, K. Komminaho, T. Luhta, M. Malinowski, S. Mertanen, S. Niemi, M. Riedel, B. Singh, L. Sito, A. Taipale, T. Törmälehto, K. Vaittinen, S. Väkevä, M. Wojdyla.

References:

Buske, S., Gutjahr, S. and Sick, S., 2009. Fresnel volume migration of single-component seismic data. Geophysics 74(6), WCA47-WCA55.

Bedrock of Finland - DigiKP. Digital map database [Electronic resource]. Espoo: Geological Survey of Finland [referred 12.04.2018]. Version 2.1.

Gaal, G., Koistinen, T., and Mattila, E. 1975, Tectonics and stratigraphy of the vicinity of Outokumpu, North Karelia, Finland. Including a structural analysis of the Outokumpu ore deposit. Geological Survey of Finland, Bulletin - Bulletin de la Commission Géologique de Finlande, 271.

Heinonen, S., Kontinen, A., Leväniemi, H., Lahti, I., Junno, N., Kurimo, M. and Koivisto, E., 2016, Sukkulansalo National Test Line in Outokumpu: A ground reference for deep exploration methods in Aatos, S. (ed.) Developing Mining Camp Exploration Concepts & Technologies – Brownfield Exploration Project 2013-2016. Geological Survey of Finland, Special Paper, 59, 163-188.

Heinonen, S., Malinowski, M., Hlousek, F., Gislason, G., Koivisto, E., Buske, S., and the COGITO-MIN Working Group, 2018. Seismic Exploration in the Kylylahti Cu-Au-Zn Mining Area: Comparison of Time and Depth Imaging Approaches. Near Surface Geoscience 2018 Conference and Exhibition, 9-12 September 2018, Porto, Portugal.

Hlousek, F., Hellwig, O., Buske, S., 2015, Improved structural characterization of the Earth's Crust at the German Continental Deep Drilling Site (KTB) using advanced seismic imaging techniques. Journal of Geophysical Research (Solid Earth), 10.1002/2015JB012330.

Koistinen, T.J., 1981, Structural evolution of an early Proterozoic stratabound Cu–Co–Zn deposit, Outokumpu, Finland. Transactions of the Royal Society of Edinburgh. Earth Sciences 72, 115–158.

Kontinen, A., Peltonen, P. and Huhma, H., 2006, Description and genetic modelling of the Outokumpu-type rock assemblage and associated sulphide deposits. Final technical report for GEOMEX JV, Workspackage Geology. Geological Survey of Finland report M10.4/2006/1.

Kukkonen, I.T., Heinonen, S., Heikkinen, P.J. and Sorjonen-Ward, P., 2012, Delineating ophiolite-derived host rocks of massive sulfide Cu-Co-Zn deposits with 2D high-resolution seismic reflection data in Outokumpu, Finland. Geophysics, 77, WC213-WC222.

Luhta, T., 2018. Petrophysical properties of the Kylylahti Cu-Au-Zn sulphide mineralization and its host rocks. Master's thesis, University of Helsinki.

Peltonen, P., Kontinen, A., Huhma, H., and Kuronen, U. 2008, Outokumpu revisited: New mineral deposit model for the mantle peridotite-associated Cu-Co-Zn-Ni-Ag-Au sulphide deposits. Ore Geology Reviews, 33, 559-617.

Economical aspect of meteorite impact craters in Fennoscandia and Baltic countries

Satu Hietala[1], Jüri Plado[2], and Lauri J. Pesonen[3]

[1]Geological Survey of Finland, P.O. Box 1237, Neulaniementie 5, FI-70211 Kuopio, Finland
[2]Department of Geology, University of Tartu, Ravila 14A, 50411 Tartu, Estonia
[3]Solid Earth Geophysics Laboratory, Physics Department, University of Helsinki, P.O. Box 64, Gustaf Hällströminkatu 2, FI-00014 Helsinki, Finland
E-mail: satu.hietala@gtk.fi

The impact crater research is a young science compared to traditional geological research but developing constantly and receiving increasing international attention. New structures are found in each year from Earth. Impact structures can host significant economic resources such as metal ore deposits, industrial material, water and gas reservoirs. In Finland and the Baltic countries, these deposits have hardly been studied in terms of economy but they may include impact collision related reserves and provide indications of regional changes in bedrock.

Keywords: impact structure, lithosphere, economic geology

1. Introduction

Cosmic collisions leave always traces even if the projectile itself is destroyed during the event. Changes in bedrock induced by impact take place at much higher temperatures and pressures than the conventional geological processes, such as volcanic activity or plate tectonics. In the small projectile cases the changes in the upper crust are local, but in the cases of huge events, the depth effects can significantly deform the crust and even the upper mantle, and contribute to the formation of economic deposits of various types. Several large meteorite impact structures throughout the world host mineral resources that are either currently mined or have the potential to become important economic ore resources in the future. Economic resources can be divided to metallic ores (Ni, Cu, Co, PGE, Au, Pb-Zn), energy resources (uranium, hydrocarbons, phosphorite), industrial materials (impact diamonds, bentonite, zeolite, bauxite, building stones, limestone), water resources (large water reservoirs, hydropower), gemstones (e.g. agate) and also educational and recreational benefits such as museums (Masaitis 1992, Grieve 2005, Pesonen et al. 1999, Reimold et al. 2005). According to Reimold et al. (2005) 55 of the existing impact structures include various types of economic deposits and 12% of them are actively exploited.

2. Economical aspects of meteorite impact craters in Fennoscandia and Baltic countries

On Earth, there are 190 confirmed impact structures which are distributed unevenly around the globe. The Fennoscandian Shield houses 16.8% of them. From the 42 impact structures in Europe (Earth Impact Database 2018), 32 are located in Fennoscandia and Baltic countries (Fig. 1).

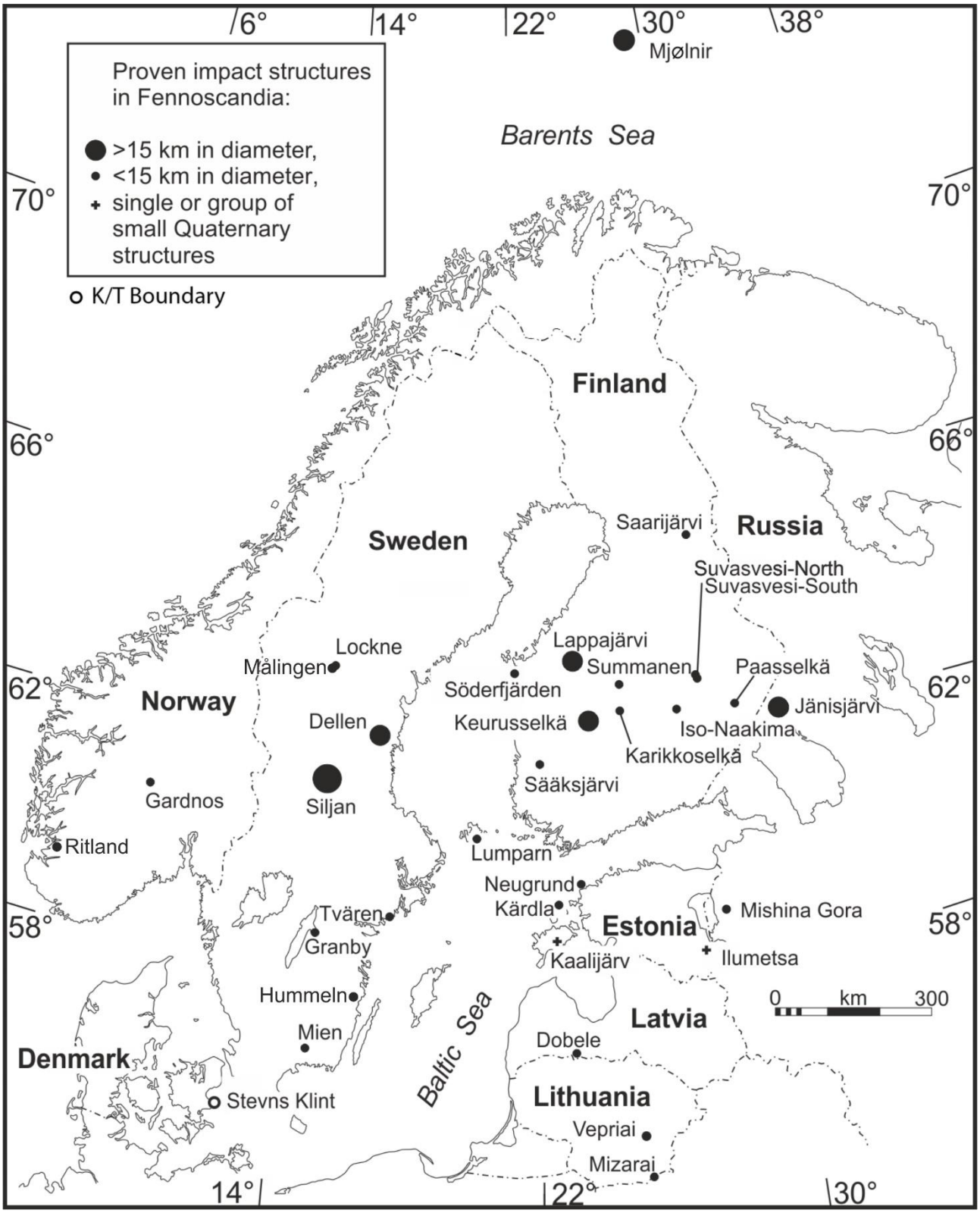

Figure 1. Proven impact structures in Fennoscandia and Baltic countries.

Economically potential impact structures Fennoscandia and Baltic countries are listed in Table 1. Most of them are utilized as tourism targets although other economic benefits could be more important and more diverse. For example, minor ore mineralizations could be impact related, like in Paasselkä (Pesonen et al. 1999), Kärdla (Suuroja 2002), Siljan (Johansson 1984), Lumparn (Bergman & Lindberg 1979) and Lockne (Sundblad 1994) structures. According to Abels et al. (2002) sulphide mineralizations of the Paasselkä could be progenetic, i.e deposits that have

already existed but may have become accessible as a direct result of the impact processes. Also, the Keurusselkä impact structure is associated with sulphidization but its economic relevance has not been studied yet. It has also been suggested that the uranium enrichment in Eastern Finland would be the result of an ancient asteroidal collision (O. Äikäs 2012, pers. comm.).

By studying impact structures, even if they don't host any economically valuable deposit, they can give important information identifying impact induced hydrothermal events which post-date the cratonization of Precambrian shields (Abels et al. 2002). For example in Kärdla, Lockne, Siljan, and Lumparn sandstones occur minor amounts of galena that are enriched in radiogenic lead which reflects remobilization of pre-impact ore and subsequent fractionation of lead isotopes via impact-induced hydrothermal activity or Caledonian fluidal activity (Eensaar et al. 2017). In Iso-Naakkima impact structure, the kaolin deposit occurs on the bottom of the crater, on top of the fragmented bedrock and could be related to post-impact hydrothermal fluids. Hydrothermal fluids have also been involved when Sääksjärvi impact agates (used as gemstones) have been crystallized. Sääksjärvi agates have crystallized in the gas vesicles of the "volcanic-like", impact melt rock less than 560 million years ago. Discovering agates could indicate the existence of a not yet found impact structure in Precambrian shield, notably if they lack younger volcanic rocks (Kinnunen and Lindqvist 1998).

Gardnos crater in Norway host impact breccia that has been exploited as decorative art stone. In Lappajärvi, impact melt rock has been used as a decorative and building stone. In addition, Lappajärvi has several other topics related to economic factors, for example, groundwater, industrial minerals like impact diamonds and zeolite-group minerals and gemstones. Lappajärvi is also an excellent tourist attraction place and especially suitable for "outdoor classroom" regarding educational items.

On an industrial scale a significant clay rock layer has been found in Saarijärvi crater and it has been estimated that under the lake is at least 100 million tones clay rock (Hyyppä and Pekkala 1987). The Lumparn structure in Aland host an economical limestone deposit but not used industrially.

Neugrund low is planned to be used as a base for marine windmills. Kärdla has as a source of mineral water and its central flatland is used for agricultural purposes: this is the case also in Söderfjärden, western Finland. Kaali crater in Estonia is a touristic site with tens of thousands visitors yearly. Tourism applies also to Ilumetsa and Söderfjärden. The buried Latvian and Lithuanian craters provide drinking water.

3. Conclusions

Economic deposits associated with Fennoscandian and Baltic meteorite impact craters are localized. Fennoscandia lacks large Vredefort- or Sudbury-sized impact structures where the post-impact hydrothermal systems have had potential to redistribute metals. Also, there are no hydrocarbon accumulations known from Fennoscandian craters. However, there are several economic benefits that impact structures are used for local or regional purposes. The Fennoscandian and Baltic countries impact structures should study better. Any summary has not yet been made of these existing and potential economic benefits.

Table 1. Economically important impact craters in Fennoscandia and Baltic countries.

Crater name	Long.	Lat.	Country	Diameter (km)	Age (Ma)	Economic interest
Lappajärvi	63°12'N	23°42'E	Finland	23	77.8 ±1.1	Summer and winter sport, education/recreation, tourism, dimension stone
Sääksjärvi	61°24'N	22°24'E	Finland	6	*ca.* 560	Agate (boulders), recreation (summer/winter sport)
Neugrund	59° 20'N	23°40'E	Estonia	8	~ 535	Energy (possible platform for windmills)
Kärdla	59° 1'N	22° 46'E	Estonia	4	~ 455	Mineral water, agricultural purposes, hydrothermal mineralization
Kaali	58° 24'N	22° 40'N	Estonia	0.11	0.0035	Tourism, education, archaeology
Ilumetsa	57° 58'N	27° 25'E	Estonia	0.08	0.0066	Tourism
Dellen	61°48'N	16°48'E	Sweden	19	89.0±2.7	Summer/winter sport, hydropower reservoir
Siljan	61°02'N	14°52'E	Sweden	65	362±1	Hydrocarbon, Pb-Zn sulphidization, winter sport
Gardnos	60°39'N	09°00'E	Norway	5	500±10	Gardnos Breccia (decorative arts)
Vepriai	55°05'N	24°35'E	Lithuania	8	160±10	Water reservoir
Dobele	56° 35'N	23° 15'E	Latvia	4.5	290 ± 35	Water reservoir

References

Abels, A., Plado, J., Pesonen L. J., Lehtinen M., 2002. The impact cratering record of Fennoscandia— A close look at the database. In Impacts in Precambrian shields. Plado J.,Pesonen L. J. (eds.) Berlin, Heidelberg: Springer. 1–58.

Bergman L., Lindberg B. 1979. Phanerozoic veins of galena in the Åland rapakivi area, southwestern Finland. Bulletin of the Geological Society of Finland, 51, 55-62.

Eensaar, J., Gaškov, M., Pani, T., Sepp, H., Somelar, P., Kirsimäe, K., 2017. Hydrothermal fracture mineralization in the stable cratonic northern part of the Baltic Paleobasin: sphalerite fluid inclusion evidence. GFF, 139, 52-62.

Grieve, R.A.F., 2005. Economic natural resource deposits at terrestrial impact structures. Geological Society, London, Special Publications, 248, 1-29.

Hyyppä J., Pekkala Y. 1987. Tutkimustyöselostus Taivalkosken kunnassa valtausalueilla Saarijärvi 1-3 (kaiv.rek.nro 3156/1-3) suoritetuista savikivitutkimuksista. Report M 06/3533/-87/1/89. Espoo: Geological Survey of Finland. In Finnish.

Johansson, Å, 1984. Geochemical studies on the Boda Pb-Zn deposit in the Siljan astrobleme, central Sweden. Geologiska Föreningens i Stockholm Förhandlingar, 106, 15-25.

Kinnunen K.A, Lindqvist K. 1998. Agate as an indicator of impact structures: An example from Sääksjärvi, Finland. Meteoritics & Planetary Science 33: 7-12

Masaitis V.L. 1992. Impact craters: Are they useful? Meteoritics 27, 21-27. Meteoritical Society, 1992, printed in USA.

Pesonen, L.J. Lahti, M., & Kinnunen, K.A. 1999. Meteorite impact structures, their economic importance and the role of geophysics. Extended Abstract Book: EAGE 61st Conference and Technical Exhibition, Helsinki, Finland. 1999.

Reimold W.U., Koeberl C., Gibson R. L. & Dressler B. O. 2005. Economic Mineral Deposits in Impact Structures: A Review. In: Koeberl C & Henkel H. 2006. Impact Tectonics, pp.479-552. Springer Science & Business Media, 27.1.2006 – 552p.

Sundblad K. 1994. Lead isotopic composition of galena associated with the Early Paleozoic meteorite impact structures at Lockne (Sweden) and Kärdla (Estonia) [abs]. In: Törnberg R (ed) 2nd International ESF workshop: The Identification and Characterization of Impacts, Lockne, Sweden, 1 p.

Suuroja K. 2002. Natural resources of the Kärdla impact structure, Hiiumaa Island, Estonia. In Plado J., Pesonen L.J. (eds) Impacts in Precambrian Shields, Springer, Berlin, 295-306.

Underground muography: The raise of geoparticle physics as a soil, orebody and rock realm imaging method

M. Holma[1,2] and P. Kuusiniemi[1,2]

[1]Muon Solutions Oy, Rakkarinne 9, 96900 Saarenkylä, Finland
[2]Arctic Planetary Science Institute, Lihtaajantie 1 E 27, 44150 Äänekoski, Finland
E-mail: marko.holma@muon-solutions.com

In the present work we explain a novel method to study soil layers, rock bodies, structures and overburdens. The method is called muography and it can be applied for any density variation study. The method is based on cosmic-ray induced muons that are produced in the upper part of Earth's atmosphere and which can penetrate deep underground. Muons can be employed to draw density variation data as they penetrate easier low density materials than those of high density. The difference is observed as the smaller or larger number of detected muons through the material under investigation.

Keywords: geoparticle physics, geophysics, cosmic rays, muons, muography, muon radiography, muon tomography, muon geotomography, detectors, imaging, density, gravity, boreholes, upper crust

1. Introduction

The crust of the Earth can be studied geophysically in many ways. Traditional methods such as various magnetic, electromagnetic, radiometric and gravimetric methods have witnessed gradual development for ever increasing sophistication and accuracy over the years. Many methods have successfully been lifted to wings, most recently by remote controlled single-aircraft drones or even large drone swarms. No wonder, hence, that the range of available geophysical exploration methods is now wider than ever before.

In all traditional methods that are based on classical physics the survey equipment can deliver only as good accuracy as the related survey instruments are designed for: the greatest details in the media under investigation are observed by instruments of whose designed specs have been specially honed for this purpose. In other words, continuing collecting data after a successful survey does not anymore increase resolution after a certain point. This is not the case in muography, an emerging state-of-the-art technique to map density variations in solid materials such as rock. *Muography* (Tanaka et al., 2009), also known as *muon radiography*, *muon tomography* and *muon geotomography*, does not belong to the family of traditional geophysical survey methods. Instead, it represents a technique that has more common with space and particle sciences than methods based on fundamental forces like magnetism, electricity, electromagnetism and gravity. Muography represents particle physics or more precisely geoparticle physics (particles interacting with the solid Earth) applied to geology. Nevertheless, from a geoscientific point of view it is just a new method to the wide range of available geophysical methods.

Similar to the gravity method, muography is a passive, non-destructive geophysical technique. Muography is based on detection of cosmic-ray induced muon particles after they have passed through the studied object. The muon flux per unit time carry important information about the average density of the material the particles passed through. If the muon detector is relocated from one place to another, objects such as geological rock bodies can be visualised from multiple directions. The picture is heavily based on the statistical methods. If the number of muons that reach the instrument is handled with dedicated algorithms, specialised particle physics methods can be applied to translate the statistical data into informative density variation maps of otherwise impenetrable rock body. In this work we describe how crystalline bedrock or soil layers can be studied employing muography.

2. History and future of muography

The use of muons for transilluminating solid objects is not by any means a new surveying method. In fact, the first pioneering experiments were carried out already in the late 1960s when Luiz Alvarez studied with his team the Belzoni chamber of the Chephren pyramid in Egypt. Muography has been used occasionally in archaeology ever after, but other applications have been rare. However, the advancements in high energy physics and particle detection during the last 15 years have assisted to unlock the potential of muography, subsequently leading to a vast range of new applications. At the same time rapidly increasing computing capabilities have led to better simulation models. Furthermore, technological development in the last decades has made it possible to design muon detection systems that are smaller than traditional systems.

The history of muography in geoscientific studies is relatively short and has so far been dominated by *surface muography*. The rapid development of the muographic imaging technologies and interpretations algorithms has gradually increased studies both in numbers and variation, and surface muography has led to *underground muography*. Surface and underground muography has now been used for example in volcano studies, fault studies and ore exploration.

There are currently at least five major driving forces that promote further use and development of muographic imaging in geosciences. First, technology is getting smaller in physical size due to general miniaturisation of technology. Second, computing power is still increasing rapidly. Third, the more muography is used in geosciences (and especially to study different types of geological challenges) the more developed and efficient the interpretation algorithms become. Fourth, more studies will lead better understanding and subsequently to better forward modelling skills. Fifth, exploration is going deeper and new discoveries are harder to make, which mean that all new methods and tools that can assist exploration are welcomed.

3. Physical principles of muography

Cosmic rays consist of high-energy particles originating mainly outside of our Solar System. These particles constantly interact with the Earth's atmosphere producing showers of secondary particles. The latter particles are electrons, gamma-rays, pions and muons (etc.), and some reach the Earth's surface. Astonishingly, regardless of energies sometimes beyond any man-made accelerator only muons and neutrinos penetrate for more than just a few meters beneath solid material, be it soil, rock or concrete. While neutrinos are difficult to detect (they can easily penetrate the Earth and billions of them pass through us every single second) muons are not. This is due to its large mass since even if the muon is very similar to an easily detected electron its mass is approximately 207 times larger than that of an electron. On ground the muon rate is approximately 150 muons per square meter every second. The number reduces significantly underground but even at 1 km of rock the number is still approximately 2 per hour. Meanwhile, the rate of neutrinos remains constant at any given depth.

While relatively small objects (up to a meter in diameter) can be transilluminated by using, e.g., X-rays, deeper penetration is needed for transilluminating large-scale objects (tens to hundreds of meters). The very high energies needed to achieve the latter are often out of reach of artificial sources. Therefore we have to rely on natural sources like muon radiation. Indeed, the heavy mass and high-energetic nature of muons makes them ideal carriers of information through large to very large objects and even (deep) underground.

4. Capabilities and applications of muography in geosciences

There are three approaches to conduct a muographic survey. In the most common application the survey system is located on ground and can hence be informally described as *surface muography*. These devices are sometimes called “muon telescopes” and they are used, e.g., in places where the target can be seen from the side due to high local relief. Most common applications include volcano imaging (Marteau et al., 2012; Nishiyama et al., 2014). Many archaeologic studies,

including scanning of pyramids, fall into this category. Since the muon detection system is located in a free space, there are no major reasons to limit the size of the survey equipment. The pros are that one can obtain highly directional data and acquire it more rapidly than below-ground surveys where the measured muon flux is diminished due to absorption of muons in the solid material between the surface and the detection system. The cons include greater logistical costs and higher operational challenges.

There are two technologies available for *underground muography*. The more used solution is to bring the afore-described surface equipment to depth (with or without some changes), for example by using mine or geotechnical tunnels. The same pros and cons are valid also for this technology. The other option is to use borehole muon technology (i.e., *borehole muography*, which is a subcategory of underground muography) that has come available just recently. As any geophysical method, also borehole muon surveys have their pros and cons. The latter include somewhat less accurate angular resolution (directional information) than those of the surface and tunnel systems. However, on the pros side there is the fact that there exists much larger number of boreholes than that of tunnels. Also logistical costs to operate and mobilise borehole muon technology are lower than those in bigger systems.

All the three muographic approaches described above can be designed in various ways, each of course having their own pros and cons in addition to those already mentioned. The most widely used muon detectors are gas-filled detectors and scintillation detectors that are based on ionisation and light detection, respectively. However, the maintenance of the former is challenging as gas-filled detectors require a continuous gas flow because of impurities and ionisation in the gas (that hamper its operation) while scintillation detectors require just power for operation. Therefore, the latter and especially plastic scintillation detectors (or plastic scintillators) are currently the main detector type even if their position resolution is worse than those of gas-filled. Scintillators are also much faster than gas-filled detectors as the light collection is faster than that of charge/ionisation.

In *borehole muography*, the cylindrical probe is lowered to the borehole like any other geophysical downhole probe. As the surveying time in a given depth is depending on the muon flux and the absorption rate of muons in material increases logarithmically as a function of depth, muon detection gets exponentially more time consuming with increasing depth. If a survey is conducted in a single depth only, the survey end product will be a 2D map of relative densities in the media (e.g., soil or rocks). Indeed, 3D-analysis is not possible by such a single-point muography. However, 3D density imaging of soil layers and bedrock can be achieved by conducting muographic surveys in various depths along the drill hole. Resolution can be further enhanced by repeating the survey in two other holes, or more, as long as the conal data clouds are at least partially superimposed. Spatial resolution can be achieved or enhanced also by combining the results with another density-sensitive survey data (e.g., gravity survey; Nishiyama et al., 2014) or by utilising some other type of geophysical (e.g., drill core petrophysical data), geological (e.g., drill core logs) or geochemical (e.g., drill core assays) data.

There are numerous applications for muography in geosciences. For example, muography can be used in delineation of ore bodies or favourable lithologies and structures by mapping density contrasts in rocks. It also offers unique opportunities for groundwater exploration, in both soil layers and crystalline bedrock. Other major applications resolve problems that are related to high-relief geological bodies, like the internal structures of volcanoes or mountains. A long-term survey or continuous monitoring is another exciting and unique way to study temporal development of density changes in geological processes (*time-lapse muography, 4D muography*). Potential applications for 4D muography include hydrological studies of soils and bedrock lithologies and crosscutting faults: for example, where and how fast does the water flow after a major raining event or thawing of snow cover in spring? Also slow and unwanted CO_2 leakage from deep geological CO_2 storage sites could potentially be monitored by continuous muon

monitoring (Kudryavtsev et al., 2012). Moreover, muography has potential to become a major technology in monitoring the long-term storage sites of nuclear waste (Clarkson et al., 2014).

5. Conclusions

Muography is a suitable method for geological studies were density information is needed. The acquired density data is completely independent of existing geophysical methods and can hence be applied with or without any previous data or if other density-sensitive methods are not suitable or accurate enough. There are, however, few prerequisites for underground muography: (1) the underground volume studied is not totally homogeneous in regard of density; (2) there is a way to install the muon detector underneath the volume of interest (e.g., a tunnel or a drill hole); and (3) you can afford to wait for weeks to months to acquire statistically enough data. The first prerequisite is obviously not valid if the very reason of the survey is to test whether the studied rock volume is homogenous or not.

Continuous technological and software development is likely to bring muography amongst the other standard research methods used in geosciences in the future. Also cumulative experience and expanding scientific community will promote this development.

References:

Clarkson, A., Hamilton, D.J., Hoek, M., Ireland, D.G., Johnstone, J.R., Kaiser, R., Keri, T., Lumsden, S., Mahon, D.F., McKinnon, B., Murray, M., Nutbeam-Tuffs, S., Shearer, C., Staines, C., Yang, G. & Zimmerman, C., 2014. GEANT4 Simulation of a Scintillating-Fibre Tracker for the Cosmic-ray Muon Tomography of Legacy Nuclear Waste Containers. Nuclear Instruments and Methods in Physics Research A: Accelerators, Spectrometers, Detectors and Associated Equipment 746, 64-73.

Kudryavtsev, V.A., Spooner, N.J.C., Gluyas, J., Fung, C. & Coleman, M., 2012. Monitoring subsurface CO_2 emplacement and security of storage using muon tomography. International Journal of Greenhouse Gas Control 11, 21-24.

Marteau, J., Gibert, D., Lesparre, N., Nicollin, F., Noli, P. & Giacoppo, F., 2012. Muons tomography applied to geosciences and volcanology. Nuclear Instruments and Methods in Physics, Research Section A: Accelerators, Spectrometers, Detectors and Associated Equipment 695, 23-28.

Nishiyama, R., Tanaka, Y., Okubo, S., Oshima, H., Tanaka, H.K.M. & Maekawa, T., 2014. Integrated processing of muon radiography and gravity anomaly data toward the realization of high-resolution 3-D density structural analysis of volcanoes: Case study of Showa-Shinzan lava dome, Usu, Japan. Journal of Geophysical Research: Solid Earth 119, 699-710.

Tanaka, H.K.M., Uchida, T., Tanaka, M., Takeo, M., Oikawa, J., Ohminato, T., Aoki, Y., Koyama, E. & Tsuji, H., 2009. Detecting a mass change inside a volcano by cosmic-ray muon radiography (muography): First results from measurements at Asama volcano, Japan. Geophysical Research Letters 36, L17302, doi:10.1029/2009GL039448.

Towards a pan-European Deep Seismic Sounding (DSS) European database: Promoting the impact, preservation, and accessibility of the existing wealth of controlled source seismic data

M. Ivandic[1], R. Carbonell[2], R. Roberts[1] and D. Marti[2]

[1]Dept of Earth Sciences, Uppsala University, Sweden
[2]Dept of Structure & Dynamics of the Earth, CSIC-Institute of Earth Sciences Jaume Almera, Barcelona, Spain
E-mail: monika.ivandic@geo.uu.se

Currently, there is no fully organized European structure for ensuring that deep seismic sounding (DSS) data is preserved for future use. Thus, within the SERA project ("The Seismology and Earthquake Engineering Research Infrastructure Alliance for Europe"), one work package aims to investigate an appropriate model for integrating DSS data into the EPOS framework. EPOS is the "European Plate Observing System", and is a project sponsored by ESFRI, the "European Strategy Forum for Research Infrastructure".

Keywords: deep seismic sounding data, data archiving, SERA/EPOS

1. Introduction

Since the 70's European Earth scientists have devoted extensive efforts to acquiring Deep Seismic Sounding (DSS) data. These projects, mostly supported by national and international agencies and research institutions are undoubtedly the base that supports all the current existing knowledge on the structure of the crust and lithosphere. These seismic experiments that resulted in unique and critical data sets are practically and logistically demanding and expensive, and many geographical areas are relatively poorly covered. Because of this, both new and old data is of great scientific importance, especially as modern analysis tools allow increasingly refined interpretations.

Currently, there is no fully organized pan-European structure for ensuring that this valuable data is properly preserved for future use and is accessible in a homogeneous and robust manner to all researchers, and furthermore in manner which will assure that the efforts of the research teams involved in their acquisition are properly acknowledged. These data alone have contributed greatly to our current understanding of the continental lithosphere of Eurasia and new analysis methods and scientific questions mean that the data continues to be used actively. Many of these projects were nationally funded within specific research programs. The list of acronyms related to key experiments and datasets is extensive, it includes: ECORS, BIRPS, DEKORP, ESCI, FIRE, HIRE, URSEIS, ESRU, EUROBRIDGE, ECORS-CROP, TRANSALP, POLAR, NFP20, EUGENO, BABEL and several others. These data sets, and new ones of the same class, are irreplaceable, and will continue to be highly relevant for studies of the deep Earth and tectonic evolution.

2. Access to raw and derived data via EPOS

The inclusion of DSS data and research infrastructures in the large portfolio of the EPOS initiative is being assessed through SERA project with a few specific goals that include: To identify and gather the relevant institutions currently holding and/or collecting such data; map and establish a first comprehensive inventory of available raw and processed data, formats, metadata, products of various levels obtained from the raw data, reports and technical documentation of past experiments; investigate access mechanisms and ownership issues where relevant; aim to join the active and passive seismology data collections.

Considerable amounts of data are already secured in various data repositories around Europe, including e.g. GFZ, Helsinki University, CSIC in Barcelona, and many others. It seems plausible that one or more of these institutions can provide the technical basis for the design of a homogeneous European system suitable for EPOS.

Aims for SERA include identifying as much such data as possible, and together with the relevant institutions finding a suitable way of making this data secure and accessible for the future. The SERA working group has already established a small, incomplete, database of DSS projects. With the help of the DSS community, the group should continue to refine the DSS project database, with a primary short-term aim of securing data which may be in danger of being lost.

Existing well-functioning DSS database systems should presumably continue to operate, but be linked to the EPOS Integrated Core Service (ICS). Where data but no proper ”database” system exists, the data should preferably be placed into an EPOS compatible database at the data-owning institution, or alternatively a data-owning institution may choose to seek a bilateral agreement with some institution running a database system. In some cases, EPOS may be able only to offer information that the data exist and who to contact about gaining access to the data.

Furthermore, some of the existing databases offer not only access to data but also to some processing tools. Pan-European coordination of such tools is a natural development in the EPOS context, and this will be further investigated, not least by dialogue with the relevant community, during the continued work within this work package.

Acknowledgements

This activity is supported by the SERA project, supported under project 730900, INFRAIA-01-2016-2017

References

Roland Roberts, Ramon Carbonell, Angeliki Adamaki, Monika Ivandic, 2018: Deep Seismic Sounding Data, **www.researchgate.net/publication/327500458_Deep_seismic_sounding_data**

Roland Roberts, Ramon Carbonell, Angeliki Adamaki, Monika Ivandic, 2018: Position Document on Future Deep Seismic Sounding (DSS) Data Accessibility, www.researchgate.net/publication/327500252_Position_Document_on_Future_Deep_Seismic_Sounding_DSS_Data_Accessibility

Preliminary studies of long-period array methods with Northern Finland Seismological Network

H. Jänkävaara[1]

[1]Oulu Mining School, Sodankylä Geophysical Observatory, University of Oulu

This extended abstract reports the first studies using the Northern Finland Seismological Network as a seismic array. The properties of the network and the procedures used to determine the suitability of the network for seismic array processing, are described. Earthquake localization using long-period, teleseismic surface waves is of particular interest.

Keywords: seismic array, earthquake localization, beampacking, long-period, applied geophysics, surface waves, teleseismic

1. Introduction

The Northern Finland Seismological Network (FN) consists of 9 broadband stations equipped by triaxial seismometers. Four stations (SGF, OUL, MSF and RNF) have been started during 2005-2008 and five new stations (KLF, OLKF, KMNF, RANF, RAJF) are now working in test regime (Kozlovskaya et al. 2016). KMNF, RANF and RAJF are the newest additions and the test data of those stations has been available at the start of 2018.

The purpose of the research is to study the suitability and possible applications of FN-network when using seismological array methods with long-period seismic signals.

2. Properties of FN-network as an array

Considering array methods, FN-network is irregularly shaped array with relatively large aperture of around 580km, which introduces some limitations in observable frequency range. In addition, errors in localization of events at distances other than teleseismic, can be prominent.

The array transfer functions (TF) with different selections of stations have been studied. Also, the improvements in the array transfer function when using external stations of nearby seismic networks (e.g. HE, UP, NS, NO and II -networks) is also studied. In addition, some attention is paid to finding the best locations for possible new stations of FN-network, so that the resolution of the array would improve.

So far, the focus of the studies has been in locating (resolving backazimuth (BAZ) of the event) teleseismic earthquakes using surface waves, the frequency band of interest being from 6.7 to 25 mHz. Using the array resolution defining procedures used by Wang (2002) and extracting the adequate information from the transfer functions, FN-network could be suitable for detecting teleseismic earthquakes using above mentioned frequency band.

3. Test Data

The earthquake detection capabilities have been tested using earthquake information from EIDA. The used catalog consists of all earthquakes around the world listed in EIDA from 1.1.2018 to 30.9.2018. The timespan includes 3587 earthquakes, but the amount should probably be increased to achieve better results. Every event with origintimes 5000 seconds or less apart from each other is excluded to make sure only one event is present in each data set used for localization. This requirement excludes 2785 events. 5 additional events are excluded because of the problems with the data files.

Additionally, the plan is to test the arrays detection capabilities particularly for events located in the arctic regions and in northern part of Russia, where the amount of permanent seismic stations is low.

4. Localization Process

Origintimes from EIDA are used to make 6000 seconds long data streams starting 500 seconds before the origintime. The data stream is bandpass filtered using the before mentioned frequency band. STA/LTA trigger is then used to find the surface wave phase. The trigger is only applied to the data trace of SGF station. Proper time offset is used when trimming the stream according to the trigger on and off times to make sure the triggered phase is included in every station's data trace. If the trigger doesn't find anything, the event is excluded. 241 events proceed to beampacking after triggering.

Beampacking method described by Schweitzer et al. (2012) is applied to supposed surface wave phase to resolve backazimuth of the event and the slowness (s_x and s_y) of the phase. The calculated BAZ is compared to the original BAZ of the event. The relation between magnitude, distance and depth and the errors in the BAZ is studied.

Array calculations and procedures are based on methods described by Schweitzer et al. (2012) and Wang (2002). Programming is done using Python together with ObsPy framework. (The ObsPy Development Team, 2017)

5. Results

The resolving of the BAZ using beampacking with long-period surface waves has been relatively successful for events with larger magnitudes and for events originating from closer epicentral distances. However, it is not possible to obtain reliable location results with surface waves if only single array is used. The whole procedure of localization can be improved by using more sophisticated trigger procedures and by using so-called multi array analysis using other long-period arrays located in the Arctic.

Acknowledgements

The study is based on the MSc Thesis in applied geophysics by H. Jänkävaara. It was partly supported by FIN-EPOS project No. 283655 and EPOS IP HORIZON 2020 project. The author thanks the staff of SGO (Hanna Silvennoinen, Janne Narkilahti and Riitta Hurskainen) for the access to data of new FN stations.

References:

Kozlovskaya, E., Narkilahti, J., Nevalainen, J., Hurskainen, R., and Silvennoinen, H. Seismic observations at the sodankylä geophysical observatory: history, present, and the future. 5:365-382, 08 2016

Schweitzer, J., Fyen, J., Mykkeltveit, S., Gibbons, S. J., Pirli, M., Kühn, D., and Kværna, T. Seismic Arrays. In Bormann, P., editor, New Manual of Seismological Observatory Practice 2 (NMSOP-2), volume 2, pages 1 - 80. Deutsches Geo-ForschungsZentrum GFZ, Potsdam, 2012. doi: 10.2312/GFZ.NMSOP-2_ch9

The ObsPy Development Team. ObsPy: A python toolbox for seismology/seismological observatories., 2017. URL https://docs.obspy.org/

Wang, J., A scheme for initial beam deployment for the international monitoring system arrays. pure and applied geophysics, 159(5):1005-1020, Mar 2002. ISSN 1420-9136. doi: 10.1007/s00024-002-8670-6. URL https://doi.org/10.1007/s00024-002-8670-6

New digital learning materials for teaching in geosciences

J. Järvinen[1], S. Piippo[1], S. Silvennoinen[1], S. Kultti[1] and E. Koivisto[1]

[1]Department of Geosciences and Geography, P.O. Box 64, FI-00014 University of Helsinki
E-mail: juha.jarvinen@helsinki.fi

The geoscience study programs at the University of Helsinki are producing new digital learning materials within the new Digiloikka project. As of 2018, these digital materials consist of: 1) GigaPan pictures, 2) 3D models and 3D maps, 3) 2D maps and other complementary materials (e.g. GPR data), and 4) educational videos for laboratory and fieldwork instructions. In the near future, these materials are used to create VR learning environments.

Keywords: photogrammetry, SfM, field teaching, GigaPan, digital leap

1. New digital learning materials

Fieldwork is a fundamental part of geosciences and nature is the most important learning environment for students. There is a constant demand for increasing the amount of field exercises. However, working outdoors is unpredictable, dependent on seasons and requires resources. With new digital learning materials, it is possible to improve and broaden the spectrum of field teaching. The Bachelor's Programme in Geosciences and the Master's Programme in Geology and Geophysics at the University of Helsinki are participating in a new project, *Digiloikka* ("Digital leap") launched by the University of Helsinki, aiming to provide resources for the study programmes to digitalize teaching. As of 2018, the digital materials produced consist of: 1) GigaPan pictures, 2) 3D models and 3D maps, 3) 2D maps and other complementary materials (e.g. GPR data), and 4) educational videos for laboratory and fieldwork instructions. Furthermore, in the near future, we are looking to combine these materials and create Virtual Reality (VR) learning environments, as well as to create a simple and optimized procedure for the continuous creation of new materials. Moving forward, we are planning to visualize various complex geological systems in VR environments.

GigaPan pictures are high-resolution panoramic images, which are photographed using a robotic GigaPan camera stand, a DSLR camera (Digital Single-Lens Reflex) and a high magnification lens. Images are then stitched together using specialized software. With GigaPan images, students can make observations and interpretations of geological formations, such as bedrock outcrops, from up close and afar (Figure 1).

3D models (Figure 2) and 3D maps are created using SfM photogrammetry (Surface from Motion: Micheletti et al., 2015). First, images are taken either by using a Drone (with Pix4D software), or preferably, using a DSLR camera, when possible. Images taken with a DSLR camera are of higher quality, hence making it possible to create models with more accurate texturing and geometry. Images and ground control data (GPS coordinates of specific locations on the mapping area) are then imported into a photogrammetry software for processing.

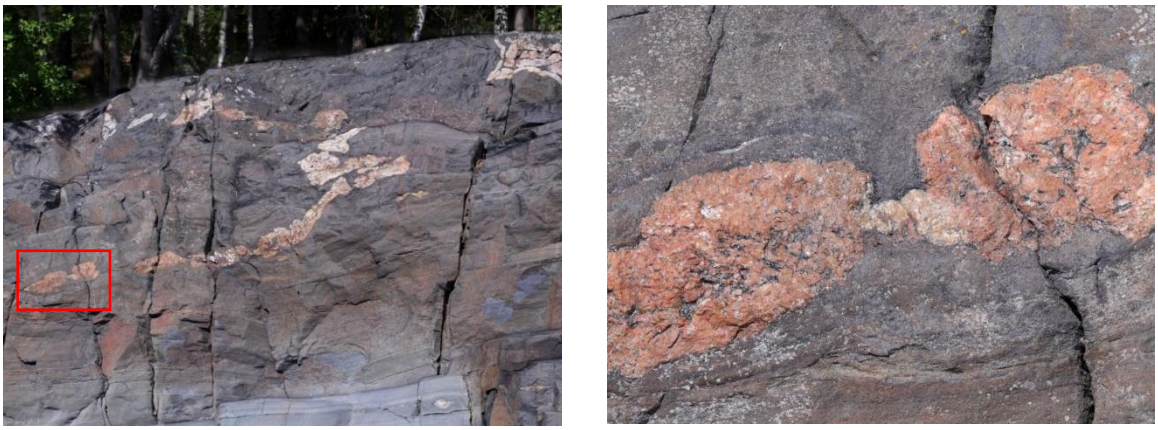

Figure 7. On the left is a GigaPan picture with low magnification, and on the right a close-up of the same image with high magnification.

Figure 8. On the left is a photogrammetric 3D model of sediment-matrix igneous breccia in Papinvuori, Tampere. On the right is a model of mylonite zone in Uutela, Helsinki.

2. Materials are open access

Materials are open access and freely to be used by other universities in their teaching of geosciences. In addition, digital materials can be used to preserve important study sites that are in danger of disappearing (for example due to human activity). The outcomes of the project are not aimed only at university students: the material will be made available for broader audience through the geologia.fi internet portal. Currently, the materials created so far are available for viewing at Sketchfab (https://sketchfab.com/HYGeo) and GigaMacro (https://viewer.gigamacro.com/HYGeo).

References:

Micheletti, N., Chandler, J.H., Lane, S.N., 2015. Structure from motion (SfM) Photogrammetry. Geomorphological Techniques, Chap. 2, Sec. 2.2 (2015). British Society

Characterisation of the structural evolution and structural control of the gold mineralisations in the Kullaa area, SW Finland

J. Kara[1], J. Manninen[1], T. Leskelä[1], P. Skyttä[1], M. Väisänen[1], M. Tiainen[2] and H. Leväniemi[2]

[1] Department of Geography and Geology, University of Turku, FI-20014 Turku, Finland
[2] Geological Survey of Finland, P.O. Box 96, FI-02151 Espoo, Finland
E-mail: jkmkar@utu.fi

Field work was conducted in the Kullaa area in SW Finland to study the tectonic evolution and structural setting of the gold mineralisations in the area. Our structural data and interpretation recognises the structural complexity associated with the mineralised zone. We suggest that the NE-SW trending faults in association with the second-order structures related to the NW-SE trending Kynsikangas shear zone have controlled the precipitation of the gold-bearing fluids.

Keywords: Shear zone, gold mineralization, Svecofennian orogeny, structural geology

1. Introduction

The Kullaa area, located in SW Finland, is characterised by several known gold occurrences (Kärkkäinen et al. 2016 and references therein) and a complex tectonic history (e.g., Pietikäinen 1994). It belongs to the central part of the 1.90-1.80 Ga Svecofennian orogen and it has been suggested that it is the western continuation of the high-grade Pirkanmaa belt (Kähkönen 2005, Nironen et al. 2016, Lahtinen et al. 2017). The area has been utilised for a small scale gold exploration since 1950s by Outokumpu Company (Eilu & Pankka 2009) and more extensively after late 1990s by the Geological Survey of Finland (Kärkkäinen et al. 2012). However, previous research has mainly focused on the geochemical features of the mineralisations and the tectonic evolution at both regional and target scales have remained ambiguous. In this study we focus on the structural evolution of the area and the structural control of the mineralisations.

The study is part of a joint-project between the Geological Survey of Finland and the University of Turku focusing on the spatial distribution of the known gold occurrences and their genetic linkage to the evolution of the regional-scale structures and lithologies in SW Finland (see also Leskelä et al. 2018, Pitkälä et al. 2018, this issue).

2. Geological setting

The study area is located within the Pomarkku block (Pietikäinen 1994) which lies between the Central Finland Granitoid Complex (CFGC) and the Satakunta sandstone basin (Fig. 1). The study area consists mostly of syn-tectonic granitoids which have intruded into the Svecofennian supracrustal rocks; paraschists and -gneisses, and mafic to intermediate metavolcanic rocks and black schists. Gabbros and diorites occur as small intrusive bodies. The Pomarkku block is bordered by two crustal scale NW-SE striking high-strain zones: the sinistral strike-slip Kynsikangas shear zone in the south (Pietikäinen 1994, this study) and the dextral oblique Kankaanpää shear zone in the north (Pajunen et al. 2008, this study). The internal structure of the Pomarkku block is characterised by E-W to ENE-WSW structural trends, including horizontal to sub-horizontal mineral-stretching lineations which are deflected towards the sub-vertical Kynsikangas zone in the south-west (Pajunen et al. 2001, Pajunen et al. 2008, Fig. 2). The bedrock of Kullaa has been metamorphosed under upper amphibolite facies condition during the regional metamorphic peak (Pietikäinen 1994, Hölttä & Heilimo 2017). The age of the metamorphisms in the area is, however, not known.

Four gold mineralizations have been identified from the area: Saarijärvi, Silmusuo, Välimäki and Kultakallio (Fig. 2). Gold occurs mostly in narrow shear zones and in narrow quartz veins of different generations within deformed and altered mafic rocks (Kärkkäinen et al. 2012).

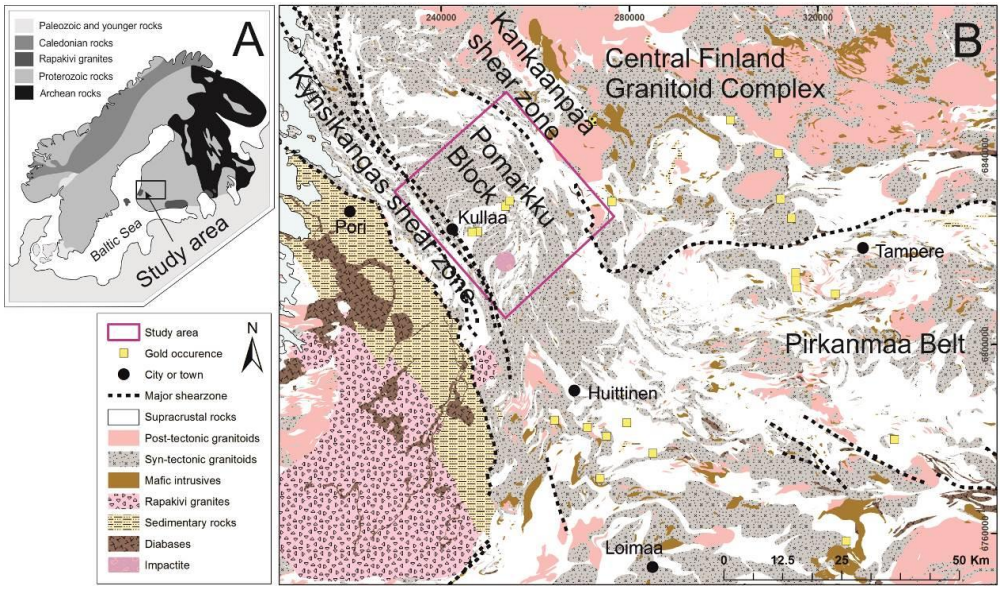

Fig. 1. A) Geological overview of the Fennoscandian shield (Koistinen et al. 2001). B) Generalised lithological map of the study area and surroundings. Geological data modified after ©Geological Survey of Finland.

3. Results

During the field work 180 measurements on lineations and fold axes and 281 measurements on foliations and axial planes were conducted. The formline map of the structural trends was composed based on the observations and the aeromagnetic map from the area (Fig. 2). The homogeneously distributed structural data from the northern part of the Pomarkku block provides the reference for the gold deposits, where the spatially associated foliation data shows more scatter, reflecting greater structural heterogeneity.

4. Discussion and conclusions

The northern part of the study area shows very gently inclined lineations and foliations which stay constant over the area. This indicates that the northern part has acted as a single block (Pajunen et al. 2008). By contrast, the dominant structural trend within the gold mineralisations is striking to NE-SW, which Kärkkäinen et al. (2016) attributed to a NE-SW striking shear zone. Our structural data and interpretation further recognizes the structural complexity associated with the mineralized zone, including NE-SW trending ductile fabrics obliquely overprinting the dominant ENE-WSW structural trends. We attribute the above NE-SW features to the presence of set of NE-SW trending faults providing the conduits for the gold-bearing fluids. The exact location of the gold mineralization have been controlled by the interplay between the NE-SW zone and second-order deformation zones related to the approximately orthogonal, NW-SW trending Kynsikangas shear zone.

In the future, U-Pb zircon dating will be performed on leucosome vein collected from a migmatised paragneiss to determine the age of metamorphism within the area

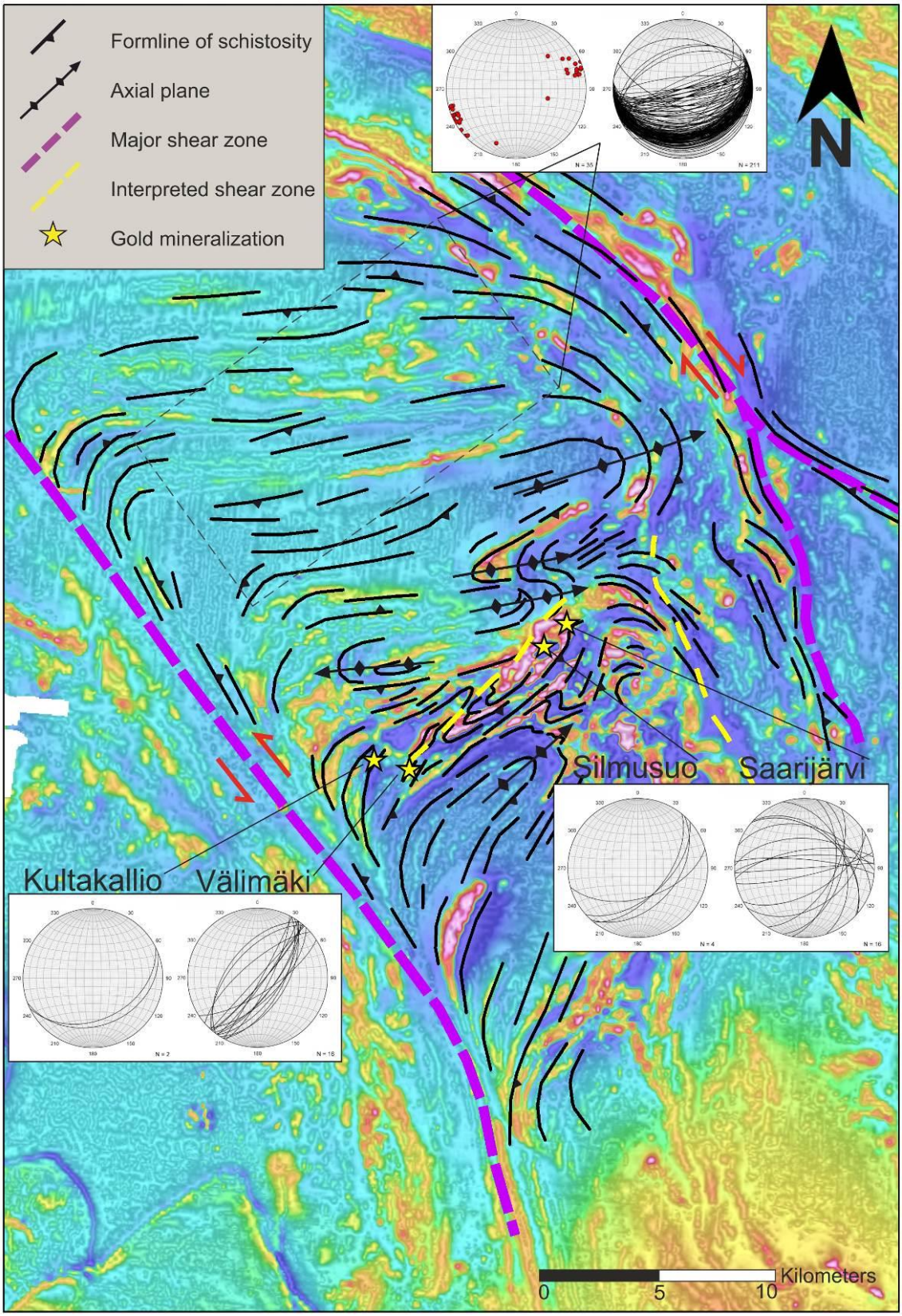

Figure 2. The formline map of the study area with Tilt Derivate (TDR) processed aeromagnetic map ©Geological Survey of Finland. Stereographic projections for the foliation data from each gold occurrence and for foliation and lineation data (red dots) from northern part of the study area for comparison.

Acknowledgements
This study was funded by the Geological Survey of Finland.

References:

Eilu, P., Pankka, H., 2009. FINGOLD - a public database on gold deposits in Finland. Version 1.1 [Electronic resource]. Geological Survey of Finland, Espoo, Finland

Hölttä, P., Heilimo, E. 2017. Metamorphic map of Finland. Geological Survey of Finland, Special Paper, 60, 77-128.

Koistinen, T., Stephens, M.B., Bogatchev, V., Nordgulen, Ø., Wennerström, M., Korhonen, J., 2001. Geological map of the Fennoscandian Shield, scale 1:2 000 000. Geological Surveys of Finland, Norway and Sweden and the North-West Department of Natural Resources of Russia.

Kähkönen, Y., 2005. Svecofennian supracrustal rocks. Developments in Precambrian Geology, 14, 343-405.

Kärkkäinen, N., Lehto, T., Pakkanen, L., Rosenberg, P. 2012. Exploration and the mineralogy of gold in the Kullaa area, southwestern Finland. Geological Survey of Finland, Special Paper, 52, 131–148.

Kärkkäinen, N., Huhta, P., Leväniemi, H., 2016. Kullaan vyöhykkeen malmipotentiaali, Saarijärven ja Kultakallion Au-mineralisaatiot. Geological Survey of Finland, Archive report, 75/2016, 42p.

Lahtinen, R., 1996. Geochemistry of Palaeoproterozoic supracrustal and plutonic rocks in the Tampere-Hameenlinna area, southern Finland. Geological Survey of Finland, 389, 113 p.

Lahtinen, R., Huhma, H., Sipilä, P., Vaarma, M., 2017. Geochemistry, U-Pb geochronology and Sm-Nd data from the Paleoproterozoic Western Finland supersuite–A key component in the coupled Bothnian oroclines. Precambrian Research, 299, 264-281.

Leskelä, T., Kara, J., Pitkälä, I., Skyttä, P., Väisänen, M., Tiainen, M., Leväniemi, H., Hokka, J., Lahaye, Y., 2018. Geochronology, geochemistry and structural setting of the Uunimäki gold mineralisation, SW Finland. In: Lithosphere 2018 Symposium, Oulu, Finland. Institute of Seismology, University of Helsinki

Nironen, M., 1999. Structural and magmatic evolution in the Loimaa area, southwestern Finland. Bulletin of the Geological Society of Finland, 71, 57-71.

Nironen, M., Kousa, J., Luukas, J., Lahtinen, R. 2016. Geological Map of Finland. 1:1 000 000. Geological Survey of Finland.

Pajunen, M., Airo, M.-L., Wennerström, M., Niemelä, R., Wasenius, P. 2001. Preliminary report: The “Shear zone research and rock engineering” project, Pori area, south-western Finland. Geological Survey of Finland, Special Paper, 31, 7–16.

Pajunen, M., Airo, M.-L., Elminen, T., Niemelä, R., Vaarma, M., Wasenius, P., Wennerström, M., 2008. Tectonic evolution of the Svecofennian crust in southeastern Finland. Geological Survey of Finland, Special Paper, 47,.15-160.

Pietikäinen, K., 1994. The geology of the Paleoproterozoic Pori Shear Zone. Michigan Tech, PhD thesis. 129p.

Pitkälä, I., Kara, J., Leskelä, T., Skyttä, P., Väisänen, M., Leväniemi, H., Hokka, J., Tiainen, M., Lahaye, Y., 2018: Shear zones and structural analysis of the Loimaa area, SW Finland. In: Lithosphere 2018 Symposium, Oulu, Finland. Institute of Seismology, University of Helsinki

Ambient noise measurements and HVSR analysis in the XSoDEx project

J. Karjalainen[1], E. Kozlovskaya [1,2], T. Pirttisalo [1], S. Heinonen [2], S. Buske [3]

[1]Oulu Mining School, Faculty of Technology, University of Oulu
[2] Geological Survey of Finland
[3] TU Bergakademie Freiberg, Germany (TUBAF)

E-mail: kjari@student.oulu.fi

In my master thesis I describe results of seismic measurements done by University of Oulu in Experiment of Sodankylä Deep Exploration (XSoDEx) project, Horizontal-to-Vertical Spectral Ratio (HVSR) analysis of the recorded ambient seismic noise data and an application of HVSR method for determination of overburden thickness at the XSoDEx measurement lines.

Keywords: HVSR, Fennoscandia, Sodankylä

1. General

Seismic data acquisition of Experiment of Sodankylä Deep Exploration (XSoDEx) project was done in collaboration of Geological Survey of Finland (GTK), TU Bergakademie Freiberg (TUBAF), Oulu Mining School (OMS) and Sodankylä Geological Observatory (SGO) during July and August 2017. The main objective was to acquire seismic reflection and refraction data by using active seismic source, but also ambient seismic noise was recorded on purpose. Ambient noise recordings were done with Sercel UNITE system owned by University of Oulu.

We utilized ambient seismic noise recordings in Horizontal-to-Vertical Spectral Ratio (HVSR) analysis of the data, also known as Nakamura's method (Nakamura, 1989) for determination of overburden thickness in the XSoDEx measurement lines.

2. Acquisition of passive seismic data

Acquisition of passive seismic data was done in cooperation of OMS and SGO. Measurements lasted two months, and data was recorded with Sercel equipment, which included 60 vertical-component geophones and 38 three-component accelerometers with Remote Autonomous Units (RAU) for each sensor (Figure 1). The data was received from RAUs through wireless connection by a special data harvester device and transmitted to a server laptop (Figure 2). RAUs were deployed at 160 m spacing around the active seismic survey line. Both one-component (1C) and three-component (3C) sensors were mixed along the line. The 3C sensors were oriented along the line in such a way, that inline component pointed to the same direction as the active measurement line was heading.

Ambient seismic noise was recorded while active seismic source was not in operation. Active seismic data was acquired in two shifts for approximately 16 h per day and the active seismic field crew was having one rest day per week. During the breaks in active seismic data acquisition, the Sercel equipment was left at the site to record ambient noise for the whole day. The resting and maintenance days were the most important time windows for ambient seismic noise recordings. The greatest concern was battery life of the data loggers, which needed to be monitored carefully. In general, batteries lasted approximately seven days for 1C and five days for 3C data loggers with used recording setup.

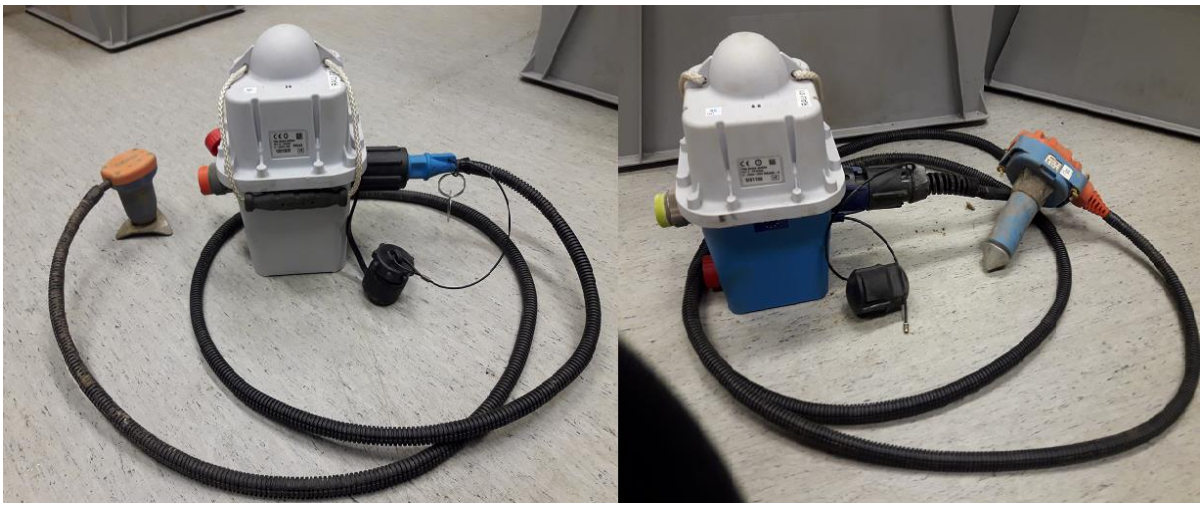

Figure 1. 1C geophone with RAU *eX* data logger (left) and 3C accelerometer with RAU-D data logger (right).

Figure 2. Server laptop, data harvester and battery charger.

3. HVSR analysis and overburden thickness determination

The HVSR analysis was made with Geopsy, which is an open source software for geophysical data processing and research. First the recorded data needed to be converted into convenient format. Miniseed format was selected, because it is plausible with HVSR analysis. As the HVSR method requires three-component recordings, the data of one-component units was not used. First, depending on the sampling rate of the recordings, the H/V spectra were calculated with 0.5-125 Hz or 0.5-250 Hz frequency range in order to get a general view from each station. When necessary, more detailed spectra with narrowed frequency range were calculated afterwards.

High-quality H/V (horizontal-to-vertical) curves were not available from every single station, so the spectra had to be visually categorised. The criteria for reliable H/V curves and clear H/V peaks are determined in SESAME (2004) report, which were utilized during the categorising process (Figure 3).

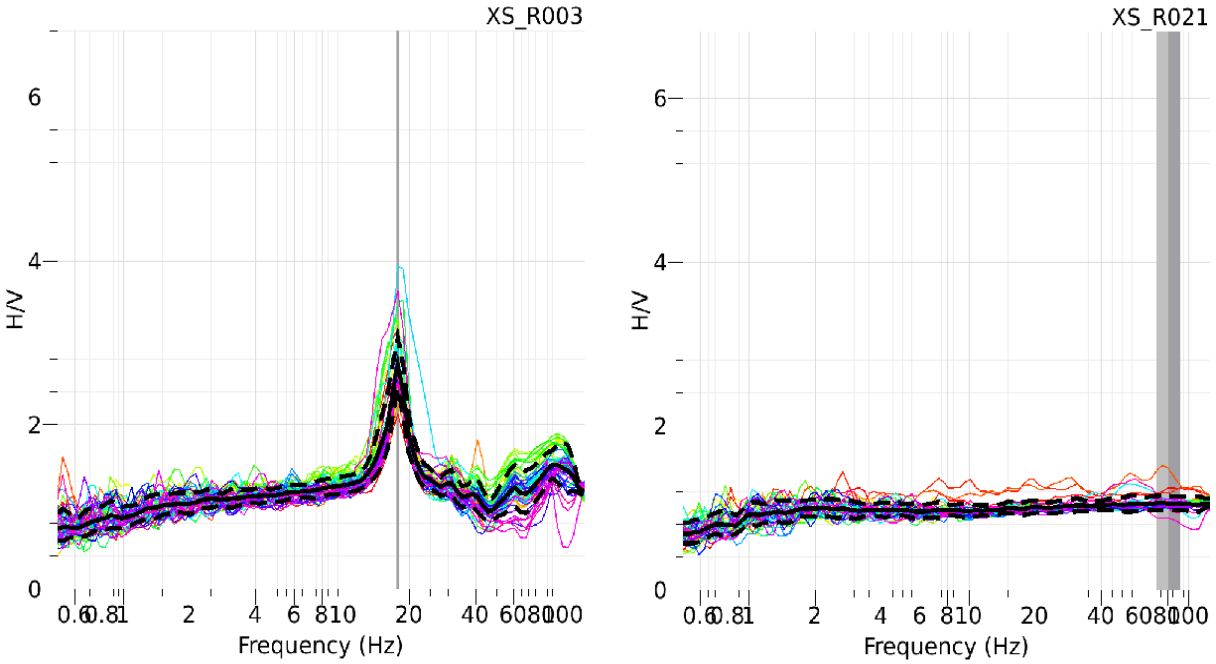

Figure 3. Two examples of different types of H/V spectra: clear peak and flat spectrum.

We took into account all the reliable curves and peaks in determination of thickness of the overburden at the location of each station. In order to facilitate future modelling, we developed a Python script to get data for all required parameters into a single file. Determination of the overburden thickness is based on the approximate relationship (Konno & Ohmachi, 1998)

$$h \approx v_s / 4f_0, \quad (1)$$

where h is overburden thickness, v_s is s-wave velocity and f_0 is the fundamental peak frequency of the H/V curve.

Drillings and excavations have been done by GTK nearby some of our stations, which provided valuable reference to the results received through HVSR analysis (GTK, 2018). This information was utilized in determination of s-wave velocity. The H/V spectra were compared with data for superficial deposits in order to further analyse behaviour of H/V curves on varying deposits (GTK, 2010). We used Esri ArcMap software for studying superficial deposit database.

4. Conclusions

The XsoDEx project was concentrating on recording seismic reflection and refraction data by using active seismic source, which partly reduced possibilities to record ambient seismic noise. However, long recording period of two months enabled the acquisition of good amount of seismic noise enabling the HVSR analysis. The clear H/V curves were not obtained for every station, due to known limitations of the HVSR technique, so those curves were left out from further analysis.

Overburden thickness can be determined through HVSR method, but s-wave velocity is necessary to be determined as accurately as possible to get reliable results. There were visible correlations between H/V curves and superficial deposits, but exceptions were also observed, when these two data sets were combined.

5. Acknowledgements

The study is a core of MSc Thesis in applied geophysics by Jari Karjalainen that was supported by Renlund Foundation in 2017. We appreciate assistance of XSoDEx field team during field work.

References:

Konno K., Ohmachi T. (1998). Ground motion characteristics estimated from spectral ratio between horizontal and vertical components of microtremor. Bulletin of Seismological Society of America 88, 228-241.

Nakamura Y. (1989). A method for dynamic characteristics estimation of subsurface using microtremor on the ground surface. Quarterly Report Railway Tech. Res. Inst., 30-1, 25-30.

SESAME (2004). Guidelines for the implementation of the H/V spectral ratio technique on ambient vibrations measurements, processing and interpretation. SESAME European research project WP12 – Deliverable D23.12.

Stratum data for superficial deposits © Geological Survey of Finland 2018.

Superficial deposits of Finland 1:200 000 © Geological Survey of Finland 2010.

Delineating the network of dolerite dykes within the Archaean Siilinjärvi carbonatite complex

T. Kauti[1], P. Skyttä[1] and A. Salo[2]

[1]Department of Geography and Geology, 20014, University of Turku, Finland
[2]Yara Suomi Oy, P.O. Box 20, 71801, Siilinjärvi, Finland
E-mail: tuomas.kauti@utu.fi

This study aims at constructing a high-detail 3D-model of the dolerite dyke network transecting the Siilinjärvi carbonatite complex. The motivation for the modelling work is to improve the estimation of the waste rock dykes within the area of interest. Our most important dataset is the unique production drilling data which is complemented with diamond drillings, 3D-photogrammetry and structural field mapping. So far we have categorised dolerite dykes based on their orientation, width and cross-cutting relations. The previously poorly understood sub-horizontal dykes are the youngest set transecting the complex. This set of dykes has been affected by limited but systematic structural overprint overprinted comprising gentle folding and oblique slip faulting. The recognized overprint and the resulting present-day geometries provide important guidelines in building the 3D-models of the dyke networks involving integration of datasets with variable coverage and resolution.

Keywords: Dolerite dyke network, carbonatite, 3D-modelling, structural analysis, Siilinjärvi

1. Introduction

The main objective of this study is to understand the nature of the 3D-network of dolerite dykes transecting the main pit of the Siilinjärvi phosphate deposit, with specific focus in the southern part of the pit where the volume of dyke material increases and totals at around 20 %. The complex has been intruded by three variably striking (NW–SE, N–S and NE–SW) sets of sub-vertical dolerite dykes (Puustinen 1971, Äikäs 1978 and Härmälä 1981) which are interconnected with sub-horizontal dykes (Sattilainen 2015). These sub-horizontal dykes cause problems to mine planning due to their unexpected occurrence – they cannot be mapped from the surface by applying conventional methods. Therefore, the importance of this study for the mining operator (Yara Suomi Oy) is to improve the reliability of the production prognosis by enhancing the prediction capacity of the location of sub-horizontal waste rock dykes in the area area of interest, towards south of the present Särkijärvi open pit.

2. Used data

The most important dataset is the unique production drilling data of Siilinjärvi which has been acquired since the start of the mining operation in 1979 (Fig. 1). The data comprises of over 200 000 short vertical boreholes based on which the mined part of the complex may be subdivided into different lithologies. The production drilling data is currently being sorted into individual dykes, which are modelled in such high detail that the true nature of dyke network can be observed. The other significant dataset comprises ca. 500 oriented diamond drillings which are used to support the modelling and delineate the probable continuations of the dolerite dykes into greater depths. The diamond drilling data covers the known deposit, including the planned open pit extension. Structural field mapping has concentrated to the southern wall of the main pit, with a total of 214 observation points from 6 elevation levels (-125 to +66 m) available so far. We have supplemented the dataset from the deepest part of the main pit with additional 30 observation points, mainly focusing on dolerite dykes. Moreover, we use 3D-photogrammetric models and waste rock level maps to adjust the dyke network models to represent the real setting of the waste rock. We used MOVE™ software for data preprocessing, integration and model building

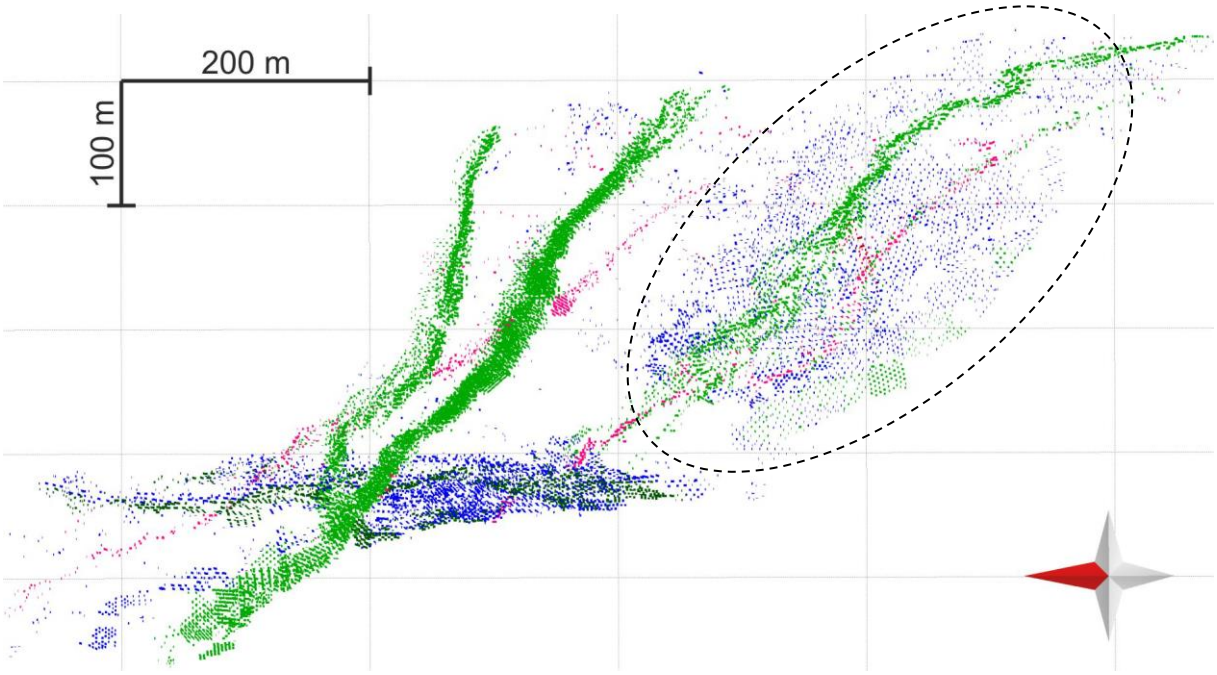

Figure 1. Production drilling data from the central part of the main pit (Särkijärvi) sorted into individual dolerite dykes. The dykes are categorized into colored sets based on their thicknesses and orientations, such as exemplified by the clearly distinguishable sub-horizontal dyke (dashed ellipse).

3. Preliminary results

Based on the field mapping and modelling work, we have been able to better delineate the occurrence of the sub-horizontal dykes and the cross-cutting relationships of the dykes (Fig. 2). Moreover, the pre-dyke structure defined by the glimmerite and carbonate rocks providing the framework for the dolerite dykes has been characterized.

- Sub-horizontal dykes are the youngest set transecting the complex.
- Displacement of the dykes occurred along vertical to steeply-dipping shears and faults. A distinct set of E-dipping faults characterized by oblique slip, E-block up, sinistral senses was observed across the whole pit.
- The hosting glimmerite shows a pre-dyke foliation with a systematic, moderate dip towards SW.
- The host rock is divided into low-strain and high-strain zones. The transition from the low to highstrain domains may be abrupt, with distinguishable from the sub-vertical carbonate banding and variable transposition of the glimmerite foliation within the high-strain domains.

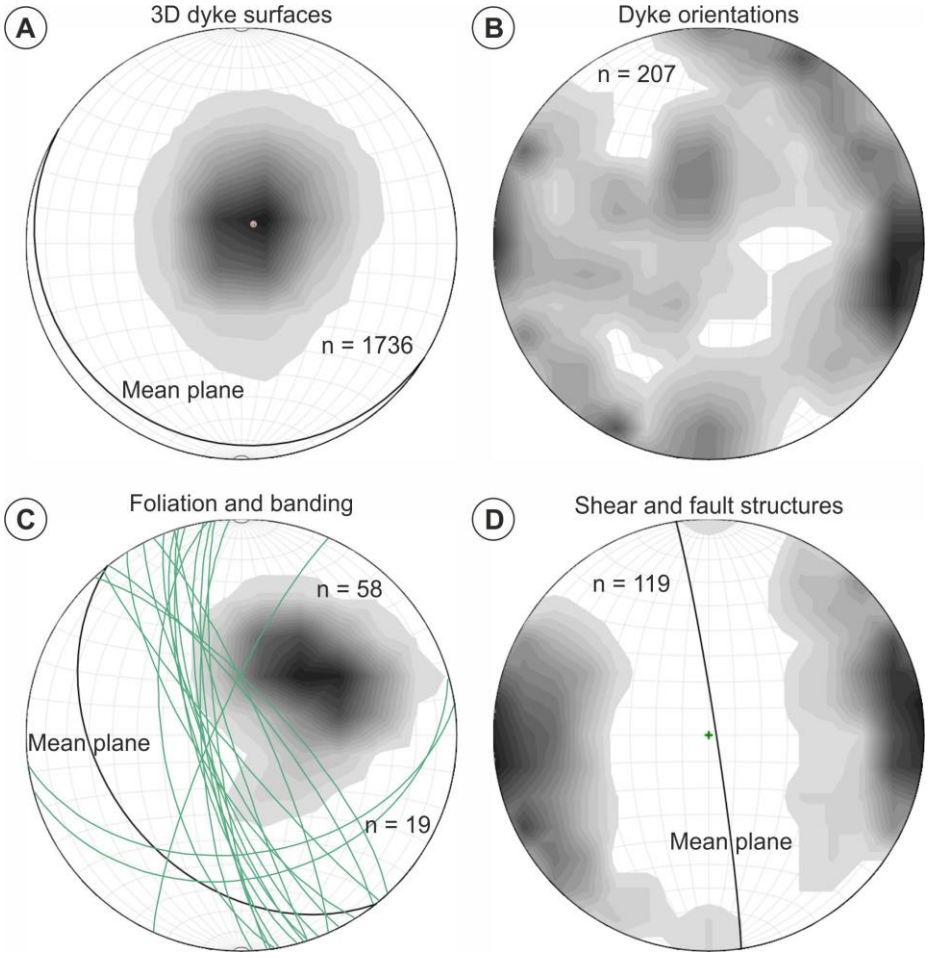

Figure 2. Structural measurements presented as pole density contours on lower-hemisphere projections. A) Modelled sub-horizontal dolerite dyke orientations (all vertices) based on the production drilling data. B) Dolerite dyke orientations measured in the field. The average width of the sub-horizontal dykes is 1–2 m while the sub-vertical ones range from 5 cm to over 30 m. C) Foliation of glimmerite (pole densities; low-strain) dips moderately towards SW and banding of carbonate rock (great circles; high-strain) dips steeply towards WSW. D) Shear and fault structures define an overall steep to vertical N–S trend.

4. Discussion and future work

For the purposes of this study, the evolution of the carbonatite complex can be divided into pre-, syn- and post-dyke stages which help understanding the structural framework of the dykes. The pre-dyke evolution involved generation of low- and high-strain zones (see Section 3), with the high-strain zones apparently controlling the emplacement of at least some of the steeply-dipping to sub-vertical dolerite dykes. However, it is not exactly clear if the oldest and most intensely deformed sub-vertical (< 0.4 m; ca. N–S) dolerite dyke set was emplaced during or after the high-strain event. The sub-vertical SE–NW to E–S striking thick (8–40 m) dolerite dykes were emplaced in the following dyking event. The youngest dykes (0.10–2 m) dips gently towards S-SE and N-NE. The relative age differences of the dyke sets are shown by the vertical shears which cause higher displacements within the older dykes with respect to the sub-horizontal ones. It is likely that shearing has taken place during the whole time period of dyke network emplacement but the rates and potential changes in the kinematics are still to be solved.

In the future, we continue to expand the modelling towards the north to cover the whole area of the mined main pit, focusing on the sub-horizontal dykes. The recently updated 3D-photogrammetry data of the S and SW pit walls will be mapped and correlated with the dyke

model generated by other datasets to reduce data gaps and to produce a coherent 3D-model. The diamond drillings will be utilized to support the interpretations and to extrapolate the models beyond the open pit volume. In the next phase of the study we will also receive new geophysical seismic profiles (through Smart Exploration project) from the area south of the main pit which are then integrated together with the previous model into the Common Earth Model.

Acknowledgements
This study is part of the Smart Exploration project (www.smartexploration.eu). The project has received funding from the European Union's Horizon 2020 Research and Innovation Programme under grant agreement no. 775971. We would like to thank Midland Valley Exploration Ltd. for the use of MOVE™ under the Academic Software Initiative and Yara Suomi Oy of seamless collaboration.

References:

Äikäs, O. 1978. Kemira Oy:n Siilinjärven kaivoksen geologinen kartoitus 1978. Geologinen tutkimuslaitos, malmiosasto, Kuopio, 4 p.

Härmälä, O. 1981. Siilinjärven kaivoksen mineraaleista ja malmin rikastusmineralogisista ominaisuuksista. Pro gradu -tutkielma, Turun yliopisto, Geologian ja maantieteen laitos, 121 p.

Puustinen, K. 1971. Geology of the Siilinjärvi carbonatite complex, eastern Finland. Bulletin de la Commission Géologique de Finlande 249, 43 p.

Sattilainen, O. 2015. 3D-modelling of the dyke network in the southern part of the Särkijärvi open pit (Siilinjärvi carbonatite). Master's thesis, University of Helsinki, Department of Geosciences and Geography, 65 p.

Testing of seismic mineral exploration methods at different scales at the Kylylahti polymetallic mine site, Eastern Finland

E. Koivisto[1], M. Malinowski[2], S. Heinonen[3], M. Riedel[1], M. Chamarczuk[2], C. Cosma[4], K. Vaittinen[5], M. Wojdyła[6] and the COGITO-MIN Working Group*

[1]Department of Geosciences and Geography, P.O. Box 68, FI-00014 University of Helsinki
[2]Institute of Geophysics, Polish Academy of Sciences, Ksiecia Janusza 64, 01-452 Warsaw, Poland
[3]Geological Survey of Finland, P.O. Box 96, FI-02151 Espoo, Finland
[4]Vibrometric Oy, 127 Taipaleentie, 01860 Perttula
[5]Boliden FinnEx Oy, Polvijärventie 22, 83700 Polvijärvi
[6]Geopartner Ltd., Skosna 39B, 30-383 Krakow, Poland
E-mail: emilia.koivisto@helsinki.fi

Building on two earlier seismic reflection campaigns in the Outokumpu ore district, the COGITO-MIN project acquired new active and passive seismic reflection data at the Kylylahti sulphide mine site in 2016. Overall, the new experiments consist of 2D measurements, a sparse active-source 3D survey, a passive seismic 3D survey, and an in-mine VSP survey utilizing novel fibre-optic DAS technology. The experiments were designed with different scales and stages of the exploration workflow in mind; from mapping of the ore host rocks at larger scale to high-resolution exploration and resource delineation. Our results demonstrate the potential of these different types of seismic data, including new, cost-effective methodologies, for different stages of exploration.

Keywords: seismic imaging, mineral exploration, Outokumpu ore district

1. COGITO-MIN seismic experiments at the Kylylahti mine site

The Outokumpu ore district contains Cu-Co-Zn-Ni-Ag-Au sulphide ore bodies. Since 1913, the area has hosted several mines. Currently, the Kylylahti mine owned by Boliden is the only operational sulphide mine in the area. Over the years, extensive geological, geochemical and geophysical surveys have taken place, including major seismic reflection campaigns in 2002 and 2008 (Kukkonen et al. 2012; Figure 1). The Outokumpu area is an ideal site for seismic exploration because the ophiolite-derived Outokumpu rock assemblage (serpentinite, carbonate, skarn and quartz rocks) hosting the semi-massive to massive sulphide mineralizations, as well as the sulphide mineralizations themselves, are strongly reflective (e.g. Kukkonen et al. 2012; Luhta et al. 2016) within their background rocks, turbiditic mica schists with black schist intercalations.

In 2016, the COGITO-MIN project acquired new types of active and passive seismic surface and borehole data at the Kylylahti mine site (Figure 1) with the aim to develop new cost-effective seismic exploration methods (Koivisto et al. 2018). The COGITO-MIN surface seismic experiments included: 1) Two 6 km long 2D seismic reflection profiles (Heinonen et al. 2017, 2018, this volume), with 10 m wireless receiver and 20 m source interval (a combination of two 9.5 t Vibroseis trucks and explosives). 2) A novel 3D passive Seismic Interferometry (SI) experiment (Chamarczuk et al. 2017, 2018, manuscript submitted to Geophysics), in which a thousand 1C seismic receivers in a 3.5 x 3 km grid, with 200 m line spacing and 50 m inline receiver interval, recorded ambient noise for a month. 3) The 3D grid was also used for a sparse 3D active-source survey with an irregular distribution of Vibroseis and explosive sources that were primarily designed for 2D and borehole measurements. Additional sources were deployed where possible to fill gaps in the source distribution. Acquisition of active-source 3D seismic data with regular source line geometry in a populated area with abundant lakes, swamps and other restrictions would not have been achievable.

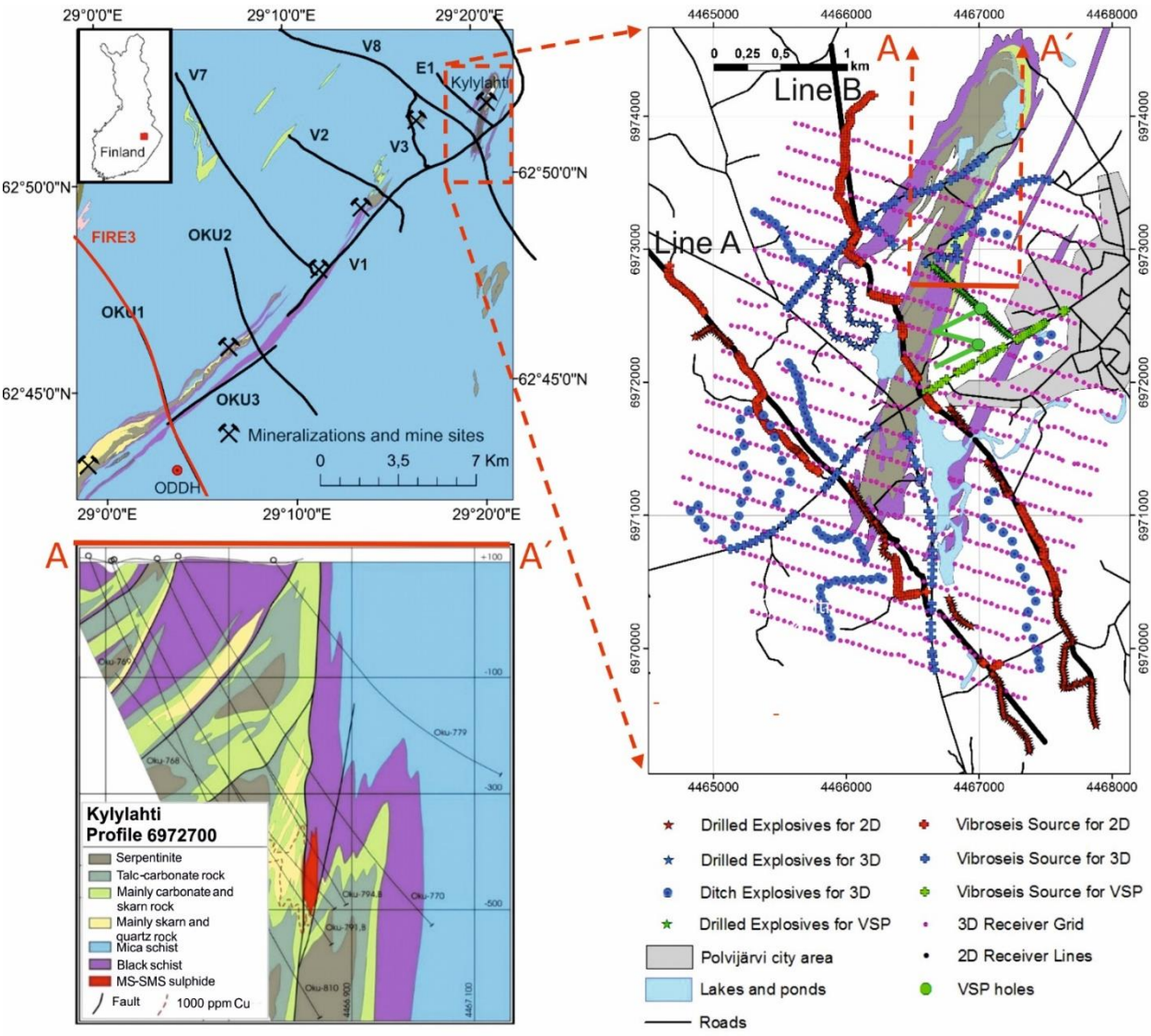

Figure 1. Top left: Crustal-scale FIRE3 and high-resolution seismic reflection profiles previously acquired in the Outokumpu area (Kukkonen et al. 2012) on the geological map (Bedrock of Finland –DigiKP). Bottom left: Geological cross-section of Peltonen et al. (2008) across the Kylylahti deposit. Right: Survey layout of the COGITO-MIN project.

The aim of the underground Vertical Seismic Profiling (VSP) survey (Riedel et al. 2017, 2018, manuscript submitted to Minerals) was to develop methods for high-resolution in-mine exploration and resource delineation, in particular for steeply dipping targets such as the Kylylahti deposit. A 3C VSP survey was performed in 4 boreholes starting from the mine tunnels (see Figure 1 for surface projections of the holes), with receivers at 2.5-5 m depth intervals over 300-500 m length and sources (time-distributed impact source VIBSIST-200) at 10-20 m intervals in the tunnels and on the surface. Additionally, to our knowledge for the first time in a hardrock mining environment, a Distributed Acoustic Sensing (DAS) VSP survey, where a fibre-optic cable is used as seismic sensor, was conducted in one borehole. The advantage of DAS is that, unlike in a conventional VSP survey, the whole borehole can be covered at once with dense measurement point spacing. This reduces the costs.

2. COGITO-MIN results and conclusions

A 3D view of the COGITO-MIN 2D profile B, 3D active-source data and VSP data from one borehole has been presented in Figure 2. 2D seismic reflection surveys provide a powerful means for understanding the larger-scale architecture of the mining and exploration fields. However, utilization of seismics for more detailed exploration targeting and mine planning typically requires a 3D seismic and/or a VSP seismic survey. For such, a well-planned, sparse active-source 3D survey can provide a cheaper alternative when the financial resources, terrain conditions or permitting do not allow for regular 3D source line geometries.

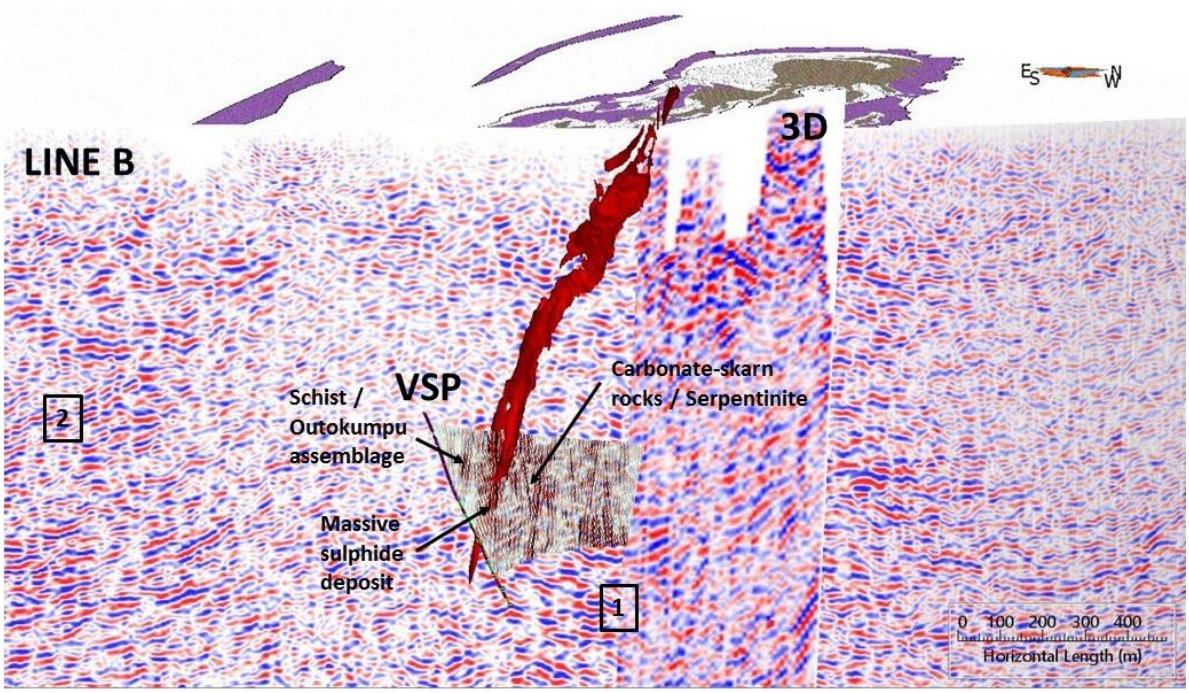

Figure 2. Example of the COGITO-MIN seismic data sets at different scales. In Kylylahti, the Outokumpu assemblage rocks appear within a tight synformal fold structure (Figure 1). In the surface seismic 2D and 3D data, this manifests as piece-wise reflectivity (indicated by 1 in the figure). More continuous reflectivity is obtained in the more optimally aligned VSP profiles (VSP data for one borehole shown in the figure), in which several known geological contacts can be identified (indicated on the figure). More continuous reflectivity in the surface seismic data is associated for example with black schist occurrences within the surrounding mica schist (indicated by 2 in the figure). The red surface is the Kylylahti sulphide deposit.

The aim of the COGITO-MIN passive seismic 3D experiment was to develop a cost-effective method for mapping the continuity of the ore host rocks through application of body-wave SI (e.g. Cheraghi et al. 2015). One application of SI is through cross-correlation of ambient noise to extract the reflection response between two receivers as if the virtual source is at one of the receiver locations. Chamarczuk et al. (2017, 2018, manuscript submitted to Geophysics) have developed a new SI workflow for processing such data acquired in the crystalline rock terrain. This workflow involves detection of body-wave events, evaluating their locations, and selective stacking over stationary-phase areas for creating virtual shot gathers. The resolution achievable with a passive SI survey is not comparable to the resolution achievable with active-source data, but the methodologies for processing passive data are developing fast and such data could be used to map the continuity of ore host rocks at a fraction of the cost of an active-source 3D survey, at least at mining sites where good distribution of (body-wave) noise sources can be expected.

The COGITO-MIN VSP images, for both the conventional 3C and the DAS VSP, have provided a detailed representation of the known geological contrasts (Figure 2) as well as of reflectors which had not been reached by previous drilling activities (Riedel et al. 2017, 2018,

manuscript submitted to Minerals). We conclude that VSP imaging provides a promising tool to guide (and reduce the costs of) drilling for in-mine exploration and resource delineation. In particular, DAS VSP surveys provide new cost-effective possibilities.

Joint interpretation of all the COGITO-MIN seismic data together with other geological and geophysical data (for example, AMT and gravity data collected along the 2D profiles) is currently underway.

Acknowledgements

The COGITO-MIN (COst-effective Geophysical Imaging Techniques for supporting Ongoing MINeral exploration in Europe) project 2016-2018 was funded through ERA-MIN. Funding for the 4 Finnish partners comes from Business Finland (former Tekes) and for the 2 Polish partners from the NCBR. *The COGITO-MIN Working Group: M. Chamarczuk, C. Cosma, N. Enescu, G. Gislason, S. Heinonen, S. Juurela, E. Koivisto, K. Komminaho, T. Luhta, M. Malinowski, S. Mertanen, S. Niemi, M. Riedel, B. Singh, L. Sito, A. Taipale, T. Törmälehto, K. Vaittinen, S. Väkevä, M. Wojdyla.

References:

Chamarczuk, M., Malinowski, M., Koivisto, E., Heinonen, S., Juurela, S. and the COGITO-MIN Working Group, 2017. Passive seismic interferometry for subsurface imaging in an active mine environment: case study from the Kylylahti Cu-Au-Zn mine, Finland. Proceedings of Exploration' 17: Seismic Methods & Exploration Workshop, 51-56.

Chamarczuk, M., Malinowski, M., Draganov, D., Koivisto, E., Heinonen, S. and Juurela, S., 2018. Seismic Interferometry for Mineral Exploration: Passive Seismic Experiment over Kylylahti Mine Area, Finland. EAGE NSG, EarthDoc, 5 p. Tu 2MIN 03

Cheraghi, S., Craven, J.A. and Bellefleur, G., 2015. Feasibility of virtual source reflection seismology using interferometry for mineral exploration: A test study in the Lalor Lake volcanogenic massive sulphide mining area, Manitoba, Canada. Geophysical Prospecting, 2015, 63, 833–848.

Heinonen, S., Malinowski, M., Gislason, G., Danaei, S., Koivisto, E., Juurela, S. and the COGITO-MIN Working Group, 2017. Active source seismic imaging in the Kylylahti Cu-Au-Zn mine area, Finland. Proceedings of Exploration' 17: Seismic Methods & Exploration Workshop, 47-50.

Heinonen, S., Malinowski, M., Hlousek, F., Gislason, G., Koivisto, E. and Buske, S., 2018. Seismic Exploration in the Kylylahti Cu-Au-Zn Mining Area: Comparison of Time and Depth Imaging Approaches. EAGE NSG: 2nd Conference on Geophysics for Mineral Exploration and Mining. EarthDoc, 5 p. Tu 2MIN P01

Koivisto, E., Malinowski, M., Heinonen, S., Cosma, C., Wojdyla, M., Vaittinen, K., Chamarczuk, M., Riedel, M., Kukkonen, I.T., 2018. From Regional Seismics to High-Resolution Resource Delineation: Example from the Outokumpu Ore District, Eastern Finland. EAGE NSG, EarthDoc, 5 p. Tu 2MIN P04

Kukkonen, I., Heinonen, S., Heikkinen, P., and Sorjonen-Ward, P., 2012. Delineating ophiolite-derived host rocks of massive sulphide Cu-Co-Zn deposits with 2D high-resolution seismic reflection data in Outokumpu, Finland. Geophysics, 77, WC213-WC222.

Luhta, T., Mertanen, S., Koivisto, E., Heinonen, S., Törmälehto, T. and Kukkonen, I., 2016. The seismic signature of the Kylylahti deposit: Initial results from new petrophysical measurements. 9th Lithosphere symposium, Programme and Extended Abstracts, 79-82.

Peltonen, P., Kontinen, A., Huhma, H. and Kuronen, U., 2008. Outokumpu revisited: New mineral deposit model for the mantle peridotite-associated Cu–Co–Zn–Ni–Ag–Au sulphide deposits. Ore Geology Reviews, 33, 559–617.

Riedel, M, Cosma, C., Komminaho, K., Enescu, N., Koivisto, E., Malinowski, M., Luhta, T., Juurela. S. and the COGITO-MIN Working Group, 2017. Seismic imaging of the Kylylahti Cu-Au-Zn ore deposit using conventional and DAS VSP measurements supported by 3D full-waveform seismic modeling. Proceedings of Exploration' 17: Seismic Methods & Exploration Workshop, 57-63.

Riedel, M., Cosma, C., Enescu, N., Koivisto, E., Komminaho, K., Vaittinen, K. and Malinowski, M., 2018. Distributed Acoustic Sensing versus Conventional VSP Imaging of the Kylylahti Polymetallic Deposit. EAGE NSG: 2nd Conference on Geophysics for Mineral Exploration and Mining. EarthDoc, 5 p. We 2MIN P12

Seismic monitoring of a hydraulic fracture stimulation

Pietari Koskenniemi, Jari Kortström, Kaiu Piipponen, Marja Uski and Tommi Vuorinen

Institute of Seismology, University of Helsinki
E-mail: kaiu.piipponen@helsinki.fi

The Enhanced Geothermal System-type power plant exploits bedrock heat by injecting cool water into a deep borehole and pumping heated water to the heat exchanger through another borehole. Water circulation between the boreholes is increased by hydraulic fracturing, i.e. by pumping fluids into the borehole under pressures high enough to fracture the rock. To control seismic risk associated with the operation, the operator implemented a three level seismic traffic light system: if earthquake magnitude and/or peak ground velocities exceeded the set limits, risk mitigation actions must be applied.

Keywords: Seismic monitoring, induced seismicity, hydraulic fracturing, deep drilling, enhanced geothermal system

1. Introduction

The first Enhanced Geothermal System (EGS) project in Finland has been initiated in the city of Espoo, southern Finland, by the Finnish power company St1. EGS-type power plant exploits bedrock heat by injecting water into a deep borehole and, after heated by geothermal heat, pumping it to the surface heat exchanger through another borehole. Hydraulic permeability between the boreholes is enhanced by hydraulic fracturing, i.e. by pumping fluids into the borehole under pressures high enough to increase the fracture aperture. Fracturing is, by definition, creating micro earthquakes, and a risk for a larger induced earthquake prevails.

Hydraulic fracturing of the first 6.4 km deep borehole was performed in June-July 2018. To control increased seismic risk associated with the operation, St1 implemented a three level (green, amber, red) seismic traffic light system (TLS): if earthquake magnitude and/or peak ground velocities exceeded the threshold limit, risk mitigation actions took place.

The city of Espoo mandated the Institute of Seismology, University of Helsinki (ISUH) to monitor the induced seismicity levels and the TLS exceedances.

Risk mitigation measures for threshold exceedance included rapid communication with Deep Heat project management and ISUH. Mitigation measures for amber conditions (ML≥1,0 and/or PGV≥1 mm/s) comprised additional monitoring and evaluation actions. If the earthquake magnitude and/or peak ground velocities exceeded the low limit for red (ML≥2,1 and PGV ≥7,5 mm/s), risk mitigation measures included immediate stop of stimulation by reducing pressure, injection rate or water volume.

2. Monitoring network

The monitoring network in Otaniemi consists of 17 stations within 10 km of the site: Eight 3C BB stations of ISUH and 12 3C short period borehole stations of ST1. The deployment provided a maximum azimuth gap of 57°, horizontal location accuracy of 200 m, and threshold magnitude of ML 0.0 in the site vicinity. Modified version of ISUH standard software (Kortström et al., 2018) was used for automatic event detection, location and size estimation.

For Traffic Light System purposes, 13 accelerometers were measuring the level of surface vibrations in sensitive locations such as hospitals and research laboratories.

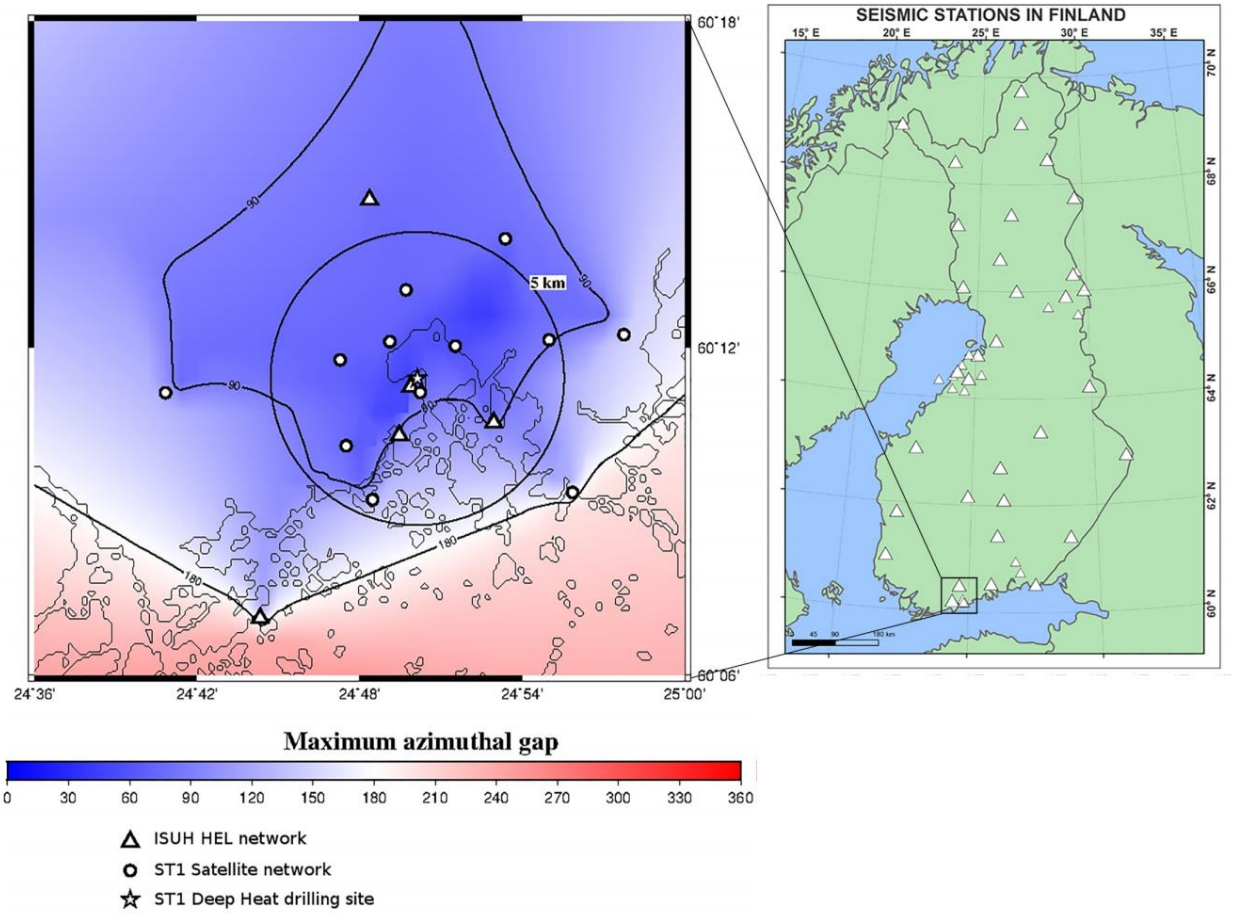

Figure 2 Temporary monitoring network used by ISUH. Three stations are outside the map area. Background colour shows the maximum azimuthal gap of the network. The inset map shows the network location in Finland.

3. Preliminary results from the induced seismicity analyses

From start of stimulation on June 4 to mid of August (three weeks after the stimulation), the system has detected close to 5000 events within a radius of 5 km from the drilling site. The largest events measured ML 1.8. They fell below the low limits of red TLS exceedance in both magnitude and peak ground velocity. However, these as well as many smaller events caused audible noise and tremors around the capital area. The smallest reported event was ML 0.5.

Over 500 events have been manually reanalysed. Preliminary focal mechanism data indicate both reverse and strike-slip type of movement. Most of the P-axes are rotated towards the direction of borehole.

References:

Ader, T. 2018. Otaniemi Geothermal Doublet, Traffic Light System for Seismic Monitoring
Kortström, J. T. Uski, M. R. Oinonen, K. J., 2018. In: Summary of the Bulletin of the International Seismological Centre. 52,1, 41-52.10.1016/j.cageo.2015.11.006

FIN-EPOS Research Infrastructure at the University of Oulu

E. Kozlovskaya[1,2], J. Narkilahti [3], J. Nevalainen [1,3], H. Silvennoinen [3], H. Jänkävaara [1,3]
[1]Oulu Mining School, Faculty of Technology, University of Oulu
[2] Geological Survey of Finland
[3] Sodankylä Geophysical Observatory, University of Oulu
E-mail: Elena.Kozlovskaya@oulu.fi

We describe the FIN-EPOS distributed research infrastructure of the Univerity of Oulu that is a part of EPOS Finnish National Research Infrastructure.

Keywords: EPOS, research infrastructure, seismic network, seismic equipment

1. EPOS ESFRI research infrastructure

The European Plate Observing System (EPOS) is the integrated solid Earth Sciences research infrastructure approved by the European Strategy Forum on Research Infrastructures (ESFRI) and included in the ESFRI Roadmap in December 2008. EPOS is a long-term integration plan of national existing RIs (http://www.epos-eu.org).

EPOS is aimed at a broad stakeholders community the following stakeholders categories:
1) Geoscience data providers 2) Scientific user community (including Academia) 3) National research organisations and funding agencies 4) Data and services providers and users outside the research community (including industry).

EPOS coordinates, collects and archives high-quality data from a range of Solid Earth science disciplines across Europe. In 2014 the EPOS consortium has been selected as one of the three ESFRI projects that are pushing the boundaries of scientific excellence, are strategically relevant for Europe, and are ready for immediate action. The implementation phase of EPOS will last till 2019. The result will be a single sustainable, permanent geophysical observational infrastructure. The three levels of EPOS are The National Research Infrastructures (NRIs) which represent the basic EPOS data providers and contribute to EPOS while being owned and managed at a national level. The Thematic Core Services (TCS) constitute the community-specific integration. They represent a governance framework where data and services are provided and where each community discusses its implementation and sustainability strategies as well as legal and ethical issues.The Integrated Core Services (ICS) represent the novel e-infrastructure consisting of services that will allow access to multidisciplinary data and data products, and synthetic data from simulations, processing, and visualization tools.

2. EPOS Infrastructure at the University of Oulu

The Finnish EPOS National Research Infrastructure is FIN-EPOS owned and managed at a national level by several organisations representing the basic geophysical and geodetic data providers in Finland. The FIN-EPOS infrastructure at the University of Oulu is distributed between Oulu Mining School of the Faculty of Technology (OMS) and Sodankylä Geophysical Observatory (SGO). The SGO is operating the permanent Northern Finland Seismological Network (FN) consisting of 9 broadband real-time seismic stations. Four stations (SGF, OUL, MSF and RNF) have been installed in 2005-2008 and five new stations (KLF, OLKF, KMNF, RANF, RAJF) were installed during the upgrade campaign in 2013-2018. Stations are equipped with STS-2 Trillium PA 120 and Trillium PH 120 seismic sensors. A regular daily data quality and SOH control is realized using a special system. The network is the data provider for EPOS TSC Seismology and TSC Antropogenic Hazard.

The SGO is also operating portable broadband equipment (11 units). Sercel Ltd. multichannel wireless seismic instrumentation of the University is operated jointly by OMS and SGO. The equipment consists of 40 3-component DSU-SA 3C MEMS sensors and 60 SG-5 1C sensors with

wireless RAU data acquisition units. The equipment is used both in passive and active seismic experiments in cooperation with Geological Survey of Finland.

3. Induced Seismicity Hub at the University of Oulu: a new contribution to FIN-EPOS

Induced seismicity hub at the University of Oulu is a new part of national FIN-EPOS infrastructure developed during 2017-2018 as a part of University of Oulu activities in EPOS Antropogenic Hazard Thematic Core Service (AH TCS: https://www.epos-ip.org/data-services/community-services-tcs/anthropogenic-hazards). The hub enables interface between national EPOS infrastructure and EPOS AH TCS and includes hardware for storage and long-term archiving of antropogenic hazard episodes related to Finland and software for preparation the data into standardized EPOS formats and for data quality control before depositing the data into TCS. The status of national research infrastructure is important for treating Intellectual Property Rights (IPR) and communication with present and potential data providers. After finalising the EPOS Implementation Phase in 2019 the hub will be supported by Oulu Mining School Research Centre.

Summanen, a new meteorite impact structure in Central Finland

T. Kreitsmann[1], L.J. Pesonen[2], S. Hietala[3], J. Lerssi[3], J. Nenonen[3] and J. Plado[1]

[1]Department of Geology, University of Tartu, Estonia, [2]Solid Earth Geophysics Laboratory, Physics Department, University of Helsinki, Finland [3]Geological Survey of Finland, Kuopio, Finland
E-mail: satu.hietala@gtk.fi

Meteorite impact cratering is a common process that affects planetary surfaces across the solar system throughout geologic time. On Earth, there are currently 190 confirmed impact structures, which are distributed unevenly around the globe. The Fennoscandian Shield houses 16.8% of them. There are currently 12 proven impact structures found in Finland. The latest discovery, Lake Summanen impact structure was proven in 2018 as based on discoveries of shatter cones and planar deformation features (PDFs) in quartz grains from erratic boulders SE from the structure. Search for meteorite impact signatures was initiated because of circular aeroelectromagnetic anomaly. Thus, Lake Summanen hides a relatively small (~2.6 km in diameter), probably simple, meteorite impact structure (Plado et al., 2018).

Keywords: impact structure, shatter cones, Summanen, lithosphere, geophysical anomaly, shock metamorphic feature.

1. Introduction

The Summanen meteorite impact structure (62°39'00''N, 25°22'30''E; ~275 km north from Helsinki; Fig. 1a) is located within the Paleoproterozoic Central Finland Granite Belt. The structure is covered with the Lake Summanen and, thus, is not directly observable. The lake is elliptical (8 × 4 km) in shape with the NW-SE elongation due to erosional influence of the Weichselian glaciation. The first hint of circular structure owes its discovery to the Geological Survey of Finland who in the early 2000`s carried out low altitude airborne geophysical mapping (Lerssi et al., 2007) that revealed a circular ~2.6 km wide aeroelectromagnetic resistivity anomaly.

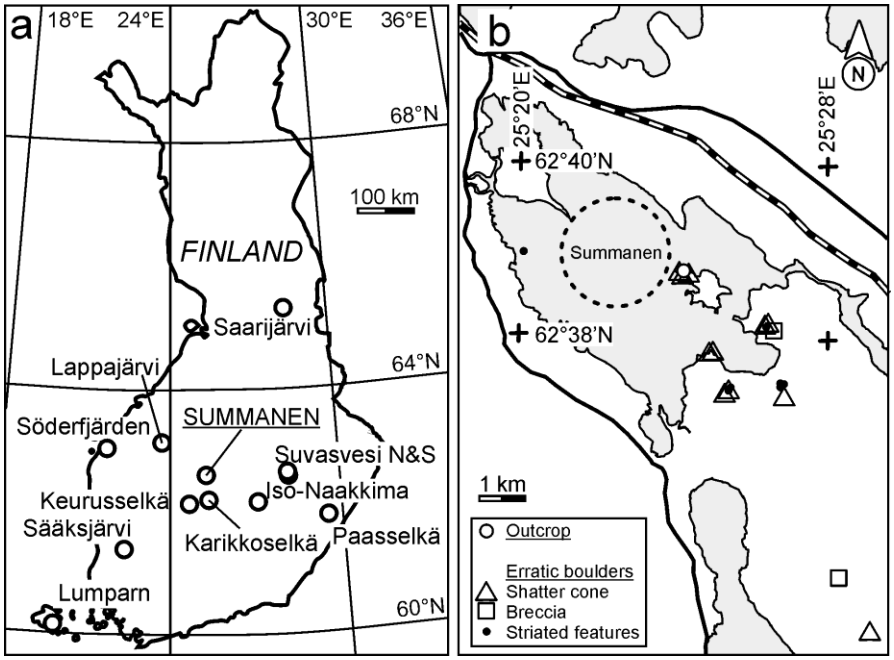

Figure 1. (a) Location of the Summanen meteorite impact structure along with other Finnish craters. (b) Location of impact-related findings in the vicinity of Lake Summanen. The dashed ring indicates the outline of the proposed crater structure as derived from aeroelectromagnetic data.

2. Methods

Geological field campaigns were conducted in 2017 to search possible impact signatures. The field-work concentrated on the south-eastern side of the lake following the ice flow direction. A few tens of erratic porphyritic granite boulders with distinct shatter cones (Fig. 1b) and striated features, and brecciated rocks were discovered. Boulder findings were GPS-referenced, described for lithology and elements of shatter cone surfaces, and sampled seventeen thin sections were prepared from breccias and rocks containing shatter cone features. Planar deformation features (PDFs) and other impact-induced high pressure mineralogical features were searched. Measurements of PDF orientations were done at the University of Tartu, Estonia, with a LOMO FS universal stage mounted on a polarizing microscope. A standard technique described by Langenhorst (2002) was followed in measuring the orientation of the c-axis, and poles to planar deformation features (PDFs) relative to the orientation of the thin section. Results were analyzed using the ANIE (a mathematical algorithm for automated indexing of PDFs in quartz grains) program by Huber et al. (2011).

3. Results

The erratic boulders in the area are generally well-rounded, but the carrying shatter cones are angular, suggesting a short travel distance. Most shatter cones were found within a distance of 5 km SE from the center of the geophysical anomalies. The outmost shatter-cone-bearing boulder was found at the distance of ~10 km from the anomalies. Most of the cones are in the fine-grained granite, but in rare cases, some have also formed in coarse-grained porphyritic granite.

Surfaces of shatter cones are curved, conical, the orientation of striations is variable, and they diverge from the apex, and striations are pervasive. Some striations on the surface show negative (concave) cone structure. The striations are diverging showing variable apical angles between 45° and 60°. The apical angles vary between 45° and 75°. The best-developed shatter cones occur in altered and fine-grained aplitic granite (Fig. 2a, b).

In two shatter-cone-bearing samples PDFs were identified. Altogether 64 measurements of the angles between host quartz c-axes and poles to PDFs were made in 60 quartz grains (Fig. 2c-e). In most cases, there was one set of PDFs per grain, usually penetrating the entire grain. Eighty-three percent of the measured angles are between 20 and 35°, which with 5° error would correspond to {1013} (22.95°) or {1012} (32.42°) in most cases. No PDFs with basal (0001) orientation were identified. All PDFs were decorated with average spacing between 5 and 8 μm. In addition to PDFs, planar fractures (PFs) were common, and in rare cases, feather features (FFs). Kink bands in biotite were abundant, including in the samples in which quartz does not display shock metamorphic features.

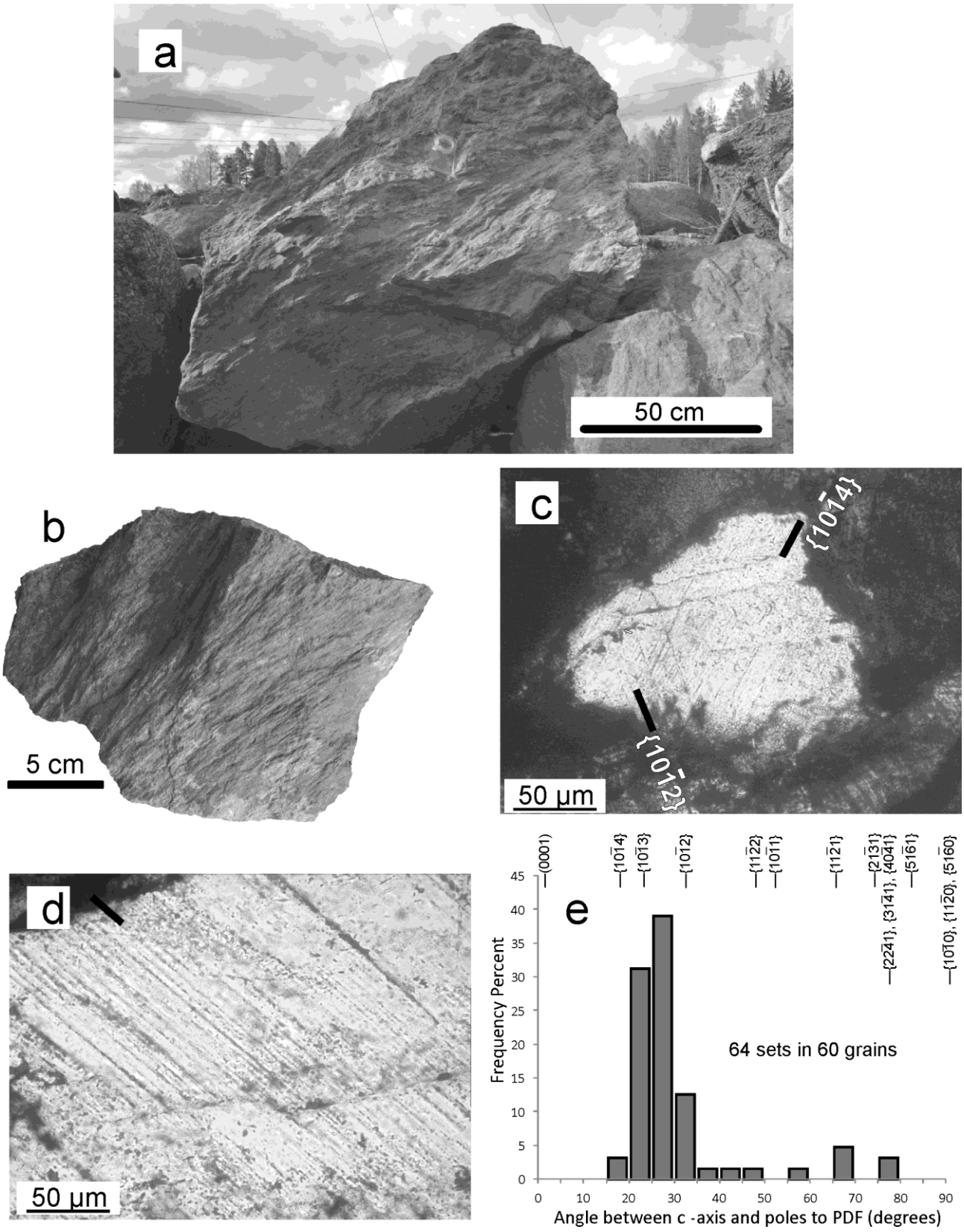

Figure 2. (a and b) Photos of shatter cone carrying boulders. (c and d) Thin section microphotographs of PDFs. (e) Histogram of angles between c-axis and poles to PDFs in 5° bins and possible corresponding PDF orientations.

4. Future studies

Age of the Summanen impact structure is still undefined, but it must be younger than 1.88 Ga. Radiometric (isotope) methods, as well paleomagnetic dating techniques will be applied to date the Summanen event. Additionally, there is a need for more comprehensive gravity mappings and 3D modellings. Seismic reflection and wide-band EM surveys may also provide additional information of the structure. The Summanen structure would be an ideal target for drilling, providing data for multidisciplinary (geology, geophysics, geochemical, and environmental) research and as such would be an ideal topic for graduate students and beyond.

Acknowledgements

Grant # IUT20-34 by the Estonian Research Council provided support for this study.

References:

Huber M., Ferrière L., Losiak A., Koeberl C., 2011. ANIE: A mathematical algorithm for automated indexing of planar deformation features in quartz grains. Meteoritics & Planetary Science, 46, 1418–1424.

Langenhorst F. 2002. Shock metamorphism of some minerals: Basic introduction and microstructural observations. Bulletin of the Czech Geological Survey, 77, 265–282.

Lerssi J., Mursu J., Niskanen M., Pajunen H., 2007. Summasjärven johtavuusanomalian tutkimukset vuosina 2005 ja 2006. Geological Survey of Finland, Report Q19/2243,2244/2007/1, 28 pp.

Plado J., Hietala S., Kreitsmann T., Lerssi J., Nenonen J., Pesonen L.J., 2018. Summanen, a new meteorite impact structure in Central Finland, Meteoritics & Planetary Science, 53.

Geothermal energy from deep bedrock in Finland – Geophysical and geological constraints

I.T. Kukkonen

[1]University of Helsinki, Dept. of Geosciences and Geopgraphy
E-mail: ilmo.kukkonen@helsinki.fi

In this presentation the exploration and use of geothermal energy in the Precambrian crystalline bedrock in Finland with the EGS principle is briefly discussed. Due to low heat flow and geothermal gradient, reservoir temperatures (>100°C) needed for production of space heating energy are attained only at the depth of about 6 km. It makes EGS projects challenging in general, and in particular with respect to drilling, stress field effects and hydraulic properties of the rock. As hydraulic conductivity is already relatively low at such depths, hydraulic stimulation is needed to enhance conductivity. Minor induced seismicity cannot be avoided, and the task is to keep the seismic activity at a level acceptable for the society and infrastructure. Regardless of the challenges, deep geothermal energy has potential also in normal continental crustal environments.

Keywords: geothermal energy, temperature, stress, hydraulic conductivity, crystalline rocks

1. General

There is a urgent societal need to reduce the use of carbon based fuels in energy production. Among the renewable energy resources, geothermal energy is one strong alternative. Although geothermal resources are much more favourable in active plate tectonic settings, such as subduction zones, spreading ridges and volcanically active areas, the potential of geothermal energy is nevertheless a valuable option even in geothermally 'cold' crystalline rock areas.

In 2014, the energy company St1 launched a pilot project in Espoo, Finland, to construct a geothermal EGS (Enhanced Geothermal System) plant at the depth of about 6 km for production of space heating energy. The produced heat will be fed into a local district heating network owned by company Fortum. The project has created an increasing interest for deep geothermal energy in Finland.

In the presentation, I review the geological and geophysical constraints of exploring and using geothermal energy from deep crystalline bedrock in Finland. The most important factors are temperature, temperature gradient, stress field and its orientation, and availability of hydraulically conductive (permeable) structures. Typically, natural hydraulic conductivity at depth is too low and it must be improved with hydraulic stimulation. It results in induced seismicity, which must be carefully considered and mitigated in EGS projects. From the technical point of view, drilling into hot considerable depths and high stress conditions requires reliable technologies for successful drilling operations and keeping the boreholes open during and after drilling.

2. Enhanced geothermal systems

Enhanced (or engineered) Geothermal Systems (EGS) comprise typically two deep boreholes drilled into a depth with high temperature at the distance of less than 1 km from each other (Figure 1). At depth, a fracture system either exists naturally or it is created in the reservoir with hydraulic stimulation, i.e., pumping fluid into the formation at pressures with exceed the opening pressure of fractures. As the bedrock is under a differential stress, increase in pore pressure will decrease the strength of the rock which eventually fails, and a small slips on fracture planes occur. One of the boreholes is the injection well for recharging cold water to the fracture system, while the other borehole is the production well, which collects the heated fluid (Figure 1).

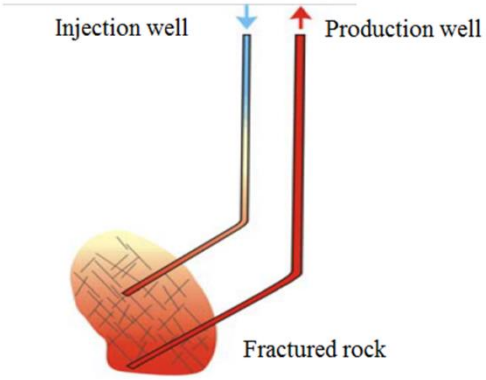

Figure 1. Enhanced geothermal system (EGS). The circulating fluid heats up in a fracture network between two deep boreholes (adapted from Piipponen, 2016).

3. Temperature

Geothermal heat flow is low (40 – 70 mW m^{-2}) in Finland), at a level typical for Precambrian terrain. Measured values in the uppermost 2 km are disturbed by the thermal signal of the last glaciation. Geothermal gradient varies from less than 10 mK/m to about 18 mK/m. The variation is due to variation in heat flow and heat production, but also to thermal conductivity variation (Fourier's first law of heat conduction) and the paleoclimatic disturbances.

Traditional power production (electricity) requires resources with temperatures exceeding 150°C. Such temperatures prevail only at depths of more than 10 km in Fennoscandia (see e.g., Veikkolainen and Kukkonen, this volume; and Figure 2). To generate heat energy for district heating systems, the resource should be at the temperature of at least 100 °C. It means about 6 km in depth. Therefore, drilling must be done into great depths, and it is far from being a simple operation. Generally, the temperature can be considered the best-known parameter in an EGS project.

3. Stress field

Rock stress increases with depth and brittle deformation prevails to about 28 km depth in the crust as revealed by the cut-off depths of earthquakes in Fennoscandia (Veikkolainen et al., 2017). The biggest principal component of the stress (σ_H) is horizontal and oriented most often SE-NW, i.e., towards the mid-Atlantic ridge (Heidbach et al., 2008). The vertical component of stress (σ_V) is the weight of the overburden, and it is usually the second largest component. The smallest component of stress is horizontal (σ_h). Mechanical behaviour of fractures and the prevailing faulting mechanism (normal, strike slip or reverse) depends on the ratios of the stress field components, the pore pressure in fractures. Increasing pore pressure decreases the normal stress on fracture planes, and improves the possibility for slip.

Although stress field is a tensor parameter, pore pressure is not. Therefore, slip will occur in fractures, which are optimally oriented to the smallest principal component of stress, i.e. perpendicular to σ_h. In southern Finland σ_h is directed roughly NE-SW, and thus the fractures most easily stimulated (opened) are oriented NW-SE.

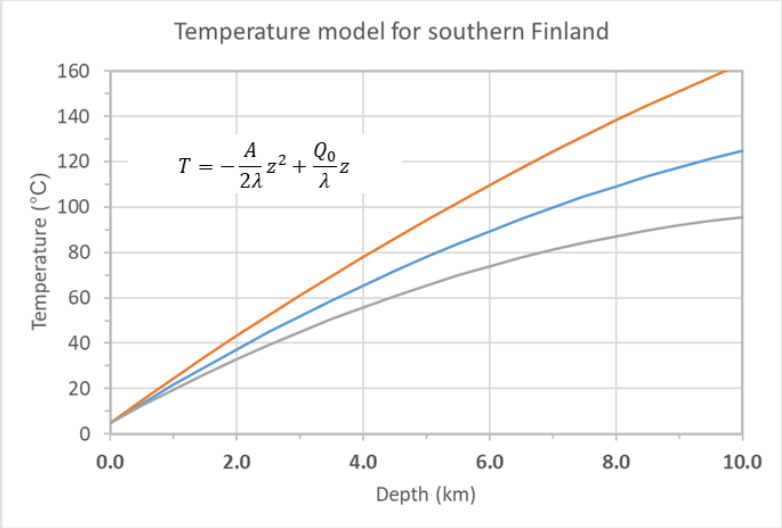

Figure 2. One-dimensional temperature model for southern Finland. Parameters for the middle curve: Q_0 = 51 mW m^{-2}, λ = 2.94 Wm^{-1} K^{-1}, A = 3.1 μW m^{-3}. The upper and lower curves show min-max estimates with conservative uncertainties assumed for the parameters.

4. Hydraulic conductivity

The exchange of heat between the hot reservoir rock and heat-carrying fluid takes place in the fracture system between the deep holes. An ideal situation would be a large volume of rock with high hydraulic conductivity and porosity. In case the fluid would be in contact with the whole volume of rock between the holes, the heat exchange would be most efficient. However, if the hydraulic conductivity is restricted to a planar system of fractures or even in a single fracture, the heat transfer is much less favourable. The heat to be mined with the EGS is stored in the rock by its heat capacity, and temperature recharge of the fracture walls takes place only by conduction. Conduction is much less efficient than advection by fluid flow. A system based on single fracture thus cools very rapidly, without reaching the life-time (15-25 years) needed to cover the investment cost. Therefore, the hydraulic properties and the spatial permeability structure are extremely important in defining the capacity of an EGS system.

Hydraulic conductivity can be improved with hydraulic stimulation. Fluid is pumped under high pressure to the reservoir between packers. Increasing pore pressure opens the fractures favourably oriented perpendicular to the smallest stress component σ_h. The success of the stimulation depends on the applied pressure, flow rate, fluid viscosity and whether the opened fractures remain open when the over pressure is removed. In oil-field stimulation, proppants (e.g. sand grain size mineral particles or synthetic materials) are typically added to the pumped fluid to keep the fractures open (Economides and Nolte, 2000).

Induced seismicity may create serious problems if the stimulation activates large faults. Well-known cases from Switzerland and Koreas have been discussed in the literature (Häring et al., 2008; Grigoli et al., 2008).

5. Discussion

Temperature gradient and deep temperature levels exclude the production of power from geothermal in the conditions of Finland. Reservoir temperatures required for power production (>150 C) would imply drilling far too deep in the crust (Figure 2). However, production of geothermal energy for space heating is possible. So far, the applications (such as the St1 project) aims at circulating down a cooled fluid of about 60°C and heating it up to about 100°C a fracture system at depth. The success of such scenarios is heavily dependent on the level hydraulic conductivity and spatial distribution of permeable structures in the reservoir.

The stress field gets very strong at depths of more than 5 km, which often results in instability problems of boreholes. Boreholes deform under high stress and break-outs are common. To keep boreholes stable a counter pressure must be applied in drilling. It means using heavy drilling muds, and for instance, mixtures of water, bentonite and barite are typical. Such a column of heavy mud may have a density of up to 2100 kg m^{-3} which then helps to increase the hydrostatic pressure in the borehole.

EGS systems have been tested in many projects, but so far, none of them has proven economical. It is mostly due to the fact that the required level of fluid flow rates and permeability have not been attained.

6. Conclusions

The most important factors for EGS systems in the crystalline rock in Finland are the reservoir temperature, temperature gradient, prevailing stress field and its orientation, and the availability of hydraulically conductive (permeable) structures, as well as mitigating induced seismicity. Regardless of the challenges, deep geothermal energy has potential also in normal continental crustal environments.

References

Economides, M.J. and Nolte, K.G. (eds), 2000. Reservoir stimulation (3rd ed.). John Wiley & Sons, Chichester.

Grigoli, F., Cesca, S., Rinaldi, A.P., Manconi, A., Lopez-Comino, J.A., Clöinton, J.F., Westaway, R., Cauzzi, C., Dahm, T. and Wiemer, S., 2108. The November 2017 Mw 5.5 Pohang earthquake: A possible case of induced seismicity in South Korea. Science, 10.1126/sience.aat2010 (2018).

Häring, M.O., Schanz, U., Ladner, F., Dyer, B.C., 2008. Characterization of the Basel 1 geothermal system. Geothermics 37, 469 - 495.

Heidbach, O., Tingay, M., Barth, A., Reinecker, J., Kurfeß, D. and Müller, B., The World Stress Map database release 2008 doi:10.1594/GFZ.WSM.Rel2008, 2008.

Piipponen, K., 2016. Modelling an Enhanced Geothermal System doublet in crystalline rock. In: Kukkonen, I.T. et al. (Eds), Lithosphere 2016 – Ninth Symposium on the Structure, Composition and Evolution of the Lithosphere in Finland. Programme and Extended Abstracts, Espoo, Finland, November 9-11, 2016. Institute of Seismology, University of Helsinki, Report S-65, pp. 109-111.

Veikkolainen, T., Kukkonen, I.T., Tiira, T., 2017. Heat flow, seismic cut-off depth and thermal modelling of the Fennoscandian Shield, Geophys. J. Int., 211, 1414–1427.

Veikkolainen, T., Kukkonen, I.T., 2018 (this volume). Heat flow and heat production in relation to geoneutrino signal near Pyhäsalmi mine.

Geochronology, geochemistry and structural setting of the Uunimäki gold mineralisation, SW Finland

T. Leskelä[1], J. Kara[1], I. Pitkälä[1], P. Skyttä[1], M. Väisänen[1], M. Tiainen[2], H. Leväniemi[2], J. Hokka[2], Y. Lahaye[2]

[1]Department of Geography and Geology, University of Turku, FI-20014 Turku, Finland
[2]Geological Survey of Finland, P.O. Box 96, FI-02151 Espoo, Finland
E-mail: tuoles@utu.fi

The Uunimäki gabbro was studied by zircon U-Pb geochronology which yielded an age of ~1.89 Ga, making it one of the oldest plutonic rocks in the Häme Belt. Geochemical analysis of the gabbro reveals that it lacks several characteristics for typical subduction zone rocks: (i) it does not have a negative Ta-Nb anomaly compared to average NMORB-composition, (ii) it shows a rather unfractionated REE pattern, (iii) it lacks clear enrichment of fluid-mobile elements (e.g. Ba, Rb, Th, Pb). Structurally, the Uunimäki gabbro is located at the intersection of several regional features: (i) steep NE-plunging folds, (ii) a ENE-WSW-trending deformation zone immediately to the north and (iii) a large N-S-trending deformation zone to the west. The gabbro itself has been deformed under both brittle and ductile conditions by primarily NW-SE-trending faults and shears.

Keywords: geochronology, geochemistry, structural geology, orogenic gold

1. Introduction

A two-year joint project between the Geological Survey of Finland (GTK) and the University of Turku was launched in the spring of 2017. Goals of the project include further structural mapping and interpretation of some previously discovered orogenic gold prospects in SW Finland (see also Kara et al. 2018, Pitkälä et al. 2018, this issue). The Uunimäki mineralisation was first discovered by GTK in 2008, during mapping of Au-critical fault and shear zones in spatially associated with gabbros (Kärkkäinen et al. 2016). The mineralisation was studied during the next decade by field mapping, till geochemistry, ground geophysical surveys and core drilling. The aim of this study is to (i) determine the age of the Uunimäki gabbro, (ii) link the mineralisation to the structural evolution of the western part of the Häme Belt, (iii) compare the hosting lithology of the Uunimäki mineralisation to the nearby Jokisivu and Palokallio gold mineralisations.

2. Geological setting

The Uunimäki mineralisation is located in the NW Häme Belt (Fig. 1) which was formed during the magmatic arc stage of the Svecofennian Orogeny at 1.90-1.87 Ga (Lahtinen et al. 2005). The lithology of the area consists of metavolcanic and metasedimentary rocks intruded by syn- and post-kinematic gabbros, diorites, tonalites, granodiorites, granites and pegmatites (Kähkönen 2005; Mäkitie et al. 2016; Nironen et al. 2016). The area has undergone polyphase deformation, with shear activity occurring post-peak metamorphism (Nironen 1999, Saalmann et al. 2010). In addition to Uunimäki, the western Häme Belt is host to other several orogenic gold occurrences (Eilu et al. 2012).

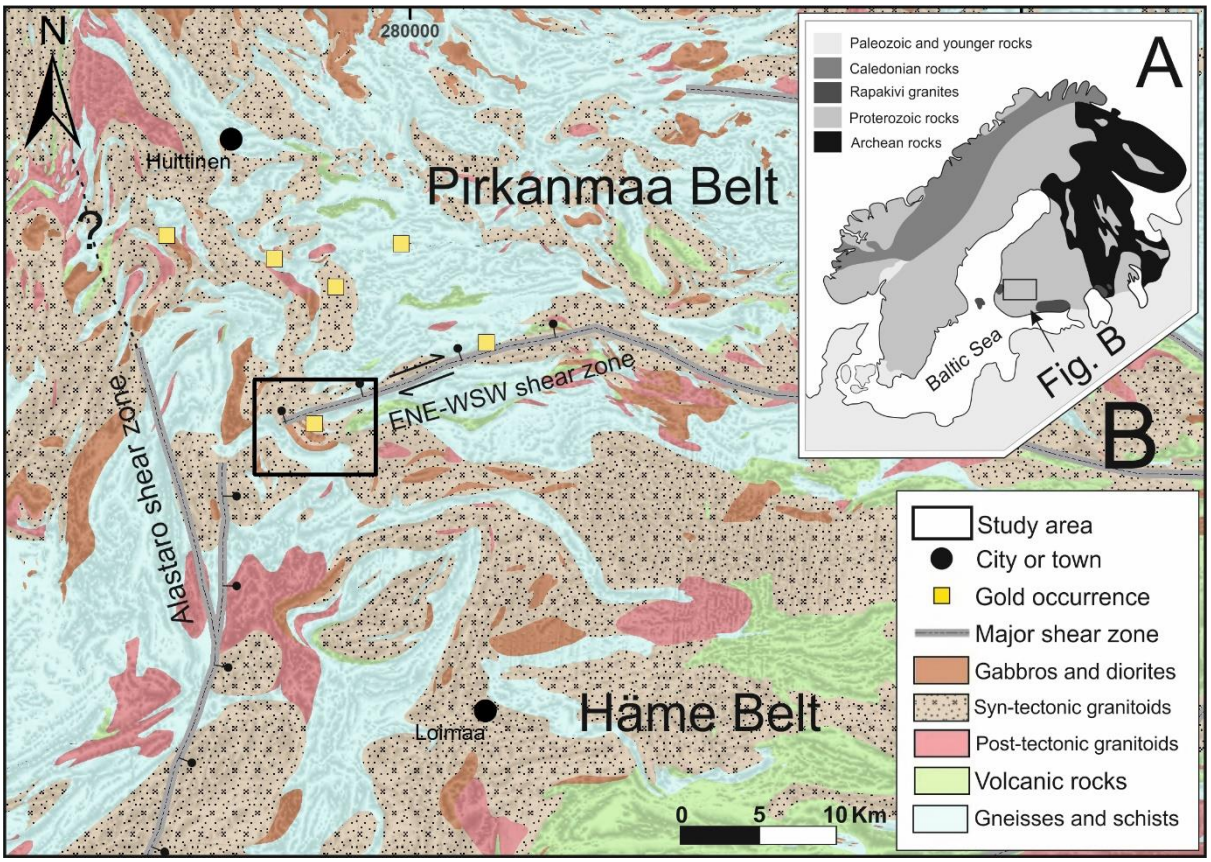

Figure 9. A: Overview of the Fennoscandian Shield modified after Koistinen et al. (2001), B: Lithological and structural map of the Häme Belt with the Uunimäki gold prospect marked by a black rectangle.

3. Petrology and geochemistry

The Uunimäki gabbro is exposed as a 1000 x 700 m large oval-shaped intrusion where the longest axis is NW-SE oriented. The gabbro is mostly medium-grained and equigranular, dark to dark-gray in color. The mineralogy of the gabbro consists of labradorite, amphibole that has been metamorphosed from clinopyroxene, biotite, and accessory ilmenite.

In the TAS-diagram the Uunimäki samples classify as gabbros due to their low SiO_2 and alkali contents. The gabbro shows slight enrichment in Fe_2O_3, Al_2O_3 and TiO_2 and depletion in MgO, K_2O and Ni compared to other gold-hosting mafic intrusive rocks in the area. Trace element concentrations show that the gabbro does not have a negative Nb-Ta anomaly which is typical for subduction zone rocks. The gabbro is only very slightly enriched in LREEs compared to HREEs. Furthermore, due to its low Th-concentration, and comparatively high Zr- and Nb-concentrations, the gabbro has more of an E-MORB affinity than a calc-alkaline volcanic arc affinity (Fig. 2).

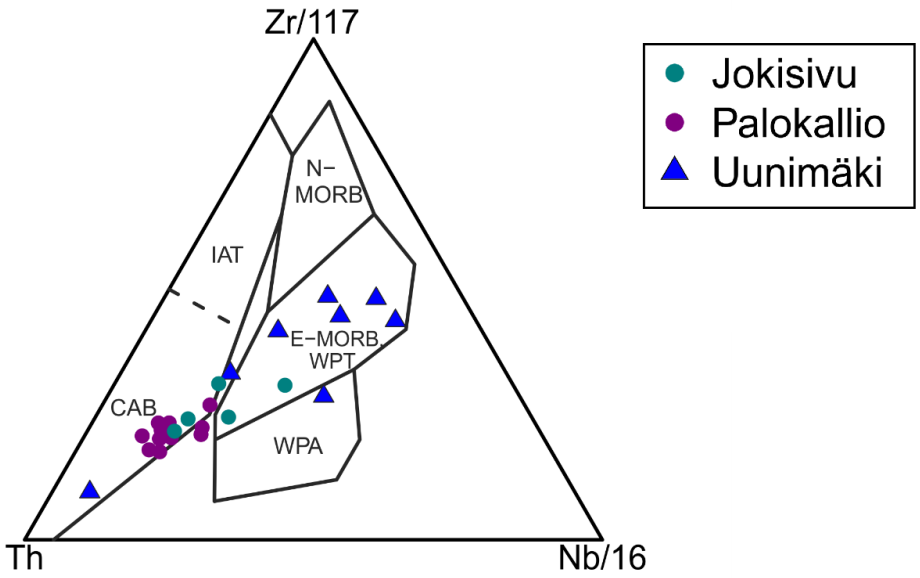

Figure 10. *Samples from the Uunimäki gabbro plotted into the Th-Nb-Zr diagram (Wood et al. 1979). Samples from the Jokisivu and Palokallio gold-hosting diorites shown for comparison.*

4. Geochronology

Zircons from an Uunimäki gabbro sample were separated for age determination. The U-Pb zircon age of the gabbro was determined in the Finnish Geoscience Research Laboratory at GTK, Espoo by laser ablation inductively coupled mass spectrometry (LA-ICP-MS). The analyses yielded a concordia age of ~1.89 Ga.

5. Structural setting

Structural mapping in the field supported by aeromagnetic geophysical maps show that the Uunimäki gabbro is located near the intersection of several regional structures. A zone of steeply NE- to E- plunging folds runs through the western Häme Belt, from Jokisivu through Uunimäki to Oripää. The folded area near Uunimäki has been reworked by two younger deformation zones: the N-S-trending Alastaro shear zone to the west, and the ENE-WSW-trending deformation zone just north of Uunimäki (Fig. 1). The Alastaro shear zone has been interpreted to be mostly a dip-slip-type zone, with the western block having a relative upwards movement. The ENE-WSW-trending shear and fault zone is also mostly dip-slip-type based on the lineation data. Some outcrops along the zone have a significant strike-slip-component as well as shown by the gentler plunging lineations associated with dextral shear sense indicators in the field. Thin sections from samples with steeply plunging lineations indicate a north-block-up sense of shear.

Though most outcrops of the Uunimäki gabbro look relatively ‘healthy’, deformation can be observed as shear bands and larger shear zones are inferred to be in topographic depressions between the individual outcrops. The gabbros close to these valleys usually appear more fractured, are crosscut by quartz veins and appear as a paler-gray in color.

6. Discussion and conclusions

The geochemical and geochronological differences between the Uunimäki gabbro and the other mafic plutonic rocks in the Häme Belt raise some questions. The gabbro does not show geochemical signatures of subduction and it is older than the other compared plutonic rocks. It is possible that the gabbro is from the same source as e.g., the Jokisivu diorite, but is simply more primitive, less fractionated. But the differences in trace element compositions raise the question

whether the gabbro could have been formed in an entirely different geotectonic environment, as the geochemical affinity of the gabbro resembles that of an EMORB rather than that of a subduction-related calc-alkaline rock.

The Uunimäki gold mineralisation fits the criteria of a typical Svecofennian orogenic gold deposit as outlined by Eilu et al. (2003): (i) the relatively small-scale shears that crosscut the Uunimäki gabbro are likely to be second-order structures caused by the nearby regional structures, (ii) the gold mineralisation at Uunimäki is hosted by a mafic intrusive rock, (iii) the host rock has been metamorphosed in amphibolite facies condition, as evidenced by the replacement of clinopyroxene with amphibole.

Acknowledgements
This study was funded by the Geological Survey of Finland.

References

Eilu, P., Ahtola, T., Äikäs, O., Halkoaho, T., Heikura, P., Hulkki, H., Iljina, M., Juopperi, H., Karinen, T., Kärkkäinen, N., Konnunaho, J., Kontinen, A., Kontoniemi, O., Korkiakoski, E., Korsakova, M., Kuivasaari, T., Kyläkoski, M., Makkonen, H., Niiranen, T., Nikander, J., Nykänen, V., Perdahl, J.-A., Pohjolainen, E., Räsänen, J., Sorjonen-Ward, P., Tiainen, M., Tontti, M., Torppa, A., Västi, K. 2012. Metallogenic areas in Finland. Geological Survey of Finland, Special Paper 53, 207-342.

Eilu, P., Sorjonen-Ward, P., Nurmi, P., Niiranen, T. 2003. A review of gold mineralization styles in Finland. Economic Geology, 98, 1329-1353.

Kara, J., Manninen, J., Leskelä, T., Skyttä, P., Väisänen, M., Tiainen, M., Leväniemi, H., 2018. Characterization of the structural evolution and structural control of the gold mineralizations in the Kullaa Area, SW Finland. Institute of Seismology, University of Helsinki, Report S-6X, xx-yy.

Koistinen, T., Stephens, M.B., Bogatchev, V., Nordgulen, Ø., Wennerström, M., Korhonen, J., 2001. Geological map of the Fennoscandian Shield, scale 1:2 000 000. Geological Surveys of Finland, Norway and Sweden and the North-West Department of Natural Resources of Russia.

Kähkönen, Y. 2005. Svecofennian supracrustal rocks. Precambrian Geology of Finland – Key to the Evolution of the Fennoscandian Shield. Developments in Precambrian Geology, 14, 343–405.

Kärkkäinen, N., Koistinen, E., Huotari-Halkosaari, T., Kuusela, J., Muhammad, S., Huhta, P. 2016. Uunimäki gold prospect, Huittinen, Southwest Finland. Geological Survey of Finland archive report 77, 55p.

Lahtinen, R., Korja, A., Nironen, M. 2005. Paleoproterozoic tectonic evolution. Developments in Precambrian Geology, 14, 481-531.

Mäkitie, H., Kärkkäinen, N., Sipilä, P., Tiainen, M., Kujala, H., Klami, J. 2016. Hämeen vyöhykkeen granitoidien luokittelua. Geological Survey of Finland archive report 33. 146p.

Nironen, M. 1999. Structural and magmatic evolution in the Loimaa area, southwestern Finland. Bulletin of the Geological Sociecity of Finland, 71, 57-71.

Nironen, M., Kousa, J., Luukas, J., Lahtinen, R. 2016. Geological Map of Finland – Bedrock 1:1 000 000. Geological Survey of Finland.

Pitkälä, I., Kara, J., Leskelä, T., Skyttä, P., Väisänen, M., Leväniemi, H., Hokka, J., Tiainen, M., Lahaye, Y., 2018. Shear zones and structural analysis of the Loimaa area, SW Finland. Institute of Seismology, University of Helsinki, Report S-6X, xx-yy.

Saalmann, K., Mänttäri, I., Peltonen, P., Whitehouse, M. J., Grönholm, P., Talikka, M. 2010. Geochronology and structural relationships of mesothermal gold mineralization in the Palaeoproterozoic Jokisivu prospect, southern Finland. Geological Magazine 147, 551-569.

Wood, D. A., Joron, J.L., Treuil, M. 1979. A re-appraisal of the use of trace elements to classify and discriminate between magma series erupted in different tectonic settings. Earth and Planetary Science Letters, 45, 326-336.

Intensity and Characteristics of Natural Remanent Magnetisation for Magnetic Data Interpretation in Sodankylä, Northern Finland

H. Leväniemi[1], S. Mertanen[1], M. Melamies[2], T. Karinen[2], S. Heinonen[1] and T. Niiranen[2]

[1]Geological Survey of Finland, P. O. Box 96, 02151 Espoo
[2]Geological Survey of Finland, P. O. Box 77, 96101 Rovaniemi
E-mail: hanna.levaniemi@gtk.fi

A new petrophysical dataset, comprising 73 outcrop samples, provides insight into natural remanent magnetisation in Sodankylä region in northern Finland. The data suggests that remanent magnetisation was blocked during the ~1.9 Ga deformation event and has been at least partially preserved. Remanent magnetisation dominates over the induced component in magnetite-bearing ultramafic volcanic rocks.

Keywords: petrophysics, remanent magnetisation, Sodankylä

1. Introduction

The Sodankylä area in northern Finland is currently one of the most lucrative mineral exploration regions in Finland due to its two significant Ni-Cu-PGE deposits, Sakatti and Kevitsa, in addition to several Au deposits. Geological Survey of Finland (GTK) conducts a regional study in Sodankylä, comprising two projects: 1) a data acquisition project XSoDEx (eXperiment of Sodankylä Deep Exploration), including a 2D seismic reflection survey (Buske et al., 2018, Heinonen et al., 2017) together with audiomagnetotelluric and gravimetric data collection, and 2) Business Finland ERDF and industry funded XL3D (Exploration Lapland 3D), which aims at producing state-of-the-art 3D exploration models of the area with the help of geophysical interpretations, data mining approaches and data integration (Niiranen & Nykänen, 2018).

The study area for these two projects expands ca. 50 km north of Sodankylä town (Figure 1) in the central part of the Central Lapland Greenstone Belt. The region is characterised by >2.2 Ga quartzites of the Sodankylä Group and >2.05 Ga Savukoski group metasediments and overlying ultramafic-mafic volcanic rocks. The complex geological history of the region culminates in ~1.9 Ga deformation related to Svecofennian collision and thrusting of the Lapland granulite belt (Hanski & Huhma, 2005).

In the XSoDEx project, we acquired a new petrophysical dataset to support geophysical data modelling and interpretation. GTK national petrophysical dataset (Korhonen et al., 1993) comprises information on density, magnetic susceptibility and intensity of remanent magnetisation for hundreds of samples in the study area, however, these samples are not oriented (for remanent magnetisation direction determination) and do not contain information on several parameters, e.g. P-wave velocities, which are useful for seismic data processing and interpretation. Thus a new outcrop sample dataset was collected along the reflection seismic profiles (see Figure 1) in autumn 2017. A technical overview of the dataset (including the measurement data) is given by Leväniemi et al. (2018).

Total number of samples in the new dataset is 73, three of which are not oriented. These data provides valuable information on petrophysical characteristics of the lithological units in the Sodankylä region especially for regional distribution and characteristics of natural remanent magnetisation NRM (remanence). In conventional magnetic data interpretation, the observed anomalies are assumed to be caused by induced magnetisation, which is aligned with the Earth's current magnetic field and proportional to magnetic susceptibility of the source. However, when strong enough, NRM can be a significant but unpredictable (in case the intensity and direction are not known) source of magnetic anomalies, as indicated e.g. by the local-scale study in the Kevitsa intrusion dunites by Montonen (2012). This paper discusses the observed petrophysical magnetic parameter data and their implications for magnetic data modelling in the Sodankylä region.

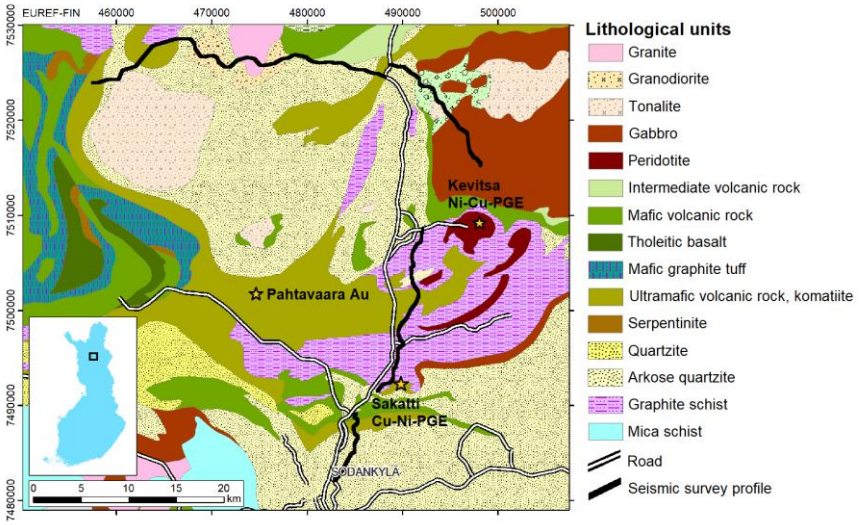

Figure 1. The XSoDEx/XL3D study area with major ore deposits.

2. Data collection, laboratory measurements and data preparation

The samples were taken with a rock hammer and oriented by setting them in their original place and marking the north direction with a compass and the horizontal level at least on two surfaces with a clinometer. The samples can be classified into 13 lithological main units, the main types of which are ultramafic volcanic rocks (15 samples), mafic plutonic rocks (12 samples) and quartzites (10 samples).

Sample preparation and petrophysical measurements were conducted at GTK's geophysical laboratory. The samples were prepared into 1-3 oriented subsamples. For each subsample, we measured density, magnetic susceptibility and resistivity by induction, intensity and direction of remanent magnetisation, porosity, P-wave velocity and resistivity by galvanic method. Königsberger ratio (Q value, ratio of remanent to induced magnetisation) was calculated for samples with magnetic susceptibility $k > 500 \times 10^{-6}$ SI, as low values indicate there are no ferromagnetic minerals that would carry remanent magnetisation. Due to the low sensitivity of fluxgate magnetometer, for remanent magnetisation analysis subsamples with intensity $J < 100$ mA/m were rejected from the data. For those samples with two or more subsamples left in the dataset, a mean direction of remanent magnetisation was calculated with the Fisher method (Fisher, 1953). A mean direction for the whole dataset was then also calculated with the same method from the remaining 40 sample directions.

3. Magnetic properties

Magnetic susceptibility and intensity of natural remanent magnetisation

Magnetic anomalies observed in any magnetic surveys are typically caused by magnetite or monoclinic pyrrhotite. Of these, magnetite-bearing rocks have higher susceptibility, often by 1-2 decades. When studying the magnetic susceptibility – Q ratio diagram (Figure 2), it becomes evident that on this region magnetic anomalies are mainly due to magnetite in ultramafic volcanic rocks (komatiites) and mafic rocks (mainly volcanic), although there are also several paramagnetic (low susceptibility) samples for these rock classes. The Q ratios indicate that there is a komatiite sample population with dominant remanence ($Q > 1$). As mineral's intensity of remanent magnetisation depends on its grain size (e.g. Butler, 1992), the magnetite in komatiites can be estimated to be moderately fine-grained.

In this diagram there are no samples from one of the major lithological units, graphite schists (Figure 1). Their susceptibilities and remanent magnetisation intensities in the dataset are very low, and it is apparent (also from airborne geophysical data) that they do not carry ferromagnetic minerals.

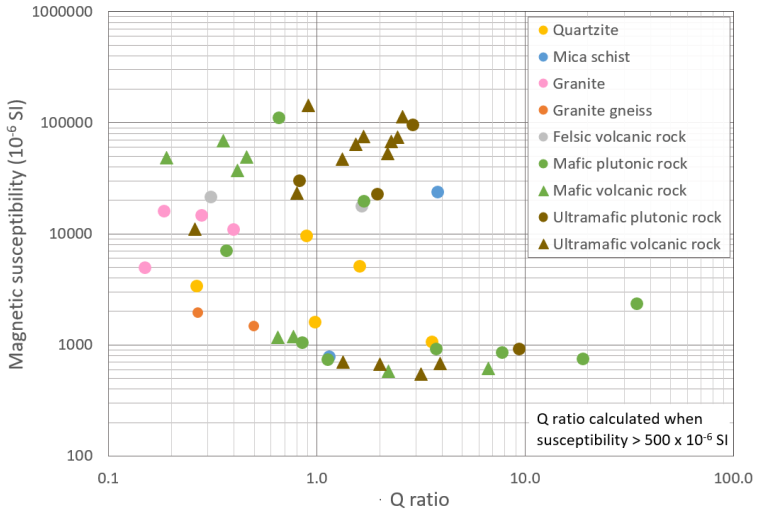

Figure 2. Magnetic susceptibility – Q ratio diagram presenting sample mean values classified according to their lithological units.

Direction of natural remanent magnetisation

The NRM directions (Figure 3) are spread quite widely, which is to be expected due to the sparse sampling in relation to the study area size. There is no obvious logic to the variation when comparing the sample directions with spatial location or their other magnetic parameter values. However, the majority of the declinations are located within the NW section with downward (positive) inclinations.

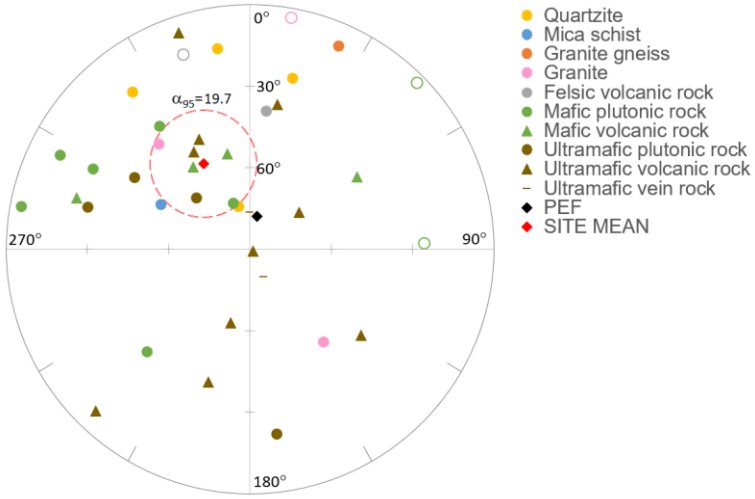

Figure 3. NRM directions according to rock class. Close symbols denote positive (downward) inclination, open symbols negative inclinations. PEF = present Earth's field.

The Fisher mean direction for all data ('site mean') has declination 331.4° and inclination 54.1°. The α_{95} confidence value for this mean is 19.7°, indicating that with 95% certainty the true mean is within this angle variation. The site mean value is close to the remanent magnetisation direction of declination ca. 345° and inclination 40-50°, observed in formations formed or overprinted during the 1.8-1.9 Ga Svecofennian orogeny (e.g. Mertanen and Pesonen, 2012). The data thus suggests that remanent magnetisation was blocked in the study area during that time and has been preserved, at least partially, from later tectonic and metamorphic events.

4. Conclusions

In the study area, the main cause for magnetic anomalies is moderately fine-grained magnetite in mafic-ultramafic volcanic rocks. A typical susceptibility range for these rocks is 20,000-100,000 x 10^{-6} SI and Königsberger ratios $Q < 1$ for the mafic rocks and $Q = 1 - 3$ for the ultramafic rocks. NRM directions suggest that remanent magnetisation was blocked during the ~1.9 Ga deformation and has been at least partially preserved. The use of these characteristic Q and NRM direction values should also be validated in magnetic modelling especially for the remanence-domaminated komatiites in order to increase reliability in constructing geological 3D models based on magnetic data.

5. Acknowledgements

The work was partly done within Business Finland ERDF funded “Exploration Lapland 3D” project, EURA2014 code A73339.

References:

Buske, S., Heinonen, S., Kozlovskaya, E., Karjalainen, J., Silvennoinen, H., 2018. Seismic exploration of mineral deposits in Northern Finland. Geophysical Research Abstracts, 20, EGU2018-13515, EGU General Assembly 2018.

Butler, R. F., 1992. Paleomagnetism: Magnetic Domains to Geological Terrains. Blackwell Scientific Publications,

Fisher, R. A,. 1953. Dispersion on a sphere. Proceedings of the Royal Society of London A217, 295–305.

Hanski, E., Huhma, H., 2005. Central Lapland greenstone belt. In: Lehtinen, M., Nurmi, P. A., Rämö, T. O. (eds) Precambrian Geology of Finland Key to the Evolution of the Fennoscandian Shield. Elsevier, Amsterdam.

Heinonen, S., Buske, S., Kozlovskaya, E., Karinen, T., Lahti, I., Niiranen, T., Leväniemi, H., Niemi, S., Silvennoinen, H., Nykänen, V., 2017. XSoDEx: Experiment of Sodankylä Deep Exploration. In: Hölttä, P., Nennonen, K., Eerola. T. (eds.) 3rd Finnish National Colloquium of Geosciences, Espoo, 15-16 March, Abstract Book, 34-35.

Korhonen, J. V., Säävuori, H., Wennerström, M., Kivekäs, L., Hongisto, H., Lähde, S., 1993. One hundred seventy eight thousand petrophysical parameter determinations from the regional petrophysical programme. In: Autio, Sini (ed.) Geological Survey of Finland, Current Research 1991-1992, 167-141.

Leväniemi, H., Melamies, M., Mertanen, S., Heinonen, S., Karinen, T., 2018. Petrophysical measurements to support interpretation of geophysical data in Sodankylä, northern Finland. Geological Survey of Finland, Open File Report 25/2018.

Mertanen, S. and Pesonen, L.J., 2012. Paleo-Mesoproterozoic Assamblages of Continents: Paleomagnetic Evidence for Near Equatorial Supercontinents. In: I. Haapala (Ed.), From the Earth’s Core to Outer Space. Lecture Notes in Earth System Sciences 137, Springer-Verlag Berlin Heidelberg 2012, 11-35.

Montonen, M., 2012. Indusoitu ja pysyvä magnetoituma kahdessa Kevitsan intruusion lävistävässä kairareiässä. Unpublished Master’s Thesis, University of Helsinki. (in Finnish)

Niiranen, T., Nykänen, V., 2018. Exploration Lapland 3D (XL3D) projekti – Ratkaisuja suurten aineistojen käsittelyyn ja geologiseen 3D mallinnukseen. Materia 2/2018, 63-64. (in Finnish)

Groundwater monitoring in postglacial faults -effect of atmospheric pressure and tide

M. Markovaara-Koivisto[1], T. Ruskeeniemi[1], P. Hänninen[1] and R. Sutinen[2]

[1]Geological Survey of Finland, PL96, 02151 Espoo, Finland
[2]Geological Survey of Finland, PL 77, 96101 Rovaniemi, Finland
E-mail: mira.markovaara-koivisto@gtk.fi

We present groundwater monitoring net established in 2017 in the northern Finland to record seasonal changes in the postglacial faults – and in the case of an earthquake. Monitoring stations are located in drill holes intersecting postglacial faults, in a river crosscutting a postglacial fault and in springs in the vicinity of the postglacial fault. The monitoring stations record electrical conductivity, temperature and water head. In addition, the stations measure snow depth and soil moisture to record surface water feed. By now one 3.3 magnitude earthquake has occurred at about 250 km distance from the closest monitoring station. It was followed by a small increase in the electrical conductivity and groundwater head in a drill hole. The increase in the groundwater head remained even after removing the effect of atmospheric pressure and tide.

Keywords: groundwater, monitoring, postglacial fault, northern Finland, earthquake

1. Introduction

Postglacial faults (PGFs) are old reactivated features or structures that have formed due to lithospheric plate stresses and postglacial land uplift (Arvidson, 1995; Wu, 1999). As they are the weakest parts of our bedrock, they are likely to reactivate as a results of the future glaciation cycles (Mattila et al. this publication). Typically bedrock faults consist of fault core and damage zone, in which the fracture number is high compared to the surrounding bedrock (Mitchell and Faulkner, 2009). Groundwater hosted in the soil on top of the bedrock and in the shallow parts of the bedrock contribute in the surficial water cycle. Deeper groundwater might be stagnant, enabling long water-rock interaction and concentration of soluble elements (Kietäväinen et al., 2013; Frape et al., 2014).

Behaviour of groundwater in occasion of an earthquake has been reported around the world (e.g. Roeloffs et al., 2003; Matsumoto et al., 2003; Woodcock and Roeloffs, 1996), but not its behaviour in faults. With automatic long-term monitoring of groundwater within fault environments we are prepared to record its behaviour in occasion of an earthquake and remove other sources by comparing the behaviour in different monitoring stations and environments.

2. Materials and methods

The monitoring of fault related groundwater in was realised by establishing nine stations in Suasselkä PGF, Isovaara-Riikonkumpu PGF, Pasmajärvi PGF and Venejärvi PGF (Figure 1). Three of the stations monitor groundwater behaviour in drill holes intersecting PGFs, two monitor spring waters in the PGFs and two in springs further away from the PGFs, and two monitor changes in a river flowing across a PGF. Monitoring begun on the 20th June 2017.

The river stations monitor hydraulic head, electrical conductivity (EC) and temperature of water upstream and downstream from the Suasselkä PGS. Also soil temperature and moisture, snow depth and air temperature are measured enabling removal of local environmental variety in the monitoring data. Spring stations measure the same parameters, added with gas content in the spring water. This is because gas bubbles have been noticed in some of the springs close to PGFs. Drill hole stations produce EC and temperature data directly from the fault zone. The sensors were carefully installed to the fault zone intersection determined beforehand by fracture logging from drill cores and measuring EC of the groundwater in the drill hole. The drill hole stations measure also soil temperature and moisture, and snow depth and air temperature. Measuring interval is 5 or 30 minutes.

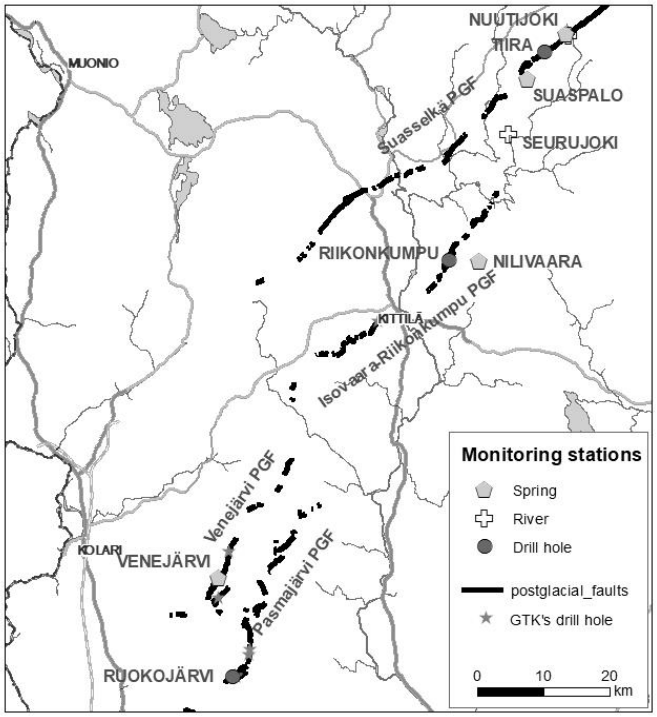

Figure 1. Location of the monitoring stations, postglacial faults and drill holes in northern Finland.

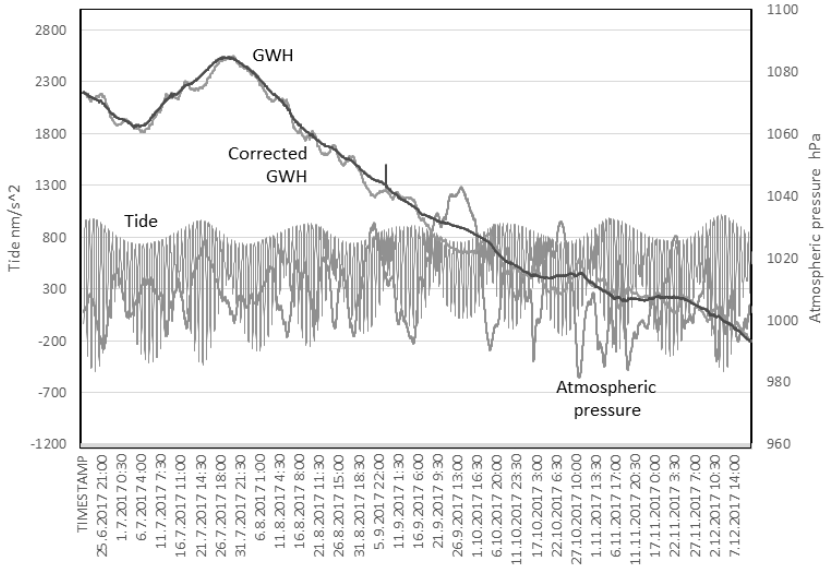

Figure 2. Effect of tide force and atmospheric pressure on groundwater head at Ruokojärvi drill hole monitoring station.

Tide and atmospheric pressure were noticed to affect the groundwater head (GWH) in the drill holes, as they showed wavy pattern and opposite behaviour with the changes in the atmospheric pressure (Fig. 2). These effects were removed from the GWH by firs simulating the tide forces with Tsof software (Van Camp and Vauterin, 2005) at the time and location of the measurements. Then the corrected GHW for the drill hole was calculated in BETCO software (Toll and Rasmussen, 2007) by using tide forces and atmospheric pressure data provided by the close by meteorological station of the Finnish Meteorological Institute (FMI).

3. Results

During the monitoring period a 3.3 magnitude earthquake (7th December 2017, Institute of Seismology, University of Helsinki) occurred at Liminka, some 250 km SSW from the Ruokojärvi monitoring station. GWH, EC and temperature of groundwater in the Pasmajärvi PGF are monitored in a drill hole at the depth of 21.5 m and 31.5 m. Figure 3 shows these parameters together with daily precipitation provided by FMI. EC at 21.5 m follows tightly GWH, which infers that the water takes part into the surface water circulation. For instance snow melt causes steep rise in both the GWH and EC. At 31.5 m depth along the drill hole, EC experiences a small descent but recovers soon after the snowmelt.

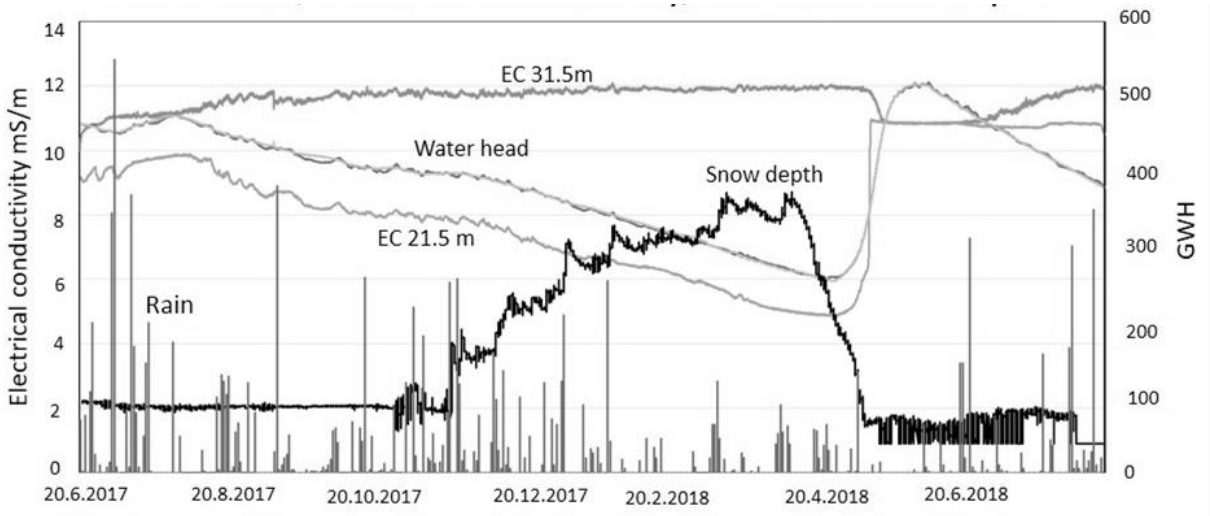

Figure 3. Monitoring data of drill hole station Ruokojärvi, where the drill hole intersects Pasmajärvi PGF. Groundwater head (histogram) is shown for both measured and atmospheric pressure+tide corrected.

Figure 4 shows the monitored parameters in December 2017, at the moment of the earthquake and possible effects recorded. The data shows three instances where EC rises both at 21.5 and 31.5 meters depth and the GWH trembles or rises even after removing the effect of atmospheric pressure and tide. These occur 1 day, 6 days and 17 days after the earthquake (7th December 2017). The recorded effects are rather small compared to the annual changes in the monitored parameters. Therefore we will continue to monitor the seasonal changes in the PGF groundwater and wait for other earthquakes closer to the monitoring stations to confirm the relationship or to identify other explanations for the observations.

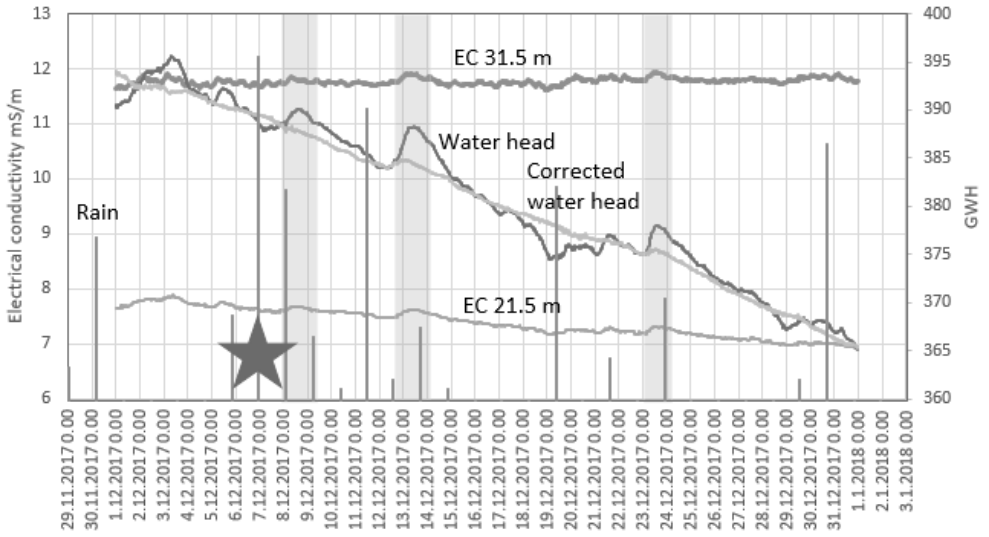

Figure 4. Possible effects of the 3.3 magnitude earthquake at Liminka 7.12.2017 (star, Institute of Seismology, University of Helsinki) on the electrical conductivity and groundwater head are marked with grey vertical bars. Daily rain is provided by Finnish Meteorological Institute.

4. Conclusions

The built monitoring station network has potential to record the effect of an earthquake on the groundwater in PGFs in spring, lake and drill hole intersection environments. Since building the monitoring network in June-October 2017 only one 3.3 magnitude earthquake has occurred, but due to the 250 km distance to our closest monitoring station, the recorded effects on the EC and GWH recorded from a drill hole were faint.

References:

Arvidsson, R., 1996. Fennoscandian earthquakes: whole crustal rupturing related to postglacial rebound. Science 274, 744–746.

Blomqvist, R., 1999. Hydrogeochemistry of deep groundwaters in the central part of the Fennoscandian Shield. Geol. Surv. Finland, Nuclear Waste Disposal Research. Report YST-101.

Kietäväinen, R., Ahonen, L., Kukkonen, I.T., Hendriksson, N., Nyyssönen, M., Itävaara, M., 2013. Characterisation and isotopic evolution of saline waters of the Outokumpu Deep Drill Hole, Finland – Implications for water origin and deep terrestrial biosphere. Applied Geochemistry, vol. 32, 37-51.

Mitchell, T. M., Faulkner, D. R., 2009. The nature and origin of off-fault damage surrounding strike-slip fault zones with a wide range of displacements: A field study from the Atacama fault zone, northern Chile. J. Struct. Geol., 31(8), 802-816.

Matsumoto, N., Kitagawa, G., Roeloffs, E.A., 2003. Hydrological response to earthquakes in the Haibara well, central Japan – I. Groundwater level changes revealed using state space decomposition of atmospheric pressure, rainfall and tidal responses. Geophysical Journal International 155, 3, 885-898.

Roeloffs, E., Snee, M., Galloway, D. L., Sorey, M. L., Farrar, C. D., Howle, J. F., Hughes, J., 2003. Water Level Changes Induced by Local and Distant Earthquakes at Long Valley Caldera, California. Journal of Volcanology and Geothermal Research 127, 3-4, 269-303.

Toll, N.J., Rasmussen, T.C., 2007. Removal of Barometric Pressure Effects and Earth Tides from Observed Water Levels. Ground water Vol 45, No. 1, p. 101-105.

Van Camp, M., Vauterin, P., 2005. Tsoft: Graphical and interactive software for the analysis of time series and earth tides. Computers and Geosciences 31, no. 5: 631–640.

Woodcock, D., Roeloffs, E., 1996. Seismically-induced water level oscillations in a fractured-rock aquifer well near Grants Pass, Oregon, Oregon Geology, 58 (2), 27-33.

Wu, P., Johnston, P. Lambeck, K., 1999. Postglacial rebound and fault instability in Fennoscandia. Geophysical Journal International 139, 657-670

On the displacement-length ratios of postglacial faults

J. Mattila[1], A. Ojala[1], T. Ruskeeniemi[1], J.-P. Palmu[1], M. Markovaara-Koivisto[1], N. Nordbäck[1], R. Sutinen[2]

[1]Geological Survey of Finland, PL96, 02151 Espoo, Finland
[2]Geological Survey of Finland, PL 77, 96101 Rovaniemi, Finland
E-mail: jussi.mattila@gtk.fi

By detailed analysis of the displacement (D) –length (L) data of postglacial faults from LiDAR-data, we show that the D-L ratios of postglacial faults are much higher than typically observed for surface ruptures of earthquakes. Based on mechanical concepts of earthquakes and observations from trenches made for paleoseismological studies, we propose that the high D-L ratios are caused by the fact that the postglacial faults are weak. The results of our study thus points to the fact that postglacial intraplate seismicity in northern Europe was mostly governed by weak faults. The discrepancy of the D-L ratios observed between the postglacial faults and recent earthquakes further requires us to ask the questions: is the approach of using length and displacement data for estimating the moment magnitudes of postglacial earthquakes reasonable?

Keywords: postglacial fault, slip profile, displacement-length ratio, Fennoscandia, earthquake

1. Introduction

Intraplate cratonic areas pose a challenge to seismic hazard assessment due to their low deformation rates and lack of large magnitude earthquakes, which makes the prediction of the long-term seismicity of such areas difficult. This is especially a concern for the seismic hazard assessment of high-level nuclear waste repositories located in intraplate settings. Although of low recurrence rate, large intraplate earthquakes do occur, as shown for example by prominent postglacial surface ruptures located in northern Europe (Kuivamäki et al., 1998; Kujansuu, 1964; Lundqvist and Lagerbäck, 1976; Olesen et al., 2004; Palmu et al., 2015). A peculiar feature of the postglacial faults, as noted by Muir Wood (1993), is that their displacement-length (D-L) ratios are high as compared to other reverse-type surface ruptures. Muir Wood (1993) did not, however, give conclusive causative reason for the observed D-L ratios, but rather speculated that these may be due to several displacement events, underestimated fault lengths or strong crust in the vicinity of the faults. With the recent availability of high-resolution LiDAR-data, it is now possible to map the surface ruptures of postglacial faults with high-precision (e.g. Mikko et al., 2015; Palmu et al., 2015) and to extract continuous displacement profiles from the scarps (Mattila et al., 2016; Ojala et al., 2017). By analyzing displacement and length data of the postglacial faults located in Finland, we explore whether the observations of high displacement-length ratios observed by Muir Wood (1993) are indeed correct and applicable to the Finnish faults. We further discuss the potential implications of the high D-L ratios for the mechanisms of postglacial earthquakes.

2. Methodology

In order to acquire detailed displacement and length data from the postglacial faults using high-resolution LiDAR data, we followed the methodology presented by Mattila et al. (2016) and Ojala et al. (2017). We extracted the displacement profiles by first manually digitising a line at the hinge of the scarp on the upthrown side and then on the hinge of the downthrown side. In the next step we projected the digitised lines on to the LiDAR-based DEM for as accurate representation of the topographic variation at the scarp hinges as possible. We then extracted the projected lines for further analysis with Rhinoceros3D software where we divided the line on the upthrown side of the scarp into a set of points separated by a one meter interval and, from these points, we then computed the closest point on the downthrown side line (Figure 1). We could then extract the vertical offset, or throw, of the scarp at 1 meter intervals by measuring the height

difference between the associated point pairs. Continuous offset profiles were then generated by collecting the height differences between all point pairs and by computing the locations of the points along the scarp. By using this data, we then computed the mean and maximum values of vertical offsets for each fault segments for further analysis. In a similar manner, we extracted the lengths of the surface ruptures from the digitised hinge lines. According to the National Land Survey of Finland (2018), the LiDAR data used in the analysis is the most accurate elevation data set available in Finland and the elevation accuracy is at maximum of 15 cm and the standard error in planimetric accuracy is 60 cm, which set the error limits for the displacement profile and length data.

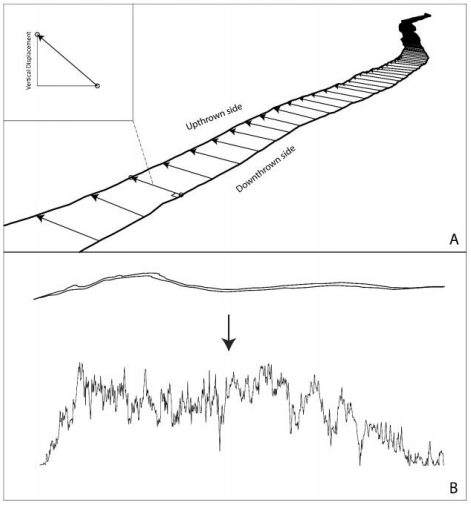

Figure 1. An example of the computation of offsets along the fault scarp. The line on the upthrown side of the scarps is divided into a set of points separated from each other by a one meter interval. Then the closest point on the downthrown side line was computed. By measuring the height difference between the point pairs, the vertical offset (or throw) of the scarp at that specific location can be defined. B) By collecting all the offset data along the fault segments, a continuous displacement profile for the scarps can be generated. From Ojala et al., 2017.

3. Results and discussion

The displacement-length data of the Finnish postglacial fault segments are shown in Figure 2, together with displacement-length data of surface ruptures of recent reverse earthquakes (Stirling et al., 2002), postglacial faults from Sweden and "geological" reverse faults (Elliott, 1976; Scholz and Cowie, 1990) that have accumulated displacement during long periods of time and many slip events and which are used here as a comparison for ruptures that have slipped only once. If isolated fault segments are consider, the Finnish postglacial faults have clearly higher D-L ratios than typically observed for reverse earthquake ruptures – the difference in the ratios is several orders of magnitude. Similar high-values are also observed for the Swedish postglacial faults, although the longest faults seem to cluster along with the trend for typical reverse earthquakes. In order to account potential uncertainties, we also plotted the D-L values for fault systems, which account for longer fault lengths and to the fact that reverse earthquake ruptures tend to be highly complex and consists of isolated fault segments. Such approach decreases the D-L ratios but the ratios are still higher than those of typical reverse earthquakes. We thus confirm the observations of (Muir Wood, 1993) and show that the D-L ratios of postglacial faults are higher than usually observed for earthquake surface ruptures.

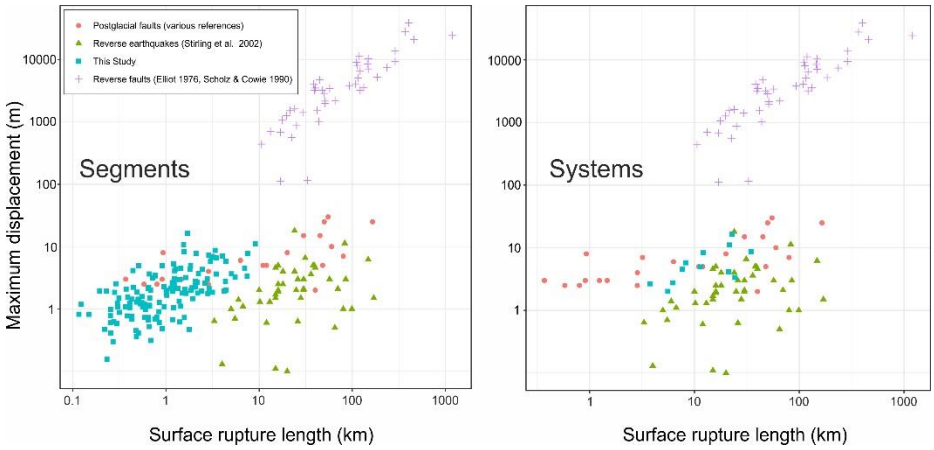

Figure 2. *Displacement-length data for Finnish postglacial fault segments (left-hand side figure) and systems (right-hand side figure), reverse earthquakes, Swedish postglacial faults and "geological" reverse faults.*

Displacement (D) –length (L) ratios of faults are proportional to the stress drop (Δσ) and fault strength (Stiffness or Young's modulus) as given by the equation (Gudmundsson, 2011):

$$\frac{D}{L} = \frac{2\Delta\sigma(1-\nu)}{E}$$

High D-L ratios may thus be explained either by high stress drops, weak faults or by a combination of these. Based on observations of postglacial faults in several trenches, the weak-fault hypothesis is a likely scenario, although we cannot exclude the possibility of high stresses either, potentially promoted by stress accumulation under the continental ice sheet during a long period of time.

4. Conclusions

The displacement length-ratios of the postglacial faults are high compared to those of typical earthquake surface ruptures and such high ratios may be explained either by extremely high stresses during the rupture or by weak faults. Direct observations of the known postglacial faults from trenches made for paleoseismological studies show that postglacial ruptures took place in old faults, often portrayed by highly weathered and fractured reactivated mylonites, promoting the weak-fault hypothesis. We cannot exclude the possibility that high-stresses also contributed to the formation of the observed high displacement-length ratios but the observations of the fault properties indicate that the fault strength did play a major role. We thus postulate that postglacial intraplate seismicity in northern Europe was mostly governed by weak faults. The high D-L ratios may also have further implications. As the moment magnitudes of paleoearthquakes are typically estimated from the observed length and displacement values and compared to those of present-day earthquakes and their moment magnitudes (Leonard, 2010; Wells and Coppersmith, 1994), the discrepancy of the D-L ratios observed here requires us to ask the question: is this approach reasonable?

References:

Elliott, D., 1976. The Energy Balance and Deformation Mechanisms of Thrust Sheets. Philos. Trans. R. Soc. Math. Phys. Eng. Sci. 283, 289–312. https://doi.org/10.1098/rsta.1976.0086
Gudmundsson, A., 2011. Rock Fractures in Geological Processes. Cambridge University Press, Cambridge. https://doi.org/10.1017/CBO9780511975684
Kuivamäki, A., Vuorela, P., Paananen, M., 1998. Indications of postglacial and recent bedrock movements in Finland and Russian Karelia. (Geological Survey of Finland Report No. YST-99). Geological Survey of Finland.
Kujansuu, R., 1964. Nuorista siirroksista Lapissa. Geologi 16, 30–36.
Leonard, M., 2010. Earthquake fault scaling: Self-consistent relating of rupture length, width, average displacement, and moment release. Bull. Seismol. Soc. Am. 100, 1971–1988. https://doi.org/10.1785/0120090189
Lundqvist, J., Lagerbäck, R., 1976. The parve fault: A late-glacial fault in the Precambrian of Swedish Lapland. Gff 98, 45–51. https://doi.org/10.1080/11035897609454337
Mattila, J., Ojala, A.E.K., Sutinen, R., Palmu, J., Ruskeeniemi, T., 2016. Digging deeper with LiDAR : Vertical slip profiles of post-glacial faults, in: Lithosphere 2016 - Ninth Symposium on the Structure, Composition and Evolution of the Lithosphere in Fennoscandia. Programme and Extended Abstracts. Presented at the Lithosphere 2016 Symposium, University of Helsinki, pp. 87–90.
Mikko, H., Smith, C.A., Lund, B., Ask, M.V.S., Munier, R., 2015. LiDAR-derived inventory of post-glacial fault scarps in Sweden. GFF 137, 334–338. https://doi.org/10.1080/11035897.2015.1036360
Muir Wood, R., 1993. A review of the Seismotectonic of Sweden (Technical Report). Svensk kärnbränslehantering (SKB), Stockholm.
National Land Survey of Finland, 2018. Laser scanning data [WWW Document]. URL http://www.maanmittauslaitos.fi/en/maps-and-spatial-data/expert-users/product-descriptions/laser-scanning-data
Ojala, A.E.K., Mattila, J., Ruskeeniemi, T., Palmu, J.P., Lindberg, A., Hänninen, P., Sutinen, R., 2017. Postglacial seismic activity along the Isovaara–Riikonkumpu fault complex. Glob. Planet. Change 157, 59–72. https://doi.org/10.1016/j.gloplacha.2017.08.015
Olesen, O., Blikra, L.H., Braathen, A., Dehls, J.F., Olsen, L., Rise, L., Roberts, D., Riis, F., Faleide, J.I., Anda, E., 2004. Neotectonic deformation in Norway and its implications: A review. Nor. Geol. Tidsskr. 84, 3–21.
Palmu, J.-P., Ojala, A.E., Ruskeeniemi, T., Sutinen, R., Mattila, J., 2015. LiDAR DEM detection and classification of postglacial faults and seismically-induced landforms in Finland: a paleoseismic database. GFF 137, 344–352.
Scholz, C.H., Cowie, P.A., 1990. Determination of total strain from faulting using slip measurements. Nature 346, 837–839. https://doi.org/10.1038/346837a0
Stirling, M., Rhoades, D., Berryman, K., 2002. Comparison of earthquake scaling relations derived from data of the instrumental and preinstrumental era. Bull. Seismol. Soc. Am. 92, 812–830.
Wells, D.L., Coppersmith, K.J., 1994. New Empirical Relationships among Magnitude, Rupture Length, Rupture Width, Rupture Area, and Surface Displacement. Bull. Seismol. Soc. Am. 84, 974–1002.

3D-density model of the Earth crust for central part of the East-European platform

O.M. Muravina[1], V.N. Glaznev[1] and M.V. Mints[2]

[1]Voronezh State University, Voronezh, Russia
[2]Geological Institute RAS, Moscow, Russia
E-mail: muravina@geol.vsu.ru

In this article we describe a method for constructing a complex density model of the lithosphere of the central part of the East European Platform, developed taking into account the particular geological structure of the study region. Seismic and geological data on the structure of the medium and petrophysical data on the density of the sedimentary cover and the upper part of the crust were used as a priori information. The incompleteness of a priori data was overcome by using the methods of stochastic estimates of unknown parameters of the structure of the medium. As a result, a density model of the lithosphere and upper mantle up to depth of 80 km was obtained. The reliability of the model is due to the compliance of the gravitational field and a priori information.

Keywords: lithosphere, crust, density, gravitational field, seismic model, inversion, simulation results

1. General

The article presents a model of the density of the crust and upper mantle of the central part of the East European Platform. The density model of the lithosphere to a depth of 80 km was the result of an inversion of the gravity field in a spherical coordinate. The inverse problem was solved for three variants of the initial models, formed on the basis of generalization and complex interpretation of a large number of geological, seismic, geothermal and petrophysical information relating to the studded area.

The adverse factor of unevenness of a priori data, caused by the scale of the object of study, was overcome using the methods of stochastic estimates of unknown parameters of the media. For example, to estimate the position of the upper crustal boundary in the model the correlation functions of stochastic potential fields in terms of the geometric parameters of the mass carrier was used. As a result we obtained an estimate of the thickness of the gravitational layer - the layer with the maximum density differentiation of rocks (Glaznev et al, 2014). The methods of stochastic modeling were also used in the construction of a thermal model of the region which needed to estimate the density of the deep layers of the lithosphere from seismic data on the velocity of rocks (Glaznev et al, 2015).

2. Method for solving the inverse problem

Inversion of the gravitational field was performed by the method of local corrections, adapted to solve the problem. The method of local correction has proven itself well when working with input data represented by large arrays of numbers, which makes it possible to effectively use it in density modeling of the lithosphere for large areas**.** The iteration process is organized as follows: at each design point, the residual gravity field is calculated for which the corresponding residual of the density of the equivalent layer is found. Then, the density residual is redistributed into the layers of the medium in accordance with an a priori given weight function. Thus, the starting model is corrected in succession. The algorithm is stable provided that the starting model is correct.

Obviously, the starting model plays an important role in ensuring the geological content of the solution. This model summarizes the known seismic, petrophysical and geological data related to the field of study. When solving an inverse problem for the regional data, the starting model is described by a significant number of parameters and is characterized by a high degree of complexity. In fact, in the process of field inversion, this model is refined within the specified

limits of variation of parameters in order to obtain a mass distribution equivalent to the observed field.

Unlike the traditional method of local corrections, we used the recursive method of approximation of the medium. The use of internal recursion allows us to divide the original elementary body into smaller elements, if necessary. The second modification concerns the method of redistributing residual density to increase the stability of the solution. At each point, the remainder is divided into a smoothed and local component. The second modification concerns the method of redistributing the density deviation in order to increase the stability of the solution. At each point, the residual is divided into a smoothed and local component. The local part is redistributed into vertical cells of a given number of upper layers. The smoothed part of the residual is redistributed into a cone with a given raster width in accordance with the principles of obtaining a "normal solution". This procedure is determined by the weight function. The weight function characterizes the measure of uncertainty in the transition from velocity to density in the layers of the medium separated by seismic and geological data. The weight function is calculated for each point of the medium.

3. Input data

As a gravity field in the Bouguer reduction, the EGM2008 model (Pavlis et al, 2012) was used, synthesized for the entire territory under consideration at an average level of the region's topography at the 5'×5' grid. The inversion procedure involved a 2D array of the reduced gravitational field, obtained after taking into account the effect of the sedimentary cover. The reduced field was set on the surface of the relief in the nodes of a regular grid (15'×15').

To create the starting model, we used the results of specialized seismic observations, seismological materials on the study of the structure of the lithosphere, generalized geological models of the sedimentary complex of the cover. Seismic data became the basis for the creation of a six-layer structural model of the structure of the lithosphere, within which further constructions were carried out. The boundary of the upper crust was estimated from the results of stochastic modeling (Glaznev et al, 2014).

The position of the Moho boundary was set of data in accordance with the model EUMOHO2007 (Grad et al, 2009). Considering the fact, that the position of the Moho surface in this model is given with some variance depending on the representativeness of the initial seismic data, three variants of starting models were formed: with a minimum, average and maximum position of the Moho boundary. For all three models, the boundaries of the "transition", "basic" and "diorite" layers changed accordingly. In all case the depth of the gravitational layer remains becomes as constant.

The inclusion of petrophysical studies in the procedure of complex modeling is a necessary condition for obtaining reliable results. Special attention was paid to the problem of maximizing the use of a large amount of known data on the density of sedimentary and crystalline rocks of the upper crust. Over several decades, more than 4,000 wells have been drilled in the region, and about 1,000,000 petrophysical determinations of crystalline and sedimentary rocks have been made. This information became the basis of the digital spatial database of petrophysical data of the region. To solve the problems of robust estimation, identification and spatial analysis of petrophysical information, the method of group accounting of arguments was effectively used for the first time. (Muravina, 2012; Muravina and Ponomarenko, 2016). The developed method for the synthesis and analysis of petrophysical information allowed the formation of three-dimensional petrophysical models of sedimentary and crystalline rocks of the upper layers of the earth's crust (Muravina and Zhavoronkin, 2015). The contribution of sedimentary rocks to the gravitational field was considered by solving the direct gravimetry problem for the corresponding petrophysical model.

Estimation of the density of the deep layers of the lithosphere was carried out on the basis of the seismic velocity model calculated from seismic velocity data and the stochastic thermal

model of the media. The transition from velocity to density values was carried out on the basis of approximation stochastic dependences of the relationship between velocity and density of the rocks, considering lithostatic pressure and temperature. Thus, density model of the media were used as set of data at the boundaries of the "gravi-active", "diorite", "basalt", “transition” layers and the upper mantle. For a uniform presentation of the data, thin gradient layers were introduced at the boundaries of each layer. As a result, a starting density model was formed as 3D array of absolute density values given in spherical coordinates at the boundaries of nine layers along a radius to a depth of 80 km. In addition, at each point of the model, amplitude restrictions on the density and the entropy values of the conditional density probability were specified.

4. Results

As a result of the inversion of the gravitational field in the spherical formulation, performed within the framework of the adopted three versions of the starting models, the corresponding three-dimensional density models of the lithosphere were calculated. Since a necessary condition for the adequacy of the effective model is to achieve a given discrepancy - the difference between the model and observed values of the fields, the most adequate model is the model with the maximum depth of the Moho border. Maps of starting and final residuals of the field for this model are shown in Figure 1.

An analysis of the data obtained shows that a strong density differentiation is characteristic of the upper layers of the crust. The main tectonic subdivisions formed in the Paleoproterozoic are to some extent reflected in the pattern of density distribution only at the upper and middle levels of the crust. The layers of the lower crust are characterized by a more homogeneous character of the density distribution. The correlation with the boundaries of tectonic structures is violated. The exception is the structure of the Dnieper-Donetsk depression, the contours of which are confidently traced to the upper mantle. Thus, as a result of a complex field inversion, a consistent three-dimensional density model of the lithosphere of the central part of the East European Platform was obtained for the first time, consistent with petrophysical materials and seismic data on the structure of the lithosphere and corresponding to the observed gravity field.

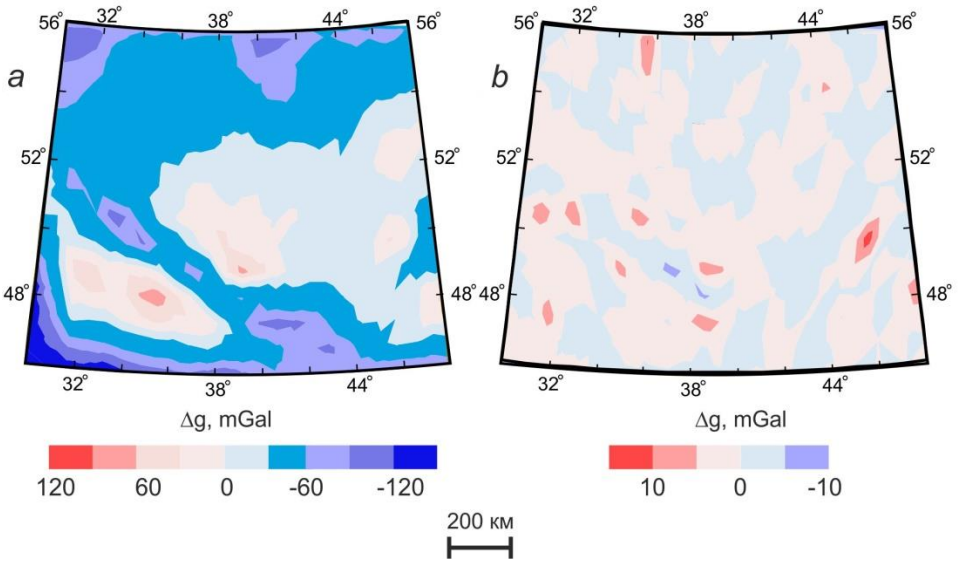

Figure 1. Starting (*a*) and final (*b*) residuals of the gravity field.

5. Conclusions

A joint analysis of the results of density modeling and geological interpretation of seismic reflection patterns allowed us to draw conclusions about the geodynamic evolution of the average Paleoproterozoic and current state of the crust (Muravina, 2016; Mints et al, 2017). It's necessary to note the main two features for 3D combined density model.

1. Spatial correlation of neotectonic dislocations have been marked as alternating density's anomalies in the upper and middle crust that form the area of abnormal tectonic stress contributing to formation of shafts in the sedimentary cover. In areas of low density crystalline basement hydrocarbon deposits may be present.

2. The structural pattern of the physical characteristics of the lithosphere region determines the existence of modern geodynamic system of radial-ring type, presumably related to the local manifestation of the endogenous activity mantle plume type which may cause radial and tangential deformation zone. Defusing tensions in these areas manifesting as modern localized intracrustal seismicity.

Acknowledgements

The research was supported by the RFBR, grants No 15-05-01214, 16-05-00975 and 18-05-00226.

References

Glaznev, V. N., Mints, M.V., Muravina, O.M., 2016. Density modeling of the central part of the East European platform, Vestnik KRAUNTS, Series of "Earth Sciences", 1 (29), 53-63 (in Russian).

Glaznev, V.N., Mints, M.V., Muravina, O.M., Raevsky, A.B., Osipenko, L.G., 2015. Complex geological-geophysical 3d model of the crust in the Ssouth-Eastern Fennoscandian shield: nature of density layering of the crust and the crust-mantle boundary, Geodynamics & Tectonophysics, 2, 133-170.

Glaznev, V. N., Muravina, O.M., Voronova, T.A., Holin, V.M., 2014. Estimation of the thickness of the gravitational crust of the Voronezh crystalline massif, Bulletin of VSU, Series Geology, 4, 78-84 (in Russian).

Grad, M., Tiira, T. and ESC Working Group, 2009. The Moho depth map of the European Plate, Geoph. J. Int., 176, 279-292.

Mints, M.V., Glaznev, V. N., Muravina, O.M., 2017. Depth structure of the crust of the southeast of the Voronezh crystalline massif according to geophysical data: geodynamic evolution in the Paleoproterozoic and the current state of the crust, Bulletin of VSU, Series Geology, 4, 5-23 (in Russian).

Muravina, O.M., 2012. The method of group accounting of arguments in the analysis of geophysical data, Geophysics, 6, 16-20 (in Russian).

Muravina, O.M., 2016. Density model of the crust of the Voronezh crystalline massif, Bulletin of VSU, Series Geology, 1, 108-114 (in Russian).

Muravina, O.M., Ponomarenko, I.A., 2016. Program implementation of the group account method for arguments in identification modeling of geological-geophysical data. Bulletin of VSU, Series Geology, 2, 107-110 (in Russian).

Muravina, O.M., Zhavoronkin, V.I., 2015. Statistical analysis of the digital basis of the Voronezh crystalline massif petrodensity map, Bulletin of VSU, Series Geology, 2, 94-99 (in Russian).

Pavlis, N.K., Holmes, S.A., Kenyon, S.C., Factor, J.K., 2012. The development and evaluation of the Earth Gravitational Model 2008 (EGM2008), J. Geoph. Res., 117. B4., doi:10.1029/2011JB008916.

EPOS Anthropogenic Hazard: Pyhäsalmi Episode

J. Nevalainen[1], E. Kozlovskaya[1] and H. Jänkävaara[1]

[1]Oulu Mining School, University of Oulu, Finland
E-mail: Jouni.nevalainen@oulu.fi

The European Plate Observing System (EPOS) is a long-term plan to facilitate integrated use of data, data products, and facilities from distributed research infrastructures for solid Earth science in Europe (EPOS, 2018a). The Geosciences from National and International research infrastructures are gathered in specific theme based packages called thematic core services. One such a theme is Anthropogenic Hazard that focuses on man triggered seismicity and other anthropogenic related phenomena that can cause harm to the works, environment and pose thread to seize the ongoing industrial operations such as mining (EPOS, 2018b). The Anthropogenic Hazard holds special data sets, called "episodes" that comprehensively descripts the geophysical process that is triggering the seismicity in different industrial infrastructures. Our work was to create Pyhäsalmi episode that focus on induced seismicity caused by underground mining operation at Pyhäsalmi mine, Pyhäjärvi, Finland.

Keywords: Induce seismicity, anthropogenic, Finland, Pyhäsalmi, mine technology.

1. General

The constantly increasing amount of high quality geoscience data has made it possible to perform multi-disciplinary research on complex research targets. This has led for the need of basic data such as base maps and research platform that would be easily and freely accessible. For this demand EPOS, the European Plate Observing System rose and it is a long-term plan to facilitate integrated use of data, data products, and facilities from distributed research infrastructures for solid Earth science in Europe (EPOS, 2018a). In addition of the high quality data, EPOS provides research e-platform, applications and visualization tools for researchers, students, industry and to public.

The geoscience data in the EPOS is classed in ten specific themes, the thematic core services. Each theme is managed by international community to agree used data formats and general content. One such a topic is Anthropogenic Hazard (AH) that focus to descript physical phenomena that can occur when complex industrial processes, and are performed under difficult environmental conditions (EPOS, 2018b). The research targets in AH consist mine environments, hydrology plant surroundings, non-conventional shale gas deposits etc. The physical phenomena are descripted with exceptional datasets, called "Episodes", which comprehensively describe a geophysical process; induced or triggered by human technological activity that can pose hazard for populations, infrastructure and the environment (EPOS, 2018b). The episode date is divided in three categories, Seismic, Technological and Geodata with corresponding metadata. The seismicity is the main geophysical method in AH as seismicity is most notable indicator of industrial impact to the bedrock (Guha, 2000). In addition AH platform offers problem specific applications to process seismic data.

2. Pyhäsalmi Episode

Pyhäsalmi mine, Central-Finland, is a deep underground mine that produces copper and zinc. Since the year 2000, the mining operation has been concentrating to Pyhäsalmi deep ore body located at depth of 900 m – 1425 m. A microseismic monitoring network was installed in 2002 due the high stress conditions that caused frequently occurring seismic events. The data for the Pyhäsalmi episode was chosen from October 2010 to March 2011 due the altering seismicity on the that time period. During this period almost 7000 seismic events occurred and a supporting pillar was collapsed due high stress in January 2011 (Pyhäsalmi, 2016).

To understand the relation between the induced seismicity and the mining operation, the technological data of Pyhäsalmi mines operation includes quarry opening location and star time, the quarry explosion data which includes both seismic observations as well explosion plans,

drillcore information, and rock mechanical reports of the mine condition. In addition it is planned to include also Pyhäsalmi mine 3D infrastructure map as soon the AH platform visualization tools are further developed. The Geodata includes geological map, lithological information from drillcore observations and in the future, a 3D geological map that is based on drillcore observations will be added to episode. Furthermore, the largest induced seismic events that has been detected by Pyhäsalmi microseismic monitoring network are compared to observations made by Finnish national seismic network. The focus is to analyse the differences in the seismic waveform content from far field and near field observations of the same events.

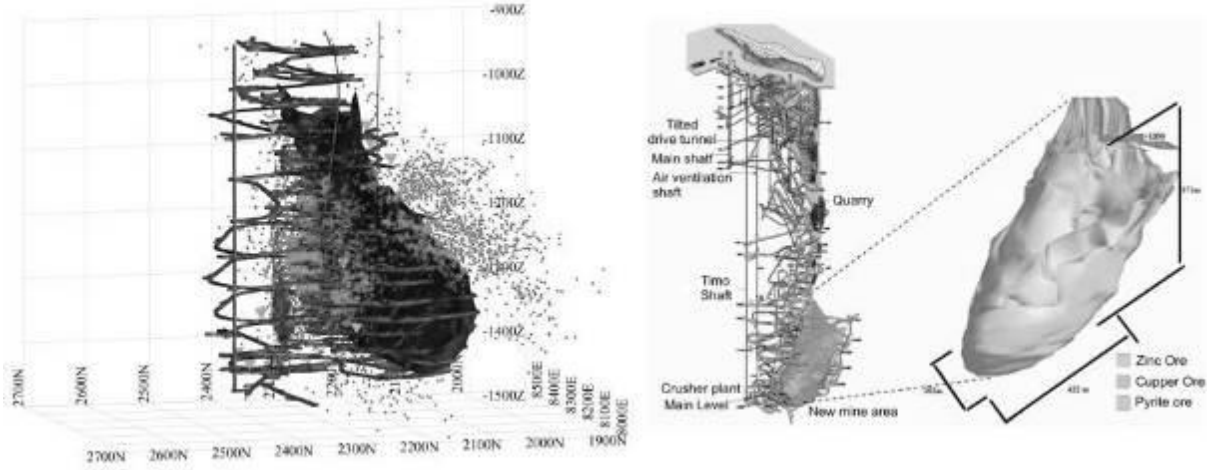

Figure 1. Left: Pyhäsalmi mine deep ore body and mine induced seismicity during the Pyhäsalmi episode. Right: Pyhäsalmi mine infrastructure.

3. Conclusion

Pyhäsalmi Episode was created to descript relationship between frequently occurring induces seismicity and mining operation at Pyhäsalmi mine, Finland. The technological data selected for the episode gives good spatial and chronical correlation with detected induced seismicity.

Acknowledgements: This work has been made within project "EPOS Implementation Phase" that has received funding from European Union's Horizon 2020 research and innovation programme under grant agreement N° 676564.

References:

EPOS, 2018a. European Plate Observing system, main webpage, https://www.epos-ip.org/. Updated 17.10.2018.

EPOS, 2018b. European Plate Observing system: Anthropogenic Hazard, webpage https://www.epos-ip.org/tcs/anthropogenic-hazards, Updated 17.10.2018.

Guha, S.K., 2000. Induced Earthquakes. Kluwer Academic Publishers, Dordrecht, Netherlands. pp. 314.

Pyhäsalmi mine, 2016. Technical report on Pyhäsalmi mine rock mechanics. Pyhäsalmi mine Ltd.

Identification of Potential Flake Graphite Ores in the Fennoscandian Shield and Utilization of Graphene (FennoFlakes)

J. Palosaari[1], S. Lund[2,3], J. Kauppila[2, 3], O. Eklund[1], R-M. Latonen[2], T. Lindfors[2], J-H. Smått[3], E. Björnvik[2], S. Sirkiä[3], J. Peltonen[3], S. Raunio[4], R. Blomqvist[4], J. Marmo[5] and S. Lukkari[5]

[1]Geology and mineralogy, Åbo Akademi University, Turku
[2]Laboratory of Analytical chemistry, Åbo Akademi University, Turku
[3]Laboratory of Physical chemistry, Åbo Akademi University, Turku
[4]Fennoscandian Resources Oy (Beowulf Mining), Turku
[5]Geological Survey of Finland, Espoo
E-mail: jenny.palosaari@abo.fi or tom.lindfors@abo.fi

This abstract will present the ongoing project FennoFlakes, a project financed by the Academy of Finland and K.H. Renlund foundation. The project merge geologists and chemists from Åbo Akademi University who work together towards the goal of filling the whole value chain from exploration of flake graphite raw material to applied applications with Finnish flake graphite.

Keywords: graphite, flake graphite, graphene, Fennoscandian shield

1. Introduction

The European commission has listed natural graphite as one of 20 critical raw materials in Europe (European commission, 2017). Our goal in this multi-disciplinary project is to identify new flake graphite ores in Finland and use this well-ordered graphite as raw material for high-end applications, like batteries for cars. The entire value chain includes identification of the ores, purification and enrichment of graphite, solution processing of graphene and high-performance proof-of-concept applications. To be successful, the project combines the expertise in geology, physical and analytical chemistry at Åbo Akademi University, as well as the expertise at the Geological Survey of Finland (GTK) and the mining industry. FennoFlakes studies and uses Finnish flake graphite from the Piippumäki and Haapamäki areas and will result in publications in high-impact journals, two PhD and 13 MSc theses. We expect that the project will contribute to increase the competitiveness of Finland as a future producer of high-quality flake graphite and make it a key player in graphene research.

2. Identification and characterisation of flake graphite

With increasing metamorphic conditions, natural graphite converts to flake graphite. During this process, the one atom thick layers – known as graphene – grow and are arranged parallel relative to each other (Buseck & Beyssac, 2014). Hence, we are focusing on high-grade metamorphic areas in the Fennoscandian shield. Graphite is often present as graphite schists or black schists, and since graphite is highly conductive, we can compare the maps of electromagnetic conductivity, and black schists with the metamorphic map of Finland. By comparing these maps, we can point out areas of interest and study them in more detail. Fieldwork in these areas is performed along with electromagnetic surveys for a better understanding on where the graphite is situated in the ground.

After sampling, thin sections are produced for analysing the graphite bearing rocks and the contact rocks. The mineral assemblages are determined, as well as the metamorphic conditions in the area. Results from XRF is also used for determining the metamorphic conditions together with mineral assemblages, different geothermometers and pseudosections.

To characterise the quality of the graphite, it is analysed with SEM, XRD and Raman spectroscopy. With SEM, we get a close-up on the graphite flakes, while with XRD and Raman spectroscopy we get information about the lattice parameters. Raman spectroscopy can also be

used as a geothermometer for determining the maximum temperatures the graphite has registered (Beyssac et. al, 2002, Rahl et. al, 2005, Palosaari et. al).

3. Enrichment and purification

Enrichment and purification of the extracted graphite rock involves three important steps: Crushing, flotation and chemical digestion. The material used is obtained from Haapamäki, and it is enriched and purified prior to the graphene exfoliation and development of applications. Selective fragmentation (SelFrag) was used as fragmentation method, since this method breaks the rock at mineral borders (Wang et al, 2011).

Prior to enrichment by conventional flotation, the fragmented graphite rock was pre-enriched by shaking table. The actual enrichment was carried out by froth flotation with methyl isobutyl carbinol as frother and kerosene as collector.

The final purification of the enriched material was carried out by chemical digestion. This means that the silicates that are left in the sample after flotation are digested in heated NaOH, HCL and HF solutions.

4. Flake graphite exfoliation

The method used for separating graphene sheets from flake graphite in this project is high shear-rate mixing. This method is based on applying shear force by a laboratory mixer to separate the graphene sheets. Restacking of the graphene sheets is prevented by the use of two different surfactants.

5. Results and future work

As the project started, we stated a hypothesis that "the higher metamorphic area – the higher quality of the flake graphite". At this stage, we can conclude that this hypothesis is accurate when examining areas with different metamorphic degrees. Our study has shown, corresponding to other studies, that the quality of the flake graphite is not affected if the area has undergone retrograde metamorphism,

By comparing the electromagnetic map, black schist map and the metamorphic map of Finland, we have pointed out several interesting areas. Based on fieldwork, Haapamäki and Piippumäki have qualified for more intensive research.

Analysis with SEM, XRD and Raman spectroscopy show that the graphite is of good quality. In SEM, we can see that the graphite flakes consists of several layers stacked parallel to each other (Figure 1). Results from XRD indicate that the flake graphite has a spacing between the graphene sheets at 0.334-0.335 nm, which is optimal for flake graphite. Results from Raman spectroscopy indicate that the graphite in Piippumäki and Haapamäki are of high quality, which is seen as the lack of D bands in the spectra. The D bands decrease and finally vanish with increasing metamorphic conditions. In Figure 2, a comparison is shown between graphite from Piippumäki (upper amphibolite facies-granulite facies) and Viistola (lower amphibolite facies). The difference is best seen in the lack of and presence of the D band in the spectrum from Piippumäki and Viistola respectively.

The enrichment tests show that the graphitic rock can be enriched to 100 % C by using a combination of different methods. A high yield of 1.15 % of few-layer graphene and single graphene layers was obtained in sodium cholate surfactant solution by using the high share-rate mixing exfoliation method. Nanocellulose was also found to be a suitable stabilizer for the graphene sheets during the exfoliation. We show that few-layer graphene and nanocellulose composite films with the electrical conductivity of 30 S cm^{-1} of and a thickness of 200 nm can easily be spray-coated on glass substrates with a standard airbrush.

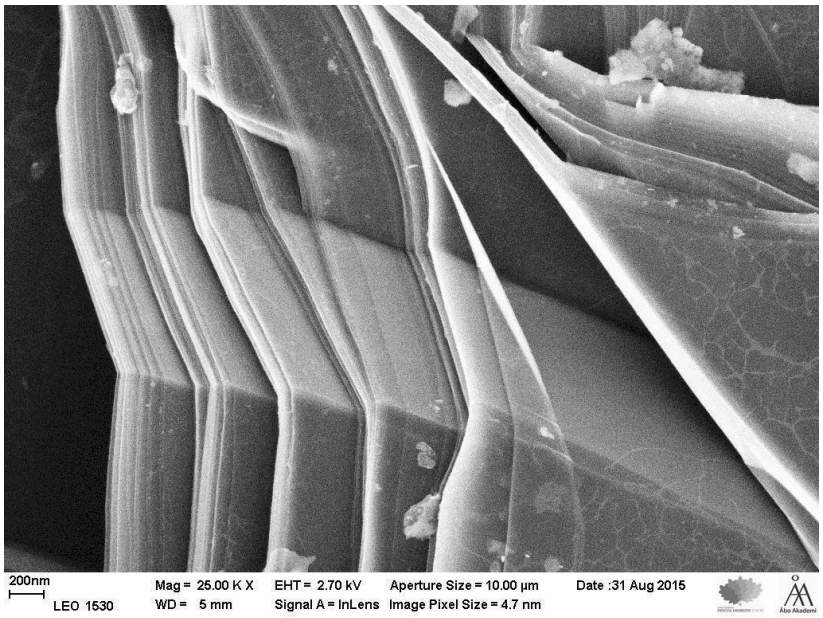

Figure 1. SEM-image of a graphite flake from Haapamäki. The flake consists clearly of parallel stacked layers. Observe the layer bent over indicated by the arrow.

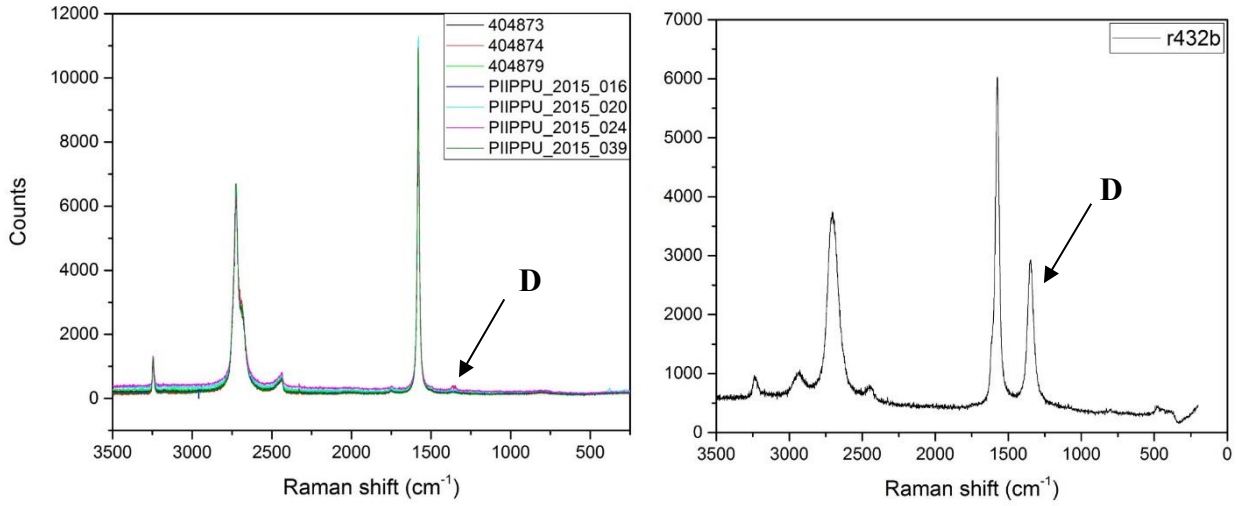

Figure 2. Raman spectra of samples from Piippumäki and Viistola. For Piippumäki, the D band is almost non-existent, while it in Viistola is clearly visible (indicated by arrows).

As for future work, collecting and comparing all the produced geological data in FennoFlakes is essential. Central topics are also to study why the graphitic carbon content vary drastically in a specified area, and if there are possible occurrences of vein graphite in eastern Finland.

References:

Beyssac, O., Goffé, B., Chopin, C. & Rouzaud, J.M., 2002. Raman spectra of carbonaceous material in metasediments: a new geothermometer. J. metamorphic Geol, 20, 859-871.

Buseck, P.R. & Beyssac, O., 2014. From Organic Matter to Graphite: Graphitization. Elements, 10, 421-426.

European commission, 2017. COMMUNICATION FROM THE COMMISSION TO THE EUROPEAN PARLIAMENT, THE COUNCIL, THE EUROPEAN ECONOMIC AND SOCIAL COMMITTEE AND THE COMMITTEE OF THE REGIONS on the 2017 list of Critical Raw Materials for the EU. https://eur-lex.europa.eu/legalcontent/EN/TXT/PDF/?uri=CELEX:52017DC0490&from=EN

Palosaari, J., Latonen, R-M., Smått, J-H., Raunio, S. & Eklund, O., Graphite prospect of Piippumäki – an example of a high-quality graphite occurrence in eastern Finland. To be submitted in October 2018.

Rahl, J.M., Anderson, K.M., Brandon, M.T. & Fassoulas, C., 2005. Raman spectroscopic carbonaceous material thermometry of low-grade metamorphic rocks: Calibration and application to tectonic exhumation in Crete, Greece. Earth and Planetary Science Letters, 240, 339-354.

Wang, E., Shi, F. & Manlapig, E., 2011. Pre-weakening of mineral ores by high voltage pulses. Minerals Engineering, 24, 455-462.

Shear zones and structural analysis of the Loimaa area, SW Finland

I. Pitkälä[1], J. Kara[1], T. Leskelä[1], P. Skyttä[1], M. Väisänen[1], H. Leväniemi[2], J. Hokka[2], M. Tiainen[2], Y. Lahaye[2]

[1] Department of Geography and Geology, University of Turku, FI-20014 Turku, Finland
[2] Geological Survey of Finland, P.O. Box 96, FI-02151 Espoo, Finland
E-mail: iiro.j.pitkala@utu.fi

Shear zones of various ages and orientations are common in Southern Finland. In the study area, E-W and N-S trending shear zones are the dominant structural feature. Mylonitic foliations were identified from the most intensely sheared rocks. Ductile shearing has mainly been of dip-slip type. Structural mapping revealed several larger map-scale folds, which appear to be relatively continuous across the study area from SE to NW. In the central area, folding interfered with the shear zones causing a complex crustal structure such as associated with the Uunimäki mineralization. Aeromagnetic and lithological maps, field observations, stereographic projections and oriented thin sections were used to determine the structural features of the study area.

Keywords: Shear zone, structural geology, fold, deformation, mylonite, aeromagnetic map

1. Introduction

The two-year project "Spatial distribution of gold mineralizations in SW Finland with respect to the crustal structure and hosting lithologies of the Häme and Pirkanmaa Belts" between the University of Turku and Geological Survey of Finland (GTK) was started in 2017. The aim is to provide information about the possible new and existing exploration targets with the structural, geochemical, geochronological and lithological data (see also Kara et al., 2018; Leskelä et al., 2018; this issue). The main objective of this study is to form a model of the structural features in the Loimaa area in SW Finland, which might have linkages with gold and other mineralisations (Fig 1).

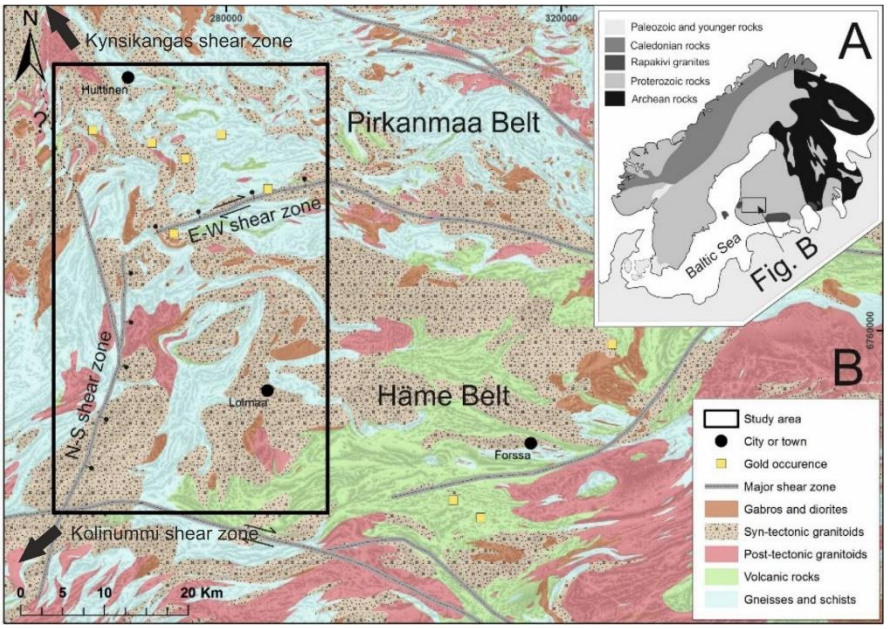

Fig. 1. A) Geological overview of the Fennoscandian shield (Koistinen et al. 2001), B) Geological map of the Häme belt presenting the study area, major shear zones and gold prospects (Bedrock of Finland – DigiKP).

2. Regional geology

The study area is located in the western end of the E-W trending Häme belt, which is part of the Svecofennian domain in the Central Fennoscandian shield (Fig. 1). The Häme Belt consist of 1.89-1.87 Ga plutonic-volcanic rocks with volcanic arc affinities (Hakkarainen, 1994; Kähkönen, 2005; Mäkitie et al., 2016), which have undergone metamorphism mainly in the amphibolite facies conditions (e.g. Nironen, 1999; Hölttä and Heilimo, 2017). The area hosts several known gold occurrences (Kärkkäinen et al., 2012).

3. Study material

The data consist of 484 bedrock observations. Tectonic features measured were the foliations, lineations, fold axes, axial surfaces, faults and, in some outcrops, fractures and veins. The main emphasis in selecting the observation targets was put in the areas of the two major shear zones. However, observations from the surrounding areas were also collected, including the major fold systems. For the kinematic renditions, oriented samples for thin sections were collected from the most promising outcrops. One sample was taken for zircon U-Pb geochronology from a granite intruding the N-S shear zone.

4. Delineation of the structural domains based on the structural data

The study area was divided into subareas based on the dominant structural signatures. The subarea division utilized both the aeromagnetic signatures of the crust, as well as field mapping data. The subareas are the ***N-S shear zone***, ***E-W shear zone***, ***North fold***, ***Alastaro fold***, ***Oripää fold*** and ***Uunimäki gold prospect*** (Fig. 2). Both shear zones are ductile, which involve strain releasing along the forming shear bands and mylonites with kinematic features. Location of the North fold between the N-S shear zone and the Kynsikangas shear zone (Fig. 1) have a potential to enlighten their correlation. The Oripää fold in the SE is the least affected by the two shear zones. The Alastaro fold is located south of Uunimäki and between the other two major fold systems, and it is more incoherent than the North fold or the Oripää fold.

4.1 Shear zone domains

The ***E-W shear zone*** (C in Fig. 2) is characterised by penetrative foliation and gneissic banding. Mylonitic foliation was observed only on a few outcrops, which characterise zones of most intense deformation. Planar and linear fabrics are mainly moderately or steeply inclined. Dextral shear sense was observed from these outcrops and thin sections. Since the collected structural data from the ***N-S shear zone*** (D1-D4 in Fig. 2) is not as homogeneous as the E-W shear zone, the area was subdivided into four subareas. Similar to the E-W shear zone, most planar and linear structures are the steeply to moderately inclined. Foliations of the southernmost subarea (D1) are NE-SW striking and the structures are most likely related to other shear zone in SW known as the Kolinummi shear zone (Fig. 1)(Väisänen and Skyttä, 2007). L-tectonites were locally observed from this subarea, while the other three subareas mainly contain S-tectonites and some S-L-tectonites. The NNE-SSW striking negative magnetic anomaly is visible on the map, possibly representing the continuation of the N-S shear zone towards SSW. Mylonitic textures and strong recrystallization of quartz characterise the structures in the next subarea towards north (D2). Mainly steeply-dipping foliations were observed, including mylonitic foliations on the best outcrops. Gently to sub-vertically plunging lineations are mainly weak to strong mineral or stretching lineations. Shear deformation-related major folding with axes plunging gently or moderately towards N-NNE was observed from subarea D3. Within the D4 sub-area the dominant structural trends are NNW-SSE.

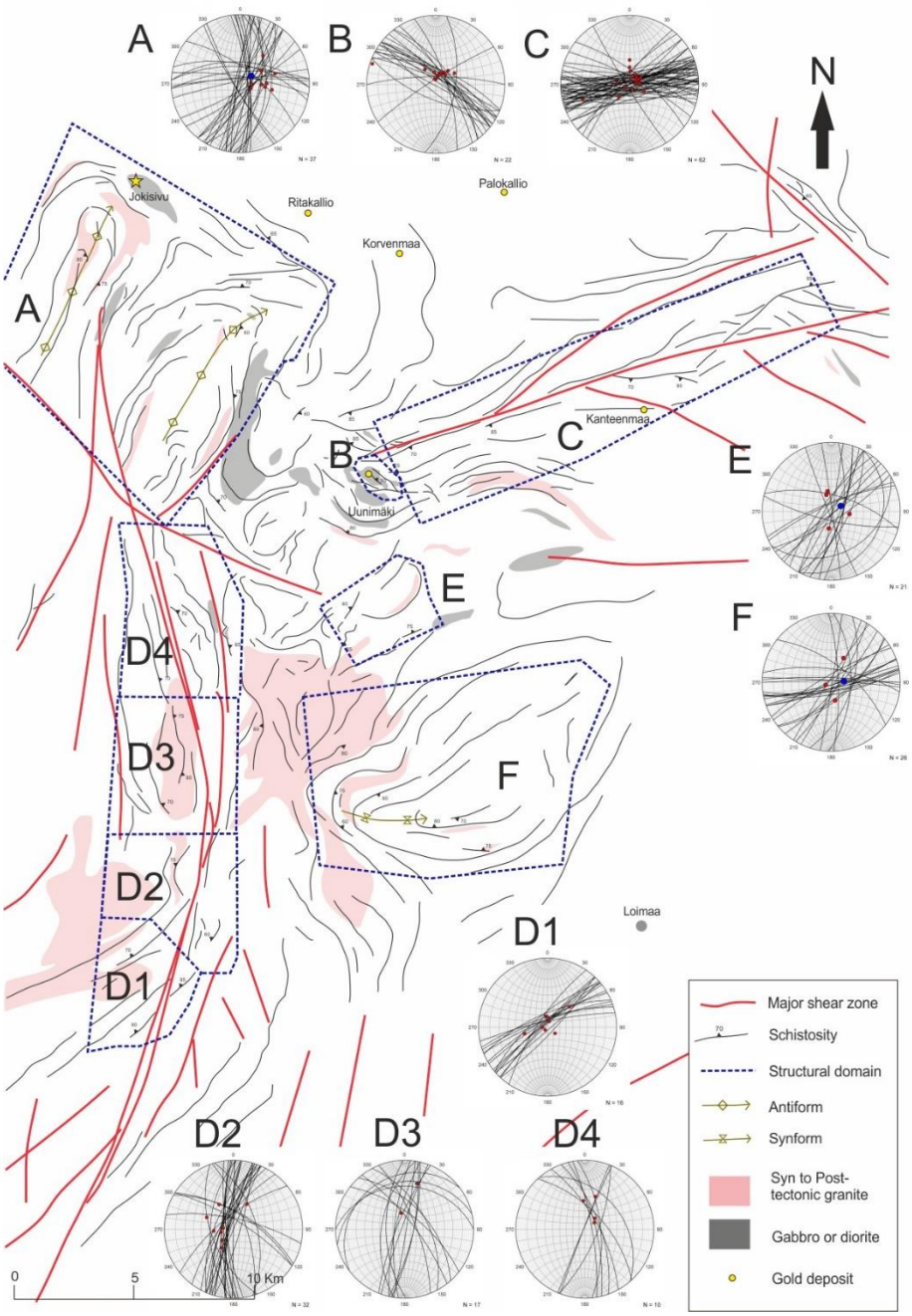

Fig. 2. Structural map of the study area, structural domains (A-F) and stereographic projections of the dominant planar (great circles) and linear (lineation; dots) features.

4.2 Folded domains

Major fold areas include the ***North fold***, ***the Alastaro fold*** and the ***Oripää fold*** (A, E and F in Fig. 2). The data collected from the Oripää fold area indicate a major synformal structure. The calculated major fold axis plunges steeply towards east (086/69). Plunges of the mineral lineations range at 47°-80°. From the North fold area, the data suggests two antiforms with steeply NE plunging fold axes (055/68). Penetrative foliation and schistosity were the most common type of planar features of the area, and some mylonitic and pseudotachylitic textures were observed from narrow zones. The more incoherent Alastaro fold south of Uunimäki contain Z and S type of folds on outcrops and the NE-plunging steep fold axis (060/72) was calculated from foliations.

5. U-Pb zircon dating

In order to estimate an age of the shear activity, a granite intruding the N-S shear zone was sampled for zircon dating. The dating was performed in the Finnish Geosciences Research Laboratory at GTK. The data revealed several age populations ranging from Archean to Paleoproterozoic. The youngest population yield an upper intercept age of ~1.87 Ga.

6. Conclusions

A continuous chain of major folds (A to F in Fig. 2) has evolved in collision prior to the generation of the major shear zones. As a result of the folding and shearing, a very complex crustal structure was generated, e.g. in mineralized Uunimäki area (B in Fig. 2). Different shear sense between the N-S and Kynsikangas shear zones indicates separate deformation events. Structures in the subarea D1 are probably related to the nearby Kolinummi shear zone in the SW (Väisänen and Skyttä 2007). The kinematic indicators within the N-S shear zone are supporting west side-up movement. The E-W shear zone shows south-side-up movement. Dextral strike-slip component has also been significant in some parts of the E-W shear zone.

The zircons from the granite within the shear zone contain several inherited populations. The youngest ~1.87 Ga population is, within errors, similar to that obtained from the nearby Oripää granite (Kurhila et al. 2005). That age was interpreted to be inherited from the source. That is also probably the case in this study.

7. Acknowledgements

This study was funded by the Geological Survey of Finland**.**

References

Bedrock of Finland - DigiKP. Digital Map Database [Electronic Resource]. Espoo: Geological Survey of Finland [referred 17.10.2018]. Version 2.0.

Hakkarainen, G., 1994. Geology and geochemistry of the Hämeenlinna-Somero volcanic belt, southwestern Finland: a Paleoproterozoic island arc. Geochemistry of Proterozoic Supracrustal rocks in Finland, 19, 85-100.

Hölttä, P., Heilimo, E. 2017. Metamorphic Map of Finland. Bedrock of Finland at the scale 1:1000 000 – Major stratigraphic units, metamorphism and tectonic evolution. Geological Survey of Finland, Special Paper, 60, 77-128.

Kara, J., Manninen, J., Leskelä, T., Skyttä, P., Väisänen, M., Tiainen, M., Leväniemi, H., 2018. Characterization of the structural evolution and structural control of the gold mineralizations in the Kullaa Area, SW Finland. Institute of Seismology, University of Helsinki, Report S-6X, xx-yy.

Koistinen, T., Stephens, M.B., Bogatchev, V., Nordgulen, Ø., Wennerström, M. Korhonen, J., 2001. Geological map of the Fennoscandian Shield, scale 1:2 000 000. Geological Surveys of Finland, Norway and Sweden and the North-West Department of Natural Resources of Russia.

Kurhila, M., Vaasjoki, M., Manttari, I., Ramo, T., Nironen, M. 2005. U-Pb ages and Nd isotope characteristics of the lateorogenic, migmatizing microcline granites in southwestern Finland. Bulletin-Geological Society of Finland, 77, 105-128.

Kähkönen, Y., 2005. Svecofennian supracrustal rocks. Developments in Precambrian Geology, 14, 343-405.

Kärkkäinen, N., Huhta, P., Lehto, T., Tiainen, M., Vuori, S. Pelkkala, M. 2012. New geochemical data for gold exploration in southern Finland. Geological Survey of Finland, Special Paper, 52, 23–46,

Leskelä, T., Kara, J., Pitkälä I., Skyttä, P., Väisänen, M Tiainen, M., Leväniemi, H., Hokka, J. Lahaye Y. Geochronology, geochemistry and structural setting of the Uunimäki gold mineralisation, SW Finland. Institute of Seismology, University of Helsinki, Report S-6X, xx-yy.

Mäkitie, H., Kärkkäinen, N., Sipilä, P., Tiainen, M., Kujala, H., Klami, J., 2016. Hämeen vyöhykkeen granitoidien luokittelua. Geological Survey of Finland archive report 33, 146p.

Nironen, M. 1999. Structural and magmatic evolution in the Loimaa area, southwestern Finland. Bulletin of the Geological Sociecity of Finland, 71, 57-71.

Väisänen, M., Skyttä, P., 2007. Late Svecofennian shear zones in southwestern Finland. GFF, 1

The Kynsikangas shear zone, Southwest Finland: Importance for understanding deformation kinematics and rheology of lower crustal shear zones

S. Reimers[1], J. Engström[2] and U. Riller[1]

[1] Universität Hamburg, Institut für Geologie, Bundesstrasse 55, 20146 Hamburg, Germany
[2] Geological Survey of Finland, P.O. Box 96, 02151 Espoo, Finland.
E-mail: sebastian.reimers@studium.uni-hamburg.de

Eroded Proterozoic orogens in southern Finland provide perfect conditions for elucidating deformation processes at lower crustal levels. The crudely N-S striking Kynsikangas Shear Zone (KSZ) belongs to a set of prominent, ductile deformation zones within the Svecofennian Orogen in SW-Finland. In order to assess the regional tectonic significance of the KSZ, knowledge of the overall deformation regime and kinematic evolution of the shear zone is necessary. Evident by the results of a detailed field-based structural analysis, the KSZ portrays well the heterogeneity of transpressive deformation at lower crustal levels and provides new constraints on the structural evolution of the Svecofennian Orogen, the internal structure and rheology of lower crustal shear zones.

Keywords: ductile shear zone, lower crust, kinematics, strain localisation, Svecofennian Orogen

1. Introduction

Unravelling deformation kinematics of shear zones on multiple scales is important for elucidating the evolution of lithotectonic terranes. This study addresses the Svecofennia Province of Finland, which formed by the amalgamation of crustal terranes at 2.0 - 1.8 Ga. This process leads to the formation of multiple sets of prominent shear zones and fault systems. One of these zones is the NW-SE striking Kynsikangas shear zone (KSZ) in the Pori area of southwest Finland (Fig. 1). The KSZ is generally interpreted as a first-order, sinistral strike-slip zone that formed under NE-SW shortening at ca. 1.8 Ga (Pajunen et al. 2008).

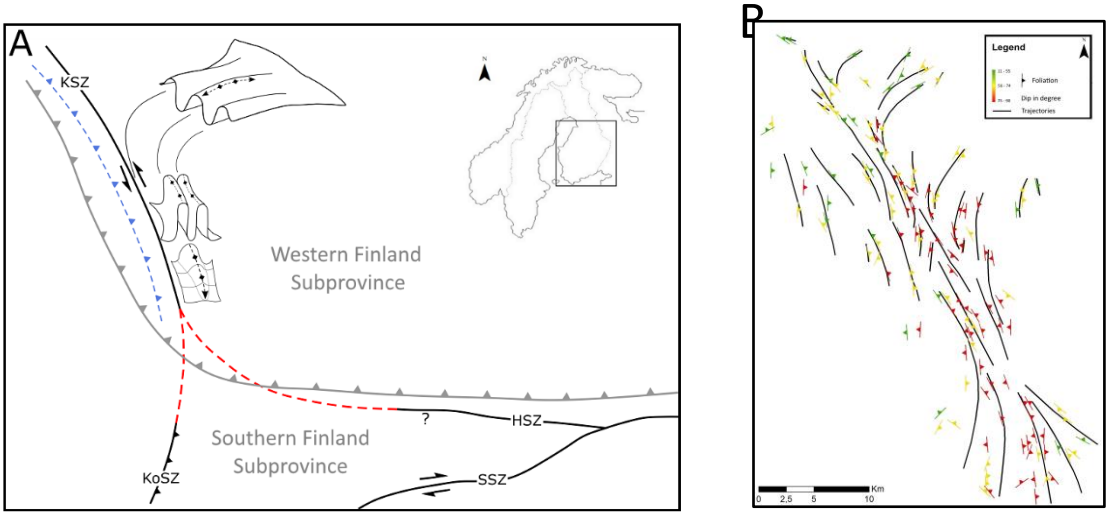

Figure 1. A: Regional tectonic relationship of prominent shear zones in southern Finland. Dashed lines mark the possible connection of the Kynsikangas Shear Zone (KSZ) with the Kolinummi (KoSZ) and the Hämeenlinna (HSZ) shear zones. The suture of Paleoproterozoic subprovinces is marked in grey. Blue dashed line indicates a proposed thrust zone. B: Map displaying trajectories and inclination of foliation planes of the KSZ.

Uncertainty of the KSZ exists regarding its internal structure, kinematic evolution, geometry, cause of shearing, age of its initiation and the depth of deformation. Moreover, it is

uncertain to what extent the KSZ is kinematically linked to the nearby Hämeenlinna and Kolenummi shear zones (Fig. 1A) (Väisänen and Skyttä, 2007, Saalmann et al. 2008) or is rather of local importance. Due to excellent exposure, the KSZ lends itself also to shed light on ongoing fundamental structural geological controversies, such as the questionable match of small-scale and regional-scale kinematic indicators of shear zones. This issue pertains to better understanding heterogeneity and rheological properties of lower-crustal shear zones.

2. Kinematic analysis

Based on the orientation of mineral foliation (S) and lineation (L) in metagranitoid rock and migmatite, the Kokemäki segment of the KSZ can be divided into and an eastern, a central and a western zone (Fig. 2). The shear zone center is characterized by strongly prolate (L>>S) mineral shape fabrics with sub-horizontal E1-axes (Fig. 3), where E1 ≥ E2 ≥ E3. By contrast, the eastern and western zones are marked by S > L fabric geometry with moderately to steeply plunging E1-axes (Fig. 3). The km-scale curvature of foliation surfaces points to an overall left-lateral sense-of-shear during ductile deformation (Fig. 1B). However, shear sense based on small-scale kinematic indicators, notably S/C fabrics, rotated rigid objects and asymmetrically folded metamorphic layers (Fig. 2) are at variance with the first-order kinematics of the KSZ (Fig. 1B). This holds in particularly for stations with known E1-axis orientations and shear directions inferred from S/C fabrics, showing large angular departures between the two. The transformation of open into isoclinal folds and the transposition of rock fabrics of the eastern segment into the central part of the KSZ (Fig. 1A) is in contrast to the rock fabrics of the western segment, leading to an asymmetric structure of the shear zone.

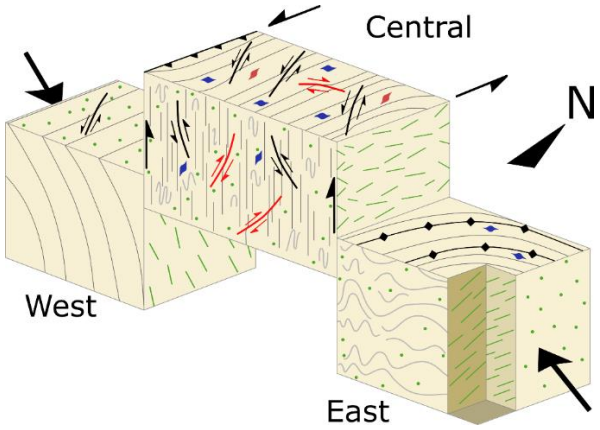

Figure 2. Schematic block diagram depicting the common structures in each segment of the Kynsikangas Shear Zone. Foliation and folds are displayed by grey lines, lineation is shown by green lines and dots. Sinistral and dextral sense of shear on C-surfaces and porphyroclasts are indicated by black and red symbols, respectively. Arrows denote shortening direction.

3. Discussion and Conclusions

Collectively, the structural and kinematic observations lead us to conclude that the KSZ formed under two different deformation regimes. Despite complex internal ductile flow, evident by the spatial variation in S-L fabric geometry and kinematics of S/C fabrics, the KSZ seems to have accommodated a strong component of left-lateral, pure shear-dominated transpression under NW-SE shortening (Fig. 4). This deformation is followed by thrusting of the central over the eastern segment under brittle conditions (Fig. 2). During ductile deformation, metamorphic fabrics and folds of the eastern segment were transposed into the KSZ. E-W shortening under brittle conditions overprint ductile fabrics and accounts for the observed asymmetry of metamorphic mineral fabrics. We also note that small-scale kinematic indicators, now routinely

used as criteria for the determination of shear-zone kinematics, do not provide reliable kinematic information in a transpressive regime, as they show highly variable sense-of-shear. This is in conflict with mesoscopic and regional-scale kinematics inferred from the curvature of foliation trajectories (Fig. 2) and questions the use of small-scale kinematic indicators for determination of the kinematics on the shear-zone scale.

Based on the branching geometry of foliation trajectories at the southern terminus of the KSZ, a physical connection of the KSZ with the Kolinummi and the Hämeenlinna shear zones is likely (Fig. 1). The pervasive and continuous deformation in rocks of the Pirkanmaa Belt and the Häme Belt indicate that the suture of the Southern and Western Finland Subdomains (Lahtinen et al. 2005) predates ductile deformation of the KSZ. Thus, the KSZ is younger than, or formed at a late stage of, terrain amalgamation in southern Finland.

Implications regarding the relationship of shape fabric geometry and its intensity and asymmetric fabrics provide new insights into the structure and rheology of lower crustal shear zones. The spatial relationship of metamorphic mineral fabrics and concentration of shear bands in the central KSZ may indicate that deformation is not exclusively dependent on temperature, but also on strain rate. In particular, shear bands may form during co-seismic deformation under the same deformation regime as metamorphic mineral fabrics. Finally, observed foliation patterns in the eastern KSZ deviate to some extent from numeric models of oblique transpression (Fig. 4).

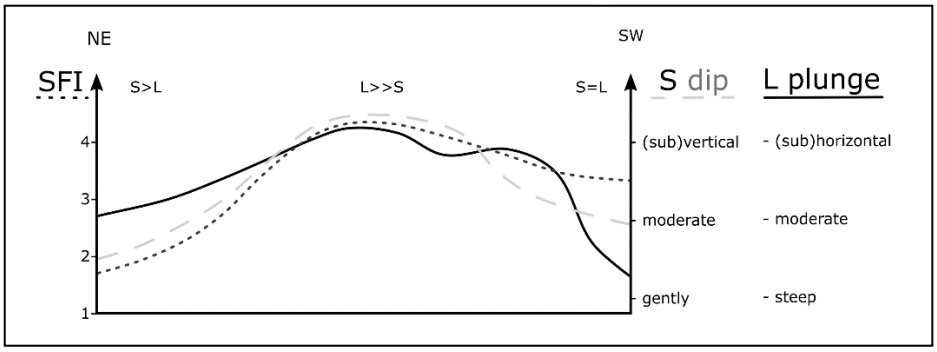

Figure 3 (top). Diagramm of the central segment of the Kynsikangas shear zone displaying shape fabric intensity (SFI), foliation (S) and lineation (L). We note a correlation in strain intensity, geometry and orientation of mineral fabrics.

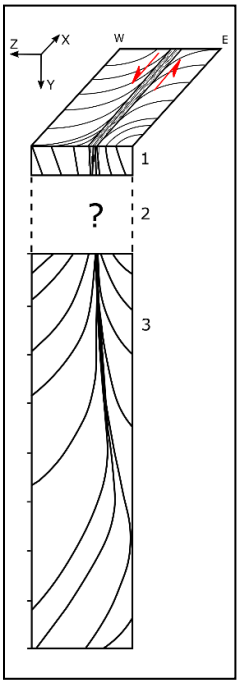

Figure 4 (right). Synoptic representation of foliation traces formed in oblique left-lateral transpression. Segment 1 represents observed foliations of the KSZ. Segment 3 is based on a numeric model by Robin and Cruden (1994). We note a mismatch in the foliation pattern in the western KSZ.

References:

Lahtinen, R., Korja, A., Nironen, M. 2005. Paleoproterozoic tectonic evolution. In: Lehtinen, M., Nurmi, P.A. and Rämö, O.T. (eds.) Precambrian Geology of Finland – Key to the Evolution of the Fennoscandian Shield. Elsevier B.V., Amsterdam, 481-532.

Robin, Y.-P. F., Cruden, A. R. 1994. Strain and vorticity patterns in ideally ductile transpression zones. Journal of Structural Geology, 16, 447-466.

Saalmann, K., Mänttäri, I., Ruffet, G., Whitehouse, M.J. 2008. Age and tectonic framework of structurally controlled palaeoproterozoic gold mineralization in the Häme Belt of southern Finland. Precambrian Research, 174, 53-77.

Pajunen, M., Airo, M.L., Elminen, T., Mänttäri, I., Niemelä, R., Vaarma, M., Wasenius, P., Wennerström, M., 2008. Tectonic evolution of svecofennian crust in southern Finland. Geol. Surv. Finl. Spec. Publ. 47, 15–184.

Väisänen, M., Skyttä, P. 2007. Late Svecofennian shear zones in southwestern Finland. GFF, 129, 55–64.

Multi-scale deformation during large impact cratering

Ulrich Riller

Universität Hamburg, Institut für Geologie, Bundesstrasse 55, 20146 Hamburg, Germany
E-mail: ulrich.riller@uni-hamburg.de

The floors of large impact structures are generally flat, contain one or more morphological rings and are dissected by radial, concentric or polygonal fracture networks. Deformation accomplishing the formation of such impact structures occurs on time and length scales ranging from seconds to thousands of years and from millimetres to tens of kilometres, respectively. Based on recent drilling of rocks underlying the peak ring of the 66 Ma Chicxulub impact structure, Mexico, field evidence from the 1.85 Ga Sudbury impact structure, Canada, and scaled analogue modelling, cratering mechanisms accounting for the observed morphological and structural characteristics are identified. In particular, the mechanisms provide evidence for the existence of acoustic fluidization during initial cratering and viscous relaxation of crust during long-term crater modification.

Keywords: impact cratering, acoustic fluidization, deformation mechanisms, long-term crustal relaxation, Chicxulub, Sudbury

1. Introduction

Hypervelocity impact is recognized as a fundamental geological process in the solar system (Melosh 1989). In particular, large meteorite impact is paramount for understanding (1) the evolution of the early Earth, (2) the geological modification of Earth's crust and surface, (3) the evolution of life and (4) the formation of giant natural resource deposits. Unravelling processes of large impact cratering on Earth is hampered by the planet's high resurfacing rates. Consequently, most of the 190 confirmed terrestrial impact structures are eroded. Only three of these, known as "the big three" qualify as large impact basins. They are: Vredefort (South Africa); Sudbury (Canada) and Chicxulub (Mexico).

Based on numerical modelling (Morgan et al. 2016), the formation of impact structures, such as the Chicxulub, containing an inner morphological ring (Fig. 1b), the so-called peak ring, starts by shock wave-induced, crustal-scale excavation of a bowl-shaped transient cavity (Fig. 2b). Gravitational instability of the cavity causes uplift of the crater centre and concomitant inward slumping of the cavity wall (Fig. 2c). Collapse and radial outward displacement of uplifted material over inward-slumped cavity wall segments followed by gravitational settling of the peak ring characterize the terminal phase of crater modification (Fig. 2d). Outstanding problems in our knowledge of large impact cratering are the mechanism of ring formation, the cause for flat floors and mechanisms of floor fracturing.

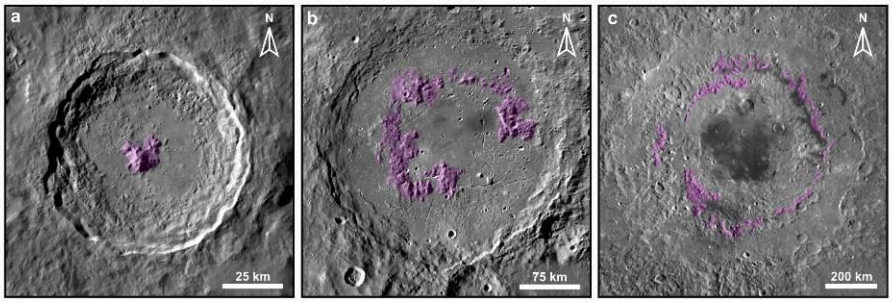

Figure 1. Typical impact structures of the Moon (http://quickmap.lroc.asu.edu). Topographically elevated areas in (a) to (c) are highlighted in magenta. (a) Central-peak crater: Tycho, (b) Peak-ring crater: Schrödinger, (c) Multi-ring impact basin: Orientale.

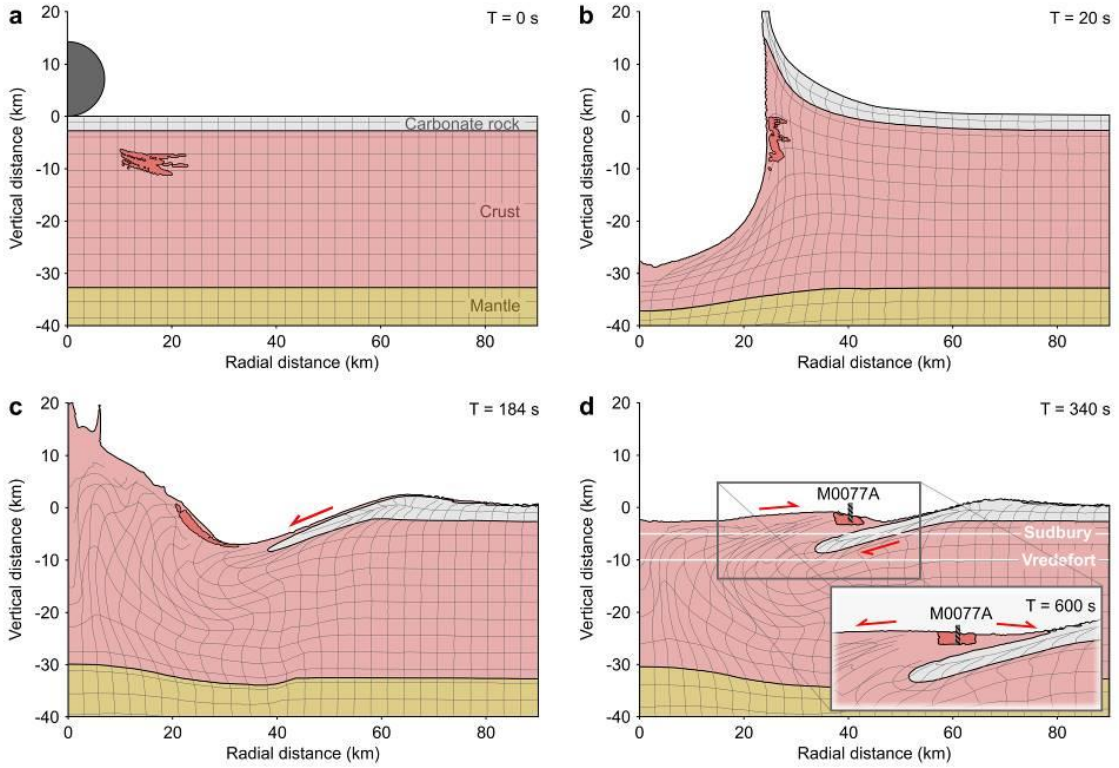

Figure 2. Formation of the Chicxulub impact structure based on numerical modelling of peak-ring crater formation (Morgan et al. 2016). A grid of tracer particles is shown to highlight the sub-crater deformation. Dark red area of crust in each panel tracks the material that eventually forms the peak ring. T denotes time in seconds after impact. Red half arrows indicate the direction of major shear displacements relative to adjacent material.

2. Short-term deformation process of cratering

The formation of the innermost topographic ring, the so-called peak ring, and the causes of target rock weakening leading to observed flat crater floors are not well understood. Constraining these mechanisms has been the prime structural geological objective of IODP-ICDP Expedition 364 "Drilling the K-Pg Impact Crater", using the ~200-km diameter Chicxulub impact structure, Mexico, as a terrestrial analogue for the formation of planetary impact basins (Morgan et al. 2016). A total of 829 meters of core was recovered from borehole M0077A drilled into the peak ring of the Chicxulub crater. From bottom to top, the core is crudely composed of: (1) pervasively shocked granitoid target rock hosting meter- to decameter-thick impact melt rock and suevite dike-like bodies, (2) a 130 m thick impact melt rock and suevite unit overlying the target rocks, and (3) a 112 m thick section of post-impact pelagic carbonate rocks. Based on visual appraisal of the drill core, prominent impact-induced deformation structures in target rock pertaining to cratering are delineated.

In addition to microscopic planar structures formed by shock metamorphism, the target rocks are replete with impact-induced, mesoscopic planar deformation structures (Riller et al. 2018). These structures include: (1) pervasive, grain-scale fractures, (2) cataclasite zones, (3) shear faults, (4) crenulated mineral foliations, and (5) ductile band structures. Structural overprinting criteria point to a relative age for these structures that can be correlated with individual cratering stages (Riller et al. 2018). In particular, pervasive fracturing preceded the other deformation mechanisms and is, thus, attributed to shock loading, decompression, and transient cavity growth (Fig. 2b). Cataclasite zones are plausible candidates for accommodating the deformation of pre-fractured target rock during transient cavity collapse and central uplift formation (Fig. 2c). As the central uplift transitions from motion upwards to outwards and downwards during collapse (Fig. 2d), cataclastic flow is superseded by shear faulting. Finally,

the formation of crenulated fabrics and ductile band structures accomplish gravitational spreading of the topographically elevated peak ring (inset in Fig. 2d).

Initial pervasive grain-scale fracturing causes a profound loss of cohesion and shear strength in target rocks at the onset of, and during, transient cavity growth (Fig. 2b). Small displacements on subsequently forming cataclasite zones across the entire rock mass is consistent with macroscopic deformation of an acoustically fluidised rock mass. In acoustic fluidization, short-wavelength, high-frequency pressure oscillations around the lithostatic pressure temporarily reduce the overburden pressure and, thus, friction between fractured target rocks (Melosh 1996). Cataclasite zones are prime candidates for the physical expression of sheared block boundaries serving as contact strain zones, during oscillation of target rock blocks. This process allows target rocks to flow rapidly over large distances during initial cratering (Fig. 2b, c). The onset of shear faulting heralds an increase in shear strain of the rock mass and waning of acoustic fluidisation. The transition from distributed cataclastic flow to localised shear-faulting illuminates the target rock regaining sufficient strength to generate and support the topography of the peak ring (Fig. 2d).

3. Long-term crater modification

Evidence of long-term modification of terrestrial craters is rather sparse, but paramount for fully understanding large-meteorite impact processes. Owing to the excellent exposure, access and post-impact tilting of impact-generated lithologies and structures, Sudbury appears to be the only large, terrestrial impact structure that allows for a structural analysis aimed at unravelling long-term modification of large impact craters. Besides providing the first quantitative structural evidence for long-term crater modification on Earth, understanding this process at Sudbury is also important for designing exploration strategies of Cu-Ni and platinum group element (PGE)-rich ore deposits.

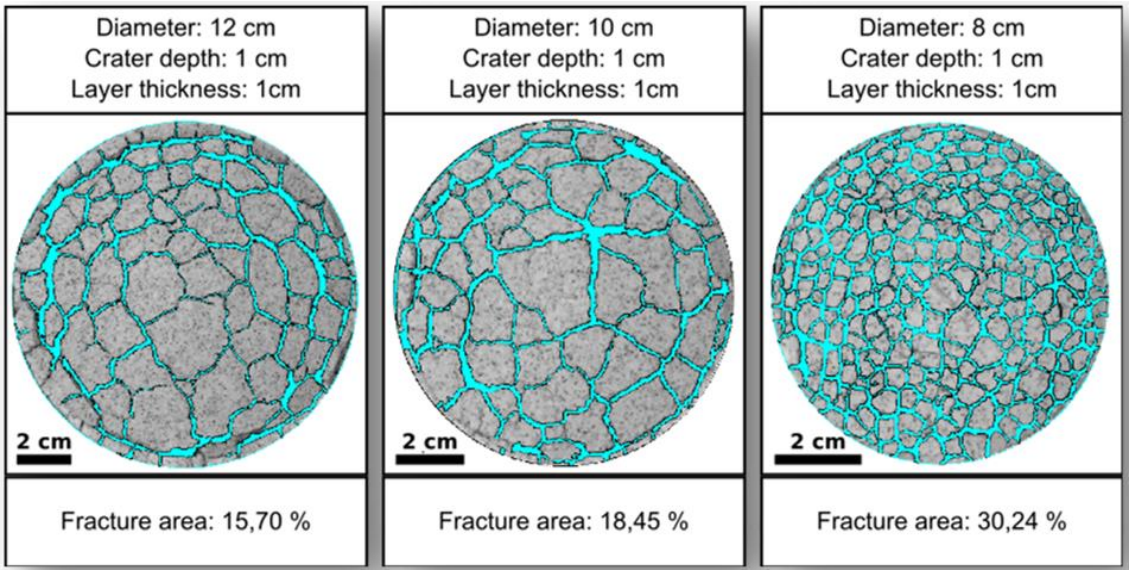

Figure 3. Fracture patterns in model crater floors with regard to crater diameter, crater depth and thickness of brittle crust.

The following structures and mineral fabrics associated with the 1.85 Ga Sudbury Igneous Complex (SIC), the deformed relic of an impact melt sheet, are traditionally attributed to the Paleoproterozoic Penokean orogeny: (1) contact-parallel igneous mineral fabrics in the SIC; (2) contact-parallel, high-temperature metamorphic fabrics in the thermal aureole of the SIC and (3) granitoid dikes, known as Offset Dikes, emanating from the SIC and derived from (partially-melted) target rocks. These structures are genetically related to cooling and solidification of the

SIC, which occurred within approximately ten thousand years after impact and, thus, substantially faster than the duration of Penokean deformation. Offset Dikes, in particular, have been interpreted as equivalents to lunar crater floor fractures. In fact, simple two-layer analogue models using viscous and granular materials for the lower and upper crust, respectively, scaled to length, time and viscosity display polygonal fractures in the model craters as a result of isostatic (i.e., viscous) re-equilibration of model crust (Fig. 3). Moreover, PGE-rich Cu-Ni sulfides occupy tensional fractures in target rocks immediately underlying the SIC. The sulfides segregated from the silicate impact melt upon cooling of the melt below about 1450°C and accumulated at the base of the melt sheet, from which they migrated into dilational target rock fractures, akin to the emplacement of Offset Dikes.

In summary, the mentioned structures have been attributed erroneously to orogenic deformation and underestimated with regard to deformation caused by long-term crater modification. In fact, they all amount to vertical thinning and horizontal extension, i.e., oblate strains, of the SIC and underlying target rocks, which is consistent with crater floor modification caused by viscous relaxation of crust known also from remote sensing studies of the lunar surface and Mercury.

4. Conclusions

Recent drilling into the peak ring of the Chicxulub impact structure, Mexico, unveiled an unprecedented record of brittle and viscous deformation mechanisms accounting for the drastic weakening of target rocks, followed by the regain of sufficient strength of rocks to build and sustain topographic rings. The observations point to quasi-continuous rock flow and, thus, acoustic fluidization as the dominant physical process controlling initial cratering. Structural analysis of impact melt rocks at Sudbury, Canada, and scaled analogue modelling suggests that crater modification of large impact structures occurs on time scales of tens of thousands of years through viscous relaxation of crust. This process is responsible for the formation of crater floor fractures, which are sinks for the accumulation of giant metal resource deposits.

5. References

Melosh, H.J. 1989. Impact cratering: a geological process. Oxford University Press, Inc., New York. 245 pages.

Melosh, H.J. 1996. Dynamical weakening of faults by acoustic fluidization. Nature 379, 601-606.

Morgan, J.V., Gulick, S.P.S., Bralower, T., Chenot, E., Christeson, G., Claeys, P., Cockell, C., Collins, G.S., Coolen, M.J.L., Ferrière, L., Gebhardt, C., Goto, K., Jones, H., Kring, D.A., Le Ber, E., Lofi, J., Long, X., Lowery, C., Mellett, C., Ocampo-Torres, R., Osinski, G.R., Perez-Cruz, L., Pickersgill, A., Poelchau, M., Rae, A., Rasmussen, C., Rebolledo-Vieyra, M., Riller, U., Sato, H., Schmitt, D.R., Smit, J., Tikoo, S., Tomioka, N., Urrutia-Fucugauchi, J., Whalen, M., Wittmann, A., Yamaguchi, K. E. and Zylberman, W. 2016. The formation of peak rings in large impact craters. Science 354, 878-882.

Riller, U., Poelchau, M.H., Rae, A.S.P., Schulte, F.M., Collins, G.S., Melosh, H.J., Grieve, R.A.F., Morgan, J.V., Gulick, S.P.S., Lofi, J., Diaw, A., McCall, N. Kring, D.A., and IODP-ICDP Expedition 364 Science Party. 2018. Rock fluidisation during peak-ring formation of large impact structures. Nature, in press.

Felsic MASH zone in southernmost Finland

A. Saukko[1], K. Nikkilä[1], O. Eklund[1] and M. Väisänen[2]

[1] Åbo Akademi University, Geology and mineralogy, Geohouse, Akademigatan 1, FI-20500 Åbo, Finland
[2] Department of Geography and Geology, FI-20014 University of Turku, Finland
E-mail: anna.saukko@abo.fi

Migmatites and related granites in southernmost Finland around Hanko Peninsula and Ekenäs archipelago are complex and vary greatly in petrology, geochemistry and field relations. We propose that a felsic MASH (melting, assimilation, storage and homogenization) processes in the middle crust can have given the area its distinct appearance.

Keywords: migmatite, granite, felsic MASH

1. Introduction

Melting, assimilation, storage and homogenization of basaltic magmas have long been thought to occur in lower crustal MASH zones, but only recently have examples of similar processes in felsic systems of the middle crust been described (Schwindinger & Weinberg, 2017). In these areas, melts from different crustal sources interact with each other, crystal mushes and restites. Signs of fluid interaction with the melt, and as an inducing agent of anatexis, are also often present.

2. Granites and migmatites in southernmost Finland

The granite and migmatite rich bedrock of southern and western Finland was formed in the margin of the Archaean Karelian craton in the Svecofennian orogeny at 1.9-1.8 Ga. This orogeny consisted of two different collisional stages and an intervening extensional stage, of which the later collision caused the most voluminous granite production. The Late Svecofennian granite-migmatite zone (LSGMZ) of metapelitic and psammopelitic migmatites goes through southern Finland in roughly WSW-ENE direction (Ehlers *et al*., 1993). In the LSGMZ, partial melting is thought to have occurred as fluid-absent incongruent melting with garnet, cordierite and sometimes orthopyroxene as peritectic minerals (Schreurs and Westra, 1986; Väisänen & Hölttä, 1999; Kriegsman, 2001). Andersen & Rämö (2018) suggest that dehydration melting is a plausible mechanism for forming late Svecofennian granites in southern Finland.

Bedrock in the southernmost part of Finland around Hanko Peninsula and Ekenäs archipelago, to the south of the LSGMZ, is characterized by migmatites on the mainland and inner archipelago, and granites in the outer archipelago (Figure 1). These migmatites are very heterogeneous and it appears that many different types of protoliths have been involved, resulting in many different types of melt. Field observations suggest that amphibolite rocks and K-feldspar bearing gneisses are the major protoliths to the migmatites. This contrasts with the migmatites in the LSGMZ.

The morphology and mineralogy of the southernmost Finland migmatites are more similar to migmatites where partial melting occurred in water-fluxed rocks, than those produced in water-absent melting (Weinberg & Hasalová, 2015). Mineralogically, the absence of garnet, cordierite, OPX and CPX are indicative of water-fluxed melting. Morphological signs of water-fluxed melting are diffuse leucosomes boundaries and the absence of melanosomes. In the migmatites, we can also see assimilation of xenoliths, which supports the idea of a mid-crustal MASH zone.

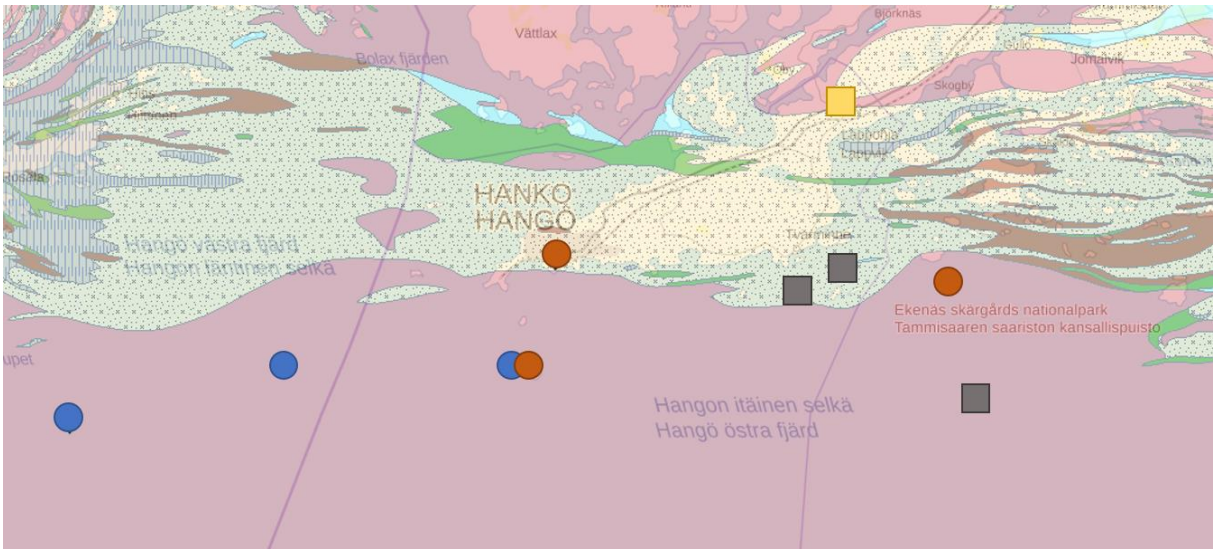

Figure 1. Lithological map of the study area. The markers denote the different rock types prevalent on some key localities. Blue circles: grey even-grained granites; orange circles: red even-grained granites; grey squares: K-feldspar megacrysts-bearing gneiss; yellow square: tonalite.

One of the most predominant rocks to the southeast of the area is a K-feldspar megacryst-bearing gneiss that occurs often together with an even-grained red granite. Field relations between these rock types are somewhat ambiguous, but they clearly interact: in places, it looks like the gneiss is partially melting into the granite, but in other places the megacryst-bearing rock looks more like an igneous granite from which the even-grained granite is separated through filter pressing. In areas with more metatexitic migmatite, megacryst-bearing gneiss appears as layers in highly metamorphosed supracrustal sequences. It is therefore difficult to say if the K-feldspar megacryst-bearing gneiss is an ortho- or a paragneiss.

The larger granite bodies in the southwest of the area are even-grained but vary in appearance from grey, magnetite fleck-bearing granite west of Hanko peninsula to red granite to the south and southeast of the peninsula. Xenoliths of the K-feldspar bearing gneiss are found in the granite bodies. Some even-grained red granites also differ from others in mineralogy and chemistry, appearing more evolved.

3. Age data

U-Pb dating of zircon from the megacryst-bearing gneiss shows ages ranging between 1900 and 1870 Ma, but in an area where the rocks look more like igneous granites, a few zircon rims also show ages at around 1830 Ma.

Our dating results show that the even-grained granites also mainly crystallised around 1830 Ma, which is also concurrent with Huhma's dating of zircon in the even-grained Hanko granite (1986). In some of the even-grained red granites, we also found zircon ages at around 1850-1840 Ma. Similar granite ages were also found in some granites in Ekenäs archipelago by Hopgood *et al.* (1983) and in Hanko by Kurhila *et al.* (2005), although all of these come with large uncertainty.

The oldest ages found in the megacryst-bearing gneisses correspond with the early volcanic arc magmatism stages and the first collisional event after it in the Svecofennian orogeny. The intervening extensional event corresponds with the rather uncertain ages in some of the even-grained red granites, so if these ages are real it is possible that some granites were formed in the area even during the extension. The 1830 Ma ages correspond to granite magmatism in the later collisional stage, and similarly to the other late Svecofennian granite sites, this appears to have been the time when granite formation was most voluminous also in southernmost Finland.

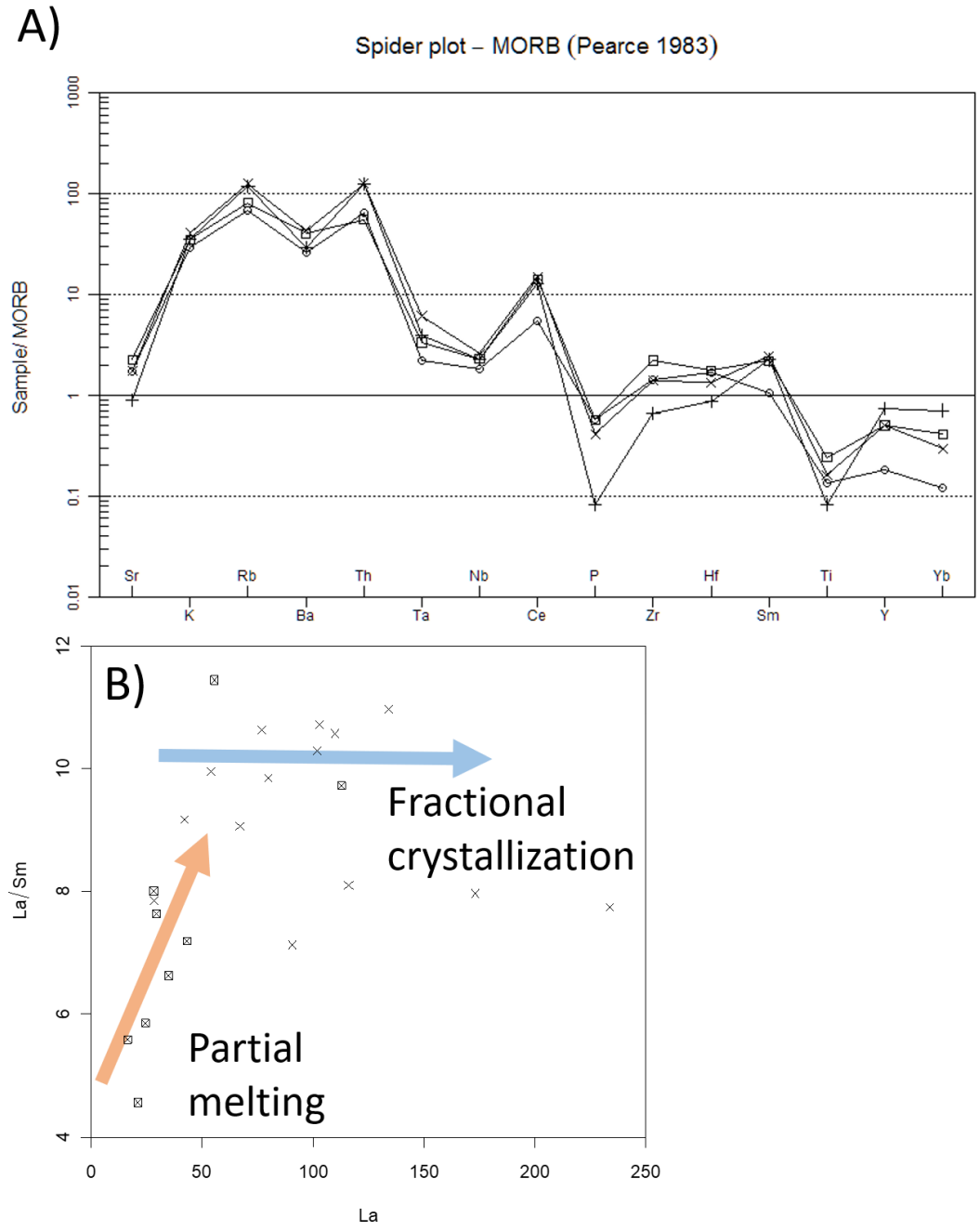

Figure 2. Geochemical trace element diagrams. A) MORB-normalized trace element spider diagram with representative tonalite (○), K-feldspar megacrysts-bearing gneiss (□), red even-grained granite (+) and grey even-grained granite (D) samples. All the rock types in the area show the same volcanic arc trend with a distinctive T-N-T anomaly. B) La vs. La/Sm diagram showing partial melting and magma differentiation trends.

4. Geochemistry

We have geochemically analysed the main rock types in the Hanko area. While the major element compositions differ greatly between different rock types, trace elements show some consistent patterns.

In trace element composition, all our sampled rock types show distinct volcanic arc features, including negative Nb, Ta and Ti anomalies (Figure 2A). This suggests that rocks stemming from the original volcanic arc have been reworked enough to form many melts that

differ from each other in appearance and in mineral and major element composition, but all still carry a very similar trace element signature. There appears to be no major influx of magmas from other sources, as even the even-grained granites show the volcanic arc pattern.

La vs La/Sm diagram (Figure 2B) shows that some of the samples follow a partial melting trend, while others follow along the fractional crystallisation trend. This is consistent with the felsic MASH zone model, as melting and crystallisation are expected to occur simultaneously.

5. Discussion

The southernmost Finland granite and migmatite area fits well with Schwindinger and Weinberg's (2017) description of a mid-crustal felsic MASH zone. Both granites and migmatites in the area show many of the melting and assimilation features characteristic to a MASH zone, but homogenisation appears to have been halted, possibly because of very rapid cooling after the orogeny. Compared to the granites in southern Finland Late Svecofennian granite-migmatite zone, where the granites appear as intruding batholiths, in southernmost Finland the granites appear to be stored by the anatectic site.

References:

Andersen, T, Rämö, O.T., 2018. Dehydration melting and granite petrogenesis in Southern Finland. In: Skyttä, P. and Eklund, O. (eds) Abstract Book 4th Finnish National Colloquium of Geosciences, Turku, 14–15 March 2018. Geological Survey of Finland, p. 58.

Ehlers, C., Lindroos, A., Selonen, O., 1993. The late Svecofennian granite-migmatite zone of southern Finland—a belt of transpressive deformation and granite emplacement. Precambrian Research Vol. 64, Issues 1–4, pp. 295-309. https://doi.org/10.1016/0301-9268(93)90083-E

Hopgood, A.M., Bowes, D.R., Kouvo, O., Halliday, A.N., 1983. U-Pb and Rb-Sr isotopic study of polyphase deformed migmatites in the Svecokarelides, southern Finland. In: Atherton, M.P., and Gribble, C.D. (Eds), Migmatites, Melting and Metamorphism. Shiva Publishers Limited, Nantwitch, England, 80—92.

Huhma, H., 1986. Sm-Nd, U-Pb and Pb-Pb isotopic evidence for the origin of the Early Proterozoic Svecokarelian crust in Finland. Geological Survey of Finland Bulletin 337.

Kriegsman, L., 2001. Quantitative Field Methods for Estimating Melt Production and Melt Loss. Phys. Chem. Earth (A), Vol. 26, No. 4-5, pp. 247-253

Kurhila, M., Vaasjoki, M., Mänttäri, I., Rämö, T., Nironen, M., 2005. U-Pb ages and Nd isotope characteristics of the lateorogenic, migmatizing microcline granites in southwestern Finland. Bulletin of the Geological Society of Finland, Vol. 77, pp. 105–128

Pearce, J. A., 1983. Role of the sub-continental lithosphere in magma genesis at active continental margins. In: Hawkesworth, C.J. and Norry, M.J. eds. Continental basalts and mantle xenoliths, Nantwich, Cheshire: Shiva Publications, pp. 230-249.

Schreurs and Westra, 1986. The thermotectonic evolution of a Proterozoic, low pressure, granulite dome, West Uusimaa, SW Finland. Contrib. Mineral. Petrol. 93, 236-250

Schwindinger, M., Weingberg, R.F., 2017. A felsic MASH zone of crustal magmas — Feedback between granite magma intrusion and in situ crustal anatexis. Lithos 284–285, 109–121. http://dx.doi.org/10.1016/j.lithos.2017.03.030

Väisänen, M., Hölttä, P. 1999. Structural and metamorphic evolution of the Turku migmatite complex, southwestern Finland. Bulletin of the Geological Society of Finland 71, Part 1, 177-218.

Weinberg R.F., Hasalová, P., 2015. Water-fluxed melting of the continental crust: A review, Lithos 212–215, 158–188. http://dx.doi.org/10.1016/j.lithos.2014.08.021

Fragmentation of the Archaean crust and its influence on the evolution of the overlying Proterozoic sequences (Northern Finland)

P. Skyttä[1]

[1]Department of Geography and Geology, University of Turku
E-mail: Pietari.skytta@utu.fi

This abstract highlights the significance of understanding the fragmentation of the Archaean continent as a key factor in controlling the evolution of the overlying Proterozoic supracrustal sequences in Northern Finland. The given example builds upon the recent findings from the Peräpohja Belt, and indicates that the understanding the apparently complex crustal structures may be more straightforward when the rigid basement block can be correctly delineated and incorporated into the structural interpretations.

Keywords: Archaean, Proterozoic, structural inheritance, Northern Fennoscandia

1. Introduction

Utilization of old structures during new deformation events is an important mechanism that provides important controls on the style and localisation of deformation e.g. when continents are rifted into pieces (e.g. Zwaan and Schreurs, 2017; Corti et al., 2018) or when brtille deformation is localised (Skyttä and Torvela, 2018). The cases of structural inheritance are of particular significance in geological domains where the older basement structures are inherited during the evolution of the overlying cover sequences, as not only the structures but also the deposition of the volcanic and sedimentary units of the cover are affected. From the exploration point of view, these are the critical factors to be understood that correct ore genetic models (e.g. Hitzman et al., 2010) may be applied and mineralization targeted.

Potential coupling between the Archaean and Palaeoproterozoic crust is particularly important in Northern Fennoscandia, where Archaean rocks from a major portion of the crust either directly exposed (e.g. Hölttä et al., 2008), or underlying the Proterozoic crust as revealed by e.g. the Nd-isotopic signatures (Mellqvist et al., 1999). Moreover, recent work has revealed a close relationship between the structural discontinuities of the Archaean basement and the evolution of the Palaeoproterozoic cover sequences within the Peräpohja Belt, Nortehrn Finland (Piippo et al., 2018; Skyttä et al., 2018), providing improved understanding of the basement-cover linkages and about the structural control of mineral deposits. The results (op. cit.) support earlier tentative models from the Kuusamo area further south-east, where the pattern of two orthogonally trending fold systems was attributed to the presence of rigid Archaean blocks controlling the strain partitioning during one single deformation event (Silvennoinen, 1972). In their work, Skyttä et al. (2018) further suggested that the geometry of the Archaean blocks would originally relate to the rifting of the Archaean continent commenced at around 2.45 Ga.

The purpose of this work is to test the concept of fragmented Archaean crust as controlling the evolution of the Proterozoic cover sequences, and whether the apparently complex structural signatures could be explained by the dynamic interaction of the rigid basement blocks and the relative thin supracrustal cover.

2. Application of the basement-cover concept

The Sattanen map sheet in the Sodankylä area was selected as a test target due to i) the apparently orthogonal structural trends, ii) pre-existing structural interpretation addressing the orthogonal fold trends to two separate structural events (Tyrväinen, 1983, and iii) the apparently relatively this supracrustal cover shown by the presence of the Archaean basement windows (Fig. 1). Introducing the NW-SE and NE-SW trending basement discontinuities into the structural

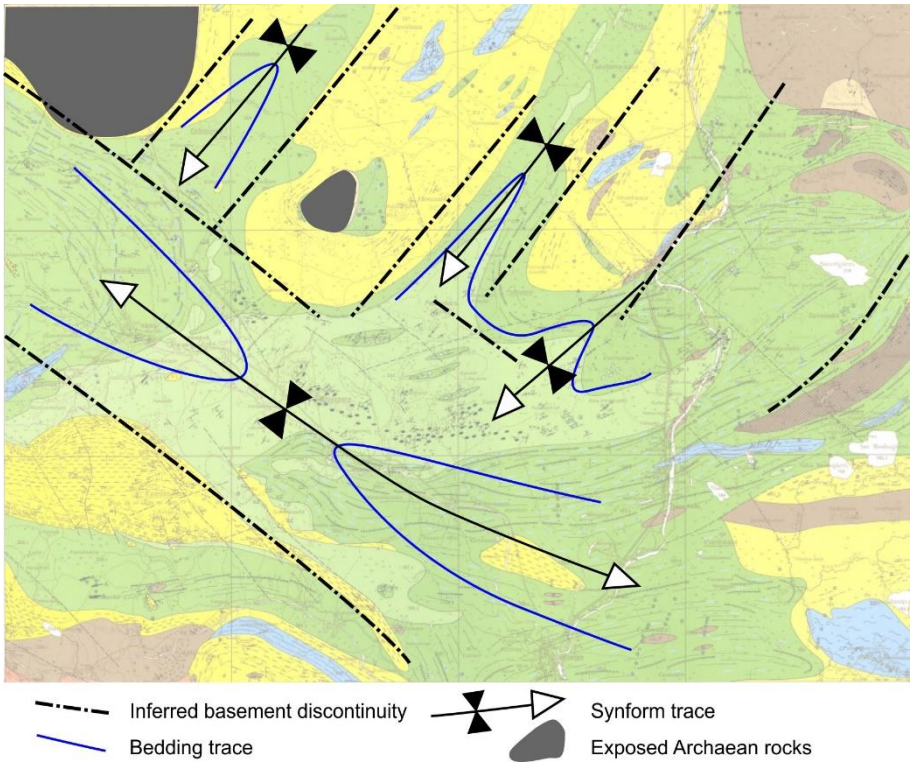

Figure 1. A structural sketch map illustrating the orthogonal structural trends defined by the inferred basement discontinuities. Explanation for the other map symbols is found in Tyrväinen (1980).

interpretations allows the apparently conflicting fold pattern to be understood as a result of one deformation event, where the contrasting trends relate to the margins of underlying fragments of the Archaean crust. The interpretation is plausible as no cross-folding may be recognised from the map patterns.

3. Conclusion

The inheritance of Archaean structures appears to explain the structural signatures of the selected test site, is assumed be a fruitful concept towards better understanding of the crustal structure in Northern Fennoscandia, and should be used as a proxy when targeting new mineral deposits, as well as when interpreting regional-scale geophysical datasets. Applying the presented approach also requires that the relationship of the structural evolution and the primary stratigraphy of the supracrustal belts is appropriately addressed.

References:

Corti, G., Molin, P., Sembroni, A., Bastow, I. D., Keir, D., 2018. Control of pre-rift lithospheric structure on the architecture and evolution of continental rifts: Insights from the Main Ethiopian Rift, East Africa. Tectonics 37, 477–496.

Hitzman, M.W., Selley, D. and Bull, S. 2010. Formation of Sedimentary Rock-Hosted Stratiform Copper Deposits through Earth History. Society of Economic Geologists 105, 627–639.

Hölttä, P., Balagansky, V., Garde, A., Mertanen, S., Peltonen, P., Slabunov, A., Sorjonen-Ward, P., Whitehouse, M. 2008. Archaean of Greenland and Fennoscandia. Episodes 31, 13–19.

Mellqvist, C., Öhlander, B., Skiöld, T., Wikström, A., 1999. The Archaean–Proterozoic Paleoboundary in the Luleå area, northern Sweden: field and isotope geochemical evidence for a sharp terrane boundary. Precambrian Research 96, 225–243.

Piippo, S., Skyttä, P., Kloppenburg, A., (2018). Linkage of crustal deformation between the Archaean basement and the Proterozoic cover in the Peräpohja Area, northern Fennoscandia. Under review at Precambrian Research (Sept 2018).

Silvennoinen, A. 1972. On the stratigraphic and structural geology of the Rukatunturi area, northeastern Finland. Gological Survey of Finland Bulletin 257. 48 pp.

Skyttä, P., Torvela, T., 2018. Brittle reactivation of ductile precursor structures: the role of incomplete structural transposition at a nuclear waste disposal site, Olkiluoto, Finland. Journal of Structural Geology 116, 253–259.

Skyttä, P., Piippo, S., Kloppenburg, A., Corti, G., (2018). 2. 45 Ga break-up of the Archaean continent in Northern Fennoscandia: Rifting dynamics and the role of inherited structures within the Archaean basement. Under review at Precambrian Research (Sept 2018).

Tyrväinen, A., 1980. Maps of Pre-Quaternary Rocks, Map Sheet 3714, Sattanen. Geological Survey of Finland, Espoo, Finland.

Tyrväinen, A. 1983. Explanation to Maps of Pre-Quaternary Rocks, Map Sheets 3713, 3714; Sodankylä and Sattanen. Volyymi: 3713; 3714, Geological Survey of Finland, Espoo, Finland.

Zwaan, F., Schreurs, G., 2017. How oblique extension and structural inheritance influence rift segment interaction: Insights from 4D analog models. Interpretation 5, SD119–SD138.

Subglacial deformations adjacent to Ristonmännikkö PGF

R. Sutinen[1] and A. Ojala[2]

[1]Geological Survey of Finland, PL 77, 96101 Rovaniemi, Finland
[2]Geological Survey of Finland, PL 96, 02151 Espoo, Finland

E-mail: raimo.sutinen@gtk.fi

Airborne LiDAR DEMs have revealed several postglacial faults (PGFs) in the interior of the former Fennoscandian Ice Sheet (FIS). One of them, called as Vaalajärvi-Ristonmännikkö PGF system in central Finnish Lapland, was verified with trenchings. The PGF-trench exhibited indication of multiple earthquake events. Here, we present morphological evidence of subglacial faulting in the area by interpreting the LiDAR-DEMs of the Late Weichselian landforms. Along the SE-trending down-ice transect from the fault, one of the striking feature is irregular groupings of straight or curvilinear and transverse-to-ice flow ridges, which are not comparable to annual or ice-marginal end moraines. We propose that some of the paleo-earthquakes were subglacial and therefore the ice crevassing created pathways for the saturated material to squeeze into the fractured ice system. At 40 km distance from the PGF, a field of arcuate/semi-circular Pulju moraines is associated with transverse-to-ice ridges forming a complex of seismic-induced subglacial landforms.

Keywords: PGF, subglacial deformation, squeezing, crevasses, seismic impact

1. Introduction

Fennoscadian shield has subjected to end- or postglacial crustal events (Arvidsson, 1996) contributing to postglacial fault (PGF) systems and subaerial deformations, such as landslides and liquefaction features (Ojala et al., 2017a; Sutinen et al., 2018a; Fig. 1). PGFs eventually have been also a dynamic driver for the subglacial bed deformations, such as the Pulju moraines (Sutinen et al., 2018b).

Transverse-to-ice flow moraines are common in the areas formerly covered by continental ice sheets, yet their morphology, size and shape are highly variable and there are no consensus about the genetic constraints. Some of the transversally oriented moraines, such as Rogen moraine or ribbed moraine are regarded as active-ice subglacial, often polygenetic, landforms (Lundqvist, 1997). Ice-marginal moraines, such as washboard moraines exhibiting crevasse-squeeze features (Ankerstjerne et al., 2015) or De Geer moraines associated with proglacial water bodies (Ojala, 2016), show regular ridge-to-ridge pattern, probably attributed to annual ice recession. Also, small end moraines may exhibit regular pattern of the ridges as a result of ice-marginal oscillations (Ham and Attig, 2001).

As far as we know, the origin of irregular fields of small transversal moraines has not linked to paleoseismicity. It is known, that modern earthquakes/icequakes e.g. in Alaska and Greenland (Ekström et al., 2006) contribute to deformations on subglacial beds. In a similar way, late glacial earthquakes may have contributed to ice-crevassing and subglacial deformations and seen now as transverse-to-ice flow morphologies in the interior part of the Fennoscandian Ice Sheet.

2. Materials and methods

In this paper we provide airborne LiDAR DEM (Digital Elevation Model) information on the group of landforms, such as transverse-to-ice flow moraine ridges and arcuate/ winding Pulju moraines with regard to their spatial coexistence with the known Vaalajärvi-Ristonmännikkö postglacial fault (PGF) system in central Finnish Lapland (Fig. 1). The airborne LiDAR DEM data is provided by the National Land Survey of Finland, applying a Leica ALS50-II laser scanner from a flight altitude of 2000 m. The LiDAR data were interpolated to a 2×2 m grid. Last-return data with generally one to three hits per m^2 allows 14-cm-vertical ground resolution.

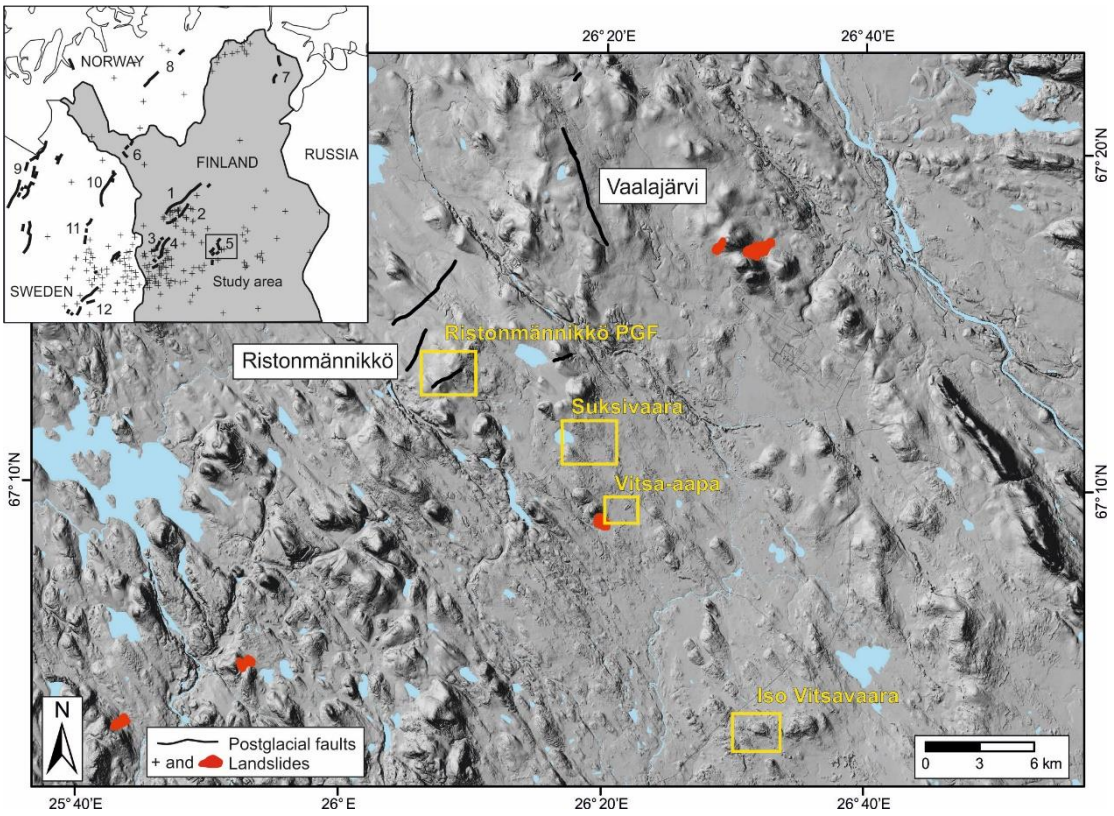

Figure 1. Vaalajärvi-Ristonmännikkö PGF system in central Finnish Lapland (#5 in the orientation map) with subsets Suksivaara, Vitsa-aapa and Iso Vitsavaara on the LiDAR DEM. PGFs and paleolandslides from Olesen et al. (2004), Lagerbäck and Sundh (2008), Sutinen et al. (2014), Mikko et al. (2015) and Ojala et al. (2017a; 2017b). 1. Suasselkä, 2. Riikonkumpu-Isovaara, 3.Venejärvi, 4.Pasmajärvi-Ruokojärvi, 5. Vaalajärvi-Ristonmännikkö, 6. Palojärvi, 7. Sevetti, 8. Stuorragurra, 9. Pärvie, 10. Lainio-Suijavaara, 11. Merasjärvi, 12. Landsjärv.

3. Results

Figure 2 shows the Ristonmännikkö PGF (location in Fig. 1) with the upthrown block facing SE. The LiDAR DEM exhibits a significant amount of straight and curvilinear moraine morphologies 40 km SE of the fault ramp. These moraines are roughly oriented transverse-to-ice flow, from northwest toward southeast. We interpret this field of moraines as subglacial deformations induced by PG faulting. The irregular spacing between the ridges indicates rather a sudden seismic-induced bed deformation than end moraine processes within the ice-margin oscillations (Ham and Attig, 2001) or regular pattern of washboard or De Geer moraines (Ankerstjerne et al., 2015; Ojala, 2016).

The Iso Vitsavaara LiDAR DEM (Fig. 3, location in Fig. 1) shows a complex of subglacial landforms constituting transverse ridges and the Pulju moraines (see Sutinen et al., 2014; 2018a; 2018b). The squeeze-up materials of the Pulju moraine has been shown to be anisotropic, but not indicative of ice-flow pattern (Sutinen et al., 2018a). Here, the transverse-to-ice ridges are 2-3.5 m high and with 50-100 m inter-spacings. Those can be seen to cover the local hills with no preference to the elevation. The arcuate/circular Pulju moraine ridges are 1-4 m high and are randomly spaced on the Iso Vitsavaara hill (Fig. 3).

Figure 2. Ristonmännikkö postglacial fault (location in Fig. 1). Photo by N. Nordbäck.

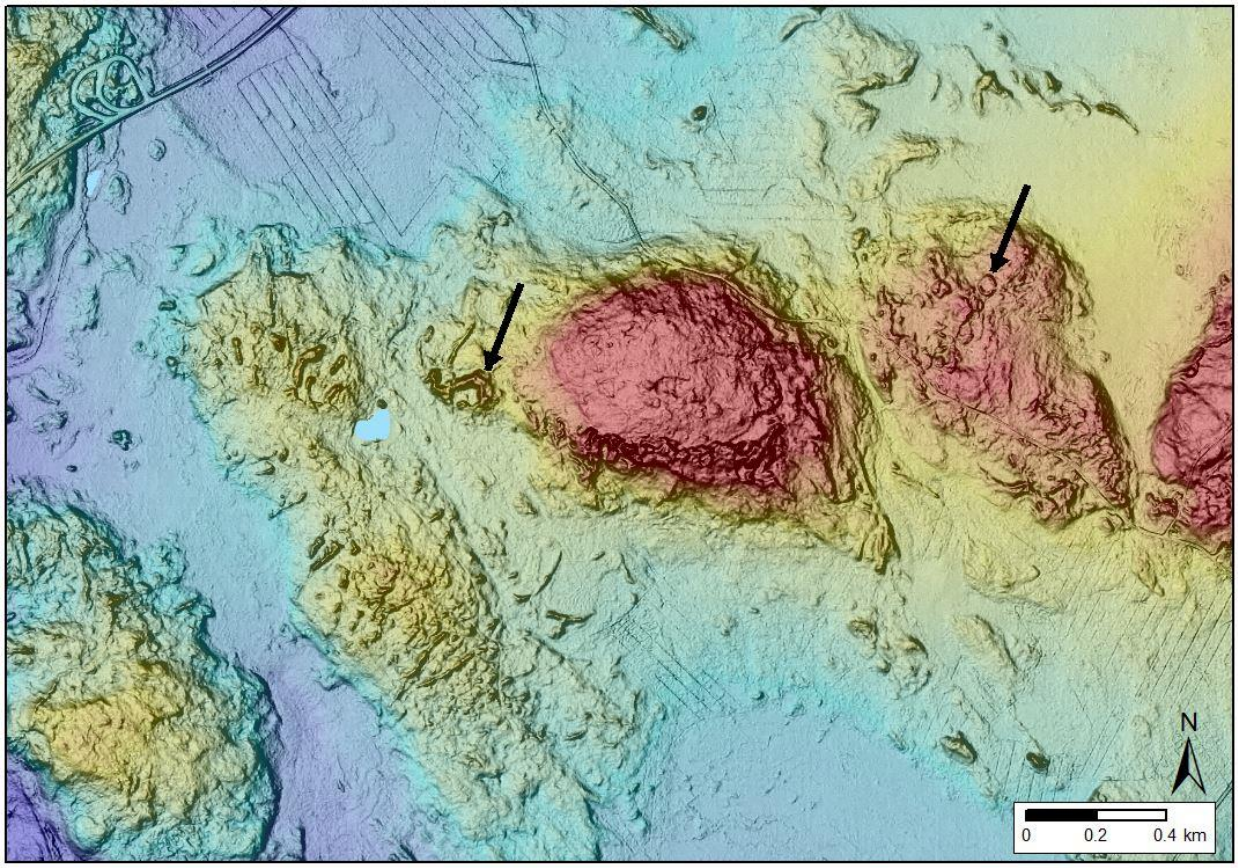

Figure 3. LiDAR DEM showing transverse-to-ice flow squeeze-up ridges and arcuate/round shaped Pulju moraines (indicated by arrows) at the Iso Vitsavaara site in central Finnish Lapland (location in Fig. 1).

The transverse-to-ice oriented ridges at the Suksivaara site, 8 km from the Ristonmännikkö PGF (location in Fig. 1), are 1-2.5-m-high and are rather randomly spaced with the separation between single ridges ranging from 100 to 300 m. Also, some minor ribbing pattern can be seen between the dominant transverse ridges, particularly in the NE part of the Suksivaara site. The minor ridges are 0.5-1 m high are the ridge-to-ridge separation ranges from 10 to 50 m. These transverse-to-ice flow ridges are deforming and/or superimposed on the NE-SE oriented ice-parallel forms, thus indicating the time difference between these morphological assemblages, i.e. the transverse ridges are younger and presumably dating back to late glacial. Some of the transverse-to-ice flow ridges show curvilinear morphologies with horns bending up-ice direction (Vitsa-aapa location in Fig. 1). The tallest ridges reach 2.5-3 m and the ridge-to-ridge spacing varies from 50 to 100 m. The morphometry of the ridges display evidence of the crevasse-squeeze up processes (Hoppe, 1952; Ankerstjerne et al., 2015). We interpret the origin of the crevasses had been subglacial event of the Ristonmännikkö PGF (Figs. 1-2). According he original squeezing hypothesis for the hummocky moraines in Norrbotten, Sweden by Hoppe (1952), the saturated bed material is forced into cavities by the ice load. We agree with this concept, but in the vicinity of the Ristomannikkö PGF, we postulate that seismic impact(s) primarily contributed to crevassing of the ice and squeeze-up of water-saturated bed materials.

References:

Ankerstjerne, S., Iverson, N.R., Lagroix, F., 2015. Origin of a washboard moraine of the Des Moines Lobe inferred from sediment properties. Geomorphology 248, 425-463.

Arvidsson, R., 1996. Fennoscandian earthquakes. Whole crustal rupturing related to postglacial rebound. Science 274, 744-746.

Ekström, G., Nettles, M., Tsai, V.C., 2006. Seasonality and increasing frequency of Greenland glacial earthquakes. Science 311, 1756-1758.

Ham, N.R., Attig, J.W., 2001. Minor end moraines of the Wisconsin Valley Lobe, north-central Wisconsin, USA. Boreas 30, 31-41.

Hoppe, G., 1952. Hummocky moraine regions with special reference to the interior of Norrbotten. Geografiska Annaler 34, 1-72.

Lagerbäck, R., Sundh, M., 2008. Early Holocene faulting and paleoseismicity in northern Sweden. Sver. Geol. Unders. C836, 80 pp.

Lundqvist, J., 1997. Rogen moraine − an example of two-step formation of glacial landscapes. Sedimentary Geology 111, 27-40.

Mikko, H., Smith, C., Lund, B., Ask, M.V., Munier, R., 2015. LiDAR-derived inventory of post-glacial fault scarps in Sweden. GFF 137, 334–338.

Ojala, A.E.K., 2016. Appearance of De Geer moraines in southern and western Finland – Implications for reconstructing glacier retreat dynamics. Geomorphology 255, 16-25.

Ojala, A.E.K., Mattila, J., Markovaara-Koivisto, M., Ruskeeniemi, T., Palmu, J-P., Sutinen, R., 2017a. Distribution and morphology of landslides in northern Finland: An analysis of postglacial seismic activity. Geomorphology, http://dx.doi.org/10.1016/j.geomorph.2017.08.045.

Ojala, A.E.K, Mattila, J., Ruskeeniemi, T., Palmu, J-P., Lindberg, A., Hänninen, P., Sutinen, R., 2017b. Characterization and timing of the Isovaara and Riikonkumpu faults in northern Finland. Global and Planetary Change 157, 59-72.

Olesen, O. Blikra, L.H. Braathen, A. Dehls, J.F. Olsen, L. Rise, L. Roberts, D. Riis, F., Faleide, J.I., Anda, E., 2004: Neotectonic deformation in Norway and its implications: a review. Norwegian Journal of Geology 84, 3-34.

Sutinen, R., Hyvönen, E., Middleton, M., Ruskeeniemi, T., 2014. Airborne LiDAR detection of postglacial faults and Pulju moraine in Palojärvi, Finnish Lapland. Global and Planetary Change 115, 24–32.

Sutinen, R., Hyvönen, E., Liwata-Kenttälä, P., Middleton, M., Ojala, A., Ruskeeniemi, T., Sutinen, A., Mattila, J., 2018a. Electrical-sedimentary anisotropy of landforms adjacent to postglacial faults in Lapland. Geomorphology, https://doi.org/10.1016/j.geomorph.2018.01.008

Sutinen, R., Hyvönen, E., Middleton, M., Airo, M.-L., 2018b. Earthquake-induced deformations on ice-stream landforms in Kuusamo, eastern Finnish Lapland. Global and Planetary Change 160, 46–60.

Magnetic disturbances driven by currents in the solid Earth and ionosphere

E.I.Tanskanen[1]

[1]ReSoLVE Centre of Excellence, Aalto University, Finland

E-mail: eija.tanskanen@aalto.fi

The Earth´s magnetic environment is continuously disturbed by ionospheric currents and solid Earth variations. Ionospheric currents are modulated by solar wind disturbances while internal variations arise from currents induced in the solid Earth. We have examined variability of geomagnetic disturbance amplitude |dB/dt| for over solar cycles 23 and the role in solid Earth currents during different solar cycle phases.

Keywords: Magnetic disturbances, ionospheric currents, ground induced currents, magnetometry, auroral substorms and ULF waves.

1. Introduction

Geomagnetic activity varies in time-scales from seconds and minutes to years and solar cycles (Figure 1). Magnetic data recorded at the surface of the Earth is a superposed signal of all disturbances from above and below. It is known that the largest role of the currents in the solid Earth in short time-scales is found during the substorm onset (Tanskanen et al., 2001). It is, however, unknown how the role of induced currents varies over the longer-time scales such as seasons and solar cycles.

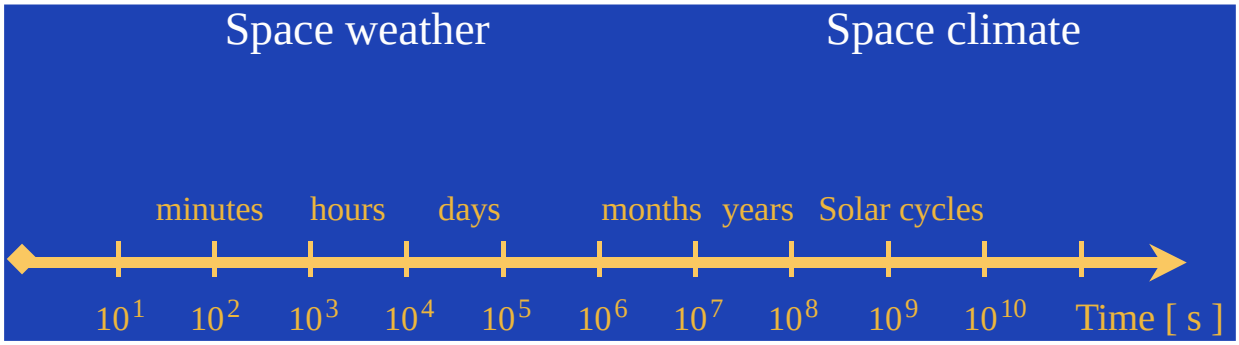

Figure 1. Geomagnetic activity varies in space weather and space climate time-scales. Space weather phenomena include ULF pulsations, auroral substorms and geomagnetic storms while space climate includes solar cycle-to-cycle variability in 11 and 22 years, and over modern solar grand maximum.

In this study we investigate how the role of induced current in the geomagnetic activity vary for the solar cycle 23 from 1998 – 2009.

2. Solar cycle variability of the role of induced currents

Magnetic field fluctuations of the north-south component |dX/dt| are computed for year from 1998 to 2009, separately for each IMAGE network station (Tanskanen, 2009). The magnetic fluctuation amplitude is shown by the red circle (Figure 2). Solar cycle variability of the

magnetic fluctuation amplitude is the largest in the auroral oval latitudes from 65 – 75 deg CGM. The largest fluctuation amplitude is found in the early declining solar cycle phase i.e. in the year 2003 while the smallest fluctuation amplitude is found in the year 2009. That is the year of the solar minimum. Then the largest fluctuation amplitudes are observed over the Svalbard. Throughout the solar cycle the smallest magnetic field fluctuation rates are seen in the southern Finland below the auroral zone.

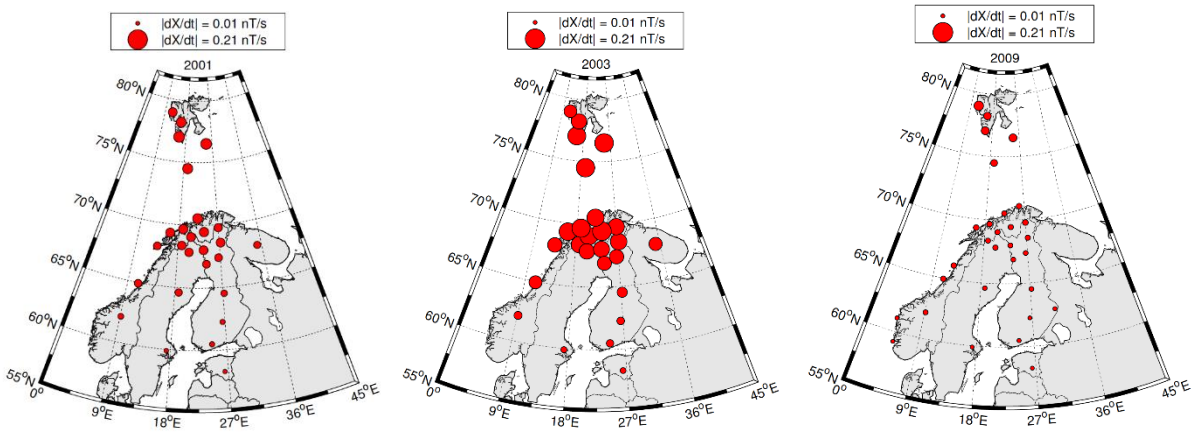

Figure 2. Magnetic field fluctuation amplitude |dX/dt| computed from the measurements by the magnetic stations in Fennoscandia for the years (a) 2001, (b) 2003, and (c) 2009.

The internal part of the magnetic field signal increase up-to the 40% during the substorm onset (Tanskanen et al., 2001) while the role of internal part decreases down to the 10-15% during the other substorm phases (growth and recovery phases) for inland stations. The role of internal part during substorm growth and recovery phases is roughly 25-30% for coastal stations, being only 10-15% less than for the substorm onset times in inland.

3. Conclusions

The role of currents induced to the solid Earth are the largest for the coastal stations and during the rapid magnetic field fluctuations for example during Pc5 pulsations and substorm onset. The largest effects from the internal sources are found during declining solar cycle phase and in winter months since then the most ULF waves in Pc5 frequency range and continuous substorm trains with rapid onsets are seen. These results are valuable when evaluating the effects of rapid magnetic field fluctuations to the current infrastructure, formulating models for space weather predictions, and building new infrastructure sensible to the space weather effects.

References:

Tanskanen, E. I., 2009, A comprehensive high-throughput analysis of substorms observed by IMAGE magnetometer network: Years 1993-2003 examined, *J. Geophys. Res. 114*, A5

Tanskanen, E.I., A. Viljanen, T.I. Pulkkinen, R. Pirjola, L. Häkkinen, A. Pulkkinen and O. Amm, 2001, At substorm onset, 40% of AL comes from underground, *J. Geophys. Res. 106*, A7, 13119-13134.

U-Pb zircon, monazite and xenotime geochronology of cordierite-anthophyllite and felsic volcanic rocks in Orijärvi, southern Finland

Teemu Vehkamäki[1], Markku Väisänen[1], Yann Lahaye[2], Matti Kurhila[2] and Bo Johanson[2]

[1]Department of Geography and Geology, FI-20014 University of Turku, Finland
[2]Geological Survey of Finland FI-02150, Espoo, Finland
E-mail: tetave@utu.fi

We sampled one felsic volcanic rock from the lower part of the Kisko formation and two cordierite-anthophyllite rocks from Orijärvi and Iilijärvi for U-Pb dating. The felsic volcanic rock yield a zircon $^{207}Pb/^{206}Pb$ weighted average age of ~1.89 Ga. The oldest zircons from the Orijärvi cordierite-anthophyllite rock give a weighted average age of ~1.89 Ga. The monazite from the same sample yield a concordia age of ~1.80 Ga and the xenotime yield a concordia age of ~1.82 Ga. The Iilijärvi cordierite-anthophyllite rock gives a monazite concordia age of ~1.82 Ga. This implies that two metamorphic pulses are recorded in the samples.

Keywords: geochronology, U-Pb, zircon, monazite, xenotime, cordierite-anthophyllite rock, felsic volcanic rock

1. Introduction

The Orijärvi area in southern Finland is historically and geologically important: it was the site of the first copper mine in Finland opened there in 1757 (Poutanen 1996). Orijärvi was also the area from where Pentti Eskola developed the theory of metamorphic facies (Eskola 1914, 1915). Since then the Orijärvi area has been a target for numerous studies focused on ore geology, geochronology, petrology, geochemistry and structural geology (eg., Latvalahti 1979, Väisänen & Mänttäri 2002, Skyttä et al. 2006, Pajunen 2008, Väisänen & Kirkland 2008, Nironen et al. 2016, Kara et al. 2018).

A special interest has been the cordierite-anthophyllite, quartz-cordierite as well as garnet and andalusite-bearing rocks which represent the metamorphic equivalents of hydrothermally altered volcanic-sedimentary rocks which are associated with the Cu-Zn-Pb mineralisations (Smith et al. 1992, Rajavuori & Kriegsman 2002, Ratsula 2016). The hydrothermal alteration is regarded to have been acting simultaneously with volcanism or at least before the regional deformation and metamorphism at c. 600 °C and 3 kbars (Latvalahti 1979, Schneiderman & Tracy 1991). The age of the metamorphism is, however, unknown. Orijärvi forms a triangular shaped low-strain area bounded by shear zones where early-stage deformation is well-preserved and the metamorphic grade is lower than outside the triangular area where the rocks are migmatitic (Ploegsma & Westra 1990, Skyttä et al. 2006).

We sampled two cordierite-anthophyllite rocks (CARs) and one felsic volcanic rock (FVR) for dating and separated zircons, monazites and xenotimes from CARs and zircons from FVR. This was done to gain better understanding of the timing of the volcanism, alteration and metamorphism. One CAR sample was collected from the vicinity of the Orijärvi mine and another CAR sample was sampled from the Iilijärvi mineralised zone 600 m to the north. The unaltered FVR was sampled from the lower part of the Kisko formation, stratigraphically above the altered rocks. Sample locations are indicated in Fig. 1.

2. Geological setting

The bedrock of Orijärvi is composed of mafic to felsic volcanic rocks and metasedimentary rocks (Kähkönen 2005). These supracrustal rocks are also accompanied with bimodal igneous rocks that represent magma chambers to the volcanic rocks (Väisänen and Mänttäri 2002, Kara et al. 2018). Based on the structural and geochemical features, bedrock in Orijärvi has been divided into four formations: the Orijärvi, Kisko, Toija and Salittu formations (Fig. 1).

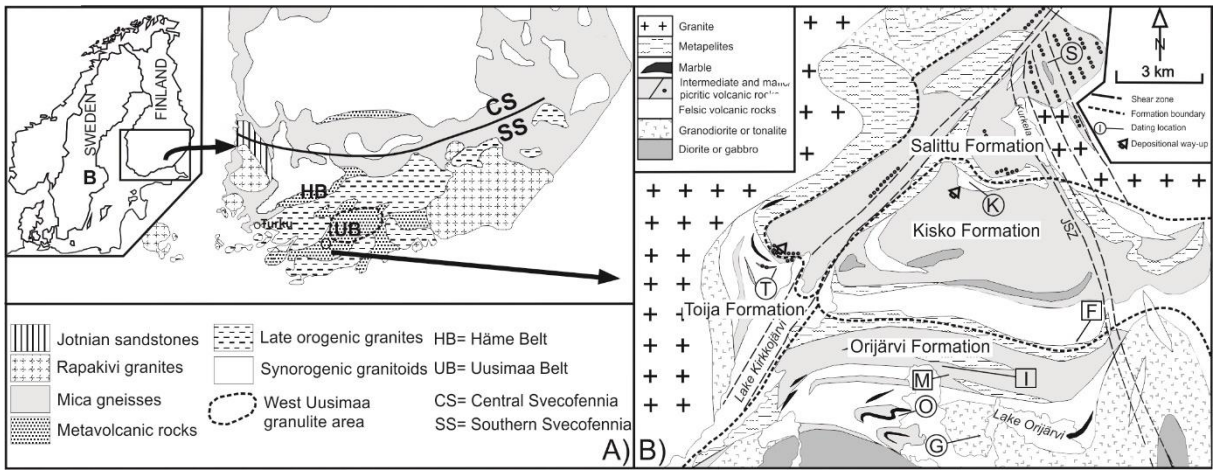

Figure 11. (A) Simplified geological map of southern Finland and (B) geological map of the Orijärvi area with previous and new sample locations indicated with circles and squares. F = felsic volcanic rock, M = Orijärvi (mine) cordierite-anthophyllite rock, I= Iilijärvi cordierite-anthophyllite rock, G = Orijärvi granodiorite (Väisänen et al. 2002), K= Kisko dacite (Väisänen & Mänttäri 2002), O = Orijärvi rhyolite (Väisänen & Mänttäri 2002) S = Salittu gabbro (Väisänen & Kirkland 2008), T = Toija felsic volcanic rock (Väisänen & Kirkland 2008). Figure is modified from Väisänen & Kirkland (2008).

The Orijärvi formation is stratigraphically the lowest one. It includes the Orijärvi granodiorite which contains mafic enclaves and shows signs of magma mingling (Kara et al. 2018). The volcanic and sedimentary rocks around the granodiorite are intensively hydrothermally altered. The zircon U-Pb age of unaltered Orijärvi rhyolite is 1895.3±2.4 Ma while the Orijärvi granodiorite is dated at 1898±9 Ma (Väisänen et al. 2002).

To the north and stratigraphically above of the Orijärvi formation lies the Kisko formation. Rocks of the Kisko Fm. are mainly felsic, intermediate and mafic volcanic and sedimentary rocks. Gabbros and plagioclase porphyries intrude the volcanic-sedimentary rocks. A dacite from the upper part of the formation yielded a U-Pb zircon age of 1878.2±3.4 Ma (Väisänen and Mänttäri 2002).

To the west and north lies the Salittu formation composing of ultramafic and mafic lavas (Schreurs et al. 1986) intercalated by metapelites and marbles. Tonalites, granoriorites and gabbros crosscut the lavas. Based on the field relationships, the Salittu formation is thought to have deposited around 1875 Ma (Väisänen and Kirkland 2008, Nironen et al. 2016).

The westernmost subarea is the Toija formation. It consists of rhyolites and pillow-basalts with metapelite and marble intercalations. The felsic volcanic rock yielded a zircon age of 1878±4 Ma with metamorphic 1815±3 Ma rims (Väisänen and Kirkland 2008).

3. Results

The U-Pb analyses were performed in the Finnish Geosciences Research Laboratory at the Geological Survey of Finland in Espoo.

Kisko felsic volcanic rock

Prismatic zircons are partly metamict, hampering the choice of intact domains for analyses spots. Consequently, many analyses are slightly discordant. However, the $^{207}Pb/^{206}Pb$ ages give a coherent weighted average age of ~1.89 Ga.

Orijärvi cordierite-anthophyllite rock

Zircons occur in many morphological types and grains are metamict and rich in inclusions. Most analyses are discordant and their $^{207}Pb/^{206}Pb$ ages form a declining trend of ages from 1901 Ma to 1786 Ma. Five oldest analyses form a distinct group and yield a weighted average age of ~1.89 Ga.

Monazites comprise both elongated and rounded grains. They yield a concordia age of ~1.80 Ga. Xenotimes are all rounded in shape and yield a concordia age of ~1.82 Ga

Iilijärvi cordierite-anthophyllite rock

Only few zircons were recovered and they all are highly discordant. Monazites are mostly rounded save a few prismatic grains. The analyses are mostly concordant and yield a concordia age of ~1.82 Ga.

4. Discussion and conclusions

The age of the Kisko felsic volcanic rock, ~1.89 Ga, is only slightly younger than the age of the Orijärvi rhyolite at 1895.3±2.4 Ma. This implies that the volcanism in the lower part of the Kisko formation continued after the deposition of the Orijärvi formation, without any hiatus in the volcanic activity as previously assumed. This also brings into question whether the previously argued stratigraphic position of the 1878±4 Ma Kisko dacite is valid (c.f. Väisänen and Mänttäri 2002, Nironen et al. 2016).

The oldest ~1.89 Ga zircon from the Orijärvi cordierite-anthophyllite rock is regarded as an igneous age of the protolith while the rest of the grains are modified by hydrothermal and metamorphic processes. The monazite and xenotime yield ages of ~1.80 Ga and ~1.82 Ga which we regard as metamorphic. The Iilijärvi monazite, however, yield an age of ~1.82 Ga, i.e., about 20 Ma older than the monazite from the Orijärvi sample even though the locations are only about 600 m apart.

The 1.82 Ga age of metamorphism and associated anatectic magmatism is common outside the Orijärvi triangle (Mouri et al. 2005, Skyttä and Mänttäri 2008, Väisänen and Kirkland 2008) related to regional granulite facies metamorphism. This implies that the lower grade Orijärvi triangle was metamorphosed simultaneously.

The 1.80 Ga metamorphism is more ambiguous but not unique. The metamorphic zircon from a gabbro within the Salittu formation yield an age of 1792±5 Ma (Väisänen and Kirkland 2008) and the titanite from the 1878±4 Ma Kisko dacite was 1798±3 Ma in age. In general, the magmatic 1.80 Ga activity is well documented in southern Finland (e.g., Rutanen et al. 2011) and it might have thermal consequences.

We conclude that the oldest volcanism in the Kisko formation started at ~1.89 Ga. The regional metamorphism in the Orijärvi triangle has had two different events at 1.82 Ga and ~1.80 Ga.

Acknowledgements
This study was funded by the Finnish Cultural Foundation.

References:

Eskola, P. 1914. On the petrology on the Orijärvi region in southwestern Finland. Bulletin de la commission géologique de Finlande 40, 279 p.

Eskola, P. 1915. Om sambandet mellan kemisk och mineralogisk sammansättning hos Orijärvitraktens metamorfa bergarter. English Summary: On the relations between the chemical and minealogical compositions in the metamorphic rocks of the Orijärvi region. Bulletin de la Commission geologique de Finland 44, 145 p.

Kähkönen, Y. 2005. Svecofennian supracrustal rocks. In: Lehtinen, M., Nurmi, P.A., Rämö, O.T., (eds.). Precambrian Geology of Finland–Key to the Evolution of the Fennoscandian Shield. Elsevier, Amsterdam, Developments in Precambrian Geology 14, 343-405.

Kara, J., Väisänen, M., Johansson, A., Lahaye, Y., O'Brien, H., Eklund, O. 2018. 1.90–1.88 Ga arc magmatism of central Fennoscandia: geochemistry, U-Pb geochronology, Sm-Nd and Lu-Hf isotope systematics of plutonic-volcanic rocks from southern Finland. Geologica Acta 16, 1-23.

Latvalahti, U. 1979. Cu-Zn-Pb ores in the Aijala-Orijarvi area, southwest Finland. Economic Geology 74, 1035–1059.

Mouri, H., Väisänen, M., Huhma, H., Korsman, K. 2005. Sm-Nd garnet and U-Pb monazite dating of high-grade metamorphism and crustal melting in the West Uusimaa area, southern Finland. GFF 127, 123-128.

Nironen, M., Mänttäri, I., Väisänen, M. 2016. The Salittu Formation in southwestern Finland, part I: Structure, age and stratigraphy. Bulletin of the Geological Society of Finland 88, 85–103.

Pajunen, M., Airo, M.L., Elminen, T., Mänttäri, I., Niemelä, R.,Vaarma, M., Wennerström, M., 2008. Tectonic evolution of the Svecofennian crust in southern Finland. Geological Survey of Finland, Special Paper 47, 15-160.

Ploegsma, M., Westra, L. 1990. The Early Proterozoic Orijärvi triangle (southwest Finland): a key area on the tectonic evolution of the Svecofennides. Precambrian Research 47, 51-69.

Poutanen, P. 1996. Suomalaisen kuparin ja sinkin juurilla: Orijärven kaivos 1757–1957. Outokumpu Oy, Gummerus, Espoo, 147 pages. (in Finnish)

Rajavuori, L., Kriegsman, L. M. 2002. Fluorine in orthoamphibole dominated Zn-Cu-Pb deposits: examples from Finland and Australia. Geological Society, London, Special Publications 204, 337-353.

Ratsula, A, 2016. Orijärven hydrotermisesti muuttuneiden kivien geokemiallinen tutkimus.,.MSc thesis, Department of Geography and Geology, University of Turku**.** 102 p. (in Finnish)

Rutanen, H., Andersson, U. B., Väisänen, M., Johansson, Å., Fröjdö, S., Lahaye, Y., Eklund, O. 2011. 1.8 Ga magmatism in southern Finland: strongly enriched mantle and juvenile crustal sources in a post-collisional setting. International Geology Review *53*, 1622-1683.

Schneiderman, J.S., Tracy, R.J. 1991. Petrology of orthoamphibole-cordierite gneisses from the Orijarvi area, Southwest Finland. American Mineralogist 76, 942-955.

Schreurs, J., Van Kooperen, P.,Westra, L. 1986. Ultramafic metavolcanic rocks of early Proterozoic age in West-Uusimaa, SW-Finland. Neues Jahrbuch für Mineralogie. Abhandlungen 155, 185–201.

Skyttä, P., Mänttäri, I. 2008. Structural setting of late Svecofennian granites and pegmatites in Uusimaa Belt, SW Finland: Age constraints and implications for crustal evolution. Precambrian Research 164, 86-109.

Skyttä, P., Väisänen, M., Mänttäri, I. 2006. Preservation of Palaeoproterozoic early Svecofennian structures in the Orijärvi area, SW Finland – Evidence for polyphase strain partitioning. Precambrian Research 150, 153–172.

Smith, M. S., Dymek, R. F., Schneiderman, J. S. 1992. Implications of trace element geochemistry for the origin of cordierite-orthoamphibole rocks from Orijärvi, SW Fin-land. The Journal of Geology, 545–559.

Väisänen, M., Kirkland, C. L. 2008. U-Th-Pb zircon geochronology on igneous rocks in the Toija and Salittu Formations, Orijärvi area, southwestern Finland: Constrains on the age of volcanism and metamorphism. Bulletin of the Geological Society of Finland 80, 73–87.

Väisänen, M., Mänttäri, I., Hölttä, P. 2002. Svecofennian magmatic and metamorphic evolution of southwestern Finland as revealed by U-Pb zircon SIMS geochronology. Precambrian Research 116, 111–127 p.

Väisänen, M., Mänttäri, I. 2002. 1.90-1.88 Ga arc and back-arc basin in the orijärvi area, SW Finland. Bulletin of the Geological Society of Finland 74, 185–214.

Heat flow and heat production in relation to geoneutrino signal near Pyhäsalmi mine

T. Veikkolainen[1,2] and I.T. Kukkonen[1]

[1]Department of Geosciences and Geography, University of Helsinki
[2]Institute of Seismology, University of Helsinki
E-mail: toni.veikkolainen@helsinki.fi

This study gives an overview of thermal environment within 150 km distance from the Pyhäsalmi zinc-copper mine which will be decommissioned in 2019. The site has hosted research activity related to nuclear physics. We have analysed geoneutrino flux in the area using a cylindrical model, and generated one-dimensional geotherms for a two-layered crust, applying upper crustal depth d = 10 km and Moho depth z_m = 55 km, Moho heat flow Q_m= 9...15 mWm^{-2}, surface heat flow Q = 32.1...46.1 mWm^{-2} from borehole data and upper crustal heat production values A_H = 0.2...2.3 μWm^{-3}. Our most plausible cylindrical model of the crust around Pyhäsalmi has Q = 39.0 mWm^{-2}, A_H = 1.21 μWm^{-3} and Q_m = 12.1 mWm^{-2}. Crustal differentiation index is D_i = 2.47 and geoneutrino flux Φ = 11.7 × 10^6 cm^{-2} s^{-1} in this case. An undifferentiated crustal cylinder with similar surface-Moho heat flow contrast would only produce Φ = 6.2 × 10^6 cm^{-2}s^{-1}. The upper crust in the immediate vicinity of Pyhäsalmi is not locally enriched in radiogenic isotopes, when compared to upper crust beyond 150 km, but separate investigations of near-field crust remain important to assess geoneutrino flux at any site with potential for a geoneutrino observatory.

Keywords: heat flow, heat production, uranium, thorium, potassium, geoneutrino

1. Introduction

The Pyhäsalmi mine in north central Finland is operated by First Quantum Minerals Ltd. to produce zinc and copper. The 1444 m deep mine is the oldest operational mine in Finland but will be decommissioned in 2019. An underground science and technology centre will be built to the mine in the Callio project (https://callio.info/), calling for knowledge of local geophysical environment. Projects related to nuclear physics have been already undertaken in the mine (Kuusiniemi et al. 2013, Enqvist et al. 2017). In the new laboratory hall at a depth of 1430 m, the share of cosmic rays in total radiation is limited to muons, and radiation from geoneutrinos could be detected more easily than in upper levels.

Geoneutrinos are electron antineutrinos resulting from beta decay series of ^{238}U and ^{232}Th. They can be detected using underground liquid scintillation detectors, yet the energy threshold of 1.8 MeV in the inverse beta decay reaction (IBD) on free protons leaves the vast majority of geoneutrinos undetected. No signal from ^{40}K and ^{235}U can be observed this way, yet a method based on neutrino-electron elastic scattering and low-background, direction-sensitive tracking detectors may provide a solution to the problem. Therefore it is becoming more important to analyze the contribution from all three major heat producing elements (U, Th and K) as a whole. This has been previously done in the vicinity of geoneutrino observatory in Sudbury, Canada, near the border of Archean and Proterozoic lithosphere (Phaneuf and Mareschal, 2014). Following the same principle in a tectonothermal environment of roughly same age range, we focus on the Finnish lithosphere around Pyhäsalmi, using heat flow and heat production data.

2. Heat production and heat flow

The standard way of determining heat production is to use radiogenic element concentration data. For this purpose, we applied the Rock Geochemical Database of Finland (Rasilainen et al. 2007). Heat production (A) [μWm^{-3}] was calculated after Rybach (1973):

$$A = \rho\,(9.52C_U + 2.56\,C_{Th} + 3.48\,C_K)\cdot 10^{-5} \quad (1)$$

where ρ is the rock density [kg/m^3] and C_U, C_{Th} and C_K are concentrations of U [ppm], Th [ppm] and K [%]. Altogether 1467 observations, 22.7% of the entire database, are located within 150 km from Pyhäsalmi mine. We assume that our mean heat production value 1.21 μWm^{-3} calculated from outcrop data in this area is representative of the regional upper crust.

Heat production is directly proportional to geoneutrino production, but the connection between surface heat flow and geoneutrino production is not simple. Surface heat flow <Q> at the center of a cylindrical layer with thickness zm, radius R, heat production <A> and lower boundary heat flow <Q_m> can be calculated as follows:

$$< \boldsymbol{Q} > - < \boldsymbol{Q_m} > = < \boldsymbol{A} > \boldsymbol{z_m}\left(\mathbf{1} + \frac{\boldsymbol{R}}{\boldsymbol{z_m}} - \sqrt{\mathbf{1} + \frac{\boldsymbol{R^2}}{\boldsymbol{z_m^2}}}\right) \quad (2)$$

Differentiation index D_i is obtained as the ratio of the average surface heat production <A_S> to the average crustal heat production <A>, i.e. Di = <A_s> zm/(<Q>-Qm). Using constraints <A_S> = 1.2 μWm-3, z_m= 55 km, <Q> = 39 mWm^{-2}, and Q_m = 12 mWm^{-2}, we end up to D_i = 2.44. For a crust with an upper crustal layer of thickness d where H = <H_S>, geoneutrino flux in a cylindrical layer can be related to the regional heat flow by (Perry et al. 2009):

$$\boldsymbol{\Phi} = \frac{\boldsymbol{\gamma(<Q>-Q_m)}}{\mathbf{2}}\left\{\frac{\boldsymbol{z_m - D_i d}}{\boldsymbol{z_m - d}}\left[\frac{\mathbf{1}}{\mathbf{2}}\mathbf{ln}\left(\mathbf{1} + \frac{\boldsymbol{R^2}}{\boldsymbol{z_m^2}}\right) + \frac{\boldsymbol{R}}{\boldsymbol{z_m}}\mathbf{atan}\left(\frac{\boldsymbol{z_m}}{\boldsymbol{R}}\right)\right] + \frac{\boldsymbol{D_i z_m}}{\boldsymbol{z_m - d}}\left[\frac{\mathbf{1}}{\mathbf{2}}\mathbf{ln}\left(\mathbf{1} + \frac{\boldsymbol{R^2}}{\boldsymbol{d^2}}\right) + \frac{\boldsymbol{R}}{\boldsymbol{d}}\mathbf{atan}\left(\frac{\boldsymbol{d}}{\boldsymbol{R}}\right)\right]\right\} \quad (3)$$

In our case R = 150 km and d = 10 km. For our two-layered crust, the influence of heat production on geoneutrino flux can be calculated from <Q>, D_i, and d. The ratio of upper to lower crustal heat production is $A_u/A_l = D_i z_m/(z_m - D_i d)$. Thickness of the lower crust is therefore 45 km, and heat production 0.333 μWm^{-3} within it. Parameter γ [J^{-1}] is ratio of neutrino activity ν [s^{-1}] to heat production per unit mass A_M [W/kg]. Using A_M values of 9.52 × 10^{-5} W kg^{-1} for U, 2.56 × 10^{-5} W kg^{-1} for Th and 3.48 × 10^{-9} W kg^{-1} for K, corresponding ν values of 7.38 × 107 s^{-1} kg^{-1}, 1.61 × 10^7 s^{-1} kg^{-1} and 2.25 × 10^4 s^{-1} kg^{-1} (Mareschal et al. 2012) and mean concentrations of heat producing elements within 150 km distance from Pyhäsalmi (1.91 ppm for U, 7.35 ppm for Th and 2.15% for K) leads to γ = 0.70 × 10^{12} J^{-1}. Hence, Equation 3 can be used to study differences in geoneutrino flux as a result of different crustal compositions. Changing the value of D_i to 1 but keeping the integrated heat production unchanged in the crust is equivalent to an evenly distributed heat production of 0.59 μWm^{-3}. Although surface heat flow is similar regardless of crustal differentiation, surface geoneutrino flux is highly dependent on near crustal sources and is therefore subject to substantial change.

For evaluation of a two-layered geotherm of the crust around Pyhäsalmi area, we used temperature-dependent thermal conductivity λ:

$$\boldsymbol{\lambda = \lambda_0}\left[\frac{\mathbf{1}}{\mathbf{1}+\boldsymbol{bT}} + \boldsymbol{c}(\boldsymbol{T} + \mathbf{273.15}\,\boldsymbol{K})^{\mathbf{3}}\right] \quad (4)$$

Here T is temperature [°C], λ_0 is thermal conductivity [Wm^{-1}K^{-1}] at the reference temperature of 25 °C and b is a pre-selected empirical parameter [1/K] dependent on lithology. In our case b=0.0008 as used by Veikkolainen et al. (2017). Radiative heat transfer is described by c, yet it

can be safely given a value of zero below temperatures of 800 °C. For b in crust, we applied a value of 0.0008. For surface value of thermal conductivity, we applied λ_0 =2.9 $Wm^{-1}K^{-1}$.

We assume here T_0 = 0 °C and q_0 = 39 mWm^{-2}. A is 1.21 μWm^{-3} (mean of point data) at depth range z = 0...10 km, and 0.33 μWm^{-3} at z = 10...55 km. Using this information, we plotted a one-dimensional geotherm of the area. To reflect the standard deviation of H within the study area, we also plotted alternative geotherms, one with A = 0.20 μWm^{-3} and another with A = 2.23 μWm^{-3}, corresponding to mean upper crustal heat production added or subtracted by one standard deviation. We required the Moho heat flow to be 12 ± 3 mWm^{-2} based on xenolith thermobarometry (Kukkonen et al. 2003) and adjusted lower and upper limits of surface heat flow accordingly. In the model with large H in upper crust, surface heat flow was 32.1 mWm^{-2} and in the model with small H in upper crust, 46.1 mWm^{-2}. Accordingly, our Moho temperature range is 494-638 °C. In terms of differentiation index, our Model 1 features D_i=2.47, Model 2 D_i=0.46 and Model 3 D_i=4.09. For geotherms, see Figure 1.

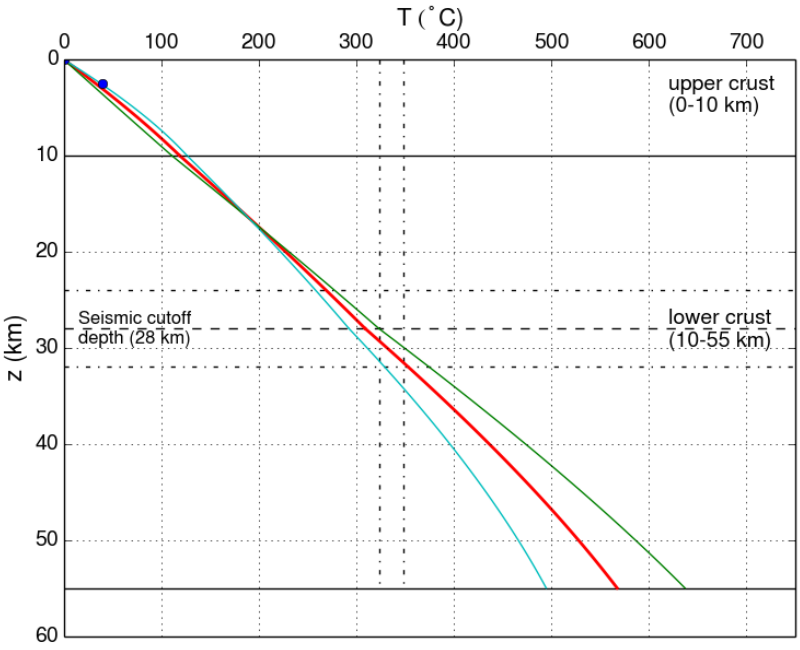

Figure 1. Geotherms for the crust of the study area, 150 km around Pyhäsalmi mine. Red curve represents the situation with A_H = 1.21 μWm^{-3}, cyan curve that with A_H = 2.23 μWm^{-3} and green curve that with A_H = 0.20 μWm^{-3}, corresponding to D_i = 2.47 (Model 1), Di = 4.09 (Model 2) and Di = 0.46 (Model 3), respectively. The temperature of 40 °C at the bottom of Outokumpu borehole (Kukkonen et al. 2011) is also shown.

In the average geotherm, upper 10 km contributes 12.1 mWm^{-2} and total crust 26.9 mWm^{-2} to heat flow in Pyhäsalmi. In the entire upper crustal heat flow contribution, the share of a cylinder of 150 km radius representing upper crust around Pyhäsalmi is as much as 96.7%. The corresponding contribution of a cylinder of 100 km radius is 95.0% and that of a cylinder of 50 km radius is 90.0%. Approximately as much as 26.7 mWm^{-2} of the crustal contribution to surface heat flow can be explained by an undifferentiated cylinder of 150 km radius and 55 km depth. Geoneutrino flux contribution in the middle of the surface of the cylinder is 6.174 × 10^6 $cm^{-2}s^{-1}$ in the undifferentiated and 11.710 × 10^6 cm^{-2} s^{-1} in the differentiated case. Differentiation nearly doubles the flux from the crust nearest to the study area. The share of upper crust is 5.299 × 10^6 cm^{-2} s^{-1} (45%) in the differentiated, but only 2.583 × 10^6 $cm^{-2}s^{-1}$ (42%) in the

undifferentiated case. The total geoneutrino flux is affected by lithospheric and asthenospheric mantle, but crustal differentiation causes most obvious changes.

3. Conclusions

Estimation of the total geoneutrino flux requires knowledge of the crustal structure also beyond the 150 km distance and integration over domains of different, often poorly known heat production constraints. The lithospheric part of geoneutrino flux should in principle be almost exclusively a result of heat production in crust, because xenolith pressure-temperature data imply very small mantle heat production A(M), 0.00-0.04 μWm^{-3} globally. The large thickness of the Fennoscandian lithosphere, 250 km, however, calls for a specific analysis for our area of interest. Even assuming a value H(M)=0.02 μWm^{-3} which is tenfold the constraint used by Veikkolainen et al. (2017) in their Fennoscandian geotherms results in a heat flow contrast of 3.9 mWm^{-2} between Moho and the base of lithosphere. Recalling our cylindrical approximation of lithospheric mantle below 55 km depth adds 0.56×10^6 $cm^{-2}s^{-1}$ to crustal geoneutrino flux, only 4.2% to total flux in case of undifferentiated and 9.0% in the case of differentiated crust. In Pyhäsalmi, the share of upper crust is ~9.5 times as large as that of mantle in the undifferentiated, and ~4.6 times as large in the differentiated case. This is due to the importance of the near-field crust and crustal differentiation for the determination of geoneutrino flux, despite the fact that crust near Pyhäsalmi is not locally enriched in radioactive elements. Although the stable intraplate location would make Pyhäsalmi a good spot for geoneutrino studies, the forthcoming Hanhikivi nuclear power plant in Pyhäjoki, 130 km from the mine site, will strongly add up to the natural geoneutrino flux in the proposed observatory area.

References:

Enqvist, T., Barabanov, I.R., Bezrukov, L.B., Gangapshev, A.M., Gavrilyuk, Y.M., Grishina, V.Yu., Gurentsov, V.I., Hissa, J., Joutsenvaara, J., Kazalov, V.V., Krokhaleva, S., Kutuniva, J., Kuusiniemi, P., Kuzminov, V.V., Kurlovich, A.S., Loo, K., Lubsandorzhiev, B.K., Lubsandorzhiev, S., Morgalyuk, V.P., Novikova, G.Y., Pshukov, A.M., Sinev, V.V., Iupecki, M.S., Trzaska, W.H., Umerov, Sh.I., Veresnikova, A.V., Virkajärvi, A., Yanovich, Y.A., Zavarzina, V.P., 2017. Towards 14 C-free liquid scintillator. J. Phys.: Conference Series 888, 012098.

Kukkonen, I.T., Kinnunen, K.A., Peltonen, P., 2003. Mantle xenoliths and thick lithosphere in the Fennoscandian Shield. Phys. Chem. Earth 28, 349-360.

Kukkonen, I.T., Rath, V., Kivekäs, L., Safanda, J., Cermak, V., 2011. Geothermal studies of the Outokumpu Deep Drill Hole, Finland: vertical variation in heat flow and paleoclimatic implications. Phys. Earth Plan. Int. 188, 9-25.

Kuusiniemi, P., Bezrukov, L., Enqvist, T., Fynbo, H., Inzhechik, L., Joutsenvaara, J., Kalliokoski, T., Loo, K., Lubsandorzhiev, B., Monto, T., 2013. Underground cosmic-ray experiment EMMA. J. Phys.: Conference Series 409, 012067.

Mareschal, J.-C., Jaupart, C., Phaneuf, C., Perry, C., 2012. Geoneutrinos and the energy budget of the Earth. J. Geodyn. 54, 43-54.

Perry, H.K.C., Mareschal, J.-C., Jaupart, C., 2009. Enhanced crustal geo-neutrino production near the Sudbury Neutrino Observatory, Ontario, Canada. Earth Plan. Sci. Lett. 288, 301-308.

Phaneuf, C., Mareschal, J.-C., 2014. Estimating concentrations of heat producing elements in the crust near the Sudbury Neutrino Observatory, Ontario, Canada. Tectonophys. 622, 135-144.

Rasilainen, K., Lahtinen, R., Bornhorst, T.J., 2007. The Rock Geochemical Database of Finland Manual. Geol. Surv. Fin., Report of Investigation 164, 38pp.

Rybach, L., 1973. Wärmeproduktionsbestimmungen an Gesteinen der Schweizer Alpen. Beiträge zur Geologie der Schweiz: Geotechnische Serie 51, 43pp.

Veikkolainen, T., Kukkonen, I.T., Tiira, T., 2017. Heat flow, seismic cut-off depth and thermal modelling of the Fennoscandian Shield, Geophys. J. Int., 211, 1414–1427.

3C Seismic Interferometry at the Polymetallic Kylylahti Deposit, Outokumpu District, Finland

S. Väkevä[1], E. Koivisto[1], G. Hillers[1], M. Chamarczuk[2] and M. Malinowski[2]

[1]Department of Geosciences and Geology (Pietari Kalmin katu 5), FI-00014 University of Helsinki, Finland
[2]Institute of Geophysics, Polish Academy of Sciences, Księcia Janusza 64, 01-452 Warsaw, Poland
E-mail: sakari.vakeva@helsinki.fi

In 2016, a three-component passive seismic survey along two 2D profiles was carried out in the Kylylahti area of Eastern Finland in association with a larger deployment of a thousand one-component (1C) receivers. This study attempts to develop a workflow for 3C seismic interferometry. The 3-by-3 correlations of the orthogonal recording components at different stations can be used to reconstruct the S-wave response or to support the 1C data interpretation. Through the application of non-conventional processing stages such as sign-bit normalization, we gain better continuity of retrieved reflections.

Keywords: seismic reflection, mineral exploration, Cu–Ni–Co deposits

1. Introduction

Theoretical advances (e.g. Wapenaar and Fokkema, 2006) have demonstrated that passive seismic ambient noise surveys allow new possibilities for seismic imaging and that the technique of seismic interferometry (SI) may provide a compelling alternative for traditional reflection surveying. SI aims at the reconstruction of the impulse response (Green's function) of an elastic system between two stations. This is equivalent to the cross-correlation (or cross-coherence) of the seismograms measured at the stations if the source is regarded as a delta function. For generalized displacement in three dimensions (elastodynamic assumption), Green's function is a tensor $\widehat{\boldsymbol{G}}_{\mathbf{qp}}(\mathbf{x_A}, \mathbf{x_B}, \boldsymbol{\omega})$ with nine components.

The suitability of SI for body-wave reflection retrieval in a mining and exploration environment was recently tested in the COGITO-MIN project at Kylylahti polymetallic mine in Eastern Finland. In the field experiment of August/September 2016, a 3D seismic array of a thousand one-component receivers was continuously recording for about 30 days in an area of 10.5 square kilometres. These data are used to develop an SI processing workflow to support mineral exploration at a mining-camp scale (Chamarczuk et al., 2017).

Parallel to the COGITO-MIN experiment, the Comprehensive Test Ban Treaty Organization (CTBTO) was using the Kylylahti mine site as a testing ground to develop an emergent technique, resonance seismometry (Labak, Lindblom and Malich, 2017). Their experiment involved the deployment of 45 three-component (3C) seismometers, planted in surface holes 30–40 cm deep, for about 30 days along two of the COGITO-MIN receiver lines. The continuous data are available as MiniSEEDs with 24 h time spans and a sample rate of 2 milliseconds.

In this work, the CTBTO data are used for developing a passive-seismic 3C interferometric workflow. The results are supported with synthetic modelling over the receiver lines.

2. Study area and methods

The Kylylahti polymetallic sulphide deposit features massive-to-semimassive sulphide ore and disseminated mineralisations. The main mineralization is a narrow ribbon in a SSW dipping hinge of a tight fold, mined at present deeper than 700 meters. The exploration environment is challenging due to the subvertical contacts between individual horizons of the Outokumpu

suite, making them difficult to detect seismically from surface. The Outokumpu rocks hosting the mineralisation are serpentinites, quartz-carbonate rocks, and tremolite-diopside skarns enfolded in deep-water turbidites and pelitic graphite schists. Kylylahti rock types can be simplified into four groups with distinct acoustic impedances: (1) mica schists and black schists formed in deep water, (2) Outokumpu ultramafics, i.e., serpentinite and soapstones, (3) metasomatic alteration rocks of previous group, and (4) massive-to-semimassive sulphide mineralisations. The groups are expected to be reflective when in contact with each other (Luhta et al., 2016).

To infer the quality of the retrieval of reflections with passive SI, the 2D finite difference code `fdelmodc` by Thorbecke and Draganov (2011) is used to set up a synthetic reference experiment. The lithological domains along the CTBTO lines are extracted from the mining operator's simplified block model and are associated with average velocities using petrophysical measurements of Luhta et al. (2016). We show that the resulting virtual shot gathers exhibit the same reflection events as a forward-modelled surface shot gather, so the interferometric workflow in general gives encouraging results.

The preprocessing stages for the actual 3C data include downsampling to 250 Hz, spectral whitening, and sign-bit normalization, which equalize the spectral content of the raw traces and mute the biasing effects of strong transients. To prevent the leaking of energy from one component to another, we can distribute energy along Green's function symmetries. We also rotate the 3×3 Green's tensor from the ZNE to the inter-station vertical, radial, and transversal coordinate system (ZRT).

The resulting coherency panels for ZRT components after rotation into the strike of the survey line are obtained from 30 days of noise. There are events in the vertical component panel that can be attributed to the impedance contrast between the host rocks of the mineralisation and its surroundings. The transverse component panel exhibits similar sparse reflectivity.

4. Conclusions

A passive seismic experiment employing a set of 45 3C seismometers deployed along two linear arrays is conducted for the CTBTO data collected at the Kylylahti deposit. Some non-conventional approaches such as the sign-bit normalization for the passive data appear to yield better continuity of reflections than those conventionally used.

Results from surface-based seismic interferometry contain reflectivity in expected areas, assuming optimal distribution of ambient-noise sources is available. Passive SI could be regarded as a standalone method for initial estimation of the target area or a supplementary tool for conventional exploration techniques for precise mapping of ore host rock continuity.

References:

Chamarczuk, M., Malinowski, M., Koivisto, E., Heinonen, S., Juurela, S. and the COGITO-MIN Working Group, 2017. Passive seismic interferometry for subsurface imaging in an active mine environment: case study from the Kylylahti Cu–Au–Zn mine, Finland. In "Proceedings of Exploration 17: Seismic Methods & Exploration Workshop" edited by G. Bellefleur and B. Milkereit, 51–56.

Labak, P., Lindblom, P. and Malich, G., 2017. Seismic field measurements in Kylylahti, Finland, in support of the further development of geophysical seismic techniques for CTBT On-site Inspections. Geophysical Research Abstracts, 19. EGU General Assembly 2017.

Luhta, T., Mertanen, S., Koivisto, E., Heinonen, S., Törmälehto, T. and Kukkonen, I., 2016. The seismic signature of the Kylylahti deposit: Initial results from new petrophysical measurements. 9th symposium on the Structure, Composition and Evolution of the Lithosphere in Finland, Programme and Extended Abstracts.

Thorbecke, J. W. and Draganov, D., 2011. Finite-difference modeling experiments for seismic interferometry. Geophysics, 76(6), H1–H18.

Wapenaar, K. and Fokkema, J., 2006. Green's function representations for seismic interferometry. Geophysics, 71(4), SI33-SI46.

Refraction seismic studies along the Kokkola–Kymi transect, Central Fennoscandia

S. Väkevä[1], T. Tiira[1], T. Janik[2], T. Veikkolainen[1], T. Skrzynik[2], A. Heinonen[1], K. Komminaho[1] and A. Korja[1]

[1]Institute of Seismology (Pietari Kalmin katu 5), FI-00014 University of Helsinki, Finland
[2]Institute of Geophysics, Polish Academy of Sciences, Ks. Janusza 64, 01-452 Warsaw, Poland
E-mail: sakari.vakeva@helsinki.fi

In 2012–2013, an uncontrolled refraction seismic survey was carried out on the Kokkola–Kymi transect (KOKKY). The line replicates the previous findings from deep seismic studies, such as a thick ~64 km crust, the presence of a high-velocity layer in the lower crust, and high Vp/Vs ratios below the Wiborg rapakivi batholith.

Keywords: deep seismic refraction, cost-effectiveness, crust, Fennoscandian shield

1. Introduction

Data for controlled-source seismic studies are acquired during campaigns on wide-angle reflection and refraction (WARR) profiles which are hundreds of kilometres long and require strong explosive sources such as TNT. Given the cost of such experiments, logistic challenges, and the regulation on experiments involving explosives in lakes, modern seismic profiling benefits from methods such as noise correlation or utilization of transient sources from industrial activities.

The 490 km Kokkola–Kymi seismic reflection line (KOKKY, Fig. 1) transects Finland in NW–SE direction and is parallel to Finnish national road number 13. In addition to the Central Finland Granitoid Complex, it crosscuts the Western and Southern Finland Subprovinces (WFS and SFS; Nironen, 2017). Sources in the KOKKY experiment are blasts from road construction sites and quarries. The applicability of quarries for seismic experiments had been previously tested in the HUKKA 2007 survey (Tiira et al. 2013). The line was surveyed in two parts: in 2012, the stations were spread along the Kokkola–Äänekoski transect, and in 2013, along the Karstula–Nuijamaa segment.

The Fennoscandian crust is generally thickest in a c.a. 400×600 km^2 area extending from the city of Joensuu across Central Finland to the Gulf of Bothnia, and in south all the way to the city of Hämeenlinna. In the Moho model by Grad et al. (2009) based on DSS surveys, the thickest crust (about 61 km) is found near the town of Heinävesi in Southern Savonia. However, results from SVEKALAPKO array seem to imply that the thickest crust is closer to 64 km (Kozlovskaya et al., 2008), and occurs beneath the Central Finland Granitoid Complex (CFGC).

2. Background of study area

The NW–SE oriented KOKKY profile studies the crustal structure of the Paleoproterozoic Svecofennian province and crosses the suture between the WFS and SFS (Nironen, 2017) at a high angle. The profile shows the Bothnian belt (BB) and Central Finland granitoid complex (CFGC) of the WFS and the Southern Savo nappe and Saimaa area of the SFS (see Nironen, 2017 for nomenclature) as well as the Wiborg rapakivi batholith (WRB). KOKKY line connects the existing deep seismic sounding (DSS) lines SVEKA81, BALTIC, FIRE 1, and FIRE 2, and is in its NW end parallel to FIRE 3A (Luosto, 1997; Kukkonen and Lahtinen, 2006). Although the DSS line FENNIA does not parallel or crosscut KOKKY

(FENNIA Working Group, 1998), they might share similar positions in relation to the Svecofennian accretionary orogen, allowing joint interpretation between them.

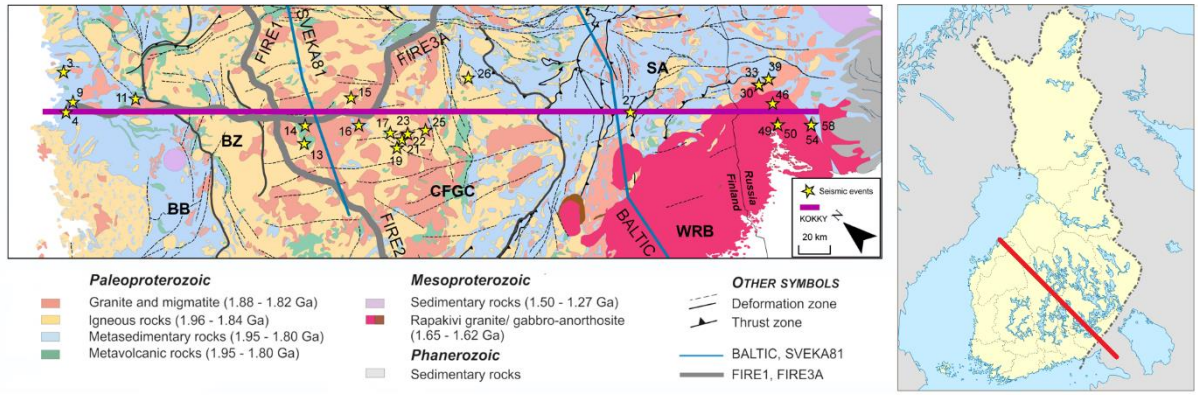

Figure 1. Location of KOKKY transect on the Finnish bedrock map along with stars indicating the locations of the industrial shots used for seismic modelling. The previous DSS lines FIRE 1, 2, 3A, SVEKA81, and BALTIC are shown in white and grey. Abbreviations: BB = Bothnian Belt, CFGC = Central Finland Granitoid Complex, HB = Häme Belt, SA = Saimaa Area, WRB = Wiborg rapakivi batholith.

The seismic structure of the central Fennoscandian shield exhibits three crustal layers, high crustal velocities, a high velocity lower crust (> 7 km/s), elevated crustal thicknesses (> 50 km), and a diffuse Moho (Kukkonen et al., 2006). Central Fennoscandian refraction studies typically point to an interface between upper crust and middle crust or other crust-internal contacts. However, since these are not always clearly visible in reflection seismic studies, they may also be due to gradual transitions in metamorphism or rock chemistry.

The Bothnian belt represents an accretionary prism of an arc complex. It is composed of metapelites and metagreywackes and minor metavolcanic units that have been deformed and metamorphosed under high-T-low-P conditions. FIRE 3A reflection seismic profile, parallel to the KOKKY line, revealed east–southeast dipping reflectors that have been correlated with the contacts of the supracrustal units on the surface (Sorjonen-Ward, 2006).

The CFGC contains strongly foliated synorogenic (1.89–1.88 Ga) and weakly oriented late orogenic (1.88–1.87 Ga) granodiorites and granites. Their anatexis took place in the crustal shortening of the continental collision stage. There is evidence of geochemically older, c.a. 2.0 Ga lithosphere (‘Keitele microcontinent’) which might have evolved into the CFGC. Some later models (Lahtinen et al., 2014) suggest that Keitele was a linear strip and it was bent into the present shape of an equidimensional sphere during the accretion of Bothnian oroclines. Remnants of the Keitele block have been variably identified on the FIRE (Finnish Reflection Experiment) lines (Lahtinen et al., 2009).

Southern Savo nappe system is a late allochtonous unit partly thrust on WFS (Nironen, 2017), and thus covers the suture between WFS and SFS. Magnetometric array studies and flight-EM measurements present the Southern Savo nappe as the easternmost limit of a conductive ribbon of graphite- and sulphide-bearing metasediments (Korsman et al., 1997). Towards south, the schists of Saimaa belt have been migmatized at 1.84–1.81 Ga. These intrusions of S-type microcline granites belong to the second-generation granitoids of the late Svecofennian leucogranite suite (Kurhila, 2011).

The Wiborg suite granites intruded SFP and the Saimaa area at around 1.63–1.53 Ga (Rämö and Haapala 2005). The BALTIC profile has previously shown that in the WRB, the

thinner crust is associated with a doubly stratified Moho, and there is a lenticular high-velocity layer right beneath the rapakivi intrusion, potentially composing anorthositic rocks (Elo and Korja, 1993; Rämö and Haapala, 2005).

3. Data acquisition

In 2012, 49 portable seismic stations were deployed in the first 200 km of the KOKKY profile. In 2013, 74 portable seismic stations were deployed in range 140 km to 440 km. There was an overlap of 60 km between the deployments. The total number of the stations was 123 and the average receiver spacing was 4 km.

Maximum perpendicular deviation of the 63 blasts near the line was 25.4 km. The averaged perpendicular offset was 14 km. As the locations of the shots were initially unknown, they were determined with the Finnish national seismic network. The inherent uncertainty in shot location and timing was reduced by comparing the locations of shots to the known quarries, mines, and road construction sites using aerial orthomosaics of the National Land Survey of Finland, digital maps, and satellite images. The origin times were estimated by extrapolating individual station arrival times using the pre-existing time-distance curves for Finland. Since there was typically more than one shot available for a single quarry, the final seismic modelling only used the 25 best-quality blasts.

4. Seismic modelling

Three techniques of seismic interpretation were used for the record sections: seismic forward modelling, tomographic inversion yielding a smooth minimum-structure velocity model, and full-waveform modelling with a 2D finite-difference code. Since the record sections are wide-angle, rays preferentially propagate horizontally, and the lateral resolution of profiles is coarser than the depth resolution. This makes refraction seismic data complementary to many other methods such as reflection seismic profiles or receiver function studies.

Forward modelling (Červený and Pšenčík, 1984) is a trial-and-error method where the interpreter builds a structured layer-cake model and adjusts velocity gradients to minimise residuals in phase arrival times. P and S phase propagation are modelled in 2D with the eikonal equation. The interpreter can also insert velocity jumps and mid-crustal reflectors when it is supported by the data. Tomographic inversion (Hobro et al., 2003), on the other hand, results in smooth velocity models by automatically adjusting seismic velocities in a regular grid. Inverted models typically have minimal structures since adjustments are gradual and the algorithms cannot by default accommodate big jumps in velocities. Full waveforms can be used to verify the resulting models also in terms of phase amplitudes.

According to the models, Moho depth varies from 54 km near Bothnian Bay to 63 km in the middle of the profile, and up to 43 km in Saimaa area. The high velocity lower crust with a homogeneous velocity of 7.35–7.4 km/s is well documented on the record sections. The layer is thickening from 4 km in SE part of the profile, reaching 18 km in its central part corresponding to CFGC, and then thinning again to about 12 km in NW part.

Upper crustal P wave velocities show an enigmatic low-velocity keel (6.0–6.2 km/s), with a thickness of ~12 km near the transition between CFGC and the Southern Savo nappe complex. However, since there are several off-line shots, the rays might also be sampling the low velocities and high attenuation of the neighbouring Raahe–Ladoga shear zone. The high-velocity anorthosite body observed in BALTIC is not seen in the present models, perhaps due to the inadequate source and receiver coverage within the WRB.

The highest Vp/Vs ratios (>1.80) observed beneath the WRB are in good agreement with the reanalysis of BALTIC profile by Janik (2010). Large Vp/Vs ratios are also observed within the high-velocity lower crust.

5. Conclusions

The results agree with previous geoscientific studies of Finland, especially for the CFGC and the north-western part. The profile extends the knowledge of the range of > 60 km deep Moho and contributes to the interpretation of the SVEKALAPKO experiment (Kozlovskaya et al., 2008).

Despite the sparse shot and receiver coverage, KOKKY line demonstrates the benefits of non-controlled seismology in further lithospheric studies.

References:

Červený, V., Pšenčík, I., 1984. Documentation of Earthquake Algorithms. SEIS83 – Numerical modeling of seismic wave fields in 2-D laterally varying layered structures by the ray method, edited by E.R. Engdahl. Report SE-35, Boulder, 36-40.

Elo, S., Korja, A. 1993. Geophysical interpretation of the crustal and the upper mantle structure in the Wiborg rapakivi granite area, southeastern Finland. Precambrian Research 64, 273-288, doi: 10.1016/0301-9268(93)90081-C.

FENNIA Working Group, 1998. P- and S-velocity structure of the Fennoscandian shield beneath the FENNIA profile in southern Finland. Institute of Seismology, University of Helsinki. Report S-38, 15 p.

Grad, M., Tiira, T., and ESC Working Group, 2009. The Moho depth map of the European Plate, Geophys. J. Int. 176, 279-292. doi: 10.1111/j.1365-246X.2008.03919.x.

Hobro, J.W., Singh, S.C., Minshull, T.A. 2003. Three-dimensional tomographic inversion of combined reflection and refraction seismic traveltime data. Geophysical Journal International 152, 79-93, doi: 10.1046/j.1365-246X.2003.01822.x.

Janik, T., 2010. Upper lithospheric structure in the central Fennoscandian shield: Constraints from P- and S-wave velocity models and VP/VS ratio distribution of the BALTIC wide-angle seismic profile. Acta Geophysica 58, 543-586, doi: 10.2478/s11600-010-0002-0.

Korsman, K., Korja, T., Pajunen, M., Virransalo, P. and the GGT/SVEKA Working Group, 1999. The GGT/SVEKA Transect: structure and evolution of the continental crust in the Palaeoproterozoic Svecofennian Orogen in Finland. Internat. Geol. Rev. 41, p. 287–333.

Kozlovskaya, E., Kosarev, G., Aleshin, I., Riznichenko, O., Sanina, I., 2008. Structure and composition of the crust and upper mantle of the Archean–Proterozoic boundary in the Fennoscandian shield obtained by joint inversion of receiver function and surface wave phase velocity of recording of the SVEKALAPKO array. Geophys. J. Intl. 175, 135–152.

Kukkonen, I.T. and Lahtinen, R. (eds), 2006. Finnish Reflection Experiment FIRE 2001–2005. Geological Survey of Finland, Special Paper 43, 247 p.

Kurhila, M., 2011. Late Svecofennian leucogranites of southern Finland: Chronicles of and orogenic collapse. PhD thesis, Department of Geosciences and Geography A8, 105 p.

Lahtinen, R., Korja, A., Nironen, M., Heikkinen, P., 2009. Palaeoproterozoic accretionary processes in Fennoscandia. Geological Society, London, Special Publications 318, 237-256, doi: 10.1144/SP318.8.

Lahtinen, R., Johnston, S. T., and Nironen, M., 2014. The Bothnian coupled oroclines of the Svecofennian Orogen: a Palaeoproterozoic terrane wreck. Terra Nova 26, 330–335.

Luosto, U., 1997. Structure of the Earth's crust in Fennoscandia as revealed from refraction and wide-angle reflection studies, in The Lithosphere in Finland – a Geophysical Perspective, edited by L.J. Pesonen, Geophysica 33, 3–16.

Nironen, M., 2017. Bedrock of Finland at the scale 1:1 000 000 – Major stratigraphic units, metamorphism and tectonic evolution. Geological Survey of Finland, Special Paper 60, 128 p.

Rämö, O.T., Haapala, I., 2005. Rapakivi granites, in Precambrian Geology of Finland – Key to the Evolution of the Fennoscandian Shield, edited by M. Lehtinen, P.A. Nurmi and O.T. Rämö, Developments in Precambrian Geology 14, 533-562.

Sorjonen-Ward, P., 2006. Geological and structural framework and preliminary interpretation of the FIRE 3 and FIRE 3A reflection seismic profiles. In: Kukkonen, I. and Lahtinen, R., eds. Finnish Reflection Experiment 2001–2005, Geological Survey of Finland, Special Paper 43, 105-159.

Tiira, T., Janik, T., Kozlovskaya, E., Grad, M., Korja, A., Komminaho, K., Hegedüs, E., Kovács, C.A., Silvennoinen, H., Brückl, E., 2013. Crustal Architecture of the Inverted Central Lapland Rift Along the HUKKA 2007 Profile. Pure and Applied Geophysics 171, 1129-1152, doi: 10.1007/s00024-013-0725-3.

Oxygen isotopes in zircon from Palaeoproterozoic post-collisional carbonatites and lamprophyres in the Fennoscandian Shield

J. Woodard[1]

[1]Geological Sciences, University of KwaZulu-Natal, Private Bag, X54001, Durban, South Africa
E-mail: jwoodard23@hotmail.com

The oxygen isotope composition of zircons from Paleaoproterozoic post-collisional carbonatites and lamprophyres in the Fennoscandian Shield has been investigated. Results show that for magmatic zircons, $\delta^{18}O$ compositions form a tight cluster with values elevated relative to typical mantle values. The consistency of these values over a wide geographic area implies the deviation from mantle values is a source characteristic and not a result of crustal contamination.

Keywords: oxygen isotopes; zircon; carbonatite; lamprophyre; post-collisional tectonics

1. Introduction

Carbonatites and lamprophyres are found in a multitude of tectonic settings worldwide (e.g. Woolley, 1989; Rock, 1991; Woolley and Kjarsgaard, 2008; Woolley and Bailey, 2012), however studies of such rocks in post-collisional extensional settings are relatively uncommon. These rock types can provide information about how the recycling of crustal material via subduction influences the geochemical and isotopic characteristics of the upper mantle. Stable oxygen isotope ratios in igneous rocks provide a tool for monitoring the recycling of supracrustal materials into melts. Regardless of age, igneous zircons in high-temperature equilibrium with the mantle have relatively uniform $\delta^{18}O$ ratios of 5.3 ± 0.3‰ (1σ, Valley et al., 1998). In mantle melts, deviation from these average values could reveal areas of source heterogeneity or give evidence of crustal contamination.

In this study, the O isotope compositions of zircons from Palaeoproterozoic (1795-1781 Ma) carbonatites and lamprophyres in the Fennoscandian Shield have been investigated. These intruded at relatively shallow levels in the crust and reflect the earliest manifestation of magmatism associated with post-collisional extension following the Svecofennian orogen (Eklund et al., 1998; Woodard and Hetherington, 2014; Woodard et al., 2014). Particularly with carbonatites, detailed isotopic studies from post-collisional orogenic settings are under-represented in the literature (e.g. Bernard-Griffiths, 1988; Schleicher et al., 1998; Hou et al., 2006; Woodard and Huhma, 2015). Specifically, studies of oxygen isotopes in zircons from these rock types representing post-collisional orogenic settings seem to be completely lacking in the literature.

2. Geological Background

At Naantali, southwest Finland, a swarm of narrow (2-60 cm) calciocarbonatite dykes intrude the Svecofennian bedrock in an area ~1 km wide and ~2 km long, surrounded by an aureole of potassic fenitization of variable intensity (Woodard and Hölttä, 2005). Woodard and Hetherington (2014) distinguished between both bright and dark domains in cathodoluminescence (CL) images of zircons and suggested that the bright domains had been affected by minor late-stage autometasomatism in the carbonatite. Emplacement of the dykes occurred at 1796 ± 9, marking the transition to a post-collisional extensional tectonic regime (Woodard and Hetherington, 2014).

The shoshonitic lamprophyre dykes in this study crop out in proximity to the paleosuture between the Archean Karelian Province and the Paleoproterozoic Svecofennian Domain.

Woodard et al. (2014) distinguished two groups of zircons in the lamprophyres: irregular fragments of large, irregularly shaped subhedral or anhedral grains (group 1) and rounded prismatic grains (group 2). Group 1 zircons were used to determine the intrusion ages for the dykes. In the North Savo region, small swarms of lamprophyre dykes intrude Late Archaean (3.1-2.7 Ga; Sorjonen-Ward and Luukkonen, 2005) gneiss in three separate areas: Lake Syväri, Lake Vuotjärvi and Niinivaara (Figure 1a). Intrusion ages (U-Pb, zircon) for these dykes are 1785 ± 5 Ma, 1790 ± 3 Ma and 1784 ± 4 Ma, respectively (Woodard et al., 2014). In the NW Ladoga region, dykes intrude Svecofennian migmatised metapelite gneiss (1.92-1.90 Ga) and pyroxene-bearing tonalite (1.88-1.86 Ga; Koistinen and Saltykova, 1999; Koistinen et al., 2001). Dykes crop out near the villages of Reuskula and Meijeri, ~15 km and ~20 km northeast respectively from the village of Lahdenpohja. Another isolated dyke crops out on Ivan's Island, south of the Jakimvarsky Gulf, while a small dyke swarm was found on Kalto Island to the north (Figure 1b). The age of the Kalto dykes was determined to be 1781 ± 20 Ma (Woodard et al., 2014).

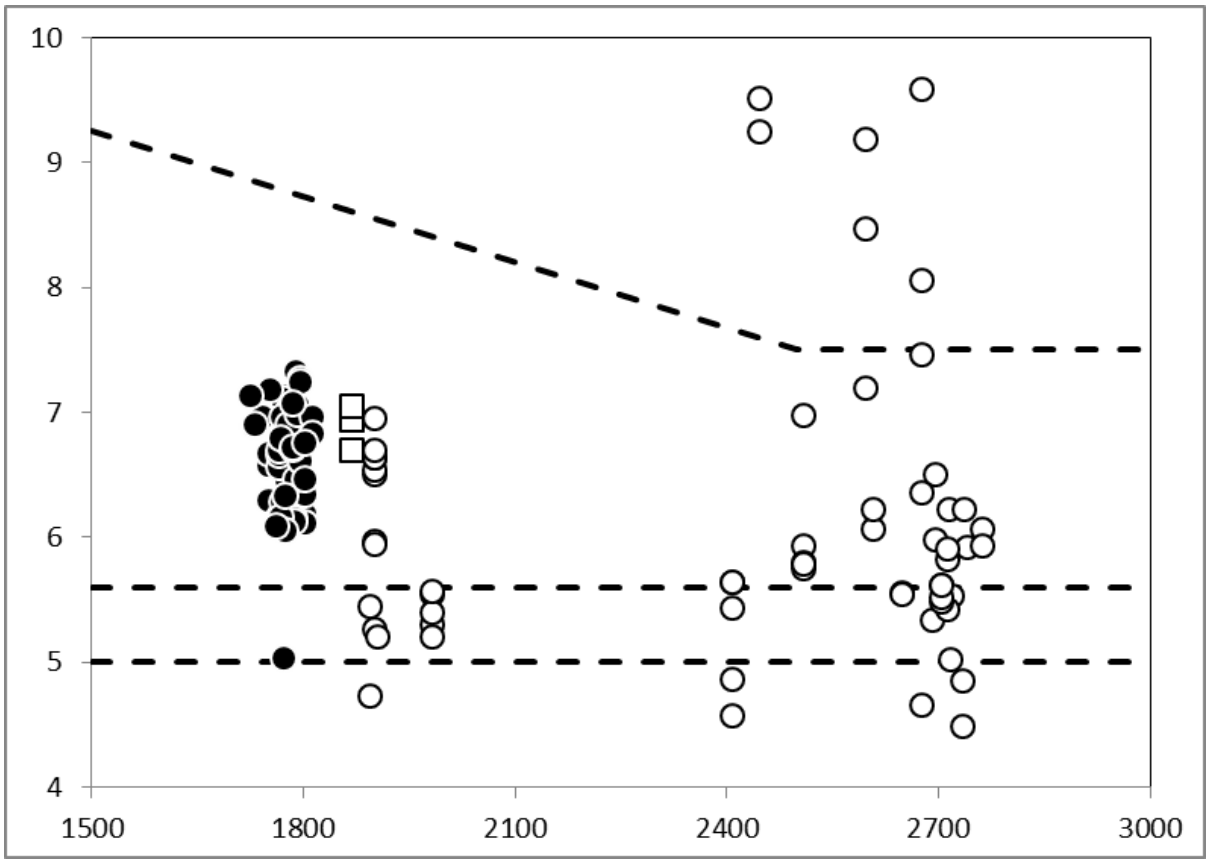

Figure 1. Plot of $\delta^{18}O$ in zircon against age. Black circles are for magmatic (CL-dark or group 1) zircons, while open symbols are for inherited (group 2) zircons. The horizontal dotted lines denote the range for mantle zircon (5.3 ± 0.3‰ 1σ, Valley et al., 1998) while the upper, inflected dotted line denotes the upper limit of the igneous zircon field as defined by Valley et al. (2005).

3.Material and Methods

The zircons in this study were the same zircons used by Woodard and Hetherington (2014) and Woodard et al. (2014) for U-Pb geochronology. Oxygen isotope compositions were measured on a Cameca IMS 1280 multicollector ion microprobe at the Swedish Museum of Natural History, Stockholm, Sweden. For the carbonatites, both CL-bright and CL-dark domains were

analysed; for the lamprophyres, both group 1 and group 2 zircons were analysed. Over the course of the each analytical session, 2-4 measurements were performed on the 91500 zircon standard after each 4-6 unknowns. A $\delta^{18}O$ value of +9.86‰ (SMOW, Wiedenbeck et al., 2004) was assumed for the 91500 zircon in data normalization and small linear-drift corrections (-0.001 - -0.007‰) were applied to each session.

4. Results and Discussion

Results from ca. 150 analytical points are plotted against age in Figure 1. Where available, the $^{207}Pb/^{206}Pb$ spot ages for the specific grains (from SIMS analyses) were used; otherwise the intrusion ages were used (sourced from Woodard and Hetherington, 2014 or Woodard et al., 2014). Magmatic zircons (CL-dark in the carbonatites; group 1 in the lamprophyres) from four samples representing each area have weighted average $\delta^{18}O$ values of 6.86 ± 0.16, 6.40 ± 0.15, 6.92 ± 0.08, and 6.58 ± 0.15; notably higher than the mantle values. Despite this deviation, there is remarkable consistency of values between samples and locations despite these rocks being dykes of varying size and separated by distances >400km. Such homogeneity argues against a model of crustal contamination, given that the heterogeneity of the Fennoscandian crust as well the unlikely scenario of all these intrusions experiencing precisely the same degree of contamination. Instead, it is more likely that the deviation represents a change in the mantle composition in the source area for these melts as a result of extended Svecofennian subduction. While this is largely circumstantial evidence that is by no means definitive, Woodard and Huhma (2015) came to the same conclusion using multiple isotopic systems from whole rock analyses of these rocks.

References:

Bernard-Griffiths., J., Peucat, J.-J., Fourcade, S., Kienast, J.-R., Ouzegane, K., 1988. Origin and evolution of 2 Ga old carbonatite complex (Ihouhaouene, Ahaggar, Algeria): Nd and Sr isotopic evidence. Contributions to Mineralogy and Petrology 100, 339-348.

Eklund, O., Konopelko, D., Rutanen, H., Fröjdö, S., Shebanov, A.D., 1998. 1.8 Ga Svecofennian post-colisional shoshonitic magmatism in the Fennoscandian Shield. Lithos 45, 87-108.

Hou, Z., Tian, S., Yuan, Z., Xie, Y., Yin, S., Yi, L., Fei, H., Yang, Z., 2006. The Himalayan collision zone carbonatites in western Sichuan, SW China: Petrogenesis, mantle source and tectonic implication. Earth and Planetary Science Letters 244, 234-250.

Koistinen, T., Saltykova, T. (eds.), 1999. Structure-lithology, metamorphism and metallogeny of the Raahe-Ladoga Zone, Map 1: Structure-lithology 1:1 000 000. Geological Survey of Finland, Espoo, Finland.

Koistinen, T., Stephens, M.B., Bogatchev, V., Nordgulen, Ø., Wennerström, M., Korhonen, J., 2001. Geological map of the Fennoscandian Shield, scale 1:2 000 000. Geological surveys of Finland, Norway and Sweden and the North-west Department of Natural Resources of Russia.

Rock, N.M.S., 1991. Lamprophyres. Glasgow: Blackie. 285p.

Schleicher, H., Kramm, U., Pernicka, E., Schidlowski, M., Schmidt, F., Subramanian, V., Todt, W., Viladkar, S.G., 1998. Enriched Subcontinental Upper Mantle beneath Southern India: Evidence from Pb, Nd, Sr, and C-O Isotopic Studies on Tamil Nadu Carbonatites. Journal of Petrology 39, 1765-1785.

Sorjonen-Ward, P., Luukkonen, E.J, 2005. Archean rocks. In: Lehtinen, M., Nurmi, P.A., Rämö, O.T. (eds.), Precambrian Geology of Finland - Key to the Evolution of the Fennoscandian Shield. Amsterdam: Elsevier B.V., 19-99.

Valley, J.W., 2003. Oxygen isotopes in zircon. In: Hanchar, J.M., Hoskin, P.W.O. (eds.), Zircon. Reviews in Mineralogy & Geochemistry 53, 343-385.

Valley, J.W., Kinny, P.D., Schulze, D.J., Spicuzza, M.J., 1998. Zircon megacrysts from kimberlite: Oxygen isotope variability among mantle melts. Contributions to Mineralogy and Petrology 133, 1-11.

Valley, J.W., Lackey, J.S., Cavosie, A.J., Clechenko, C.C., Spicuzza, M.J., Basei, M.A.S., Bindeman, I.N., Ferreira, V.P., Sial, A.N., King, E.M., Peck, W.H., Sinha, A.K., Wei, C.S., 2005. 4.4 billion years of crustal maturation: oxygen isotope ratios of magmatic zircon. Contributions to Mineralogy and Petrology 150, 561-580.

Wiedenbeck, M., Hanchar, J.M., Peck, W.H., Sylvester, P., Valley, J., Whitehouse, M., Kronz, A., Morishita, Y., Nasdala, L., Fiebig, J., Franchi, I., Girard, J.P., Greenwood, R.C., Hinton, R., Kita, N., Mason, P.R.D.,

Norman, M., Ogasawara, M., Piccoli, P.M., Rhede, D., Satoh, H., Schulz-Dobrick, B., Skar, O., Spicuzza, M.J., Terada, K., Tindle, A., Togashi, S., Vennemann, T., Xie, Q., Zheng, Y.F., 2004. Further characterisation of the 91500 zircon crystal. Geostandards and Geoanalytical Research 28, 9–39.

Woodard, J., Hetherington, C.J., 2014. Primary carbonatite in a post-collisional tectonic setting: geochronology and emplacement conditions at Naantali, SW Finland. Precambrian Research 240, 94-107.

Woodard, J., Hölttä, P., 2005. The Naantali alvikite vein-dykes: a new carbonatite in southwestern Finland. Geological Survey of Finland, Special Paper 38, 5-10.

Woodard, J., Huhma, H., 2015. Paleoproterozoic mantle enrichment beneath the Fennoscandian Shield: isotopic insight from carbonatites and lamprophyres. Lithos 236-237, 311-323.

Woodard, J., Kietäväinen, R., Eklund, O., 2014. Svecofennian post-collisional shoshonitic lamprophyres at the margin of the Karelia Craton: implications for mantle metasomatism. Lithos 205, 379-393.

Woolley, A.R., 1989. The spatial and temporal distribution of carbonatites. In: Bell, K. (ed.), Carbonatites: genesis and evolution. London: Unwin Hyman, 15-37.

Woolley, A.R., Bailey, D.K., 2012. The crucial role of lithospheric structure in the generation and release of carbonatites: geological evidence. Mineralogical Magazine 76, 259-270.

Woolley, A.R., Kjarsgaard, B.A., 2008. Carbonatite occurrences of the world: map and database. Geological Survey of Canada, 28, Open File 5796.